The composition and characterization of the organic-walled resting cysts of dinoflagellates: Implications for the preservation of organic matter

Dissertation zur Erlangung des Doktorgrades der Naturwissenschaften
(Dr. rer. Nat) am Fachbereich Geowissenschaften
der Universität Bremen

Vorgelegt von

Kara Bogus

Bremen, October 2011

Bogus, Kara 31st of October, 2011

Department of Geosciences/EUROPROX, Universität Bremen, Klagenfurter Strasse, D-28359 Bremen, Germany

Erklärung

Hiermit versichere ich, dass ich

1. die Arbeit ohne unerlaubte fremde Hilfe angefertigt habe,

2. keine anderen als die von mir angegebenen Quellen und Hilfsmittel benutzt habe und

3. die den benutzten Werken wörtlich oder inhaltlich entnommenen Stellen als solche kenntlich gemacht habe.

Bremen, den 31. Oktober 2011

Kara Bogus

Gutachter:

Frau PD Dr. Karin Zonneveld

Frau Prof. Dr. Gesine Mollenhauer

Tag des Kolloquiums:

27.01.2012

Chaos is inherent in all compounded things. Strive on with diligence.

- *-Buddha*

Let us take what the terrain gives.

- *-Amos Tversky*

Preface

This study was funded by the Deutsche Forschungsgemeinschaft (DFG) International Graduate College "Proxies in Earth's History" (EUROPROX) as a collaboration between the University of Bremen, Bremen, Germany and the National Oceanography Centre Southampton, University of Southampton, Southampton, UK. This cumulative work is submitted as a dissertation under the supervision of PD Dr. Karin A.F. Zonneveld (University of Bremen) and Prof. Ian C. Harding (University of Southampton).

The thesis includes four first author manuscripts (Chapters 5-8) that are preceded by introductory material (Chapters 1-4) and followed by general conclusions and scientific prospects (Chapter 9). References to literature cited in the text are given at the end of each chapter. The first two manuscripts are submitted to peer-reviewed journals (*Biogeoscience*s and *Review of Palaeobotany and Palynology*). The remaining two are in preparation for submission and are thus manuscript drafts. All raw data discussed in the manuscripts are depicted in numerous appendices and will be made available on Pangaea. Also included in two appendices are the abstracts of two co-author papers that were submitted during this project. In both cases, both data and written sections were contributed.

Acknowledgements

I first need to thank my supervisors, Karin Zonneveld and Ian Harding, for their interest, support, constructive criticism, and enthusiasm. I am very grateful to have been given this opportunity. I also thank them for fruitful discussions and their willingness to let me make decisions on my own, even if it proved less than helpful. I owe enormous thanks to Gerard Versteegh, without whom this project would not have been at all what it is, or really even possible. I thank Gesine Mollenhauer for what I am sure will be a thoughtful, thorough and constructive review of this thesis.

To all the people who provided various types of assistance in Bremen, especially the members of AG Willems and EUROPROX, I am incredibly indebted. I give many thanks to Sabine Kasten and Gerhard Bohrmann for their comments on my first manuscript. Additionally, I am very appreciative of Ross Williams and Shir Akbari at the NOCS for training me on FTIR analysis and palynological preparation, respectively. Further appreciation is given to John Marshall for providing assistance with the fluorescence microscope. Special thanks to those colleagues, in Bremen, Southampton and beyond, who I am lucky enough to also call friends: Ilham Bouimetarhan, Sonja Heinrich, Tim Haarmann, David Fischer, Ulrike Holzwarth, Anna Dustira, Lizeth Avendano, Ana Borrero, Monica Molina, Eithne Tynan, Marion LeFoll, and Adam Charles.

A very special thank you is necessary for Stefanie Dekeyzer, who was effectively my other half these past three years. Without her, cruises would have been all work, the office would have been all play, and I would not have nearly as much Phil Collins memorabilia.

I also need to thank my non science-y friends for unwavering support and the ability to listen patiently when I whinged. Thank you Jill, Trisha, and Emma. Another special thank you to Tony Hayes, as no matter what god-awful hour I left the university, dinner and a hug were always ready.

This thesis is dedicated to my parents, Janet and Bob, my brother and sister, Adam and Cassie, my grandmother Evelyn, and Sedona, my furry stress relief. I love you dearly, appreciate your patience and am eternally grateful that you rarely asked “how’s the Ph.D going?” when it got close to the end.

Table of Contents

Summary

Understanding the mechanisms behind the degradation and chemical transformations of organic matter (OM) after deposition and burial in marine sediments is a crucial component for understanding the global carbon cycle in its entirety, as OM represents a major reservoir of organic carbon. One way to investigate factors affecting OM preservation is through the analysis of palynomorphs, which are organic-walled microfossils. Palynomorphs, including dinoflagellate cysts, are important tools in the geosciences as they are used in fossil fuel exploration, biostratigraphy, paleoclimatology, and paleoceanography. Thus, processes affecting the palynomorph record are important for researchers in both academia and industry to understand.

This work focused on one specific palynomorph, the organic-walled resting cysts of dinoflagellates (dinoflagellate cysts). These cysts are sexually produced during a dormant stage in the dinoflagellate life cycle and are composed of a non-hydrolyzable, refractory biopolymer called "dinosporin" that is poorly characterized. As a result of the recalcitrant nature of dinoflagellate cysts, they have a long and rich sedimentary record. This makes them ideal proxies (i.e. representatives of parameters that can no longer be directly measured) for paleoenvironmental work. However, different species of dinoflagellate cysts have demonstrated varying sensitivites to aerobic degradation, and this selective preservation potential has implications for the interpretation of the sedimentary proxy record.

Therefore, the rapidity and extent of selective aerobic degradation on the dinoflagellate cyst record was examined in the first study presented in this thesis. In addition to the dinoflagellate cysts, other OM-based proxies were also investigated in recently deposited sediments along meter-scale lateral oxygen gradients at the sediment-water interface (SWI) in the northeastern Arabian Sea (Pakistan continental margin). The results suggested that a small change in the oxygen content at the SWI was sufficient to induce selective degradation that significantly altered most of the studied OM-based proxies. The affected proxies included indicators for sediment alteration (higher plant alkane index, alcohol preservation index, and diol oxidation index), and productivity (cholesterol, dinosterol, and dinoflagellate cysts). In terms of the dinoflagellate cyst

signal, the peridinioid (P) dinoflagellate cysts (produced by heterotrophic taxa) degraded faster at an oxygenated SWI than the gonauylacoid (G) taxa (produced by photoautotrophic taxa) and, as a result, a G/P ratio reflected redox changes at the SWI.

The peridinioid dinoflagellate cyst species clearly demonstrated a higher sensitivity to oxidation; however, it is not known why this was the case. It is quite plausible that differences in the dinosporin composition could explain the selective degradation of the peridinioid dinoflagellate cysts. Thus, the second study in this work investigated whether there are different cyst wall chemistries between the P- and G-dinoflagellate cysts. The results suggested that the gonyaulacoid dinoflagellate cysts have a dinosporin composition that is most likely carbohydrate-based, and possibly even cellulosic. This significantly differs from the results of the peridinioid dinoflagellate cysts, which showed evidence of amide bonds in the dinosporin biomacromolecule. The differences in composition were attributed to the different ecologies (i.e. photoautotrophy vs. heterotrophy) of the groups. This is the first time a difference in dinosporin composition has been demonstrated and suggests that it may be possible to predict the paleoecology of extinct dinoflagellates based on the chemistry of their cysts. Furthermore, it may explain the selective preservation of the different dinoflagellate cyst taxa, as a dinosporin composition with more nitrogen-based functional groups may be more labile than a carbohydrate-based structure.

In light of the observed differences in cyst wall chemistry between the P and G dinoflagellate cyst species, the next study in this work further investigated variability that may be present in the dinosporin composition. However, in this case, variation in dinosporin composition was explored within different species of a single dinoflagellate cyst genus. The Paleocene-Eocene thermal maximum (PETM)-marker genus *Apectodinium* includes several morphologically similar species, which made it an appropriate genus for study. The results showed clear differences in the cyst wall chemistry of the morphospecies, suggesting that dinosporin composition may be taxon specific. Furthermore, the dinosporin composition was shown to be a better indicator of different dinoflagellate cyst species than quantitative morphological characteristics. The high diversity of dinosporin appears to be an intrinsic property of the dinoflagellate cysts and may reflect rapidly changing environmental conditions, such as fluctuations in salinity and temperature, which would have to have occurred prior to and during cyst formation.

Finally, the diagenesis of the dinosporin biomacromolecule was investigated in an analysis of Cretaceous age material. Multiple species of gonyaulacoid dinoflagellate cysts, which was the group that exhibited a carbohydrate-based composition in extant species, were examined from a succession from the Otto Gott claypit (near Sarstedt, Germany). This succession was deposited during the late Hauterivian-early Barremian (Lower Cretaceous) and includes the Hauptblätterton, an organic rich deposit. The analyses showed diagenetic changes such as a reduction in oxygen-containing functional groups, and increases in the aliphatic and aromatic content in the dinosporin macromolecule. These alterations are analogous to changes seen in other resistant biopolymers and indicate that the analyzed dinosporin represents a geomacromolecule.

Essentially, this cumulative work represents the most comprehensive attempt to characterize the composition of dinoflagellate cyst walls to date. The composition of dinosporin and the environmental and taphonomic processes that influence this composition are important to understand both for oceanographic reconstructions, as the cyst wall chemistry can influence the preservation potential of individual species, and for describing the chemical transformations that OM undergoes after deposition on the sea floor.

Zusammenfassung

Ein fundiertes Verständnis der Mechanismen, welche den Abbau und die chemische Umwandlung organischen Materials (OM) nach dessen Ab- und Einlagerung in marinen Sedimenten steuern ist essentiell wichtig für das Verständnis des gesamten Kohlenstoffkreislaufs, da organisches Material ein Hauptreservoir dessen darstellt. Eine Möglichkeit zur Untersuchung jener Einflussfaktoren, welche die Erhaltung von OM steuern, ist die Analyse von Palynomorphen. Bei diesen handelt es sich um organisch-wandige Mikrofossilien. Sie umfassen die Gruppe der Dinoflagellaten-Zysten und sind wichtige Werkzeuge für geowissenschaftliche Analysen. Sie werden zur Exploration fossiler Brennstoffe, zur Biostratigraphie, in der Paläoklimatologie und Paläozeanographie genutzt. Es ist daher, universitär, wie auch industriell, sehr wichtig zu verstehen, welche Prozesse auf Palynomorphe des fossilen Archivs einwirken.

Die vorliegende Arbeit konzentriert sich auf spezifische Palynomorphe, namentlich die organischwandigen Zysten von Dinoflagellaten (Dinozysten). Diese Zysten werden im dormanten Stadium des Dinoflagellaten-Lebenszyklus geschlechtlich produziert und bestehen aus einem nicht-hydrolisierbaren, refraktären Biopolymer, dem bisher nur wenig beschriebenen „Dinosporin“. Auf Grund des hohen Erhaltungspotentials von Dinozysten sind diese umfangreich in sedimentären Archiven erhalten. Sie stellen damit hervorragende Proxies (stellvertretende Anzeiger für vergangene Umweltbedingungen, welche außerhalb des Zeitraums instrumenteller Aufzeichnungen liegen) für Paläoumweltrekonstruktionen dar. Ihre Interpretation wird jedoch dadurch erschwert, dass Dinozysten verschiedener Arten unterschiedlich stark unter Sauerstoffeinfluss abgebaut werden. Die selektive Erhaltung der Dinozysten hat Auswirkungen auf die Interpretation des sedimentären Proxy-Archivs.

Die erste in dieser Arbeit vorgestellte Studie befasst sich daher mit Geschwindigkeit und Ausmaß des selektiven, aeroben Dinozysten-Abbaus. Ferner wurden weitere OM basierte Proxies entlang meter-skaliger, lateraler Sauerstoff-Gradienten an der Sediment-Wasser-Grenzfläche (englisch: SWI von „sediment-water-interface) in frisch abgelagerten Sedimenten des nordöstlichen Arabischen Meeres (pakistanischer Kontinentalrand) untersucht. Die Ergebnisse der Untersuchung legen

nahe, dass bereits kleine Änderungen des Sauerstoffsgehalts an der SWI ausreichten, um selektiven Abbau zu induzieren, welcher die meisten der OM-basierten Proxies veränderte. Verschiedene Proxies wie etwa der höherer-Pflanzen-Alkan-Index, der Alkohol-Erhaltungs-Index, der Diol-Oxidations-Index (Veränderungs-Indizes) als auch Cholesterol, Dinosterol und Dinozysten (Produktivitäts-Indizes) waren betroffen. Bezüglich des von den Dinoflagellaten abgeleiteten Signals bauten sich die peridinoiden (P) Dinozysten (produziert von heterotrophen Taxa) an der sauerstoffreichen SWI schneller ab als die gonauylacoiden (G) Taxa (welche von photoautotrophen Dinoflagellaten produziert werden). Daher spiegelte das G/P Verhältnis Veränderungen der Redox-Bedingungen an SWI wider.

Die peridinoiden Dinozysten-Arten waren gegenüber Oxidation deutlich empfindlicher; eine Erklärung hierfür konnte nicht gefunden werden. Möglicherweise spielen beim selektiven Abbau der peridinoiden Dinozysten Unterschiede der Dinosporin-Zusammensetzung eine Rolle. Dies war Motivation für die zweite Studie der vorliegenden Arbeit, in welcher untersucht wurde, ob sich der Aufbau der Zysten-Wände von P- und G-Dinozysten chemisch unterscheidet. Die Ergebnisse legen nahe, dass sich die gonyaulacoiden Dinozysten aus Dinosporin aufbauen, höchstwahrscheinlich auf Kohlenhydrat- und möglicherweise Zellulosebasis. Sie unterscheiden sich damit deutlich von den peridinoiden Dinozysten, welche Anzeichen von Amid-Bindungen innerhalb der Dinosporin-Biomakromoleküle aufweisen. Die Unterschiede bezüglich des Aufbaus werden auf verschiedene ökologische Präferenzen (z.B. Photoautotrophie im Gegensatz zu Heterotrophie) der verschiedenen Gruppen zurückgeführt. In dieser Arbeit wurde zum ersten Mal ein Unterschied der Dinosporin-Zusammensetzung nachgewiesen. Dies impliziert die Möglichkeit, Paläoökologien ausgestorbener Dinoflagellaten-Arten gegebenenfalls auf der Grundlage ihrer Zysten-Chemie zu rekonstruieren. Ferner besteht die Möglichkeit, dass die unterschiedliche Erhaltung verschiedener Dinoflagellaten-Taxa auf Unterschiede des Dinosporin-Aufbaus zurückgehen, wobei Gruppen mit einem höheren Anteil an Stickstoff-basierten funktionalen Gruppen möglicherweise labiler sind, als solche mit einem höheren Anteil Kohlenhydrat-basierter funktionaler Gruppen.

Die festgestellten Unterschiede zwischen P- und G-Dinozysten bezüglich des chemischen Aufbaus ihrer Zysten-Wände gaben Anlass für die dritte Studie dieser Arbeit. In dieser wurden weitere Unterschiede der Dinosporin-Zusammensetzung untersucht. In

der Studie wurden Unterschiede zwischen verschiedenen Arten innerhalb einer einzigen Gattung untersucht. Die Gattung *Apectodinium* (kennzeichnend für das für das paläozäne-eozäne Temperaturmaximum) umfasst verschiedene, morphologisch ähnliche Arten und eignete sich daher für diese Studie. Die Ergebnisse zeigten deutliche Unterschiede im chemischen Aufbau der Zysten-Wände der verschiedenen Arten. Dies legt nahe, dass die Dinosporin-Zusammensetzung Taxon-spezifisch sein kann. Es konnte ferner gezeigt werden, dass die Zusammensetzung des Dinosporins besser zur Artbeschreibung geeignet ist, als quantitativ morphologische Merkmale. Die vielfältigen Unterschiede des Dinosporins scheinen ein wesentliches Merkmal der Dinozysten zu sein und spiegeln möglicherweise sich schnell verändernde Umweltbedingungen vor und nach der Zystenbildung wider, wie etwa Schwankungen von Salinität und Temperatur.

Abschließend wurde die diagenetische Umwandlung von Dinosporin-Makromolekülen an kreidezeitlichen Proben untersucht. Verschiedene Arten gonyaulacoider Dinozysten (jene Gruppe, welche bei ausgestorbenen Arten einen Kohlenhydrat-basierten Aufbau zeigte) aus einer Ablagerungsabfolge der Otto Gott Tongrube (nahe Sarstedt, Deutschland) wurden untersucht. Die Abfolge wurde während des späten Hauteriviums bis frühen Barremimums (untere Kreide) gebildet und umfasst Hauptblätterton, eine organik-reiche Ablagerung. Die Untersuchung zeigte diagenetische Veränderungen wie zum Beispiel die Reduzierung Sauerstoff-enthaltender funktioneller Gruppen und eine Zunahme des aliphatischen und aromatischen Anteils der Dinosporin-Makromoleküle. Diese Veränderungen sind denen anderer resistenter Biopolymere ähnlich und legen nahe, dass das untersuchte Dinosporin ein Geo-Makromolekül darstellt.

Im Kern stellt diese kumulative Arbeit den zur Zeit umfassendsten Ansatz dar, den Aufbau von Dinozysten-Wänden zu beschreiben. Es ist aus zwei Gründen wichtig, den Aufbau des Dinosporins und die Umwelt- wie auch Fossilisationsprozesse, welche diesen bestimmen, zu verstehen. Zum einen um dadurch ozeanographische Rekonstruktionen zu ermöglichen und zum anderen um die Umwandlung organischen Materials nach seiner Ablagerung am Meeresboden zu beschreiben.

List of Figures

Chapter 6

Chapter 7

Chapter 8

List of Tables

List of Abbreviations

OM	Organic matter
SWI	Sediment-water interface
AOM	Amorphous organic matter
FTIR	Fourier transform infrared spectroscopy
GS-MS	Gas chromatography-mass spectrometry
HPLC-MS	High performance liquid chromatography-mass spectrometry
HPA	Higher plant alkane
API	Alcohol preservation index
DOXI	Diol oxidation index
G/P	Gonyaulacoid/peridinioid
GDGT	Glycerol dibiphytanyl glycerol tetraether
TEX_{86}	Tetraether index of 86 carbon atom tetraethers based on GDGT moieties
TEX_{86}^{L}	Tetraether index of 86 carbon atom tetraethers as a logarithmic function, excluding the crenarchaeol regioisomer
TEX_{86}^{H}	Tetraether index of 86 carbon atom tetraethers as a logarithmic function
OMZ	Oxygen minimum zone
G-cyst	Gonyaulacoid dinoflagellate cyst; produced by photosynthetic taxa
P-cyst	Peridinioid dinoflagellate cyst; produced by heterotrophic taxa
PETM	Paleocene-Eocene thermal maximum

Chapter 1

Introduction

1.1 General introduction

Proxy variables, entities that can represent environmental parameters, are important tools that are used to help explain atmospheric pCO_2 variations over time (Zonneveld et al., 2010). As pCO_2 variations can be related to changes in climate (Berner, 1989; Siegenthaler and Sarmiento, 1993), proxies are therefore important in terms of climatic reconstructions. Proxies for marine productivity can be especially useful as primary productivity draws CO_2 into the surface waters of the ocean and converts it into organic matter (OM) through photosynthesis. A fraction of this OM, termed export production, then settles through the water column, is deposited on the sea floor and is eventually buried. This process is termed the biological pump and serves to link marine productivity, sedimentary carbon burial and climate (Raven and Falkowski, 1999). Thus, marine biota play an important role in the carbon cycle, and proxies derived from these organisms are essential tools in paleoclimate and paleoceanographic work.

After deposition on the sea floor, organic matter, including OM-based proxies, is subjected to a range of different processes that are together called diagenesis (Killops and Killops, 2004). At the end of diagenesis, the remaining OM, which has been highly altered from its original form, is known as kerogen (Crum Brown, 1912; Durand, 1980). Kerogen is difficult to characterize, as it is a complex and heterogeneous mixture of OM and insoluble in many organic solvents (Vandenbroucke and Largeau, 2007). However, discrete and biologically identifiable aspects of kerogen, such as organic microfossils that are composed of non-hydrolyzable biomacromolecules (de Leeuw et al., 2006) and so highly resistant to degradation, can be used to provide information on the chemical transformations that OM has experienced and thus provide information on the composition of marine kerogen.

Dinoflagellates are unicellular protists existing as biflagellate, mainly photosynthetic cells, which thrive in the upper water column of lakes and oceans as well as rivers, ponds and ice (Fensome et al., 1996). The majority of dinoflagellates are found in marine environments (1700 extant species out of about 2000) from the tropics to the

high latitude polar oceans, though the highest concentrations are in coastal temperate waters (Taylor et al., 2008). Some species of dinoflagellates produce an organic-walled resting cyst in preparation for a dormant stage of their life cycle (Head, 1996). These cysts are sensitive indicators for changing upper water column conditions (Marret and Zonneveld, 2003) and are composed of non-hydrolyzable OM (e.g. de Leeuw et al., 2006). Thus, they represent one proxy that can be used both in paleoenvironmental studies (Sluijs et al., 2005) as well as studies on the nature of marine kerogen (de Leeuw et al., 2006; Versteegh et al., 2007).

Dinoflagellate cysts are thus extremely useful microfossils and their sedimentary record is a valuable resource for many disciplines, including paleoclimatology, paleoceanography, biostratigraphy and the petroleum industry. However, it is known that certain species of dinoflagellate cysts are more sensitive to oxidation/aerobic degradation (e.g. Dale, 1976; Hopkins and McCarthy, 2002; Zonneveld et al., 2008). This has implications for the interpretation of the sedimentary dinoflagellate cyst record, as the original assemblage signal, which is used for reconstructions of surface water conditions, may be overprinted. Thus, the sedimentary dinoflagellate cyst signal potentially represents a mixture of upper water column and redox changes (McCarthy et al., 2000; Zonneveld et al., 2007). In order to provide more information on the selective aerobic degradation of dinoflagellate cysts and to attempt to explain the causes for it, the following themes were investigated.

1.2 Scientific objectives

Essentially, this thesis is split into two topics. The first evaluates the effects of lateral oxygen gradients at the sediment-water interface on selected OM-based proxies, including dinoflagellate cysts. The second part of this thesis investigates the composition of dinosporin, the least studied of the resistant biomacromolecules (de Leeuw et al., 2006), through the use of micro-Fourier transform infrared (FTIR) spectroscopy. In order to utilize the full potential of dinoflagellate cysts in providing information on OM preservation, it is essential to understand their initial composition and the factors that can affect this composition. Some of the major factors were evaluated in three separate, but related studies.

The specific questions addressed in this work are:

(1) Does selective aerobic degradation show significant overprinting of OM-based proxy signals along a short spatial scale and with small changes in bottom water oxygen content at the sediment-water interface?
(2) What, if any, are the compositional differences in the wall chemistry of dinoflagellate cysts derived from oxidation sensitive and resistant dinoflagellate cysts?
(3) Can some of other factors that may influence the cyst wall chemistry be identified?
(4) Are there any chemical changes in the dinoflagellate cyst walls that can be specifically attributed to diagenetic processes?

1.3 Outline

The next chapter in this thesis (**Chapter 2**) presents a brief discussion on the global carbon cycle and diagenesis. Particular emphasis is placed on processes affecting organic matter (OM) after deposition and its incorporation into marine kerogen. Finally, there is a short discussion on resistant biomacromolecules with a focus on the uncertainties regarding their initial structures. The following chapter (**Chapter 3**) discusses some aspects of dinoflagellates including brief descriptions of their biology and ecology. Additionally, discussions on cyst formation, morphology, applications and preservation are presented.

As this thesis is an integration of palynology and geochemistry, various methodologies and analytical devices were employed. Therefore, **Chapter 4** gives a basic explantion about the primary analytical techniques that were used. These methods include palynological procedures, and micro-Fourier transform infrared (FTIR) spectroscopy. Furthermore, gas chromatography-mass spectrometry (GC-MS) and high performance liquid chromatography-mass spectrometry (HPLC-MS) were particularly important for the biomarker work described in Chapter 5 and so are described briefly.

Chapter 5 is entitled “The effect of meter-scale lateral oxygen gradients at the sediment-water interface on selected organic matter based alteration, productivity, and temperature proxies” and has been submitted to *Biogeosciences*. It is a study of the effects of changing bottom water concentrations on the preservation of OM-based

proxies. The investigated proxies were divided into 3 groups: sediment alteration (higher plant alkane index [HPA], alcohol preservation index [API], alkyldiol oxidation index [DOXI]), export production (indices based on phytol, cholesterol, dinosterol and peridinioid and gonyaulacoid dinoflagellate cyst ratio [G/P]), and temperature (glycerol dibiphytanyl glycerol based indices [TEX_{86}, TEX_{86}^{L}, and TEX_{86}^{H}]). The majority of the proxies, including the dinoflagellate cysts, showed clear effects of selective aerobic degradation. However, the temperature proxies and the productivity proxy derived from phytol were more strongly influenced by local sedimentary factors.

Chapter 6 is the first attempt to elucidate possible reasons for the observed species-specific sensitivity to aerobic degradation in dinoflagellate cysts. It is titled "Differences in composition between organic-walled resting cysts produced by autotrophic and heterotrophic dinoflagellate taxa" and is a manuscript in preparation. Gonyaulacoid dinoflagellate cysts, which are resistant to oxidation, are produced by photosynthetic dinoflagellates and were shown to have a dinosporin composition that is carbohydrate-based, and possibly even cellulosic. This significantly differed from the oxidation-sensitive peridinioid dinoflagellate cysts, produced by heterotrophic taxa, which showed evidence of nitrogen-containing functional groups in the cyst wall. These differences in composition are probably due to the different ecologies (i.e. photoautotrophy vs. heterotrophy) of the dinoflagellates that produce the cyst types, and represents the first time differences in the cyst biomacromolecule has been demonstrated between these two groups. The variations in the cyst wall composition are further speculated to account for the difference in lability between the gonyaulacoid and peridinioid dinoflagellate cysts.

The **Chapter 7** manuscript, "The composition and diversity of dinosporin in species of the *Apectodinium* complex (Dinoflagellata)", has been submitted to *Review of Palaeobotany and Palynology*. It investigated the structure and compositional variability of dinosporin derived from the late Paleocene dinoflagellate cyst genus *Apectodinium.* This genus includes morphologically similar species, and the geochemical results showed a high diversity of dinosporin composition, suggesting that it may be taxon specific. The micro-FTIR analysis was shown to be a better technique for separating the dinoflagellate cyst species of this genus than quantitative morphometrics. We proposed that the high diversity in the cyst wall biomacromolecule is an intrinsic property of the dinoflagellate

cysts and may be a response to rapidly changing environmental conditions, such as fluctuations in salinity and temperature.

In **Chapter 8**, "Diagenetic changes in dinosporin composition in Early Cretaceous gonyaulacoid dinoflagellate cysts" (in preparation), changes in the dinoflagellate cyst wall chemistry as a result of diagenesis were investigated. Gonyaulacoid dinoflagellate cysts, shown to have a carbohydrate-based composition, were examined in a succession from the Otto Gott claypit (near Sarstedt, Germany). This succession was deposited during the late Hauterivian-early Barremian and includes the Hauptblätterton, an organic rich horizon. By comparing the dinosporin composition of numerous gonyaulacoid cyst species from this interval to modern gonyaulacoid cysts, we were able to describe some possible diagenetic changes that had occurred in the dinosporin structure. These included a reduction in ether bonds and other oxygen-containing functional groups, and increases in carbon-carbon and carbon-hydrogen bonds, which correspond to increases in the aliphatic and aromatic content of the cyst wall macromolecule.

Finally, **Chapter 9** presents the main conclusions of this thesis and discusses some remaining open questions. Furthermore, it provides some suggestions for subsequent research regarding the elucidation of dinoflagellate cyst wall chemistry.

References

Berner, R.A., 1989. Biogeochemical cycles of carbon and sulfur and their effect on atmospheric oxygen over Phanerozoic time. *Palaeogeography, Palaeoclimatology, Palaeoecology*, 73, 97-122.

Crum Brown, 1912. In: Carruthers, R.G., Caldwell, W., Steuart, D.R. *The oil shales of the Lothians*. HMSO, Edinburgh. 201 pp.

de Leeuw, J.W., Versteegh, G.J.M., van Bergen, P.F., 2006. Biomacromolecules of algae and plants and their fossil analogues. *Plant Ecology*, 182, 209-233.

Durand, B., 1980. Sedimentary organic matter and kerogen: Definition and quantitative importance of kerogen. In: Durand, B. (Ed.), *Kerogen, Insoluble Organic Matter from Sedimentary Rocks.* Editions Technip, Paris. pp 13-34.

Dale, B., 1976. Cyst formation, sedimentation, and preservation: factors affecting dinoflagellate assemblages in recent sediments from Trondheimsfjord, Norway. *Review of Palaeobotany and Palynology*, 22, 39-60.

Fensome, R.A., Riding, J.B., Taylor, F.J.R., 1996. Dinoflagellates. In: Jansonius, J., McGregor, D.C. (Eds.), *Palynology: principles and applications*. American Association of Stratigraphic Palynologists Foundation, Dallas, pp. 107-169.

Head, M.J., 1996. Modern dinoflagellate cysts and their biological affinities. In: Jansonius, J., McGregor, D.C. (Eds.), Palynology: Principles and Applications. American Association of Stratigraphic Palynologists Foundation, Dallas, Texas, pp. 1197-1248.

Hopkins, J.A., McCarthy, F.M.G., 2002. Post-depositional palynomorph degradation in Quaternary shelf sediments: a laboratory experiment studying the effects of progressive oxidation. *Palynology*, 26, 167-184.

Killops, S.D., Killops, V.J., 2004. *An Introduction to Organic Geochemistry*. Wiley-Blackwell, 408 pp.

Marret, F., Zonneveld, K.A.F., 2003. Atlas of modern organic-walled dinoflagellate cyst distribution. *Marine Micropaleontology*, 125, 1-200.

McCarthy, F.M.G., Gostlin, K.E., Mudie, P.J., Scott, D.B., 2000. Synchronous palynological changes in early Pleistocene sediments off New Jersey and Iberia, and a possible paleoceanographic explanation. *Palynology*, 24, 63-77.

Raven, J.A., Falkowski, P.G., 1999. Oceanic sinks for atmospheric CO_2. *Plant, Cell and Environment*, 22, 741-755.

Siegenthaler, U., Sarmiento, J.L., 1993. Atmospheric carbon dioxide and the ocean. *Nature*, 365, 119-125.

Sluijs, A., Pross, J., Brinkhuis, H., 2005. From greenhouse to icehouse; organic-walled dinoflagellate cysts as paleoenvironmental indicators in the Paleogene. Earth-Science Reviews, 68, 281-315.

Taylor, F.J.R., Hoppenrath, M., Saldarriaga, J.F., 2008. Dinoflagellate diversity and distribution. *Biodiversity and Conservation*, 17, 407-418.

Vandenbroucke, M., Largeau, C, 2007. Kerogen origin, evolution and structure. *Organic Geochemistry*, 38, 719-833.

Versteegh, G.J.M., Blokker, P., Marshall, C.P., Pross, J., 2007. Macromolecular composition of the dinoflagellate cyst *Thalassiphora pelagica* (Oligocene, SW Germany). *Organic Geochemistry*, 38, 1643-1656.

Zonneveld, K.A.F., Bockelmann, F., Holzwarth, U., 2007. Selective preservation of organic-walled dinoflagellate cysts as a tool to quantify past net primary production and bottom water oxygen concentrations. *Marine Geology*, 237, 109-126.

Zonneveld, K.A.F., Versteegh, G.J.M., Kodrans-Nsiah, M., 2008. Preservation and organic chemistry of Late Cenozoic organic-walled dinoflagellate cysts: A review, *Marine Micropaleontology*, 68, 179-197.

Zonneveld, K.A.F., Versteegh, G.J.M., Kasten, S., Eglinton, T.I., Emeis, K.C., Huguet, C., Koch, B.P., de Lange, G.J., de Leeuw, J.W., Middelburg, J.J., Mollenhauer, G., Prahl, F.G., Rethemeyer, J., Wakeham, S.G., 2010. Selective preservation of organic matter in marine environments; processes and impact on the sedimentary record. *Biogeosciences*, 7 483-511.

Chapter 2

The carbon cycle and organic matter preservation

2.1 Global carbon cycle

A comprehensive understanding of the carbon cycle is important for several reasons. Carbon is a universal component in living things so that understanding the flow of carbon approximates the flow of living matter in the biosphere. Carbon dioxide and methane, common forms of carbon, are two of the most potent greenhouse gases. Though methane is 25 times more potent (Schlesinger, 2005), CO_2 has received the most attention for several reasons. It is predicted to contribute over half of the increase in radiative forcing during the next century, has a long residence time in the atmosphere-ocean system, and the major cause of its increase is the burning of fossil fuels, which is something that can be regulated (Reilly et al., 1999). The study of the carbon cycle involves the assessment of CO_2 in Earth's atmosphere in relation to natural processes that add or remove CO_2 to and from that reservoir. Thus, knowledge of past pCO_2 changes can provide information on climatic changes.

Carbon dioxide concentrations are controlled by various processes that add/remove it to/from the atmosphere, and most of these processes are cyclical (Schlesinger, 2005). For example, photosynthesis removes CO_2 through the reaction:

$$(1) \qquad CO_2 + H_2O \rightarrow CH_2O + O_2$$

which is, in turn, compensated by the return of CO_2 through O_2 consumption via OM degradation:

$$(2) \qquad CH_2O + O_2 \rightarrow CO_2 + H_2O.$$

The global carbon cycle consists of many of these balanced processes that take place at different rates and timescales (Berner, 2004), which together give rise to the overall global biogeochemical carbon cycle.

2.1.1 Abiotic carbon cycle

This aspect of the global carbon cycle (Fig. 2.1a) comprises processes that would occur even without life on Earth. One of the most basic is the carbonate-silicate cycle. This is driven by the reaction of atmospheric CO_2 with the Earth's crust, causing the chemical weathering of rocks. CO_2 is transferred to the oceans as bicarbonate (HCO_3^-). This bicarbonate is removed from seawater through calcium carbonate ($CaCO_3$) deposition. Through the subduction of oceanic crust, this deposited material is returned to the atmosphere via volcanic emanations. The amount of carbon moving through this subcycle is relatively small (Schlesinger, 2005). Another subcycle involves the dissolution of CO_2 in water through the reaction:

$$(3) \qquad CO_2 + H_2O \rightarrow H^+ + HCO_3^- \rightarrow H_2CO_3.$$

As the pCO_2 rises, more CO_2 is dissolved in the surface waters of the oceans so that atmospheric CO_2 is regulated by the chemical equilibrium of dissolved CO_2, bicarbonate and carbonate in seawater. Thus, the primary control on atmospheric CO_2 concentrations is carbon sequestration and storage in the ocean (Berner, 1982; Siegenthaler and Sarmiento, 1993). The net uptake of CO_2 by the oceans is about 2 Pg C yr^{-1} (Sabine et al, 2004), which is about 20 times more than consumption by rock weathering (Andrews and Schlesinger, 2001). The total uptake by the oceans is determined by the downward mixing of surface waters into the deep sea via thermohaline circulation (Broecker, 1997). However, the rate at which this equilibrium leads to uptake or release of carbon is a slow process (Schlesinger, 2005).

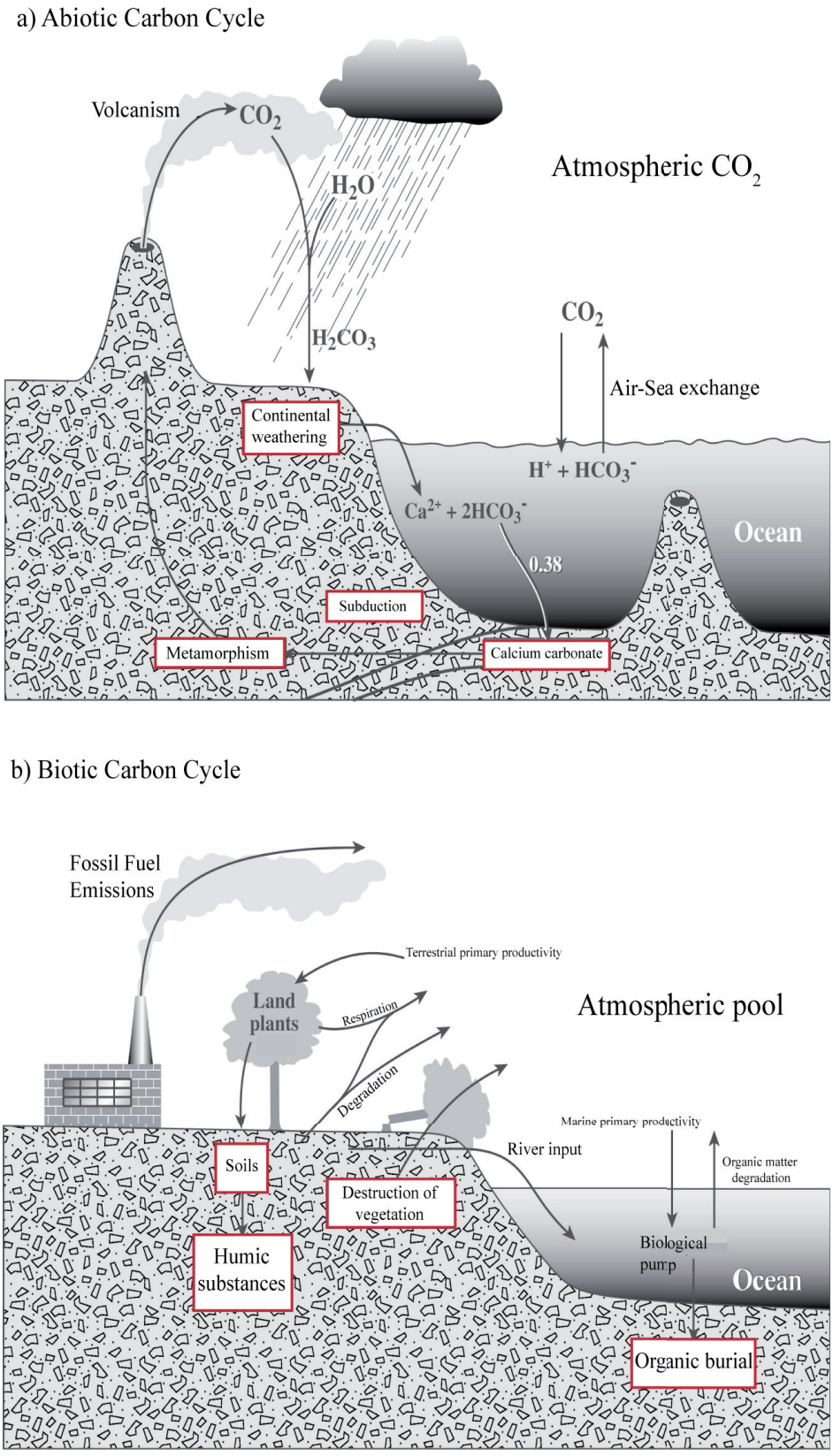

Figure 2.1: A simplified scheme depicting the abiotic (a) and biotic (b) subcycles within the global carbon cycle. Modified from Schlesinger (2005).

2.1.2 Biotic carbon cycle

This facet of the global carbon cycle (Fig. 2.1b) is completely dependent on the presence of life, as photosynthesis [Eq. (1)] and respiration [Eq. (2)] facilitate the movement of CO_2. Photosynthetic organisms remove CO_2 from the atmosphere and produce organic matter (OM) [Eq. (1)], which is referred to as primary production. The two main groups of primary producers are algae and higher plants. As solar energy is the catalyst for photosynthesis, life for these organisms is therefore restricted to the photic zone, i.e. land surfaces and the upper hundred meters of the water column. This represents a direct link between the ocean and the atmosphere, so that proxies analyzed from the sediment column that reflect upper water column conditions at their time of production also provide information on climate change. The sequestration of organic carbon into marine sediments represents the major global sink for organic carbon (Berner, 1982) due to higher erosion, degradation and weathering on land. More than 90% of organic carbon burial occurs in deltaic, continental shelf and upper slope sediments, which indicates that these margins are the largest marine sink (Berner, 1989; Hedges and Keil, 1995). The biotic transformation of CO_2 into OM and subsequent transport out of the photic zone, called export production, is a process referred to as the biological pump (Raven and Falkowski, 1999). The biological pump serves to facilitate the movement of OM to the sea floor where it can be buried and stored.

2.2 Diagenetic processes and kerogen

As OM settles through the water column, is deposited on the sea floor and is buried, it is subjected to processes collectively called diagenesis. Diagenesis takes place under conditions of relatively low temperature and pressure. As material is buried deeper within the sediment column, the sediments themselves undergo compaction and consolidation. Simultaneously, a decrease in water content and an increase in temperature occur (thermal maturation). These processes, along with biotic and abiotic degradation, transform characterizable OM into a heterogeneous complex termed kerogen (Fig. 2.2). Kerogen is specifically defined as an insoluble and non-hydrolyzable heterogeneous mixture of complex bio- and geomacromolecules (Durand, 1980). Kerogen is considered one of the most recalcitrant organic materials on Earth (Hedges and Keil, 1995) and is also the most abundant. More than 99.9% of the carbon present in Earth's crust is found in sedimentary rocks with about 20% representing organic carbon

and the bulk (> 90%) of that present as kerogen (Berner, 1989). As this thesis is limited to the marine realm, the following discussion refers to processes involved in the degradation of OM in the ocean.

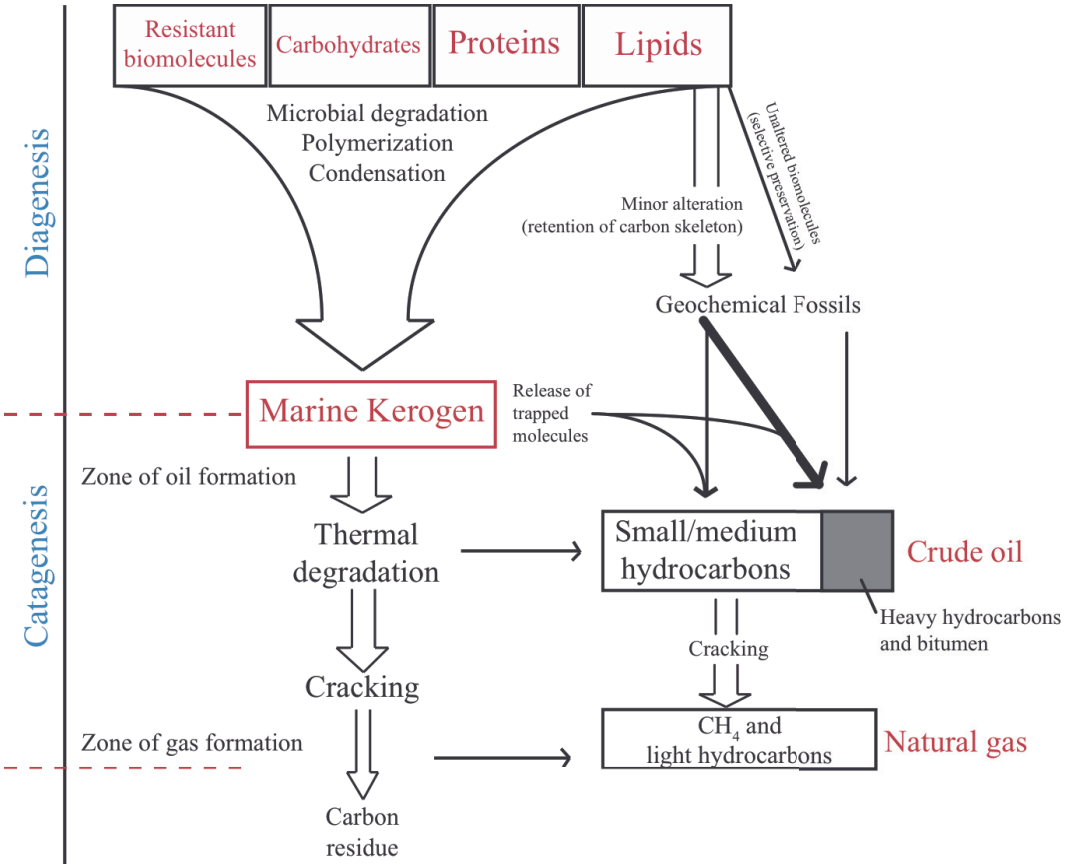

Figure 2.2: Simplified scheme depicting processes affecting OM within the sediment column. Modified and redrawn from Tissot and Welte (1984).

2.2.1 Early diagenesis (syn-depositional)

On average, only 0.1-2.0% of the total OM produced from primary production will end up buried in marine sediments (e.g. Sarnthein et al., 1988; Berner, 1989; Hedges and Keil, 1995) as the vast majority is recycled within the water column (e.g. Wakeham et al., 2002). After this small fraction of OM is deposited on the sea floor, it undergoes extensive biological, physical and chemical alterations. In general, the quality and quantity of available OM components influences the rate of OM degradation (Lee, 1992; Henrichs, 1992), but the extent to which a specific compound is preserved can depend upon different processes (Hedges and Keil, 1995). A dominant proportion of OM is

degraded following a characteristic pathway of oxidation reactions, including the reduction of O_2, NO_3^-, MnO_2, Fe_2O_3, and SO_4^{2-} (Fig. 2.3), depending on sequential redox horizons (Froelich et al., 1979; Bender and Heggie, 1984).

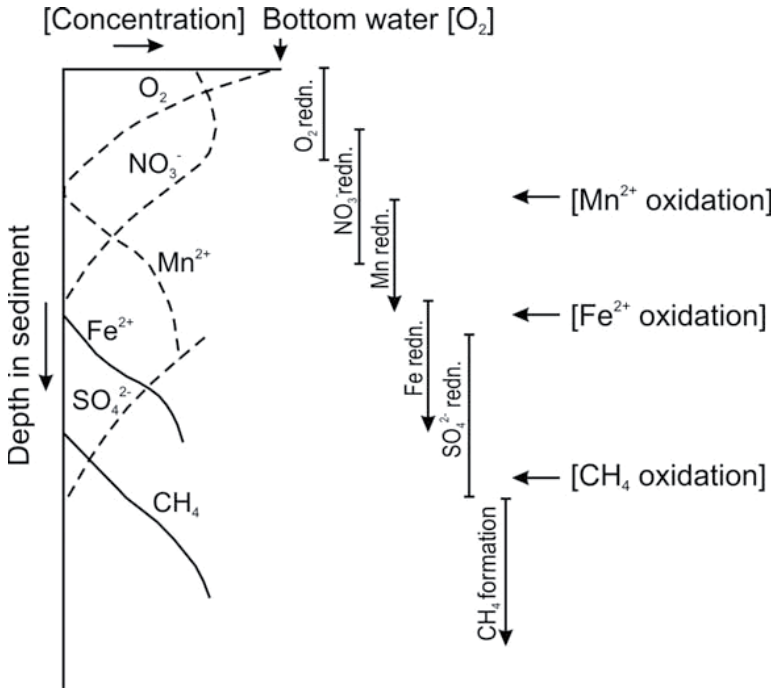

Figure 2.3: Schematic representation of redox horizons for early organic matter degradation as measured from sediment pore water. From Bockelmann (2007).

O_2 is described as the most relevant oxidant in continental margin settings (Hartnett et al., 1998; Hulthe et al., 1998; Hedges et al., 1999). On a global scale, aerobic decomposition is the major process of OM degradation, as anoxic processes, such as sulfate reduction, consume only 10% as much OM (Henrichs and Reeburgh, 1987). Therefore, one of the primary controls on OM preservation is the oxygen concentration in bottom waters and pore waters (Paropkari et al. 1992; 1993; Keil et al., 1994a; Cowie et al., 1995; 1999; van der Weijden et al., 1999) and the O_2 exposure time (Hartnett et al., 1998). Other factors can also influence the extent of preserved OM. These include bioturbation and physical mixing (Arzayus and Canuel, 2004), which essentially increase the O_2 exposure time, as well as sediment accumulation rate, adsorption (Hedges and Keil, 1995), metal oxide presence (Aller, 1994; Hedges and Keil, 1995), lateral transport (Arthur et al., 1998; Mollenhauer et al., 2007; 2008), and winnowing (Pedersen et al., 1992).

Aerobic OM degradation is known to be a selective process (e.g. Hulthe et al., 1998; Hedges et al., 1999) with a large proportion occurring after initial deposition at the sediment-water interface (e.g. Canuel and Martens, 1996). Lipid biomarkers, also called chemical or molecular fossils, are biosynthesized compounds derived from specific sources (Killops and Killops, 2004), while palynomorphs are discrete particles of OM that can be reliably linked to distinct species. Both groups of proxies provide (paleo)-environmental information, but have also demonstrated selective degradation (e.g. Zonneveld et al., 2010). Examples where this has been documented include the Madeira F1 turbidite (Zonneveld et al., 1997; Hoefs et al., 2002), the Mediterranean S1 sapropel (Zonneveld et al., 2001; Versteegh et al., 2010) and along the oxygen minimum zone (OMZ) of the Arabian Sea (Sinninghe Damsté et al., 2002). Chapter 5 presents a specific case along the northeastern Arabian Sea OMZ where OM-based proxies show a highly selective sensitivity to short O_2 exposure times and small lateral oxygen gradients at the sediment-water interface.

2.2.2 Kerogen formation and composition

At the end of diagenesis, the fraction of OM that has escaped degradation is called kerogen (Fig. 2.2). The composition of kerogen depends on the OM that evades degradation and remains in marine sediments, so that kerogen is mainly derived from the biota of the upper water column (e.g. Vandenbroucke and Largeau, 2007). However, as only an extremely small fraction of OM from the upper water column (0.1-2 %) is buried in marine sediments, the chemical composition of kerogen is quite different from that of living organisms (Vandenbroucke and Largeau, 2007). The kerogen composition also depends on the biochemical alteration processes that have taken place (see Section 2.2.1) so that regions with different source organisms and depositional conditions will produce kerogens with different compositions.

There are a number of different ways that particulate and molecular aspects of kerogen can be preserved. They include (1) the selective preservation pathway, which is based on the degradability of the individual OM components (e.g. Tegelaar et al., 1989; 1991; Briggs, 1999), (2) the condensation pathway where oxidative polymerization (e.g. Tissot and Welte, 1984; Versteegh et al., 2004; Gupta et al., 2006) or natural sulfurization (e.g. Sinninghe Damsté et al., 1989; van Dongen et al., 2003) converts the more labile aspects of the OM into a more refractory form and (3) the physical protection pathway

whereby adsorption or encapsulation of labile OM makes it unreachable for degradative enzymes (e.g. Keil et al., 1994b; Hedges and Keil, 1995; Mayer, 1994a, b; Bergamaschi et al., 1997; Ransom et al., 1998; Keil and Cowie, 1999).

All of the diagenetic processes compounded with the initial composition of the OM produce a heterogeneous and complex macromolecular structure (Fig. 2.4). Kerogen is notoriously difficult to analyze due to the fact that it is insoluble in most organic solvents (Durand, 1980). Identifiable aspects of kerogen include discrete organic-walled microfossils called palynomorphs, which derive from plants or animals in the terrestrial or marine realm and encompass acritarchs, dinoflagellate cysts, chitinozoa, fungal and plant spores, pollen grains, green/blue algae, and scolecodonts (Jansonius and McGregor, 1996). The term palynomorph does not include other microfossil elements like wood fragments, plant cuticles and amorphous organic matter (AOM). This entire kerogen fraction, containing palynomorphs and other microfossil elements, is called phytoclasts (Bostick, 1971). The palynomorph fraction of kerogen in particular is important because it represents biological sources at a low taxonomic level, thus linking biology with geology.

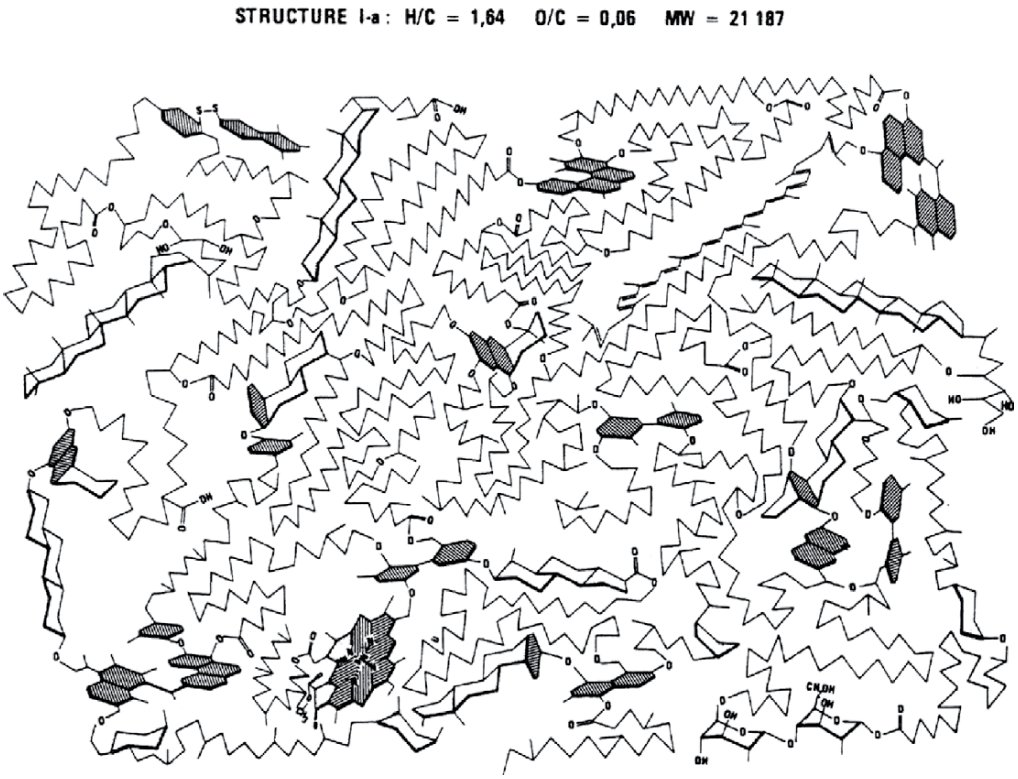

Figure 2.4: Example of the structure of an immature kerogen (Type I; Green River shale, UT, USA) to illustrate its complex nature. From Behar and Vandenbroucke (1987).

2.3 Resistant biomacromolecules

While most plants and algae have limited preservation potential, some have resistant biomacromolecules as part of their cell walls or produce fossilizable components during their life cycle (e.g. van Bergen et al., 1995; 2004). As a result, there is a rich fossil record of palynomorphs from higher plants and algae. These include non-hydrolyzable algal walls, pollen, spores, and dinoflagellate cysts. From studies of extant organisms, there seem to be two biochemical pathways that lead to the production of resistant biomacromolecules: the acetate-malate pathway (leading to algaenan, cutin/cutan) and the phenylpropanoid pathway (leading to sporopollenin, dinosporin) (de Leeuw et al., 2006).

There are many problems associated with analyzing the structure of these macromolecules after they are incorporated into the sedimentary record (Versteegh and Blokker, 2004). First, the isolation of sufficient quantities of pure, monotypic samples is difficult and time-consuming (as they must, in most cases, be individually picked), and contamination by other OM components can lead to misinterpretation (e.g. Blokker et al., 2000). Second, there may a dearth of recent counterparts for comparison, as is the case for acritarchs and extinct taxa (Versteegh and Blokker, 2004). Finally, diagenetic processes may have transformed the original biomacromolecule into a more stable geomacromolecule, which can obscure the interpretation of the original structure. These processes include natural sulfurization of biomolecules (e.g. Sinninghe Damsté et al., 1989; Sinninghe Damsté and de Leeuw, 1990; Kok et al., 2000; Versteegh et al., 2007) or oxidative polymerization (e.g. Stankiewicz et al., 2000; Kuypers et al., 2002; Versteegh et al., 2004; Gupta et al., 2006). The latter could account for the relatively higher contribution of aliphatic components generally found in fossil biopolymers compared to extant organisms, and originate from the migration of lipids from within (i.e. from cell contents) or external (i.e. from the sediment) to the microfossil. Evidence for oxidative polymerization is not limited to palynomorphs; it is found in fossilized algal (Versteegh et al., 2004), archaeal (Kuypers et al., 2002), arthropod (e.g. Briggs et al., 1995; Stankiewicz et al., 2000) and plant cuticle (Mösle et al., 1997; 1998; Collinson et al., 1998) biopolymers as well. In the case of algal- and plant-derived biomacromolecules, discussed briefly in the following sections, the exact original structure and transformation pathways are still incompletely understood. This paucity of data, especially involving the dinoflagellate cysts, led directly to one of the major aims of this work.

2.3.1 Cutin/cutan

Cutan is a non-hydrolyzable aliphatic biopolymer present in well-preserved fossil cuticles of higher plants and is distinct from cutin, the biopolyester present in plant cuticles (de Leeuw and Largeau, 1993). There has been an ongoing debate about how extensive the presence of cutan is in living plant material and whether it is primarily a diagenetically produced geomacromolecule (e.g. Mösle et al., 1997; 1998; Collinson et al., 1998). In most species, it seems to be formed diagenetically from either cutin (Tegelaar et al., 1991) or cuticular waxes (Collinson et al., 1998). However, it is a significant component in drought-adapted CAM plants, which led to the hypothesis that it is produced as an adaptation to drought conditions (Boom et al., 2005).

2.3.2 Sporopollenin

This macromolecule is the extremely resistant and non-hydrolyzable component of pollen and spore walls (Brooks and Shaw, 1978). It can be preserved for millions of years and resist high temperature metamorphism (Bernard et al., 2007; 2009). It is currently thought that sporopollenin consists of several types depending on whether the parent organism is a fern, gymnosperm or angiosperm, although composition variations also occur within the same pollen or spore wall, depending upon the exine layer examined (e.g. de Leeuw et al., 2006). This suggests that sporopollenin is actually a suite of chemically different biopolymers. The first type of sporopollenin is made up of oxygenated aromatic building blocks derived from *para*-coumaric and ferulic acids (Fig. 2.5), while the second type is aliphatic (e.g. Domínguez et al., 1999); this structure is currently unknown. The phenolic components in *para*-coumaric and ferulic acids absorb UV-B radiation (Rozema et al., 2001a, b) and sporopollenin chemistry is currently being investigated as a possible proxy for stratospheric ozone levels (e.g. Blokker et al., 2006; Watson et al., 2007).

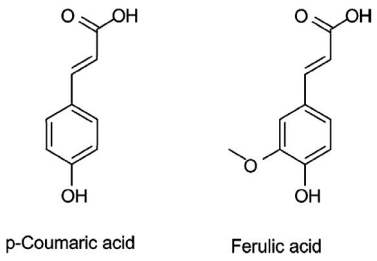

Figure 2.5: Building blocks of sporopollenin. From Watson et al. (2007).

Despite the pre-dominantly aromatic sporopollenin signal in extant species, almost all fossil sporopollenins that have been analyzed demonstrate a composition that is a mixture of aliphatic and aromatic moieties (van Bergen et al., 1993; 2004). Degradation

experiments (e.g. Yule et al., 2000) have shown that sporopollenin first exhibits a relative increase in aliphatic content with increasing thermal degradation and then becomes dominated by aromatic components. Therefore, these structural changes represent the effects of taphonomic processes.

2.3.3 Algaenan

Algaenans are the best studied of the resistant biomacromolecules and are hydrolysis resistant aliphatic compounds (Tegelaar et al., 1989) with three generally proposed structures (Versteegh and Blokker, 2004). The first is common in most Chlorophyceae and consists of building blocks of linear, even-numbered carbon chains (C_{22-34}) with ether and ester bond cross-linkages (Fig. 2.6a; Blokker et al., 1998; 1999). The second type, found in the chlorophyte *Botryococcus braunii*, consists of monomers of unsaturated aliphatic aldehydes and hydrocarbons cross-linked by acetal and ester bonds (Fig. 2.6b; e.g. Simpson et al., 2003). The third type is produced by Eustigmatophyta and composed of mid-chain, long chain (C_{28-36}) diols and alkenols (C_{30-32}) and odd (C_{25-29}) unsaturated hydrocarbons, cross-linked by ether bonds (Fig. 2.6c; e.g. Gelin et al., 1997). Algaenans have mainly been found in fresh water species of Chlorophyta (Versteegh and Blokker, 2004), although there may be some bias as fresh water algae species are better studied than marine ones. Fossil algaenans appear

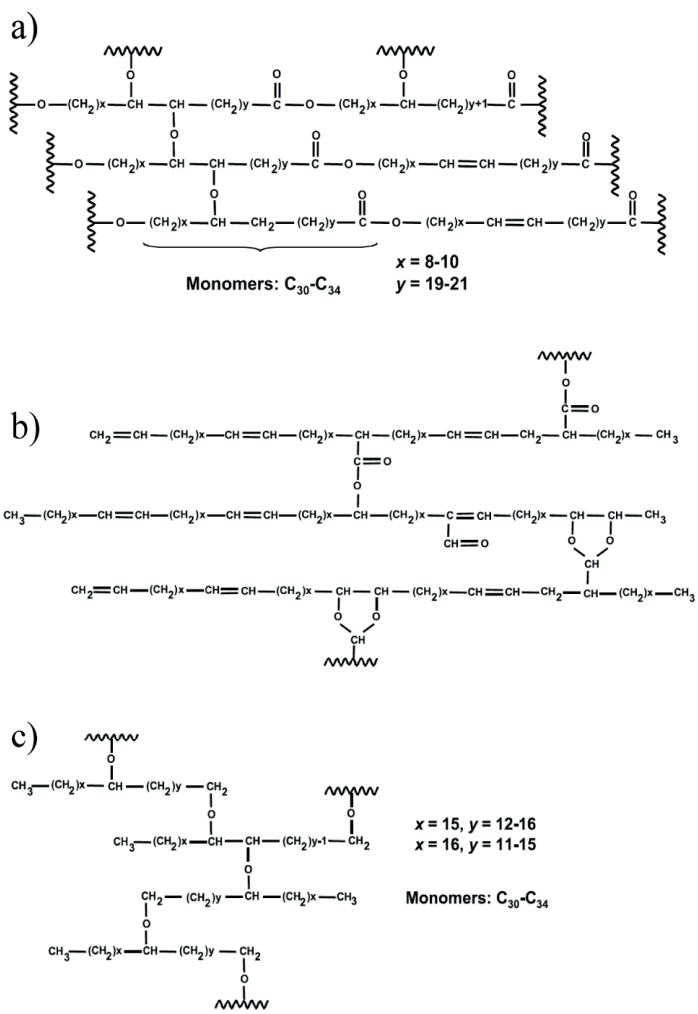

Figure 2.6: Structures of the aliphatic biomacromolecule algaenan (from Versteegh and Blokker, 2004).

to bear little resemblance to modern representatives, with the exception of those from Chlorophyta (Versteegh and Blokker, 2004). This is a result of diagenetic processes such as oxidative polymerization altering the original biopolymer structure, which can complicate the interpretation/classification of algaenan-containing fossils (e.g. Arouri et al., 1999; 2000; Blokker et al., 2001).

2.3.4 Dinosporin

This thesis primarily focuses on this biomacromolecule, which is also the least studied. "Dinosporin" is the term for the resistant biopolymer comprising dinoflagellate resting cysts (Fensome et al., 1993). This microfossil group has a long sedimentary record, having appeared 245-208 million years ago, and evolved a high diversity of forms and life strategies (Hackett et al., 2004; Chapter 3 and references therein). Algaenan has been demonstrated to be a component in the motile cell wall of one species of Dinophyta (*Gymnodinium cantenatum*; Gelin et al., 1999), although studies of dinosporin suggest that it is a significantly different biopolymer from algaenan (Kokinos et al., 1998; de Leeuw et al., 2006; Versteegh et al., 2007; Versteegh et al., in press; Chapters 5-7). Dinosporin has also previously been called sporopollenin-like (Fensome et al., 1993) although more recent studies dispute this (e.g. Kokinos et al., 1998; Versteegh et al., in press; Chapter 7).

Previous research had suggested that dinosporin was a primarily aromatic compound with isoprenoid long chain aliphatics derived from tocopherol (Kokinos et al., 1998). However, recent research suggests that dinosporin does not contain significant amounts of long chain aliphatics, nor is it primarily aromatic, but that it is carbohydrate-based (Versteegh et al., in press). The studies presented in this thesis concur that a carbohydrate-based composition for dinosporin derived from autotrophic dinoflagellates is very probable, and that a cellulosic dinosporin is even possible. However, dinosporin from heterotrophic dinoflagellates differs dramatically, mainly due to evidence for amide bonds (Chapter 6). Furthermore, dinosporin seems to be taxon specific as species within the same genus exhibit different compositions (Chapter 7), so that dinosporin may be more accurately thought of as a suite of biopolymers. Finally, as with all studies of biomacromolecules, diagenetic alteration of the original biomacromolecule changes the composition as some functional groups are removed and new structures are formed, which is illustrated for dinosporin in Chapter 8.

References

Aller, R.C., 1994. Bioturbation and remineralization of sedimentary organic matter: effects of redox oscillation. *Chemical Geology*, 114, 331-345.

Andrews, J.A., Schlesinger, W.H., 2001. Soil CO_2 dynamics, acidification, and chemical weathering in a temperate forest with experimental CO_2 enrichment. *Global Biogeochemical Cycles*, 15, 149-162.

Arouri, K., Greenwood, P.F., Walter, M.R., 1999. A possible chlorophycean affinity of some Neoprotoerozoic acritarchs. *Organic Geochemistry*, 30, 1323-1337.

Arouri, K., Greenwood, P.F., Walter, M.R., 2000. Biological affinities of Neoproterozoic acritarchs from Australia: microscopic and cheical characterization. Organic Geochemistry, 31, 75-89.

Arthur, M.A., Dean, W.E., Laarkamp, K., 1998. Organic carbon accumulation and preservation in surface sediments of the Peru margin. *Chemical Geology*, 152, 273-286.

Arzayus, K.M., Canuel, E.A., 2004. Organic matter degradation in sediments of the York River estuary: Effects of biological vs. physical mixing. *Geochimica et Cosmochimica Acta*, 69, 455-463.

Behar, F., Vandenbroucke, M., 1987. Chemical modeling of kerogens. *Organic Geochemistry*, 11, 15-24.

Bender, M.L., Heggie, D.T., 1984. Fate of organic carbon reaching the sea floor: a status report. *Geochimica et Cosmochimica Acta*, 48, 977-986.

Bergamaschi, B.A., Tsamakis, E., Keil, R.G., Eglinton, T.I., Montluçon, D.B., Hedges, J.I., 1997. The effect of grain size and surface area on organic matter, lignin and carbohydrate concentrations, and molecular composition in Peru Margin sediments. *Geochimica et Cosmochimica Acta*, 61, 1247-1260.

Bernard, S., Bezerara, K., Beyssac, O., Menguy, N., Guyot, F., Brown, G.E. Jr., Goffé, B., 2007. Exceptional preservation of fossil plant spores in high-pressure metamorphic rocks. *Earth and Planetary Science Letters*, 262, 257-272.

Bernard, S., Benzerara, K., Beyssac, O., Brown, G.E., Stamm, L.G., Duringer, P., 2009. Ultrastructural and chemical study of modern and fossil sporoderms by Scanning Transmission C-ray Microscopy (STXM). *Review of Palaeobotany and Palynology*, 156, 248-261.

Berner, R.A., 1982. Burial of organic carbon and pyrite sulfur in the modern ocean: Its geochemical and environmental significance. *American Journal of Science*, 282, 451-473.

Berner, R.A., 1989. Biogeochemical cycles of carbon and sulfur and their effect on atmospheric oxygen over Phanerozoic time. *Palaeogeography, Palaeoclimatology, Palaeoecology*, 73, 97-122.

Berner, R.A., 2004. *The Phanerozoic Carbon Cycle: CO_2 and O_2*. Oxford University Press, New York, 150 pp.

Blokker, P., Schouten, S., van den Ende, H., de Leeuw, J.W., Hatcher, P.G., Sinninghe Damsté, J.S., 1998. Chemical structure of algaenans from the fresh water algae *Tetraedron minimum*, *Scenedesmus communis* and *Pediastrum boryanum*. *Organic Geochemistry*, 29, 1453-1468.

Blokker, P., Schouten, S., de Leeuw, J.W., Sinninghe Damsté, J.S., van den Ende, H., 1999. Molecular structure of the resistant biopolymer in the zygospore cell walls of *Chlamydomonas monoica*. *Planta*, 207, 539-543.

Blokker, P., Schouten, S., de Leeuw, J.W., Sinninghe Damsté, J.S., van den Ende, H., 2000. A comparative study of fossil and extant algaenans using ruthenium tetroxide degradation. *Geochimica et Cosmochimica Acta*, 64, 2055-2065.

Blokker, P., van Bergen, P., Pancost, R., Collinson, M.E., de Leeuw, J.W., Sinninghe Damsté, J.S., 2001. The chemical structure of Gloeocapsamorpha prisca micro-fossils: Implications for their origin. *Geochimica et Cosmochimica Acta*, 65, 885-900.

Blokker, P., Yeloff, D., Boelen, P., Broekman, R.A., Rozema, J., 2006. The occurrence of *p*-coumaric acid and ferulic acid in fossil plant materials and their use as a UV-proxy. *Plant Ecology*, 182, 197-207.

Bockelmann, F., 2007. Selective preservation of organic-walled dinoflagellate cysts in Quaternary marine sediments: An oxygen effect and its application to paleoceanography. PhD thesis, University of Bremen, 130 pp.

Boom, A., Sinninghe Damsté, J.S., de Leeuw, J.W., 2005. Cutan, a common aliphatic biopolymer in cuticles of drought-adapted plants. *Organic Geochemistry*, 36, 596-601.

Bostick, N.H., 1971. Thermal alteration of clastic organic particles as an indicator of contact and burial metamorphism in sedimentary rocks. *Geoscience and Man*, 3, 83-92.

Briggs, D.E.G., 1999. Molecular taphonomy of animal and plant cuticles: selective preservation and diagenesis. *Philosophical Transactions of the Royal Society B, Biological Sciences*, 354, 7-17.

Briggs, D.E.G., Kear, A.J., Baas, M., de Leeuw, J.W., Rigby, S., 1995. Decay and composition of the hemichordate *Rhabdopleura*: implications for the taphonomy of graptolites. *Lethaia*, 28, 15-23.

Broecker, W.S., 1997. Thermohaline circulation, the Achilles heel of our climate system: Will man-made CO_2 upset the current balance. *Science*, 278, 1582-1588.

Brooks, J., Shaw, G., 1978. Sporopollenin; a review of its chemistry, palaeochemistry and geochemistry. *Grana*, 17, 91-97.

Canuel, E.A., Martens, C.S., 1996. Reactivity of recently deposited organic matter: Degradation of lipid compounds near the sediment-water interface. *Geochimica et Cosmochimica Acta*, 60, 1793-1806.

Collinson, M.E., Mösle, B., Finch, P., Scott, A.C., Wilson, R., 1998. Structure, biosynthesis and biodegradation of cutin and suberin. *Ancient Biomolecules*, 2, 251-265.

Cowie, G.L., Hedges, J.I., Prahl, F.G., de Lange, G.J., 1995. Elemental and major biochemical changes across an oxidation front in a relict turbidite: an oxygen effect. *Geochimica et Cosmochimica Acta*, 59, 33-46.

Cowie, G.L., Calvert, S.E., Pedersen, T.F., Schulz, H., von Rad, U., 1999. Organic content and preservational controls in surficial shelf and slope sediments from the Arabian Sea (Pakistan Margin). *Marine Geology*, 161, 23-38.

Domínguez, E., Mercado, J.A., Quesada, M.A., Heredia, A., 1999. Pollen sporopollenin: degradation and structural elucidation. *Sexual Plant Reproduction*, 12, 171-178.

de Leeuw, J.W., Largeau, C., 1993. A review of macromolecular organic compounds that comprise living organisms and their role in kerogen, coal and petroleum formation. In: Engel, M.H., Macko, S.A., (Eds.), *Organic Geochemistry: principles and applications.* Plenum Publishing Corp., New York. pp. 23-72.

de Leeuw, J.W., Versteegh, G.J.M., van Bergen, P.F., 2006. Biomacromolecules of algae and plants and their fossil analogues. *Plant Ecology*, 182, 209-233.

Durand, B., 1980. Sedimentary organic matter and kerogen: Definition and quantitative importance of kerogen. In: Durand, B. (Ed.), *Kerogen, Insoluble Organic Matter from Sedimentary Rocks.* Editions Technip, Paris. pp 13-34.

Fensome, R.A., Taylor, F.J.R., Norris, G., Sarjeant, W.A.S., Wharton, D.I., Williams, G.L., 1993. A classification of fossil and living dinoflagellates. *Micropaleontology Press Special Paper*, 7, 351 pp.

Froelich, P.H., Klinkhammer, G.P., Bender, M.L., Luedtke, N.A., Heath, G.R., Cullen, D., Dauphin, P., Hammond, D., Hartmann, B., 1979. Early oxidation of organic matter in pelagic sediments of the eastern equatorial Atlantic: suboxic diagenesis. *Geochimica et Cosmochimica Acta*, 43, 1075-1090.

Gelin, F., Boogers, I., Noordeloos, A.A.M., Sinninghe Damsté, J.S., Riegman, R., de Leeuw, J.W., 1997. Resistant biomacromolecules in marine microalgae of the classes Eustigmatophyceae and Chlorophyceae: geochemical applications. *Organic Geochemistry*, 26, 659-675.

Gelin, F., Volkman, J.K., Largeau, C., Derenne, S., Sinninghe Damsté, J.S., de Leeuw, J.W., 1999. Distribution of aliphatic, nonhydrolyzable biopolymers in marine microalgae. *Organic Geochemistry*, 30, 147-159.

Gupta, N.S., Collinson, M.E., Briggs, D.E.G., Evershed, R.P., Pancost, R., 2006. Reinvestigation of the occurrence of cutan in plants: implications for the leaf fossil record. *Paleobiology*, 32, 432-449.

Hackett, J.D., Anderson, D.M., Erdner, D., Bhattacharya, D., 2004. Dinoflagellates: a remarkable evolutionary experiment. *American Journal of Botany*, 91, 1523-1534.

Hartnett, H.E., Keil, R.G., Hedges, J.I., Devol, A.H., 1998. Influence of oxygen exposure time on organic carbon preservation in continental margin sediments. *Nature*, 391, 572-574.

Hedges, J.I., Keil, R.G., 1995. Sedimentary organic matter preservation: an assessment and speculative synthesis. *Marine Chemistry*, 49, 81-115.

Hedges, J.I., Hu, F.S., Devol, A.H., Hartnett, H.E., Tsamakis, E., Keil, R.G., 1999. Sedimentary organic matter preservation: a test for selective degradation under oxic conditions. *American Journal of Science,* 299, 529-555.

Henrichs, S.M., 1992. Early diagenesis of organic matter in marine sediments: progress and perplexity. *Marine Chemistry*, 39, 119-149.

Henrichs, S.M., Reeburgh, W.S., 1987. Anaerobic mineralization of marine sediment organic matter: Rates and the role of anaerobic processes in the oceanic carbon economy. *Geomicrobiology Journal*, 5, 191-237.

Hoefs, M.J.L., Rijpstra, W.I.C., Sinninghe Damsté, J.S., 2002. The influence of oxic degradation on the sedimentary biomarker record I: Evidence from Madeira Abyssal Plain turbidites. *Geochimica et Cosmochimica Acta,* 66, 2719-2735.

Hulthe, G., Hulth, S., Hall, P.O.J., 1998. Effect of oxygen on the degradation rate of refractory and labile organic matter in continental margin sediments. *Geochimica et Cosmochimica Acta*, 63, 1319-1328.

Jansonius, J., McGregor, D.C., 1996. Chapter 1: Introduction. In: Jansonius, J., McGregor, D.C., (Eds.), *Palynology: principles and applications*. American Association of Stratigraphic Palynologists Foundation, Dallas, 1-10.

Keil, R.G., Cowie, G.L., 1999. Organic matter preservation through the oxygen-deficient zone of the NE Arabian Sea as discerned by organic carbon: mineral surface area ratios. *Marine Geology*, 161, 13-22.

Keil, R.G., Hu, F.S., Tsamakis, E.C., Hedges, J.I., 1994a. Pollen in marine sediments as an indicator of oxidation of organic matter. *Nature*, 369, 639-641.

Keil, R.G; Montluçon, D.B., Prahl, F.G., Hedges, J.I., 1994b. Sorptive preservation of labile organic matter in marine sediments. *Nature*, 370, 549-551.

Killops, S.D., Killops, V.J., 2004. *An Introduction to Organic Geochemistry*. Wiley-Blackwell, 408 pp.

Kok, M., Schouten, S., Sinninghe Damsté, J.S., 2000. Formation of insoluble, nonhydrolyzable, sulfur-rich macromolecules via incorporation of inorganic sulfur species into algal carbohydrates. *Geochimica et Cosmochimica Acta*, 64, 2689-2699.

Kokinos, J.P., Eglinton, T.I., Goñi, M.A., Boon, J.J., Martoglio P.A., Anderson, D.M., 1998. Characterization of a highly resistant biomacromolecular material in the cell wall of a marine dinoflagellate resting cyst. *Organic Geochemistry*, 28, 265-288.

Kuypers, M.M.M., Blokker, P., Hopmans, E.C., Kinkel, H., Pancost, R.D., Schouten, S., Sinninghe Damsté, J.S., 2002. Archaeal remains dominate marine organic matter from the early Albian oceanic anoxic event 1b. *Palaeogeography, Palaeoclimatology, Palaeoecology*, 185, 211-234.

Lee, C., 1992. Control on organic carbon preservation: The use of stratified water bodies to compare intrinsic rates of decomposition in oxic and anoxic systems. *Geochimica et Cosmochimica Acta*, 56, 3323-3335.

Mayer, L.M., 1994a. Surface area control of organic carbon accumulation in continental shelf sediments. *Geochimica et Cosmochimica Acta*, 58, 1271-1284.

Mayer, L.M., 1994b. Relationships between mineral surfaces and organic carbon concentrations in soils and sediments. *Chemical Geology*, 114, 347-363.

Mösle, B., Finch, P., Collinson, M.E., Scott, A.C., 1997. Comparison of modern and fossil plant cuticles by selective chemical extraction monitored by flash pyrolysis-gas chromatography-mass spectroscopy and electron microscopy. *Journal of Analytical and Applied Pyrolysis*, 40-41, 585-597.

Mösle, B., Colllinson, M.E., Finch, P., Stankiewicz, B.A., Scott, A.C., Wilson, R., 1998. Factors influencing the preservation of plant cuticles: a comparison of morphology and chemical composition of modern and fossil examples. *Organic Geochemistry*, 29: 1369-1380.

Mollenhauer, G., Inthorn, M., Vogt, T., Zabel, M., Sinninghe Damsté, J.S., Eglinton, T.I., 2007. Aging of marine organic matter during cross-shelf lateral transport in the Benguela upwelling system revealed by compound-specific radiocarbon dating. *Geochemistry, Geophysics, Geosystems*, 8, Q09004, doi: 10.1029/2007GC001603.

Mollenhauer, G., Eglinton, T.I., Hopmans, E.C., Sinninghe Damsté, J.S., 2008. A radiocarbon-based assessment of the preservation characteristics of crenarchaeol and alkenones from continental margin sediments. *Organic Geochemistry*, 39, 1039-1045.

Paropkari, A.L., Prakash Babu, C., Mascarenhas, A., 1992. A critical evaluation of depositional parameters controlling the variability of organic carbon in Arabian Sea sediments, *Marine Geology*, 107, 213-226.

Paropkari, A.L., Prakash Babu, C., Mascarenhas, A., 1993. New evidence for enhanced preservation of organic carbon in contact with the oxyen minimum zone on the western continental slope of India. *Marine Geology*, 111, 7-13.

Petersen, T.F., Shimmield, G.B., Price, N.B., 1992. Lack of enhanced preservation of organic matter in sediments under the oxygen minimum on the Oman Margin. *Geochimica et Cosmochimica Acta*, 56, 545-551.

Ransom, B., Kim, D., Kastner, M., Wainwright, S., 1998. Organic matter preservation on continental slopes: importance of mineralogy and surface area. *Geochimica et Cosmochimica Acta*, 62, 1329-1346.

Raven, J.A., Falkowski, P.G., 1999. Oceanic sinks for atmospheric CO_2. *Plant, Cell and Environment*, 22, 741-755.

Reilly, J., Prinn, R., Harnisch, J., Fitzmaurice, J., Jacoby, H., Kicklighter, D., Melillo, J., Stone, P., Sokolov, A., Wang, C., 1999. Multi-gas assessment of the Kyoto Protocol. *Nature*, 401, 549-555.

Rozema, J., Noorkijk, A.J., Broekman, R.A., van Beem, B.M., 2001a. (Poly)phenolic compounds in pollen and spores of Antarctic plants as indicators of solar UV-B. *Plant Ecology*, 154, 11.

Rozema, J., Broekman, R.A., Blokker, P., Meijkamp, B.B., de Bakker, N., van de Staaij, N.J., van Beem, A., Ariese, F., Kars, S.M., 2001b. UV-B absorbance and UV-B absorbing compounds (*para*-coumaric acid) in pollen and sporopollenin: the perspective to track historic UV-B levels. *Journal of Photochemistry and Photobiology B*, 62, 108-117.

Sabine, C.L., Feely, R.A., Gruber, N., Key, R.M., Lee, K., Bullister, J.L., Wanninkhof, R., Wong, C.S., Wallace, D.W.R., Tilbrook, B., Millero, F.J., Peng, T-H., Kozyr, A., Ono, T., Rios, A.F., 2004. The oceanic sink for anthropogenic CO_2. *Science*, 305, 367-371.

Sarnthein, M., Winn, K., Duplessy, J.C., Fontugne, M.R., 1988. Global variations of surface ocean productivity in low and mid-latitudes: Influence on CO_2 reservoirs of the deep ocean and atmosphere during the last 21,000 years. *Paleoceanography*, 3, 361-399.

Schlesinger, W.H., 2005. The Global Carbon Cycle and Climate Change. In: Sinnott-Armstrong, W., Howarth, R.B. (Eds.), *Perspectives on Climate Change: Science, Economics, Politics, Ethics*, Advances in the Economics of Environmental Research, Vol. 5, Emerald Group Publishing Limited, pp. 31-53.

Siegenthaler, U., Sarmiento, J.L., 1993. Atmospheric carbon dioxide and the ocean. *Nature*, 365, 119-125.

Simpson, A.J., Zhang, X., Kramer, R., Hatcher, P.G., 2003. New insights on the structure of algaenan from *Botryococcus braunii* race A and its hexane insoluble botryals based on multidimensional NMR spectroscopy and electrospray-AMSS spectrometry techniques. *Phytochemistry*, 62, 783-796.

Sinninghe Damsté, J.S., de Leeuw, J.W., 1990. Organically-bound sulphur in the geosphere: state of the art and future research. *Organic Geochemistry*, 16, 1077-1101.

Sinninghe Damsté, J.S., Rijpstra, W.I.C., Kock-Van Dalen, A.C., de Leeuw, J.W., Schenck, P.A., 1989. Quenching of labile functionalized lipids by inorganic sulfur species: evidence for the formation of sedimentary organic compounds at the early stages of diagenesis. *Geochimica et Cosmochimica Acta*, 53, 1343-1355.

Sinninghe Damsté, J.S., de las Heras, F.X.C., van Bergen, P.F., de Leeuw, J.W., 1993. Characterization of Tertiary Catalan lacustrine oil shales; Discovery of extremely organic sulphur-rich Type I kerogens. *Geochimica et Cosmochimica Acta*, 57, 389-415.

Sinninghe Damsté, J.S., Rijpstra, W.I.C., Reichart, G.J., 2002. The influence of oxic degradation on the sedimentary biomarker record II. Evidence from Arabian Sea sediments. *Geochimica et Cosmochimica Acta*, 66, 2737-2754.

Stankiewicz, B.A., Briggs, D.E.G., Michels, R., Collinson, M.E., Flannery, M.B., Evershed, R.P., 2000. Alternative origin of aliphatic polymer kerogen, *Geology*, 28, 559-562.

Tegelaar, E.W., de Leeuw, J.W., Derenne, S., Largeau, C., 1989. A reappraisal of kerogen formation. *Geochimica et Cosmochimica Acta*, 53, 3103-3106.

Tegelaar, E.W., Kerp, H., Visscher, H., Schenck, P.A., de Leeuw, J.W., 1991. Bias of the paleobotanical record as a consequence of variations in the chemical composition of higher vascular plant cuticles. *Paleobiology*, 17, 133-144.

Tissot, B.P., Welte, D.H., 1984. *Petroleum Formation and Occurrence.* Springer, Berlin, 699 pp.

van Bergen, P.F., Collinson, M.E., de Leeuw, J.W., 1993. Chemical composition and ultrastructure of fossil and extant salvinialean microspore massulae and megaspores. *Grana Supplement I*, 18-30.

van Bergen, P.F., Collinson, M.E., Briggs, D.E.G., de Leeuw, J.W., Scott, A.C., Evershed, R.P., Finch, P., 1995. Resistant biomacromolecules in the fossil record. *Acta Botanica Neerlandica*, 44, 319-345.

van Bergen, P.F., Blokker, P., Collinson, M.E., Sinninghe Damsté, J.S., de Leeuw, J.W., 2004. Structural biomacromolecules in plants: what can be learnt from the fossil record? In: Hemsley, A.R., Poole, I., (Eds.), *Evolution of Plant Physiology*. Elsevier, Amsterdam, pp. 133-154.

Vandenbroucke, M., Largeau, C, 2007. Kerogen origin, evolution and structure. *Organic Geochemistry*, 38, 719-833.

van der Weijden, C.H., Reichart, G.J., Visser, H.J., 1999. Enhanced preservation of organic matter in sediments deposited within the oxygen minimum zone in the northeastern Arabian Sea. *Deep-Sea Research Part I*, 46, 807-830.

van Dongen, B.E., Schouten, S., Baas, M., Geenevasen, J.A.J., Sinninghe Damsté, J.S., 2003. An experimental study of the low-temperature sulfurization of carbohydrates. *Organic Geochemistry*, 34, 1129-1144.

Versteegh, G.J.M., Zonneveld, K.A.F., 2002. Use of selective degradation to separate preservation from productivity. *Geology*, 30, 615-618.

Versteegh, G.J.M., Blokker, P., 2004. Resistant macromolecules of extant and fossil microalgae. *Phycological Research*, 52, 325-339.

Versteegh, G.J.M., Blokker, P., Wood, G., Collinson, M.E., Sinninghe Damsté, J.S., de Leeuw, J.W., 2004. An example of oxidative polymerization of unsaturated fatty acids as a preservation pathway for dinoflagellate organic matter. *Organic Geochemistry*, 35, 1129-1139.

Versteegh, G.J.M., Blokker, P., Marshall, C.P., Pross, J., 2007. Macromolecular composition of the dinoflagellate cyst *Thalassiphora pelagica* (Oligocene, SW Germany). *Organic Geochemistry*, 38, 1643-1656.

Versteegh, G.J.M., Zonneveld, K.A.F., and de Lange, G.J.: Selective aerobic and anaerobic degradation of lipids and palynomorphs in the Eastern Mediterranean since the onset of sapropel S1 deposition, Mar. Geol., 278, 177-192, 2010.

Versteegh, G.J.M., Blokker, P., Bogus, K., Harding, I.C., Lewis, J., Oltmanns, S., Rochon, A., Zonneveld, K.A.F., in press. Flash pyrolysis and infrared spectroscopy of cultured and sediment derived *Lingulodinium polyedrum* (Dinoflagellata) cyst walls. *Organic Geochemistry.*

Wakeham, S.G., Peterson, M.L., Hedges, J.I., Lee, C., 2002. Lipid biomarker fluxes in the Arabian Sea, with a comparison to the equatorial Pacific Ocean, *Deep Sea Research Part II*, 49, 2265 2301.

Watson, J.S., Sephton, M.A., Sephton, S.V., Self, S., Fraser, W.T., Lomax, B.H., Gilmour, I., Wellman, C.H., Berrling, D.J., 2007. Rapid determination of spore chemistry using thermochemolysis gas chromatography-mass spectrometry and micro-Fourier transform infrared spectroscopy. *Photochemical and Photobiological Sciences*, 6, 689-694.

Yule, B.L., Roberts, S., Marshall, J.E.A., 2000. The thermal evolution of sporopollenin. *Organic Geochemistry*, 31, 859-870.

Zonneveld, K.A.F., Versteegh, G.J.M., de Lange, G.J., 1997. Preservation of organic walled dinoflagellate cysts in different oxygen regimes: a 10,000 years natural experiment. *Marine Micropaleontology*, 29, 393-405.

Zonneveld, K.A.F., Versteegh, G.J.M., de Lange, G.J., 2001. Palaeoproductivity and post-depositional aerobic organic matter decay reflected by dinoflagellate cyst assemblages of the Eastern Mediterranean S1 sapropel. *Marine Geology*, 172, 181-195.

Zonneveld, K.A.F., Versteegh, G.J.M., Kasten, S., Eglinton, T.I., Emeis, K.C., Huguet, C., Koch, B.P., de Lange, G.J., de Leeuw, J.W., Middelburg, J.J., Mollenhauer, G., Prahl, F.G., Rethemeyer, J., Wakeham, S.G., 2010. Selective preservation of organic matter in marine environments; processes and impact on the sedimentary record. *Biogeosciences*, 7 483-511.

CHAPTER 3

DINOFLAGELLATES

3.1 Biology of dinoflagellates

3.1.1 Cell structure

Dinoflagellate motile cells (size range 20 -200 µm) are able to migrate vertically through the water column (Taylor and Pollingher, 1987) through the use of two asymmetrical flagella, transverse and longitudinal (Fig. 3.1). The flagella lie in surface grooves: the ribbon-like transverse flagellum, which provides forward propulsion, is situated in the cingulum and the longitudinal flagellum, which provides steering, in the sulcus (Fensome et al., 1993). The cytoplasm of dinoflagellates contains typical eukaryotic organelles including: rough and smooth endoplasmic reticulum, Golgi apparatus, lipid and starch grains, and food vacuoles. However, the genetic systems in the nucleus and mitochondria as well as the presence of peridinin plastids are completely unique to dinoflagellates (e.g. Schnepf and Elbrächter, 1999; Nash et al. 2007, Slamovits et al. 2007).

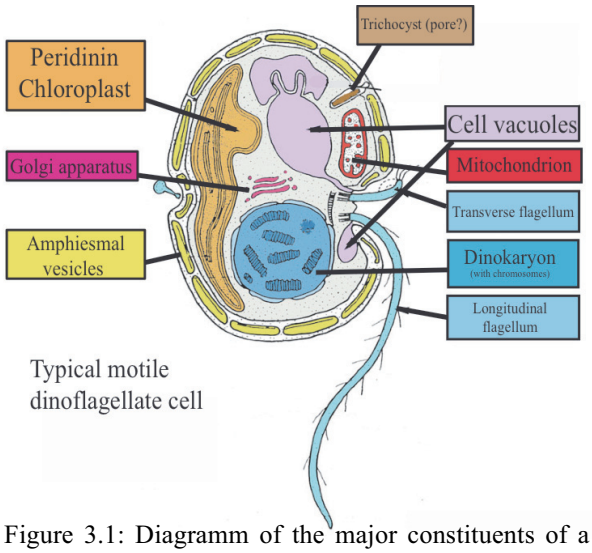

Figure 3.1: Diagramm of the major constituents of a motile dinoflagellate cell. Modified from Taylor (1987).

The outer cortical region of a dinoflagellate is also distinctive. This entire structural complex is called the amphiesma (Fig. 3.1) (Morrill and Loeblich, 1983). The amphiesmal vesicles are a single layer present beneath the cell membrane that play a structural role in the cell, and are penetrated by trichocysts, which are the most common type of what are assumed to be exit apertures (Taylor, 1987). Thecal plates, if present, are internal to the cell membrane, composed of cellulose and lie within the amphiesmal vesicles. Not every dinoflagellate species produces theca, those that do are called thecate and those that do not are referred

to as athecate. The cellulose-based thecal plates abut one another tightly with the juncture areas referred to as sutures; the arrangement of the thecal plates (or amphiesmal vesicles in athecate taxa) is referred to as tabulation, which is a distinguishing characteristic of different dinoflagellate lineages (e.g. Taylor, 1987; Matthiessen et al., 2005). Generally, five basic types are recognized: prorocentroid, dinophysoid, gymnodinioid, gonyaulacoid and peridinioid; while the most relevant types to this work are the gonyaulacoid and peridinioid types (Fig. 3.2). These types have well developed thecal plates and are generally produced by autotrophic and heterotrophic taxa, respectively (Matthiessen et al., 2005).

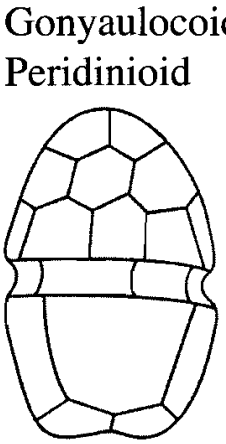

Figure 3.2: Tabulation pattern of the dinoflagellate group mainly used in this thesis. From Matthiessen et al. (2005).

3.1.2 Life cycle

The dinoflagellate life cycle can be quite complex (Fig. 3.3); the following description is a simplified scheme. The life cycle consists of four main parts: growth (mitotic and asexual), sexuality (meiotic), quiescence (sexual or asexual immobile phase with a low metabolic rate) and senescence (population decline and death) (e.g. von Dassow and Montresor, 2011). The motile life stages (i.e. growth) are usually haploid and population growth normally happens through asexual division, as this is faster and thus preferred during optimal environmental conditions (e.g. Anderson and Lindquist, 1985). However, sexual reproduction is necessary as it allows for genetic recombination and thus, genetic variability (von Dassow and Montresor, 2011). During sexual reproduction (i.e. sexuality), two haploid cells, called gametes, fuse to form a diploid cell, termed a planozygote. The planozygote can then transition to a quiescent state through the formation of an environmentally resistant resting cyst (hypnozygote) during which the cell ceases swimming, expels its flagella and becomes surrounded by a continuous wall (Taylor, 1987). This hypnozygote may be organic-, calcareous- or, rarely, siliceous-walled (e.g. Fensome et al., 1999). In this study, the hypnozygote is defined as an organic-walled non-motile resting cyst.

Encystment occurs mainly after blooms and may be influenced by specific environmental factors such as temperature, day length, irradiance and/or low nutrient

levels (e.g. Anderson and Lindquist, 1985; Taylor, 1987) as well as an endogenous encystment rhythm (e.g. Anderson and Kaefer, 1987). About 15% of extant species have been discovered to participate in cyst formation (Head, 1996), though it can be as high as 28% in temperate regions (Persson et al., 2000). Dinoflagellate cyst formation processes are incompletely understood (e.g. von Dassow and Montresor, 2011); however, cyst formation appears to be a self-assembly process (J. Lewis, personal communication). After the expulsion of the flagella, the outer cell membrane swells and the cyst membrane forms from material available in the cell. Cyst formation is a poorly understood process, as it is rarely observed and/or obscured by the thecal plates and cell content (Rochon et al., 2009). However, Rochon et al. (2009) provided a description; in brief, the formation of the cyst membrane begins within the cell when the flagella are expelled, the outer membrane then swells (100 µm diameter) during which the theca dislocate and the thecal plates fall off, and if the cyst has projections, they grow within the space of the membrane over a period of a few minutes to an hour. When process growth is completed, the outer membrane ruptures and the cyst is released.

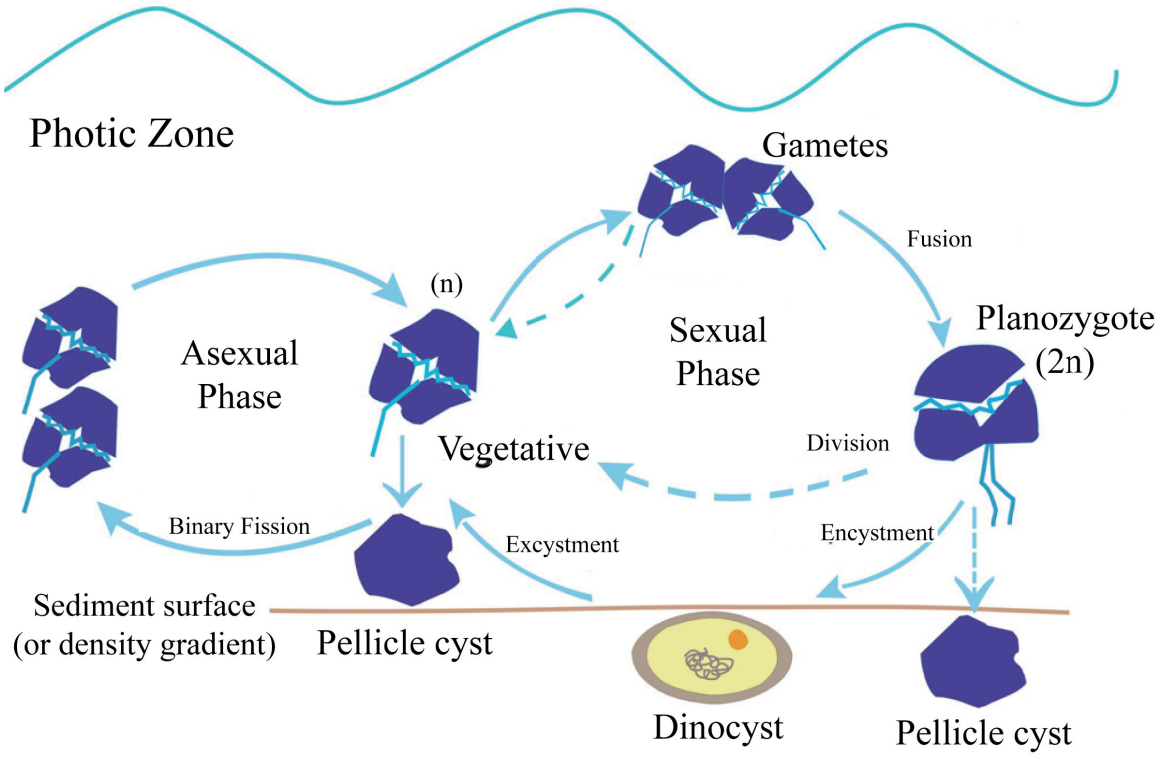

Figure 3.3: Dinoflagellate life cycle. Modified from Walker (1984).

Dinoflagellate cysts can remain dormant in sediments for up to a century without suffering deleterious consquences (Ribeiro et al., 2011) and can thus serve an important ecological role as "seed banks", which allow for recurrent blooms and the expansion of geographic distributions (Matsuoka and Fukuyo, 2000). Individual dinoflagellate cysts probably never settle on the sea floor in the open ocean because if the cysts sink a considerable distance, the emerging motile stage cannot return to the photic zone based on their swimming speeds (Sournia, 1982). Instead, the cysts likely accumulate at density gradients (e.g. above the pycnocline) or complete their cyst stage at a rate that allows for successful excystment before the cyst sinks to too great a depth (Dale, 1992). Excystment can be triggered or inhibited by several factors such as bottom water anoxia, low temperature or nutrient/light availability (Anderson, 1980; Dale, 1983). It should be noted that species can deviate from the previously described life cycle. Some species do not produce a resting cyst so that the planozygote undergoes meiosis and division without the production of a dinoflagellate cyst (e.g. Figueroa and Bravo, 2005) while in other species, the gametes revert to an asexual phase and instead undergo binary fission rather than fusion (Figueroa and Bravo, 2005; Figueroa et al., 2006).

3.1.3 Life strategies

In photosynthetic dinoflagellates, which have chloroplasts and can produce their own sugars and organic materials via photosynthesis, the most common chloroplast type is the peridinin plastid (Schnepf and Elbrächter, 1999). Peridinin is a carotenoid found only in dinoflagellates; other photosynthetic pigments include chlorophyll-*a*, c_2, b-carotene, diadinoxanthin and dinoxanthin (Jeffrey et al., 1975). The life strategy of many dinoflagellate taxa includes heterotrophy; these species do not possess chloroplasts and must consume other organisms or organic detritus to obtain nourishment. In heterotrophic taxa, feeding occurs by osmotrophy and/or phagotrophy. In direct phagocytosis, the cytostome (cell mouth) distends extensively as whole prey organisms are ingested (Fig. 3.4a), whereas other feeding strategies may use a penduncle to pierce the prey's cell membrane and suck the contents out, much like a straw (Fig. 3.4b; Schnepf and Elbrächter, 1992) or a pallium, which is a pseudopodial feeding veil that extends out of the dinoflagellate and surrounds the prey (Fig. 3.4c). Digestive enzymes are then secreted and the prey is digested extracellularly in the pallium (Jacobson and Anderson, 1992). Both the autotrophic and heterotrophic life strategies are complicated by the fact

that many dinoflagellate species participate in a mixture of the two (i.e. mixotrophy), which has been noted to be more common that originally thought (Fensome et al., 1996). In these cases, heterotrophic species can acquire chloroplasts from their prey (i.e. kleptochloroplasts) and utilize them, thus becoming photosynthetic themselves, while some photosynthetic species have been discovered to possess food vacuoles (Stoecker, 1999).

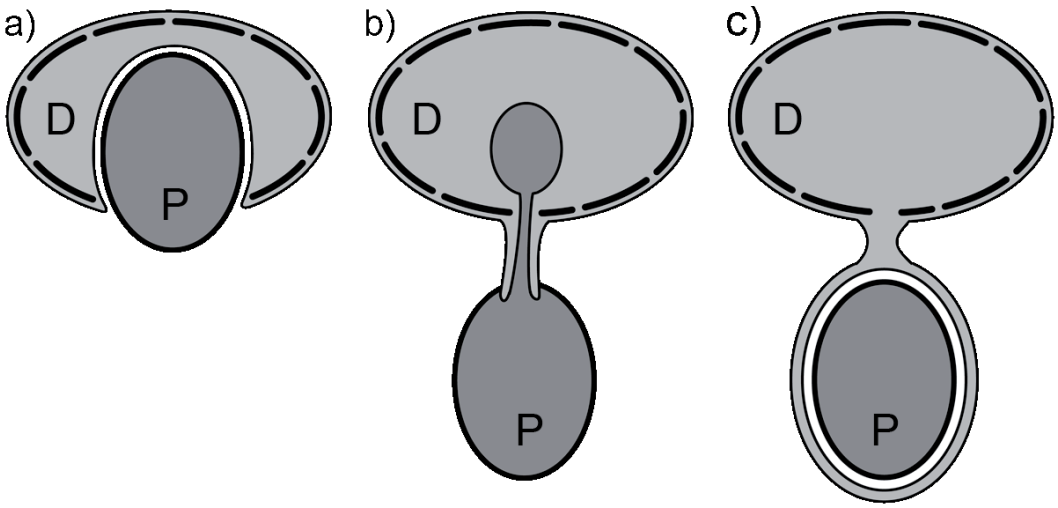

Figure 3.4: Common feeding strategies of heterotrophic dinoflagellates (a) direct phagocytosis, (b) peduncle feeding, and (c) pallium feeding. D= dinoflagellate, P= prey.

3.1.4 Cyst characteristics

Dinoflagellate cysts can be even more complex in their morphology than the motile phase (Wall and Dale, 1968), and their morphological features are the primary means of identification. The following descriptions are generally after Taylor (1987). There are three main forms of a cyst body. A proximate cyst shape varies from spherical to peridinioid and usually does not possess extensive projections, though some ornamentation may reflect the position and shape of the thecal plates, cingulum and sulcus from the motile form. A chorate cyst is characterized by variable ornamentation that functions as support for the planozygotic cell wall. A specific example of chorate cyst formation was shown for *Lingulodinium polyedrum* (motile form of *L. machaerophorum*; Kokinos and Anderson, 1995). The cyst shape is generally spherical, subspherical or ovoid. A cavate cyst consists of two or more clearly separated wall layers with a cavity or cavities between these layers. Cyst walls can be composed of up to four layers of a resistant biopolymer termed dinosporin (see Section 2.4.4) and may vary in

color from transparent to dark brown (Fensome et al., 1993). The cyst wall surface ranges from completely featureless to highly elaborate and is taxon specific. For example, in the autotrophic species discussed in Chapter 6, the paratabulation is expressed in the form of septa for *Impagidinium patulum* (Fig. 3.5a), and gonal (i.e. at paraplate junctions) processes in *Spiniferites pachydermus* (Fig. 3.5b) while no relationship between paratabulation and the distribution of processes is seen in *Operculodinium centrocarpum* (Fig. 3.5c).

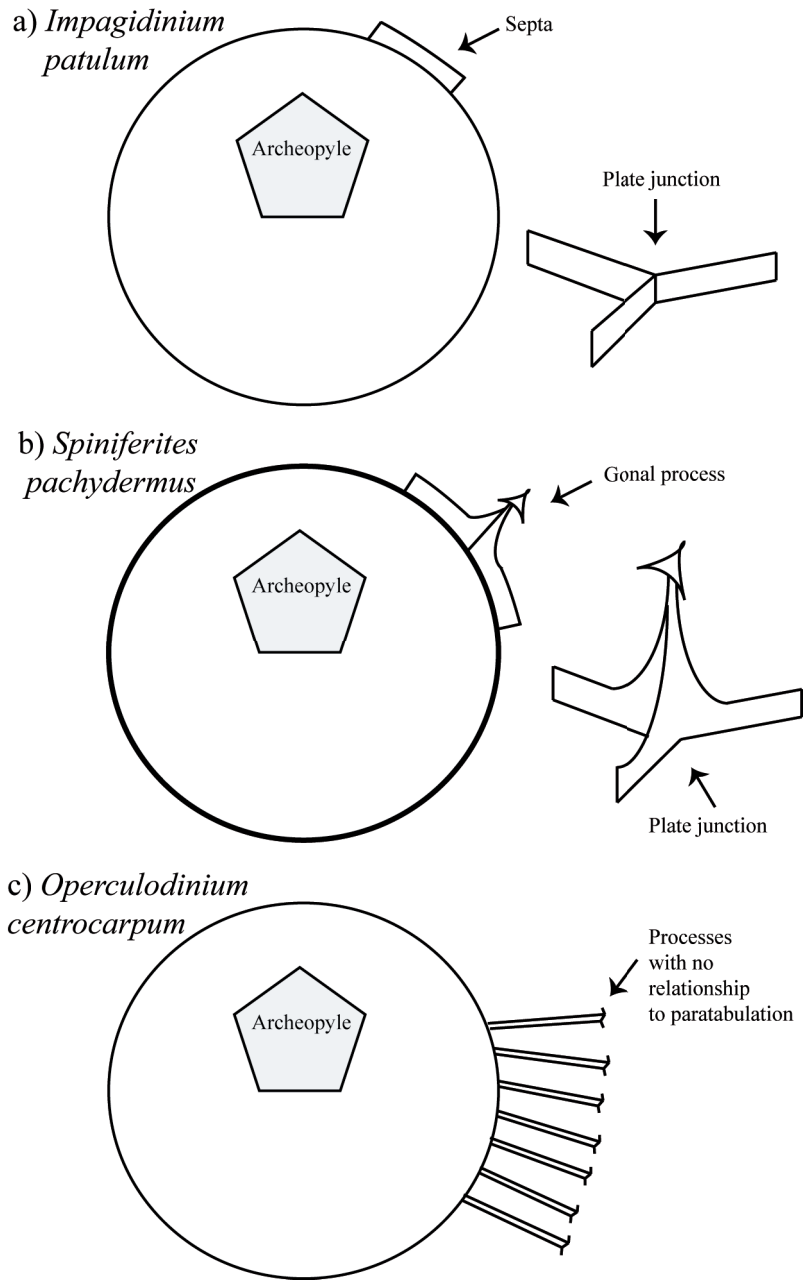

Figure 3.5: Diagrammatic illustration of the different cyst ornamentations seen in certain gonyaulacoid dinoflagellate cysts. Modified and redrawn from Zonneveld (2011).

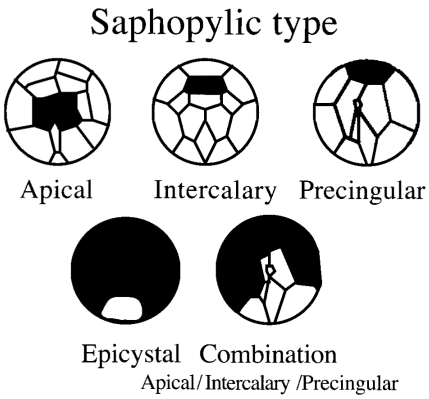

Figure 3.6: Archeopyle types in Peridiniales and Gonyaulacales. From Matthiessen et al. (2005).

One of the most defining morphological features of a dinoflagellate cyst is the archeopyle, as its type and shape is characteristic for an individual species. The archeopyle is an opening formed as a result of the excystment of the cell. There are three main archeopyle types (after Matsuoka, 1985). A saphopylic archeopyle has sutures that correspond to paraplate boundaries and part of the cyst wall associated with the archeopyle (i.e. operculum) is detached from the cyst body. Most modern cysts belonging to the Peridiniales and Gonyaulacales have this archeopyle type (Fig. 3.6). A theropylic archeopyle also follows paraplate boundaries but the operculum is usually still attached to the cyst due to the incomplete development of the archeopyle sutures. A cryptopylic archeopyle has archeopyle sutures that do not reflect paratabulation. The archeopyle form itself can be either chasmic (slit-like) or tremic (hole-like).

3.2 Dinoflagellate ecology

Dinoflagellates, along with diatoms and coccolithophorids, comprise most of the marine eukaryotic phytoplankton and, as such, are important primary producers. They usually dominate in oligotrophic waters while phytoplankton in more nutrient rich surface waters contain mostly diatoms, or a combination of diatoms and dinoflagellates (Taylor and Pollingher, 1987). Roughly half of dinoflagellate species are autotrophic (Gaines and Elbrächter, 1987), so light is a major limiting factor as are nutrients (i.e. nitrate, phosphate) and essential trace elements (i.e. iron; Taylor and Pollingher, 1987). In general, dinoflagellates are more diverse in tropical waters than in polar waters and tend to be more abundant and diverse in the warmer months of the year (Matthiessen et al., 2005). This is due to the fact that temperature has a direct effect on metabolic rates as well as an indirect effect on the vertical stability of the water column. Furthermore, marine dinoflagellates are euryhaline so they can dwell in environments as diverse as epicontinental seas or estuaries, near shore environments, and the open ocean.

In addition to existing as free-living cells, dinoflagellates also participate as symbionts (termed zooxanthellae) and even parasites (Taylor et al., 2008). Dinoflagellates are symbionts in many invertebrates including cnidarians (e.g. Karako-

Lampert et al., 2004; Thornhill et al., 2009), sponges (e.g. Garson et al., 1998; Schönberg and Loh, 2005), mollusks (e.g. Trench et al., 1981; Ishikura et al., 2004), and other protists, including radiolarians (e.g. Gast et al., 2003) and foraminifera (e.g. Garcia-Cuetos et al., 2005; Siano et al., 2010). Perhaps the most famous example of dinoflagellate symbiosis is their association with corals and reef ecosystems (e.g. Coffroth and Santos, 2005). Symbiotic relationships provide the other organism with additional nutrients (Yellowlees et al., 2008), and can contribute to their ecological success (Douglas, 2003).

3.3 Practical applications of dinoflagellate signals

Though the motile stage is rarely preserved, dinoflagellate cysts have been used extensively in paleoclimatology and paleooceanography studies (e.g. Fensome et al., 1993; Marret and Zonneveld, 2003; Fensome and Williams, 2004). In addition to the use of dinoflagellate cysts in climatic and oceanic reconstructions, dinoflagellates are important organisms of study in other areas. Of the cyst-producing dinoflagellates, a number are harmful when the population explodes in a bloom. Specifically, more than 16 have been known to cause "red tides" (so-called due to the accumulation of carotenoid pigments that cause seawater to be discolored golden or red) and 7 to be toxic (Matsuoka and Fukuyo, 2000). Some of these toxins can cause serious harm to other marine organisms, including fish (Heil et al., 2001; Cembella et al., 2002) and humans (e.g. Steidinger, 1993; Backer et al., 2003). These deleterious effects of certain dinoflagellate species' blooms have economic implications for industry, notably fisheries and tourism.

3.3.1 Lipids and genetics

It is also possible to use other dinoflagellate-derived compounds as proxies. One of the most commonly used is 4α, 23, 24-trimethyl-5α-cholest-22*E*-en-3β-ol (i.e. dinosterol), a sterol that is mainly produced by certain dinoflagellate lineages (e.g. Boon et al., 1979; Volkman et al., 1993; 1999) as a membrane lipid. There has been some recent discussion on the observed discrepancy between the relationship of dinoflagellate cyst abundance and dinosterol concentrations with studies either showing a weak (e.g. Marret and Scourse, 2002) or nonexistent (Pinturier-Geiss et al., 2002; Sangiorgi et al., 2005) correlation. This may be related to differences in the species that manufacture dinosterol as a membrane lipid and those that produce dinoflagellate cysts (Boere et al., 2009).

Additionally, the high lability of dinosterol as well as peridinioid cysts (Section 3.3.4) may result in the overprinting of any correlation as a better relationship was seen after the inclusion of dinosterol degradation products (e.g. Mouradian et al., 2007; Chapter 5). Finally, isotopic studies on dinosterol have shown some promise as a salinity proxy (Sachs and Schwab, 2011) and dinoflagellate DNA has been used to trace dinoflagellate inputs to sediments (Boere et al., 2009) as well as in reconstructions of phytoplankton assemblages (Boere et al., 2011).

3.3.2 Importance of dinoflagellate cysts in Recent paleoenvironmental studies

Since dinoflagellate cysts are composed of resistant OM, they are more refractory than organisms with a carbonate or siliceous backbone as these are subject to dissolution (Matthiessen, 1995). Many studies have documented the geographic distribution of modern (i.e. Quaternary) dinoflagellate cysts in marine sediments in relation to environmental conditions (e.g. Wall et al., 1977; Rochon et al., 1999; Marret and Zonneveld, 2003). These datasets illustrate the connections between global environmental conditions, such as temperature, salinity and productivity/eutrophication, and general dinoflagellate cyst distribiutions. The work of Wall et al. (1977) first identified a proximal to distal distribution of dinoflagellate cyst signals in which specific taxa were classified as neritic to oceanic, based on the premise that many dinoflagellate species are adapted to specific surface water conditions. For example, changes in the dinoflagellate cyst species present in an assemblage can be used to trace broad salinity gradients and water mass stratification (Pemberton et al., 2004), nutrient availability and water temperature (Dale, 1996) and even ecosystem stress (Bradford and Wall, 1984). As well, empirical studies are able to interpret regional assemblages in terms of more localized productivity/eutrophication, salinity, temperature and sea ice changes (e.g. de Vernal et al., 2001; Dale et al., 1999; Esper et al., 2002; Pospelova et al., 2002; Sangiorgi and Donders, 2004; Vink et al., 2000; Zonneveld, 1997; Zonneveld et al., 2001a).

In order to accurately utilize dinoflagellate cysts as environmental proxies, an actuo-paleontological approach is considered ideal because it traces the factors that affect the living dinoflagellate community and transforms it into the fossil dinoflagellate cyst record (Fig. 3.7). Plankton studies provide valuable information on individual species but are basically random records of a given locality at a particular point in time (Matthiessen et al., 2005), although this patchiness can be rectified by sampling over several seasons at

the same location (e.g. Dale et al., 1999). Moored sediment traps can illustrate seasonal and interannual variations in plankton production and distribution, as well as changes in fluxes and sedimentation (Honjo, 1996). Despite their usefulness in tracking these changes, comprehensive sediment trap studies are still not all that common (e.g. Matsuoka, 1992; Dale, 1992; Dale and Dale, 1992; Mudie, 1996; Montresor et al., 1998; Harland and Pudsey, 1999; Zonneveld and Brummer, 2000; Godhe et al., 2001; Morquecho and Lechuga-Devéze, 2004; Tamelander and Heiskanen, 2004). However, processes such as degradation, lateral transport and predatory grazing can all overprint the original planktonic signal during settling through the water column. Dinoflagellates are a common component of marine snow, but dinoflagellate cysts have not been observed in fecal pellets (Alldredge et al., 1998). Nonetheless, aggregate formation, something that dinoflagellate cysts do participate in, may be more important than fecal pellet incorporation for the export of dinoflagellate cysts to the sea floor (Mudie, 1996), so it is likely that dinoflagellate cysts are not significantly degraded as they sink through the water column (Zonneveld and Brummer, 2000). At the sediment-water interface, seasonal ecological information is generally lost, as the sediments are an integration of multiple years depending on the local sedimentation rate. Furthermore, after deposition on the seafloor, the dinoflagellate cyst community is subjected to biotic and abiotic degradative processes (Sections 2.2.1; 3.3.4; Chapter 5), all of which can further overprint photic zone ecological information. Despite these limitations and uncertainties, dinoflagellate cysts have proven to be very sensitive indicators of environmental changes in surface waters (e.g. Reichart and Brinkhuis, 2003), once the relationship between specific dinoflagellate species and oceanographic conditions is known.

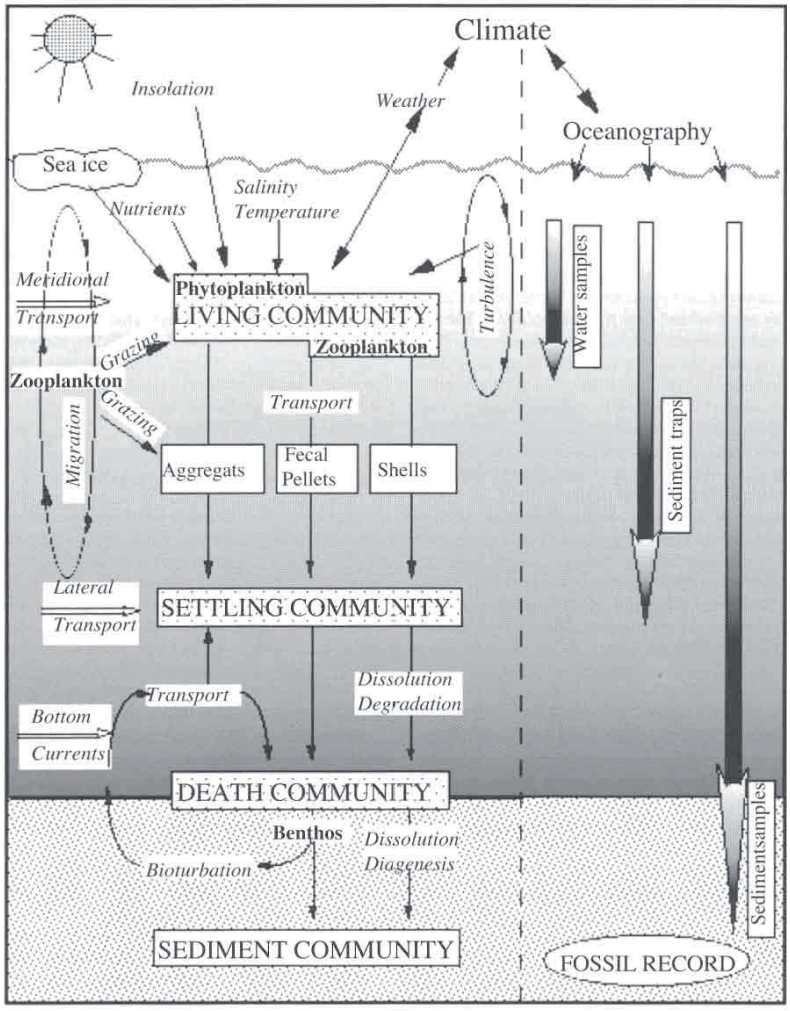

Figure 3.7: Diagramm illustrating the actuo-paleontological approach for linking environmental information to the sedimentary record using dinoflagellate cysts, and factors influencing the relationship. From Matthiessen et al. (2005).

3.3.3 Importance of dinoflagellate cysts in pre-Quaternary paleoenvironmental studies

The actuo-paleontological approach provides information on certain oceanographic conditions that are important for specific taxa. This information can then be used to represent environmental conditions; however, this is more difficult for pre-Quaternary assemblages because the number of extant species decreases going back through time. Even so, using the knowledge gleaned from work on Recent assemblages, correlations to pre-Quaternary oceanographic and climatic changes have successfully been made, and have provided essential paleoenvironmental information (Sluijs et al., 2005 and references therein). Reconstructions for temperature (e.g. Sluijs et al., 2006; 2011), salinity changes (e.g. Crouch et al., 2003; Harding et al., 2011), and productivity (e.g. Sluijs and Brinkhuis, 2009) can all be inferred from changes in the dinoflagellate cyst

assemblage and the appearance/disappearance of specific taxa. In one example, the dinoflagellate cyst genus *Apectodinium* is a well-documented, nearly global, indicator for the onset of the Paleocene-Eocene thermal maximum (e.g. Crouch et al., 2001; Sluijs et al., 2006), a short (Westerhold et al., 2009) and intense period of extreme global warmth (e.g. Weijers et al., 2007). This entire period is well constrained by the first and last appearance of this dinoflagellate cyst genus in the higher latitudes (e.g. Crouch et al., 2001; 2003; Sluijs et al., 2006; Sluijs and Brinkhuis, 2009).

Dinoflagellate cysts have shown to be applicable environmental proxies since they first appeared in the fossil record (Fensome et al., 1993). The earliest conclusive dinoflagellate evidence is from the Mesozoic (MacRae et al., 1996). In pre-Mesozoic strata, dinoflagellate evidence is rare, absent or unrecognized. However, there are indications that dinoflagellates may have first appeared in the Precambrian and that their appearance as we can recognize them today developed during evolutionary radiations in the Mesozoic. For example, pre-Mesozoic dinoflagellates probably had different tabulation and may have lacked a cingulum and sulcus (Fensome et al., 1999). So, it is quite possible that some Paleozoic acritarchs may represent dinoflagellates (e.g. Downie, 1973; Butterfield and Rainbird, 1998). Additionally, an analysis of dinoflagellate-based steroids shows intriguing evidence for a dinoflagellate presence well before the Triassic (Moldowan et al., 1996; Moldowan and Talyzina, 1998). Even more intriguing is the fact that the presence of dinosterane correlates well with acritarch species abundance in the Proterozoic (Fensome et al., 1999), where some specific spiny acritarch genera were concluded to be dinosterane producers (Moldowan and Talyzina, 1998).

The first confirmed dinoflagellate cyst is from the earliest mid-Triassic (Fensome et al., 1999). Triassic and early Jurassic dinoflagellate cyst records display low species diversity and simple cyst morphologies (Fig. 3.8). By the mid- to late Jurassic, practically all the major variations present in the gonyaulacoids and peridinioids were present (Fensome et al., 1999). There was also an increase in both diversity and morphological complexity, which continues well into the Cretaceous (MacRae et al., 1996). There are several peaks in diversity in the Cretaceous (Albian and Maastrichtian) and the early Eocene (MacRae et al., 1996) after which diversity decreases to the modern value (Fig. 3.8). The dinoflagellate cyst diversity trend shows parallels to sea level with highstands reflecting higher diversity and vice versa (Haq et al., 1987; MacRae et al., 1996.).

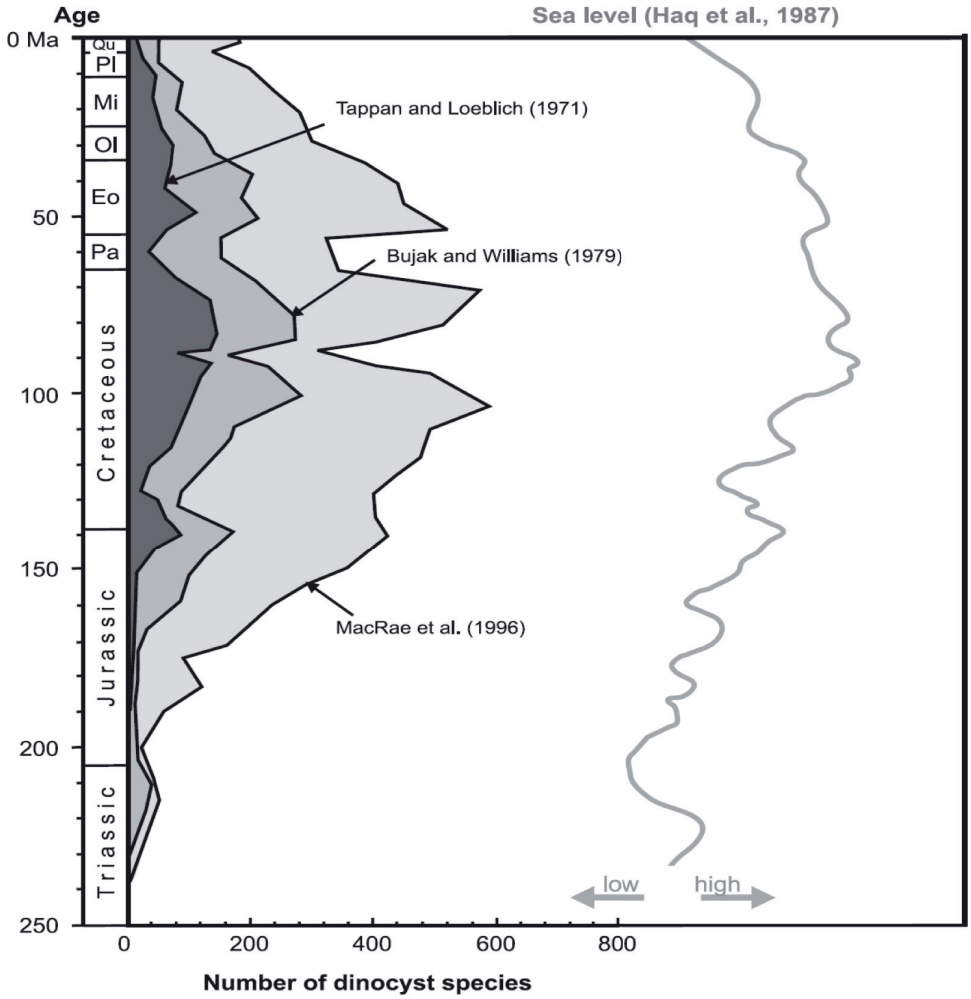

Figure 3.8: Three different curves demonstrating the diversity of dinoflagellate cysts since their first confirmed appearance in the Triassic, in relation to sea level. From Sluijs et al. (2005), after MacRae et al. (1996).

3.3.4 Selective dinoflagellate cyst preservation

Since the motile form of dinoflagellates rarely fossilizes, the dinoflagellate record is extremely biased towards the minority of species that form resting cysts. A rare exception of sorts is the case of dinocasts discussed in Versteegh et al. (2004), where cell material was fossilized through polymerization. Thecae are cellulosic in nature, which is generally considered a labile biopolymer; thecal remains have never been reported in deep sea sediments (Dale, 1992) though they have been found in anoxic lacustrine sediments (McCarthy et al., 2011). It has been known for some time that certain extant species of cysts suffer from selective oxic degradation (Table 3.1), which has the possibility of complicating the interpretation of the original surface water signal (Zonneveld et al., 1997; 2001). Studies showing selective cyst degradation are based on

laboratory (e.g. Dale, 1976; Hopkins and McCarthy, 2002) and degradation (e.g. Kodrans-Nsiah et al., 2008) experiments, sediment trap studies (Dale, 1992), and marine sediments (e.g. Zonneveld et al., 1997; 2001; Chapter 5). Despite the fact that the selective preservation of dinoflagellate cyst taxa is well documented, it is rarely considered when interpreting fossil assemblages, which can lead to misinterpretations of changing oceanographic conditions like productivity when the dinoflagellate cyst assemblage actually reflects changing redox conditions (e.g. McCarthy et al., 2000).

Table 3.1: Classification scheme of dinoflagellate cysts according to their species selective sensitivity to oxidation (adapted from Zonneveld et al., 2001).

Sensitive (S-) cysts	Resistant (R-) cysts	Moderately resistant (MR-) cysts
Brigantedinium spp.	*Impagidinium aculeatum*	*Bitectatodinium spongium*
Cyst of *Diplopelta parva*	*Impagidinium paradoxum*	*Lingulodinium machaerophorum*
Cyst of *Protoperidinium americanum*	*Impagidinium patulum*	*Operculodinium centrocarpum*
Cyst of *Protoperidinium monospinum*	*Impagidinium sphaericum*	*Operculodinium longispinigerum*
Cyst of *Protoperidinium stellatum*	*Impagidinium* spp.	*Spiniferites membranaceous*
Dubridinium spp.	*Nematosphaeropsis labyrinthus*	*Spiniferites mirabilis*
Echinidinium aculeatum	*Operculodinium israelianum*	*Spiniferites pachydermus*
Echinidinium bispiniformum	*Pentapharsodinium dalei*	*Spiniferites ramosus*
Echinidinium granulatum	*Polysphaeridium zoharyi*	*Spiniferites* spp.
Echinidinium transparantum		
Echinidinium delicatum		
Echinidinium spp.		
Leipokatium invisitatum		
Lejeunacysta oliva		
Lejeunacysta sabrina		
Lejeunacysta spp.		
Polykrikos kofoidii		
Quinquecuspis concreta		
Selenopemphix nephroides		
Selenopemphix quanta		
Stelladinium robustum		
Trinovantedinium applanatum		
Votadinium calvum		
Xandarodinium xanthum		

In general, spherical brown cysts, such as *Brigantedinium* spp. and *Echinidinium* spp., are known to be particularly sensitive to degradation, whereas the Gonyaulacales are generally considered more resistant (Fig. 3.9; Zonneveld et al., 2001; Versteegh and Zonneveld, 2002). There are essentially two different explanations for the observed selective destruction of cysts. The first is the individual cyst species sensitivity to oxidation, which has been postulated to result from differences in the cyst wall chemistry (Zonneveld et al., 2008; Chapter 6). The second is benthic preference as spherical brown cysts are prefentially degraded by the activity of benthic deposit feeders (Persson and Rosenberg, 2003). Since the presence of benthic organisms is also dependent on oxygen

concentrations in the bottom water, it can be said that oxygen, either directly or indirectly, is responsible for the selectivity of dinoflagellate cyst preservation after deposition. It has been shown that selective degradation of dinoflagellate cysts is a rapid process (Kodrans-Nsiah et al., 2008; Chapter 5) and this work suggests that most likely explanation for the differential taphonomy is a systematic difference in the composition of the cyst wall (i.e. dinosporin).

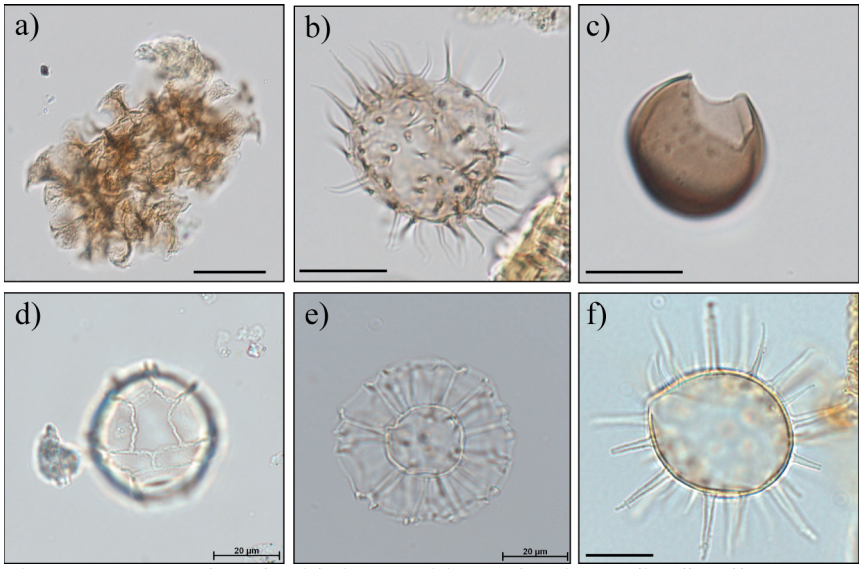

Figure 3.9: Examples of oxidation sensitive and resistant dinoflagellate cysts: a) cyst of *Polykrikos schwartzii*, b) *Echinidinium* spp., c) *Brigantedinium* spp., d) *Impagidinium patulum*, e) *Nematosphaeropsis labyrinthus*, f) *Lingulodinium machaerophorum*. Photos a-c are from the Benguela upwelling region (GeoB 2341; see Chapter 6). Photos d-f are from Marret and Zonneveld (2003). Scale bars are 20 µm.

References

Alldredge, A.L., Passow, U., Haddock, S.H.D., 1998. The characteristics and transparent exopolymer particle (TEP) content of marine snow formed from thecate dinoflagellates. *Journal of Plankton Research*, 20, 393-406.

Anderson, D.M., 1980. Effects of temperature conditioning on development and germination of *Gonyaulax tamarensis* (Dinophyceae) hypnozygotes. *Journal of Phycology*, 16, 166-172.

Anderson, D.M., Kaefer, B.A. 1987. An endogenous annual clock in the toxic marine dinoflagellate *Gonyaulax tamarensis*. *Nature*, 325, 616-617.

Anderson, D.M., Lindquist, N.L., 1985. Time-course measurements of phosphorus depletion and cyst formation in the dinoflagellate *Gonyaulax tamarensis* Lebour. *Journal of Experimental Marine Biology and Ecology*, 86, 1-13.

Anderson, D.M., Lively, J.J., Reardon, E.M., Price, C.A., 1985. Sinking characteristics of dinoflagellate cysts. *Limnology and Oceanography*, 30, 1000-1009.

Backer, L.C., Fleming, L.E., Rowan, A., Cheng, Y.-S., Benson, J., Pierce, R.H., Zaias, J., Bean, J., Bossart, G.D., Johnson, D., Quimbo, R., Baden, D.G., 2003. Recreational exposure to aerosolized brevetoxins during Florida red tide events. *Harmful Algae*, 2, 19-28.

Berner, R.A., 1989. Biogeochemical cycles of carbon and sulfur and their effect on atmospheric oxygen over Phanerozoic time. *Palaeogeography, Palaeoclimatology, Palaeoecology* (*Global and Planetary Change Section),* 75, 97-122.

Boere, A.C., Rijpstra, W.I.C., Versteegh, G.J.M., Volkman, J.K., Sinninghe Damsté, J.S., Coolen, M.J.L., 2009. Later-Holocene succession of dinoflagellates in an Antarctic fjord using a multi-proxy approach: paleoenvironmental genomics, lipid biomarkers, and palynomorphs. *Geobiology*, 7, 265-281.

Boere, A.C., Sinninghe Damsté, J.S., Rijpstra, W.I.C., Volkman, J.K., Coolen, M.J.L., 2011. Source-specific variability in post-depositional DNA preservation with potential implications for DNA based paleoecological records. *Organic Geochemistry*, 42, 1216-1225.

Boon, J.J., Rijpstra, W.I.C., de Lange, F., de Leeuw, J.W., 1979. Black Sea sterol – a molecular fossil for dinoflagellate blooms, *Nature*, 277, 125-126.

Bradford, M.R., Wall, D.A., 1984. The distribution of recent organic-walled dinoflagellate cysts in the Persian Gulf, Gulf of Oman, and northwestern Arabian Sea. *Palaeontographica*, 1192, 16-84.

Brenner, W.W., Biebow, N., 2001. Missing autofluorescence of recent and fossil dinoflagellate cysts – an indication of heterotrophy? *Neues Jahrbuch fuer Geologie und Palaeontologie, Abhandlungen*, 219, 229-240.

Butterfield, N.J., Rainbird, R.H., 1998. Diverse organic-walled fossils, including "possible dinoflagellates", from the early Neoproterozoic of arctic Canada. *Geology*, 26, 963-966.

Cembella, A.D., Quilliam, M.A., Lewis, N.I., Bauder, A.G., Dell'Aversano, C., Thomas, K., Jellett, J., Cusack, R.R., 2002. The toxigenic marine dinoflagellate *Alexandrium tamarense* as the probable cause of mortality of caged salmon in Nova Scotia. *Harmful Algae*, 1, 313-325.

Coffroth, M. A., Santos, S.R., 2005. Genetic diversity of symbiotic dinoflagellates in the genus *Symbiodinium*. *Protist*, 156, 19-34 .

Combourieu-Nebout, N., Paterne, M., Turon, J.L., Siani, G., 1998. A high-resolution record of the last deglaciation in the central Mediterranean Sea: Palaeovegetation and palaeohydrological evolution, Quaternary Science Review, 17, 303-317.

Crouch, E.M., Heilmann-Clausen, C., Brinkhuis, H., Morgans, H.E.G., Rogers, K.M., Egger, H., Schmitz, B., 2001. Global dinoflagellate event associated with the late Paleocene thermal maximum. *Geology*, 29, 315-318.

Crouch, E.M., Dickens, G.R., Brinkhuis, H., Aubry, M.P., Hollis, C.J., Rogers, K.M., Visscher, H., 2003. The *Apectodinium* acme and terrestrial discharge during the Paleocene-Eocene thermal maximum: new palynological, geochemical, and calcareous nannoplankton observations at Tawanui, New Zealand. *Palaeogeography, Palaeoclimatology, Palaeoecology*, 194, 387-403.

Dale, B., 1976. Cyst formation, sedimentation, and preservation: factors affecting dinoflagellate assemblages in recent sediments from Trondheimsfjord, Norway. *Review of Palaeobotany and Palynology*, 22, 39-60.

Dale, B., 1983. Dinoflagellate resting cysts: "benthic plankton". In: Fryxell, G.A., (Ed.), *Survival strategies of the algae*. Cambridge University Press, pp 69-136.

Dale, B., 1986. Life cycle strategies of oceanic dinoflagellates. UNESCO Technical Papers in Marine Science, 49, 65-72.

Dale, B., 1992. Dinoflagellate contributions to the open ocean sediment flux. In: Honjo, S., (Ed.), *Dinoflagellate contributions to the deep sea*. Ocean Biocenosis Series 5, Woods Hole, 1-31.

Dale, B., 1996. Dinoflagellate cyst ecology: modeling and geological applications. In: Jansonius, J., McGregor, D.C. (Eds.), Palynology: Principles and Applications. American Association of Stratigraphic Palynologists Foundation, Salt Lake City, Utah, pp. 1249-1275.

Dale, A.M., Dale, B., 1992. Dinoflagellate contributions to the sediment flux of the Nordic Seas. In: Honjo, S., (Ed.), *Dinoflagellate contributions to the deep sea*. Ocean Biocenosis Series 5, Woods Hole, 45-75.

Dale, T., Rey, F., Heimdal, B.R., 1999. Seasonal development of phytoplankton at a high latitude oceanic site. *Sarsia*, 84, 419-435.

de Vernal, A., Matthiessen, J., Mudie, P.J., Rochon, A., Boessenkool, K.P., Eynaud, F., Grøsfjeld, K., guiot, J., Hamel, D., Harland, R., Head, M.J., Kunz-Pirrung, M., Loucheur, V., Peyron, O., Pospelova, V., Radi, T., Turon, J.-L., Voronina, E., 2001. Dinoflagellate cyst assemblages as tracers of sea-surface conditions in the northern North Atlantic, Arctic and sub-Arctic seas: the new "n-677" data based and its application for quantitative paleoceanographic reconstruction. *Journal of Quaternary Science*, 16, 681-698.

Douglas, E.A., 2003. Coral bleaching – how and why? *Marine Pollution Bulletin*, 46, 385-392.

Downie, C., 1973. Observations on the nature of acritarchs. *Palaeontology*, 16, 239-259.

Esper, O., Zonneveld, K.A.F., Willems, H., 2002. Distribution of organic-walled dinoflagellate cysts in surface sediments of the southern Ocean (Atlantic sector) between the Subtropical Front and Weddell Gyre. *Marine Micropaleontology*, 46, 177-208.

Fensome, R.A., Williams, G.L., 2004. *The Lentin and Williams index of fossil dinoflagellates 2004 Edition.* American Association of Stratigraphic Palynologists, Contributions Series, 42, 909 pp.

Fensome, R.A., Taylor, F.J.R., Norris, G., Sarjeant, W.A.S., Wharton, D.I., Williams, G.L., 1993. A classification of fossil and living dinoflagellates. *Micropaleontology Press Special Paper*, 7, 351 pp.

Fensome, R.A., Riding, J.B., Taylor, F.J.R., 1996. Dinoflagellates. In: Jansonius, J., McGregor, D.C. (Eds.), *Palynology: principles and applications*. American Association of Stratigraphic Palynologists Foundation, Dallas, pp. 107-169.

Fensome, R.A., Saldarriaga, J.F., Taylor, F.J.R., 1999. Dinoflagellate phylogeny revisited: reconciling morphological and molecular based phylogenies. *Grana*, 38, 66-80.

Figueroa, R.I., Bravo, I., 2005. Sexual reproduction and two different encystment strategies of *Lingulodinium polyedrum* (Dinophyceae) in culture. *Journal of Phycology*, 41, 370-379.

Figueroa, R.I., Bravo, I., Garcés, E., 2006. The multiple routes of sexuality in *Alexandrium tailori* (Dinophyceae) in culture. *Journal of Phycology*, 42, 1028-1039.

Gaines, G., Elbrächter, M., 1987. Heterotrophic nutrition. In: Taylor, F. J. R. (Ed.), *The biology of dinoflagellates*. Botanical Monographs Volume 21, Blackwell Scientific Publications, Oxford, pp. 224-268.

Garcia-Cuetos, L., Pochon, X., Pawlowski, J., 2005. Molecular evidence for host-symbiont specificity in sorittid foraminifera. *Protist*, 156, 399-412.

Garson, M.J., Flowers, A.E., Webb, R.I., Charan, R.D., McCaffrey, E.J., 1998. A sponge/dinoflagellate association in the haplosclerid sponge *Haliclona* sp.: cellular origin of cytotoxic alkaloids by Percoll density gradient fractionation. *Cell Tissue Research*, 293, 365-373.

Gast, R.J., Beaudoin, D.J., Caron, D.A., 2003. Isolation of symbiotically expressed genes from the dinoflagellate symbiont of the solitary radiolarian *Thalassicolla nucleata*. *Biological Bulletin*, 204, 210-214.

Godhe, A., Norén, R. Kuylenstierna, M., Ekberg, C., Karlson, B., 2001. Relationship between planktonic dinoflagellate abundance, cysts recovered in sediment traps and environmental factors in the Gullmar Fjord, Sweden. *Journal of Plankton Research*, 23, 923-938.

Haq, B.U., Hardenbol, J., Vail, P.R., 1987. Chronology of fluctuating sea levels since the Triassic. *Science*, 235, 1156-1167.

Harding, I.C., Charles, A.J., Marshall, J.E.A., Pälike, H., Roberts, A.P., Wilson, P.A., Jarvis, E., Thorne, R., Morris, E., Moremon, R., Pearce, R.B., Akbari, S., 2011. Sea-level and salinity fluctuations during the Paleocene-Eocene thermal maximum in Arctic Spitsbergen. *Earth and Planetary Science Letters*, 303, 97-107.

Harland, R., Pudsey, C.J., 1999. Dinoflagellate cysts from sediment traps deployed in the Bellingshausen, Weddell and Scotia seas, Antarctica. *Marine Micropaleontology*, 37, 77-99.

Head, M.J., 1996. Modern dinoflagellate cysts and their biological affinities. In: Jansonius, J., McGregor, D.C. (Eds.), Palynology: Principles and Applications. American Association of Stratigraphic Palynologists Foundation, Dallas, Texas, pp. 1197-1248.

Heil, C.A., Glibert, P.M, Al-Sarawi, M.A., Faraj, M., Behbehani, M., Husain, M., 2001. First record of a fish-killing *Gymnodinium sp*. bloom in Kuwait Bay, Arabian Sea: chronology and potential causes. *Marine Ecology Progress Series*, 214, 15-23.

Honjo, S., 1996. Fluxes of particles to the interior of the open oceans. In: Ittekkot, V., Schaefer, P., Honjo, S., Depetris, P.J., (Eds.), *Particle flux in the ocean*. John Wiley and Sons, Chichester, 91-154.

Hopkins, J.A., McCarthy, F.M.G., 2002. Post-depositional palynomorph degradation in Quaternary shelf sediments: a laboratory experiment studying the effects of progressive oxidation. *Palynology*, 26, 167-184.

Ishikura, M., Hagiwara, K., Takishita, K., Haga, M., Iwai, K., Maruyama, T., 2004. Isolation of new *Symbiodinium* strains from tridacnid giant clam (*Tridacna crocea*) and sea slug (*Pteraeolidia ianthina*) using culture medium containing giant clam tissue homogenate. *Marine Biotechnology*, 6, 378-385.

Jacobson, D. M., Anderson, D. M., 1992. Ultrastructure of the feeding apparatus and myonemal system of the heterotrophic dinoflagellate *Protoperidinium spinulosum*. *Journal of Phycology*, 28, 69-82.

Jeffrey, S. W., Sielicki, M., Haxo, F.T., 1975. Chloroplast pigment patterns in dinoflagellates. *Journal of Phycology*, 11, 374-384.

Karako-Lampert, S., Katcoff, D.F., Achituv, Y., Dubinsky, Z., Stambler, N., 2004. Do clades of symbiotic dinoflagellates in scleractinian corals of the Gulf of Eilat (Red Sea) differ from those of other coral reefs? *Journal of Experimental Marine Biology and Ecology*, 311, 301-314.

Kodrans-Nsiah, M., de Lange, G.J., and Zonneveld, K.A.F.: A natural exposure experiment on short-term species-selective aerobic degradation of dinoflagellate cysts, Rev. Palaeobot. Palynol., 152, 32-39, 2008.

Kokinos, J.P., Anderson, D.M., 1995. Morphological development of resting cysts in cultures of the marine dinoflagellate *Lingulodinium polyedrum* (=*L. machaerophorum*). *Palynology*, 19, 143-166.

MacRae, G., Fensome, R.A., Williams, G.L., 1996. Fossil dinoflagellate diversity, originations, and extinctions and their significance. Canadian Journal of Botany, 74, 1687-1694.

Marret, F., Scourse, J., 2002. Control of modern dinoflagellate cyst distribution in the Irish and Celtic seas by seasonal stratification dynamics. *Marine Micropaleontology*, 47, 101-116.

Marret, F., Zonneveld, K.A.F., 2003. Atlas of modern organic-walled dinoflagellate cyst distribution. *Marine Micropaleontology*, 125, 1-200.

Matsuoka, K., 1985. Archeopyle structure in modern gymnodinialean dinoflagellate cysts. *Review of Palaeobotany and Palynology*, 44, 217-231.

Matsuoka, K., 1992. Seasonal variability of palynomorphs in a JT-03 sediment trap settled in the Japan Trench. *Bulletin of the Faculty of Liberal Arts*, Nagasaki University, Natural Science, 32, 221-233.

Matsuoka, K., Fukuyo, Y., 2000. *Technical guide for modern dinoflagellate cyst study*. WESTPAC-HAB/WESTPAC/IOC, 77 pp.

Matthiessen, J., 1995. Distribution patterns of dinoflagellate cysts and other organic-walled microfossils in recent Norwegian-Greenland Sea sediments. *Marine Micropaleontology*, 24, 307-334.

Matthiessen, J., de Vernal, A., Head, M., Okolodkov, Y., Zonneveld, K.A.F., Harland, R., 2005. Modern organic-walled dinoflagellate cysts in Arctic marine environments and their (paleo-) environmental significance. *Palaeontologische Zeitschrift*, 79, 3-51.

McCarthy, F.M.G., 2011. *Freshwater dinoflagellates in paleolimnological studies*. IX International Conference on Modern and Fossil Dinoflagellates (DINO9), Liverpool, UK. Abstract.

McCarthy, F.M.G., Gostlin, K.E., Mudie, P.J., Scott, D.B., 2000. Synchronous palynological changes in early Pleistocene sediments off New Jersey and Iberia, and a possible paleoceanographic explanation. *Palynology*, 24, 63-77.

Moldowan, J.M., Dahl, J., Jacobson, S.R., Huizinga, B.J., Fago, F.J., Shetty, R., Watt, D.S., Peters, K.E., 1996. Chemostratigraphic reconstruction of biofacies: molecular evidence linking cyst-forming dinoflagellates with pre-Triassic ancestors. *Geology*, 24, 159-162.

Moldowan, J.M., Talyzina, N.M., 1998. Biogeochemical evidence for dinoflagellates in the Early Cambrian. *Science*, 281, 1168-1170.

Montresor, M., Zingone, A., Sarno, D., 1998. Dinoflagellate cyst production at a coastal Mediterranean site. *Journal of Plankton Research*, 20, 2291-2312.

Morquecho, L., Lechuga-Nevéze, C.H., 2004. Seasonal occurrence of planktonic dinoflagellates and cyst production in relationship to environmental variables in subtropical Bahía Concepcíon, Gulf of California. *Botanica Marina*, 47, 313-322.

Mouradian, M., Panetta, R.J., de Vernal, A., Gélinas, Y., 2007. Dinosterols or dinocysts to estimate dinoflagellate contributions to marine sedimentary organic matter? *Limnology and Oceanography*, 52, 2569-2581.

Mudie, P.J., 1996. Pellets of dinoflagellate-eating zooplankton. In: Jansonius, J., McGregor, D.C., (Eds.), *Palynology: Principles and applications.* American Association of Stratigraphic Palynologists, Salt Lake City, pp. 1087-1089.

Nash, E. A., Barbrook, A.C., Edwards-Stewart, R.K., Bernhardt, K., Howe, C.J., Nisbet, R.E., 2007. Organization of the mitochondrial genome in the dinoflagellate *Amphidinium carterae. Molecular Biology and Evolution,* 24, 1528-1536.

Pemberton, K., Rees, A.P., Miller, P.I., Raine, R., Joint, I., 2004. The influence of water body characteristics on phytoplankton diversity and production in the Celtic Sea. *Continental Shelf Research*, 24, 2011.

Persson, A., Godhe, A., Karlson, B., 2000. Dinoflagellate cysts in recent sediments from the West coast of Sweden. *Botanica Marina*, 43, 69-79.

Persson, A., Rosenberg, R., 2003. Impact of grazing and bioturbation of marine benthic deposit feeders on dinoflagellate cysts. *Harmful Algae*, 2, 43-50.

Pinturier-Geiss, L., Méjanelle, L., Dale, B., Karlsen, D.A., 2002. Lipids as indicators of eutrophication in marine coastal sediments. *Journal of Microbiological Methods*, 48, 239-257.

Pospelova, V., Chmura, G.L., Boothman, W.S., Latimer, J.S., 2002. Dinoflagellate cyst records and human disturbance in two neighboring estuaries, New Bedford Harbor and Apponagansett Bay, Massachusetts (USA). *Science of the Total Environment*, 298, 81-102.

Reichart, G.J., Brinkhuis, H., 2003. Late Quaternary *Protoperidinium* cysts as indicators of paleoproductivity in the northern Arabian Sea. *Marine Micropaleontology*, 49, 303-315.

Ribeiro, S., Berge, T., Lundholm, N., Andersen, T.J., Abrantes, F., Ellegaard, M., 2011. Phytoplankton growth after a century of dormancy illuminates past resilience to catastrophic darkness. *Nature Communications*, 2, doi: 10.1038/ncomms1314.

Rochon, A., de Vernal, A., Turon, J.L., Matthiessen, J., Head, M.J., 1999. Distribution of recent dinoflagellate cysts in surface sediments from the North Atlantic Ocean and adjacent seas in relation to sea-surface parameters. *American Association of Stratigraphic Palynologists Contribution Series*, 35, 1-146.

Rochon, A., Lewis, J., Ellegaard, M., Harding, I.C., 2009. The *Gonyaulax spinifera* (Dinophyceae) "complex": Perpetuating the paradox? *Review of Palaeobotany and Palynology*, 155, 52-60.

Sachs, J.P., Schwab, V.F., 2011. Hydrogen isotopes in dinosterol from the Chesapeake Bay estuary. *Geochimica et Cosmochimica Acta*, 75, 444-459.

Sangiorgi, F., Donders, T.H., 2004. Reconstructing 150 years of eutrophication in the north-watern Adriatic Sea (Italy) using dinoflagellate cysts, pollen and spores. *Estuarine, Coastal and Shelf Science*, 60, 69-79.

Sangiorgi, F., Fabbri, D., Comandini, M., Gabbianelli, G., Tagliavini, E., 2005. The distribution of sterols and organic-walled dinoflagellate cysts in surface sediments of the North-western Adriatic Sea (Italy). *Estuarine, Coastal and Shelf Science*, 64, 395-406.

Schnepf, E., Elbrächter, M., 1992. Nutritional strategies in dinoflagellates: a review with emphasis on cell biological aspects. *European Journal of Protistology*, 28, 3-24.

Schnepf, E., Elbrächter, M., 1999. Dinophyte chloroplasts and phylogeny-a review. *Grana*, 38, 81-97.

Schönberg, C.H.L., Loh, W.K.W., 2005. Molecular identity of the unique symbiotic dinoflagellates found in the bioeroding demosponge *Cliona orientalis*. *Marine Ecological Progress Series*, 299, 157-166.

Siano, R., Montresor, M., Probert, I., Not, F., de Vargas, C., 2010. *Pelagodinium* gen. nov. and *P. béli* comb. nov., a dinoflagellate symbiont of planktonic foraminifera. *Protist*, 161, 385-399.

Slamovits, C. H., Saldarriaga, J.F., Larocque, A., Keeling, P.J., 2007. The highly reduced and fragmented mitochondrial genome of the early-branching dinoflagellate *Oxyrrhis marina* shares characteristics with both apicomplexan and dinoflagellate mitochondrial genomes. *Journal of Molecular Biology*, 372, 356-368.

Sluijs, A., Brinkhuis, H., 2009. A dynamic climate and ecosystem state during the Paleocene Eocene Thermal Maximum: inferences from dinoflagellate cyst assemblages on the New Jersey shelf. *Biogeosciences*, 6, 1755-1781.

Sluijs, A., Pross, J., Brinkhuis, H., 2005. From greenhouse to icehouse; organic-walled dinoflagellate cysts as paleoenvironmental indicators in the Paleogene. Earth-Science Reviews, 68, 281-315.

Sluijs, A., Schouten, S., Pagani, M., Woltering, M., Brinkhuis, H., Sinninghe Damsté, J.S., Dickens, G.R., Huber, M., Reichart, G.J., Stein, R., Matthiessen, J., Lourens, L.J., Pedentchouk, N., Backman, J., Moran, K., Expedition 302 Scientists, 2006. Subtropical Arctic Ocean temperatures during the Palaeocene/Eocene thermal maximum. *Nature*, 441, 610-613.

Sluijs, A., Bijl, P.K., Schouten, S., Röhl, U., Reichart, G.-J., Brinkhuis, H., 2011. Southern ocean warming, sea level and hydrological change during the Paleocene-Eocene thermal maximum. *Climate of the Past,* 7, 47-61.

Steidinger, K., 1993. Some taxonomic and biologic aspects of toxic dinoflagellates. In: Falconer, I.R., (Ed.), *Algal Toxins in Seafood and Drinking Water*. Academic Press, New York, 224 pp.

Stoeker, D.K., 1999. Mixotrophy among Dinoflagellates. *Journal of Eukaryotic Microbiology*, 46, 397-401.

Sournia, A., 1982. Form and function in marine phytoplankton. *Biological Revue*, 57, 347-394.

Tamelander, T., Heiskanen, A.S., 2004. Effects of spring bloom phytoplankton dynamics and hydrography on the composition of settling material in the coastal northern Baltic Sea. *Journal of Marine Systems*, 52, 217-234.

Taylor, F.J.R., 1987. *The Biology of Dinoflagellates*. Botanical Monographs, Blackwell Scientific Publications, Oxford, 785 pp.

Taylor, F.J.R., Hoppenrath, M., Saldarriaga, J.F., 2008. Dinoflagellate diversity and distribution. *Biodiversity and Conservation*, 17, 407-418.

Taylor, F.J.R., Pollingher, U., 1987. The ecology of dinoflagellates. In: Taylor, F.J.R., (Ed.), *The Biology of Dinoflagellates*. Blackwell Scientific Publications, Oxford, pp. 398-529.

Thornhill, D.F., Xiang, Y., Fitt, W.K., Santos, S.R., 2009. Reef endemism, host specificity and temporal stability in populations of symbiotic dinoflagellates from two ecologically dominant Caribbean corals. *PLoS ONE*, 7, e6262.

Trench, R.K., Wethey, D.S., Porter, J.W., 1981. Observations on the xymbiosis with zooxanthellae among the *Tridacnidae* (Mollusca, Bivalvia). *Biological Bulletin*, 161, 180-198.

Versteegh, G.J.M., Zonneveld, K.A.F., 2002. Use of selective degradation to separate preservation from productivity. *Geology*, 30, 615-618.

Versteegh, G.J.M., Blokker, P., Wood, G., Collinson, M.E., Sinninghe Damsté, J.S., de Leeuw, J.W., 2004. An example of oxidative polymerization of unsaturated fatty acids as a preservation pathway for dinoflagellate organic matter. *Organic Geochemistry*, 35, 1129-1139.

Vink, A., Zonneveld, K.A.F., Willems, H., 2000. Organic-walled dinoflagellate cysts in western equatorial Atlantic surface seiments: Distributions and their relation to environment. *Review of Palaeobotany and Palynology*, 112, 247-286.

Volkmann, J.K., Barrett, S.M., Dunstan, G.A., and Jeffrey, S.W.: Geochemical significance of the occurrence of dinosterol and other 4-methyl sterols in a marine diatom, Org. Geochem., 20, 7-15, 1993.

Volkman, J.K., Rijpstra, W.I.C., de Leeuw, J.W., Mansour, M.P., Jackson, A.E., and Blackburn, S.I., 1999. Sterols of four dinoflagellates from the genus *Prorocentrum*, Phytochem., 52, 659-668.

von Dassow, P., Montresor, M., 2011. Unveiling the mysteries of phytoplankton life cycles: patterns and opportunities behind complexity. *Journal of Plankton Research*, 33, 3-12.

Walker, L. M., 1984. Life histories, dispersal and survival in marine, planktonic dinoflagellates. In: Steidinger, K. A., Walker, L. M., (Eds.), *Marine Plankton Life Cycle Strategies*. CRC press, Florida, USA, pp 19-34.

Wall, D., Dale, B., 1968. Modern dinoflagellate cysts and evolution of the Peridiniales. *Micropaleontology*, 14, 265–304.

Wall, D., Dale, B., Lohmann, G.P., Smith, W.K., 1977. The environmental and climatic distribution of dinoflagellate cysts in modern marine sediments from regions in the North and South Atlantic Oceans and adjacent seas. *Marine Micropaleontology*, 2, 121-200.

Weijers, J.W.H., Schouten, S., Sluijs, A., Brinkhuis, H., Sinninghe Damsté, J.S., 2007. Warm arctic continents during the Palaeocene-Eocene thermal maximum. *Earth and Planetary Science Letters*, 261, 230-238.

Westerhold, T., Röhl, U., McCarren, H.K., Zachos, J.C., 2009. Latest on the absolute age of the Paleocene-Eocene Thermal Maximum (PETM): New insights from exact stratigraphic position of key ash layers +19 and -17. *Earth and Planetary Science Letters*, 287, 412-419.

Yellowlees, D., Rees, T.A.V., Leggat, W., 2008. Metabolic interactions between algal symbionts and invertebrate hosts. *Plant Cell and Environment*, 31, 679-694.

Zonneveld, K.A.F., 2011. Determination key of modern dinoflagellate cysts. University of Bremen, Bremen, Germany. 34 pp., 10 pl.

Zonneveld, K.A.F., Versteegh, G.J.M., de Lange, G.J., 1997. Preservation of organic-walled dinoflagellate cysts in different oxygen regimes: a 10,000 year natural experiment. *Marine Micropaleontology*, 29, 393-405.

Zonneveld, K.A.F., Brummer, G.J.A., 2000. (Palaeo-) ecological significance, transport, and preservation of organic-walled dinoflagellate cysts in the Somali Basin, NW Arabian Sea. *Deep-Sea Research Part II*, 47, 2229-2256.

Zonneveld, K.A.F., Hoek, R.P., Brinkhuis, H., Willms, H., 2001a. Geographical distributions of organic-walled dinoflagellate cysts in surficial sediments of the Benguela upwelling region and their relationship to upper ocean conditions. Progress in Oceanography, 48, 25-72.

Zonneveld, K.A.F., Versteegh, G.J.M., de Lange, G.J., 2001b. Palaeoproductivity and post-depositional aerobic organic matter decay reflected by dinoflagellate cyst assemblages of the Eastern Mediterranean S1 sapropel. *Marine Geology*, 172, 181-195.

Zonneveld, K.A.F., Versteegh, G.J.M., Kodrans-Nsiah, M., 2008. Preservation and organic chemistry of Late Cenozoic organic-walled dinoflagellate cysts: A review, *Marine Micropaleontology*, 68, 179-197.

Chapter 4

Methods

4.1 Palynological methods

Palynology is the study of OM-based microscopic fossils (palynomorphs, see Section 2.2.2) and a subdiscipline of geology and paleontology. It is a useful subject for providing biostratigraphic and (paleo-) ecological information. Accurate sample processing and identification techniques are thus essential procedures in order to avoid contamination or alteration of a palynomorph assemblage. While some authors describe their methodology in detail (e.g. Riding and Kyffin-Hughes, 2004 and references therein), many others do not besides mentioning that a "standard" palynological technique was used. However, this description is fairly unclear as many different processing, identification and quantification techniques are available and routinely used.

4.1.1. Processing

Palynomorphs are usually (though not necessarily; e.g. Riding Kyffin-Hughes, 2004) extracted from the sediment and sedimentary rock matrix by treatment with concentrated acids. These acids digest certain components of the overall matrix and, in essence, isolate the palynomorphs for study. Ideally, the procedure does not affect the size, shape, and preservation of the palynomorphs. Most procedures use HCl to dissolve the carbonate fraction and HF to remove silicate minerals (Doher, 1980). After each step, the residue is neutralized. Methods of neutralization vary though the most common is rinsing with deionized or distilled water (e.g. Mertens et al., 2009). The addition of KOH can also be used, as in Chapter 5. However, neutralization with KOH can cause swelling of the palynomorphs and, if the solution becomes alkaline, the rapid selective destruction of protoperidiniacean cysts (≤ 5 min; e.g. Mertens et al., 2009). Thus, extreme care must be taken to ensure that the solution does not become alkaline. In all other studies in this thesis where chemical treatments were used, residues were neutralized with distilled water.

The resulting residue can be further "cleaned" and concentrated by a brief oxidizing treatment, commonly with nitric acid (Funkhouser and Evitt, 1959), ultrasonication, density separation, decantation and/or sieving (Ediger, 1986). All of these processes separate the palynomorphs from extraneous organic matter; however, all have disadvantages. Oxidizing agents like nitric acid have been shown to selectively destroy palynomorphs (Dale, 1976; Schrank, 1988; Hopkins and McCarthy, 2002). Prolonged ultrasonic treatment can destroy more delicate dinoflagellate cysts (McIntyre and Norris, 1964; Hodgkinson, 1991), so a maximum time of 60 seconds is recommended (Mertens et al., 2009). Finally, significant amounts of material can be lost during decanting and sieving procedures (Lignum et al., 2008; Mertens et al., 2009), although decanting over a sieve and using a maximum sieve size of 15 μm can minimize these losses. In the end, the type of procedure used should depend on the specific sample and intended analyses. For example, if a sample contains significant amounts of siliclastic or organic material, a sieve mesh size < 15 μm is impractical. Furthermore, if the cysts are intended for geochemical analyses, oxidizing agents should be avoided and care taken to prevent contamination. In this particular work, the preparation methods varied slightly and details are given in each individual study. For the most part, processing steps follow recommendations in Mertens et al. (2009).

4.1.2 Identification

Dinoflagellate cysts are traditionally identified to the species level through the use of a light microscope. The important morphological characteristics for cyst identification are the shape of the cyst body and its ornamentation, wall structure and color, paratabulation, and archeopyle (Matsuoka and Fukuyo, 2000). However, this technique is not without its caveats. For example, most cysts have, in contrast to the motile forms, a spherical to peridinioid shape. Additionally, while the archeopyle type is useful, especially in the determination of higher classification ranks, it is not always visible and in the case of cells that failed to excyst, may not even be present. Thus, cyst identification based on a single morphological characteristic is not always reliable and the most accurate identifications are based on a combination of several features.

4.1.3 Quantification

Palynomorph assemblage data can be presented qualitatively or quantitatively. Generally, qualitative data are depicted as the % abundance of a given taxa within the entire assemblage, and is a measure of the species diversity. The main source of error here is observer bias, which is influenced by the experience of the observer as well as the ambiguity of the taxa and/or specimen (Mertens et al., 2009). Despite this bias, reproducibility of relative abundance data is generally good. In contrast, reproducibility of quantitative data is more problematic and primarily depends on the processing method (Mertens et al., 2009). There are two main types of quantification: the first is via the marker-grain method (Stockmarr, 1971) and the second is the volumetric method (Dale, 1976; Holzwarth et al., 2007). The marker-grain method involves the addition of *Lycopodium clavatum* Linnaeus (Stag's horn clubmoss) tablets before acid treatment. A known number of spores are contained in the calcium carbonate-based tablet so that quantification of the number of cysts per gram in a sample is possible (Lignum et al., 2008). Concentrations based on the volumetric method involve concentrating the residue to a specific volume, mounting an aliquot on a slide and counting the entire slide. The volumetric method was used in this work when quantification was performed (Chapter 5).

4.2 Fourier Transform Infrared (FTIR) spectroscopy

Infrared radiation is a form of electromagnetic energy. When this energy is directed at a sample of unknown material (i.e. a dinoflagellate cyst), molecules within the sample absorb some of the energy while the rest is transmitted (passes through). The absorbed IR radiation causes a permanent dipole movement, which results in characteristic vibrational frequencies for a particular bond type. Thus, absorption peaks that appear in the resulting sample's signal, called a spectrum, correspond to the vibrational frequencies of the atomic bond types and are reproducible as well as characteristic (e.g. Coates, 2000). In a spectrum, the combination of functional group frequencies (x-axis) and the band intensities (y-axis) comprise the overall signal of the sample. An interpretation of the spectrum can provide information on structural features of a compound (e.g. functional groups, aromaticity, unsaturation; see Fig. 4.1). Furthermore, that information can be qualitative (i.e. identification of particular functional groups as well as local orientation) as well as quantitative. A given absorption peak increases proportionately with the

number of times that specific bond type is present (Coates, 2000). Thus, the size of a peak corresponds to the amount present in the sample. While FTIR analysis gives an overall idea of the chemical nature of a sample, it does not provide conclusive information as to the way chemical bonds are arranged into a macromolecular structure.

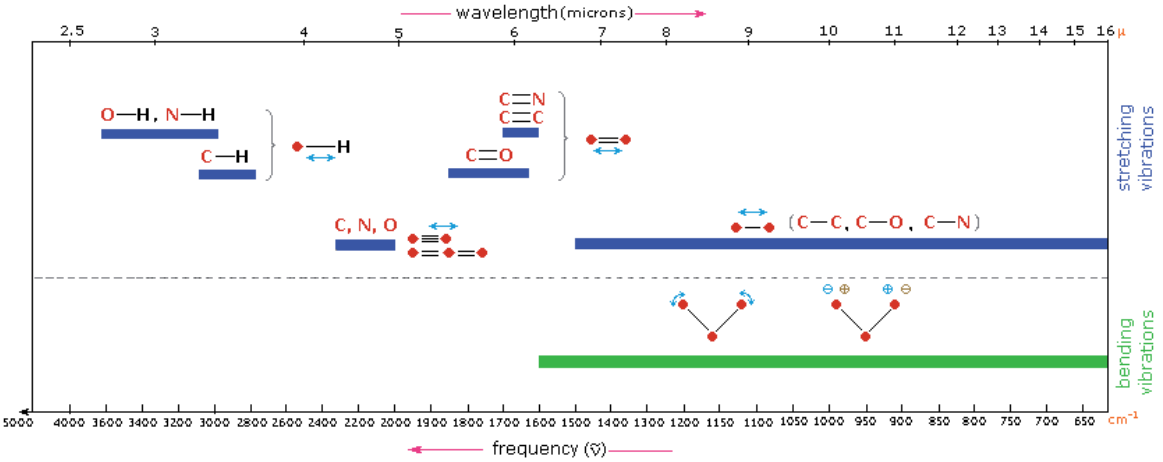

Figure 4.1: Simplified scheme showing characteristic vibrational movement and absorption frequencies for different bond types. Bending and stretching refer to types of motion (angular changes). From Reusch (2011).

FTIR has previously been used to characterize torbanites (e.g. Landais et al., 1993), acritarchs (e.g. Marshall et al., 2005; Javaux and Marshall, 2006), fossil plant cuticles (Mösle et al., 1998; Collinson et al., 1998), fossil arthropods (Stankiewicz et al., 1998), sporopollenin (Yule et al., 2000; Zimmermann, 2010), and algaenan (e.g. Derenne et al., 1997; Allard and Templier, 2000). It has also been proposed as a relatively fast method for the speciation of different pollen grains (e.g. Pappas et al., 2003). In terms of its utilization in the analysis of dinoflagellate cysts, it has been used on a couple of occasions in investigations of cyst wall chemistry (e.g. Kokinos et al., 1998; Versteegh et al., 2007). However, these analyses were carried out on a culture sample and a monotypic assemblage, respectively, and a greater amount of material was available for analysis. In this thesis, the FTIR machine was coupled to a microscope, which allowed for the analysis of single dinoflagellate cysts.

4.2.1 Sample preparation

FTIR and micro-FTIR differ slightly in their sample preparation. FTIR requires pressing the sample into, for example, a KBr pellet, while in micro-FTIR a specimen is placed on a salt slide and analyzed directly. The specimen generally needs to be larger than 20 µm.

Thus, this is a large advantage over FTIR, as individual specimens can be analyzed accurately and preparation time is significantly reduced because the isolation of large quantities of palynomorphs is not necessary.

Due to the fact that micro-FTIR has not been used to analyze dinoflagellate cysts before, there is no standard preparation technique available. However, the method used in this thesis was modified from Versteegh et al. (2007) and Javaux and Marshall (2006). One possible source of error can be the inadvertent alteration of the chemical composition of the dinoflagellate cyst. For example, the use of oxidizing agents (Versteegh et al., 2007) or hydroxides (i.e. KOH) has the potential to modify functional groups (e.g. deprotonating carboxylic acids into carboxylates). In the case of lithified samples, the use of strong acids cannot be avoided, as they are the best method to separate dinoflagellate cysts from the rock matrix (Section 4.1.1). However, only HF was used for lithified sediment in this work (Chapter 7; 8) as the samples contained very little carbonate. For the Recent samples (Chapter 6), no chemical treatments were used. While this eliminates prospective alteration that may occur from the acids, it can still produce complications, as the FTIR absorption of silica occurs in the same range as ether bonds (Coates, 2000; discussed in Chapter 6).

4.2.2 Analytical components

Mechanistically, FTIR spectroscopy is quite simple. It consists of two parts: an optical bench coupled to a computer. The optical bench comprises the IR source, the interferometer, where spectral encoding takes place, and the detector. The optical bench measures the intensity of the coded infrared beam after it passes through the sample. The resulting signal, called an interferogram, contains the intensity information of all the frequencies in the beam. The computer then reads the interferogram, and using the FT algorithm, decodes the intensity information for each frequency, which produces the final spectrum for the sample. Further advantages of FTIR include that it is non-destructive to the sample; for example, the specimens analyzed in Chapter 6 are the same specimens that were also used in the fluorescence photography. Furthermore, the measurements themselves require no calibration, the data do not need extensive manipulation after collection (spectra are essentially raw data), and the assignment of major frequency groups is fairly straightforward (Reusch, 2011). The major frequency group identification

is generally based on comparisons to published spectra (e.g. Colthup et al., 1990; Pandey et al., 1999; Coates, 2000).

4.2.3. Quantification

As mentioned previously, FTIR is also a quantitative method, as the absorption intensity increases proportionately with atomic bond presence. Quantification was generally performed very simply in this work through use of the software available with the FTIR (OMNIC 3.1). The program ImageJ64 was also used when spectra were compared to previously published FTIR spectra, as this program creates a pixilated area to integrate. In both cases, quantification involved integrating the areas under an absorption peak after baseline correction in absorbance mode. Absorbance mode is preferred for quantitative analyses because it is really the parameter that reflects concentration. It can be operationally defined as a measure of the quantity of light that a dinoflagellate cyst neither transmits nor reflects, while the transmittance is a ratio of the light intensity that has passed through the dinoflagellate cyst to the initial light intensity. Therefore, absorbance units are proportional to the amount of a certain bond type and the transmittance is a percentage. It is possible to convert between the two parameters and both are presented in the literature (e.g. Pandey, 1999; Yule et al., 2000; Foster et al., 2002; Steemans et al., 2010; Versteegh et al., in press). In this thesis, spectra are presented using either absorbance or transmittance. In order to allow for the comparison between spectra, peak areas can either be normalized or compared via the use of ratios. The use of ratios is preferred as it allows for the comparison of the spectral band strength between specimens and species without closed sum effects.

4.3 Chromatographic methods

Chromatography coupled to mass spectrometry is a category of analytical techniques that allow for complex mixtures of chemicals to be physically separated, identified, and quantified. It is used in this work to identify and quantify lipid biomarkers in Chapter 5. The chromatography component separates the compounds and the mass spectrometer (MS) provides detailed structural information for individual identification. In gas chromatography (GC), the compounds are separated in a gaseous phase while in liquid

chromatography, such as high performance liquid chromatography (HPLC), the separation is achieved in the liquid phase.

GC-MS is a good method for the analysis of relatively low molecular weight compounds, which must also be sufficiently volatile and thermally stable. In contrast, HPLC-MS allows for the analysis a wider range of compounds. These include higher molecular weight compounds, compounds with higher polarity, and more thermally labile compounds. Both of these methods are particularly useful in paleoclimatology for identifying and tracing contributors to the OM of the water column and sedimentary record (e.g. Eglinton and Eglinton, 2008).

4.3.1 Sample preparation

Generally, samples are first solvent extracted to isolate the "extractable" (i.e. not adsorbed) lipid components. Thus, only those components, which are soluble in the chosen solvent mixture end up in the extract. Compounds more tightly bound to the sediment matrix (i.e. bound lipids) are not analyzed unless additional steps are performed, such as saponification of the sediment. In GC-MS, further modifications, such as the derivitization of functional groups to produce sufficiently amenable low molecular weight compounds, are generally necessary. As HPLC-MS can accomodate compounds with a higher molecular mass, polarity and lability, the number of procedures required after lipid extraction to make compounds amenable for analysis is much reduced. Specific procedural details used in this work are discussed in Chapter 5.

4.3.2 Analytical components

The following brief description is taken from Killops and Killops (2004). In GC-MS, a sample is injected into the gas chromatograph, vaporized and moved onto the chromatographic column by an inert carrier gas such as helium. As the sample moves through the capillary column, individual components are separated by their interaction with the column coating (stationary phase; usually silica) and the carrier gas (mobile phase; He). As the sample moves along the capillary, the oven, which houses the capillary column, can be programmed to increase the temperature gradually. Thus, the separation of compounds present in the sample is achieved in two parts: (1) through interactions with the stationary phase and (2) temperature. Compounds that interact with

the stationary phase quickest and have a low boiling point elute from the column sooner. The time from injection to when elution occurs is referred to as the retention time (RT). Knowing the RT for a given compound can provide some information towards the identification because, assuming GC conditions remain the same, a compound will always elute from the column at about the same RT (Fig. 4.2).

As the separated compounds from the sample elute from the GC column, and enter the MS, they are bombarded by a stream of electrons. This energy is enough to knock an electron off of the organic molecules, producing fragments in a characteristic and reproducible way. Some of these fragments are charged ions (resonant ions) that can be detected by the MS. As the patterns of fragmentation are characteristic for different organic compounds, they are thus identifiable. The mass of the fragment divided by the charge is called the mass to charge ratio (m/z). As most compounds have a charge of +1, the m/z usually represents the molecular mass of the fragment. A grouping of four electromagnets, termed a quadrapole, focuses the fragments through a slit and an associated computer directs the quadrapoles to allow certain m/z fragments through to the detector. The computer program has the quadrapoles cycle through a range of m/z values many times per second with the full range cycle called a scan. Each scan produces a graph with the x-axis depicting the m/z and the y-axis representing signal intensity for each of the detected fragments. Overall, this graph is referred to as a mass spectrum and is a useful tool for identifying and quantifying unknown organic compounds (Fig. 4.2).

In HPLC-MS, the principles are essentially the same; thus only the differences are mentioned. Through the HPLC, the injected sample remains in liquid form, and the mobile phase is a solvent mixture. Thus, separation is achieved via interaction with the stationary phase (silica) and the eluent, which increases in polarity over time. The HPLC is coupled to a MS via a specialized interface, such as an atmospheric pressure chemical ionization (APCI) interface, which serves to, as the name suggests, ionize the molecules as they elute from the capillary column. Essentially, as the compounds elute, the solution is introduced to a pneumatic nebulizer and desolvated, then ionized through interaction with the corona discharge and collisions with vaporized solvent molecules before being transferred to the MS.

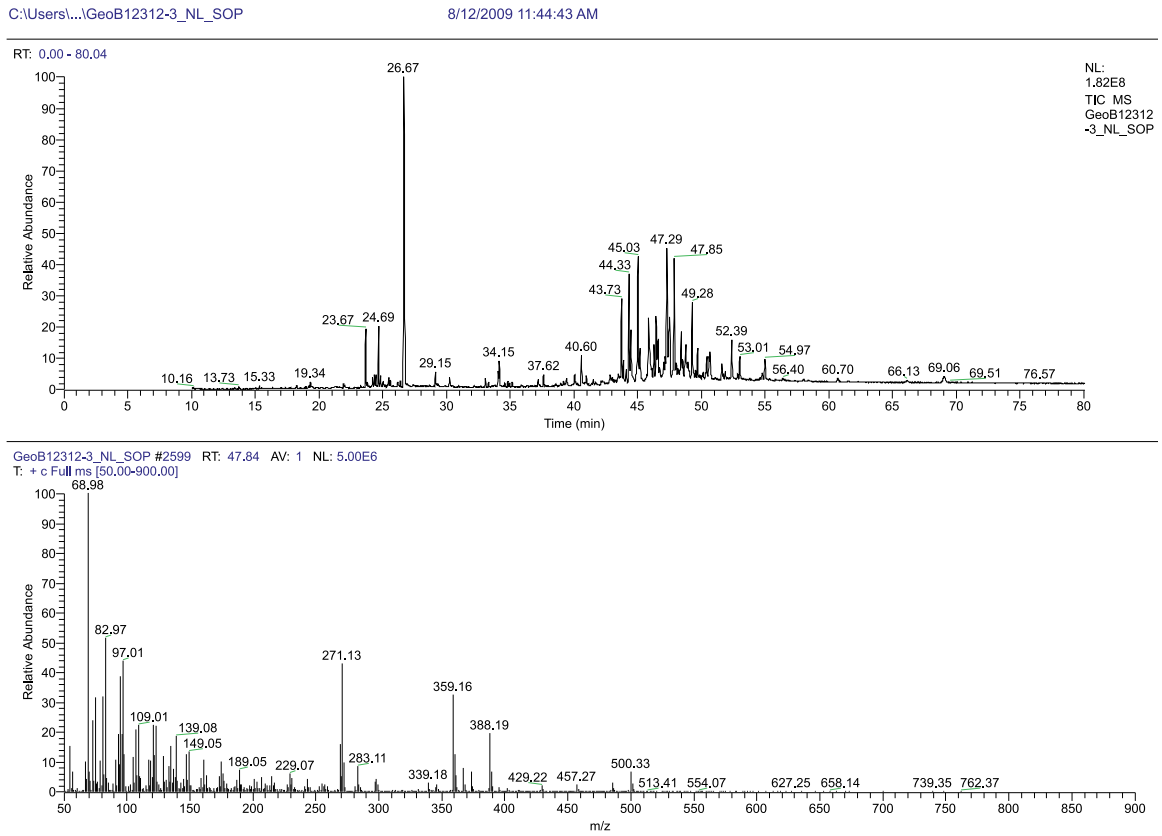

Figure 4.2: An example of a GC-MS run of neutral lipids from the northeastern Arabian Sea (GeoB 12312). Top window is the GC showing compounds elute at specific RTs. Bottom window is the mass spectrum of dinosterol (RT=47.85).

4.3.3 Quantification

Essentially, quantification of the analyzed compounds is performed through comparison of its peak size to a standard (e.g. Huguet et al., 2006). In the GC-MS analysis in Chapter 5, a mixture of standards was added to the solution prior to derivatization. Unfortunately, quantifying with a GC-MS means that the relative response factors of the compounds are not known, and thus assumed to be 1. As a result, this is not the most robust method of quantification. However, as the specific reason for the analysis was to compare the relative change in concentrations between samples, this method is considered sufficient. For the HPLC-MS analysis, the relative abundance of compounds was used, so no standards were needed.

References

Allard, B., Templier, J., 2000. Comparison of neutral lipid profile of various trilaminar outer cell wall (TLS)-containing microalgae with emphasis on algaenan occurrence. *Phytochemistry*, 54, 369-380.

Coates, J., 2000. Interpretation of Infrared Spectra, A Practical Approach. In: Meyers, R.A. (Ed.), *Encyclopedia of Analytical Chemistry*. John Wiley and Sons Ltd., pp. 10815-10837.

Collinson, M.E., Mösle, B., Finch, P., Scott, A.C., Wilson, R., 1998. Structure, biosynthesis and biodegradation of cutin and suberin. *Ancient Biomolecules*, 2, 251-265.

Colthup, N.B., Daly, L.H., Wiberly, S.E., 1990. *Introduction to Infrared and Ramna Spectroscopy*. Academic Press Limited, London, 282 pp.

Dale, B., 1976. Cyst formation, sedimentation, and preservation: factors affecting dinoflagellate assemblages in recent sediments from Trondheimsfjord, Norway. *Review of Palaeobotany and Palynology*, 22, 39-60.

Derenne, S., Largeau, C., Hetényi, M., Brukner-Wein, A., Connan, J., Lugardon, B., 1997. Chemical structure of the organic matter in a Pliocene maar-type shale: Implicated *Botryococcus* race strains and formation pathways. *Geochimica et Cosmochimica Acta*, 61, 1879-1889.

Doher, L.I., 1980. Palynomorph separation procedures currently used in the paleontology and stratigraphy laboratories, US Geological Survey. *Geological Survey Circular*, 830, 1-29.

Ediger, V.S., 1986. Sieving techniques in palynological sample processing with special reference to the MRA system. *Micropaleontology*, 32, 256-270.

Eglinton, T.I., Eglinton, G., 2008. Molecular proxies for paleoclimatology. *Earth and Planetary Science Letters*, 275, 1-16.

Foster, G.B., Stephenson, M.H., Marshall, C., Logan, G.A., Greenwood, P.F., 2002. A revision of *Reduviasporonites* Wilson 1962: Description, illustration, comparison and biological affinities. *Palynology*, 26, 35-58.

Funkhouser, J.W., Evitt, W.R., 1959. Preparation techniques for acid-insoluble microfossils. *Micropaleontology*, 5, 369-375.

Hodgkinson, R.L., 1991. Microfossil processing: a damage report. *Micropaleontology*, 37, 320-326.

Holzwarth, U., Esper, O., Zonneveld, K., 2007. Distribution of organic-walled dinoflagellate cysts in sediments of the Benguela upwelling system in relationship to environmental conditions. *Marine Micropaleontology*, 64, 91-119.

Hopkins, J.A., McCarthy, F.M.G., 2002. Post-depositional palynomorph degradation in Quaternary shelf sediments: a laboratory experiment studying the effects of progressive oxidation. *Palynology*, 26, 167-184.

Huguet, C., Hopmans, E.C., Febo-Ayala, W., Thompson, D.H., Sinninghe Damsté, J.S., Schouten, S., 2006. An improved method to determine the absolute abundance of glycerol dibiphytanyl glycerol tetraether lipids. *Organic Geochemistry*, 37, 1036-1041.

Javaux, E.J., Marshall, C.P., 2006. A new approach in deciphering early protist paleobiology and evolution: combined microscopy and microchemistry of single Proterozoic acritarchs. *Review of Palaeobotany and Palynology*, 139, 1-15.

Killops, S.D., Killops, V.J., 2004. *An Introduction to Organic Geochemistry*. Wiley-Blackwell, 408 pp.

Kokinos, J.P., Eglinton, T.I., Goñi, M.A., Boon, J.J., Martoglio P.A., Anderson, D.M., 1998. Characterization of a highly resistant biomacromolecular material in the cell wall of a marine dinoflagellate resting cyst. *Organic Geochemistry*, 28, 265-288.

Landais, P., Rochdi, A., Largeau, C., Derenne, S., 1993. Chemical characterization of torbanites by transmission micro-FTIR spectroscopy: origin and extent of compositional heterogeneities. *Geochimica et Cosmochimica Acta*, 57, 2529-2539.

Lignum, J., Jarvis, I., Pearce, M.A., 2008. A critical assessment of standard processing methods for the preparation of palynological samples. *Review of Palaeobotany and Palynology*, 149, 133-149.

Marshall, C.P., Javaux, E.J., Knoll, A.H., Walter, M.R., 2005. Combined micro-Fourier transform infrared (FTIR) spectroscopy and micro-Raman spectroscopy of Proterozoic acritarchs: a new approach to palaeobiology. *Precambrian Research*, 138, 208-224.

Matsuoka, K., Fukuyo, Y., 2000. Technical guide for modern dinoflagellate cyst study. WESTPAC-HAB/WESTPAC/IOC, 77 pp.

McIntyre, D.J., Norris, G., 1964. Effect of ultrasound on Recent spores and pollen. *New Zealand Journal of Science*, 7, 242-257.

Mertens, K.N., Verhoeven, K., Verleye, T., Louwye, S., Amorim, A., Ribeiro, S., Deaf, A.S., Harding, I.C., De Schepper, S., González, C., Kodrans-Nsiah, M., de Vernal, A., Henry, M., Radi, T., Dybkjaer, K., Poulsen, N.E., Feist-Burkhardt, S., Chitolie, J., Heilmann-Clausen, C., Londeix, L., Turon, J.L., Marret, F., Matthiessen, J., McCarthy, F.M.G., Prasad, V., Pospelova, V., Kyffin Hughes,

J.E., Riding, J.B., Rochon, A., Sangiorgi, F., Welters, N., Sinclair, N., Thun, C., Soliman, A., van Nieuwenhove, N., Vink A., Young, M., 2009. Determining the absolute abundance of dinoflagellate cysts in recent marine sediments: The *Lycopodium* marker-grain method put to the test. *Review of Palaeobotany and Palynology*, 157, 238-252.

Mösle, B., Colllinson, M.E., Finch, P., Stankiewicz, B.A., Scott, A.C., Wilson, R., 1998. Factors influencing the preservation of plant cuticles: a comparison of morphology and chemical composition of modern and fossil examples. *Organic Geochemistry*, 29: 1369-1380.

Pandey, K.K., 1999. A study of chemical structure of soft and hardwood and wood polymers by FTIR spectroscopy. *Journal of Applied Polymer Science*, 71, 1969-1975.

Pappas, C.S., Tarantillis, P.A. Harizanis, P.C., Polissiou, M.G., 2003. New method for pollen identification by FT-IR spectroscopy. *Applied Spectroscopy*, 57, 23-27.

Reusch, W., 2011. Introduction to Spectroscopy. Department of Chemistry handbook, Michigan State University, Lansing, http://www2.chemistry.msu.edu/faculty/reusch/VirtTxtJml/Spectrpy/spectro.htm.

Riding, J.B., Kyffin-Hughes, J.E., 2004. A review of the laboratory preparation of palynomorphs with a description of an effective non-acid technique. *Revista Brasileira de Paleontologia*, 7, 13-44.

Schrank, E., 1988. Effects of chemical processing on the preservation of peridinioid dinoflagellates: a case study from the Late Cretaceous of NE Africa. *Review of Palaeobotany and Palynology*, 56, 123-140.

Stankiewicz, B.A., Mastalerz, M., Hof, C.H.J., Bierstedt, A., Flannery, M.B., Briggs, D.E.G., Evershed, R.P., 1998. Biodegradation of the chitin-protein complex in crustacean cuticle. *Organic Geochemistry*, 28, 67-76.

Steemans, P., Lepot, K., Marshall, C.P., Le Hérissé, A., Javaux, E.J., 2010. FTIR characterisation of the chemical composition of Silurian miospores (cryptospores and trilete spores) from Gotland, Sweden. *Review of Palaeobotany and Palynology*, 162, 577-590.

Stockmarr, J., 1971. Tablets with spores used in absolute pollen analysis. *Pollen et Spores*, 13, 615-621.

Versteegh, G.J.M., Blokker, P., Marshall, C.P., Pross, J., 2007. Macromolecular composition of the dinoflagellate cyst *Thalassiphora pelagica* (Oligocene, SW Germany). *Organic Geochemistry*, 38, 1643-1656.

Versteegh, G.J.M., Blokker, P., Bogus, K., Harding, I.C., Lewis, J., Oltmanns, S., Rochon, A., Zonneveld, K.A.F., in press. Flash pyrolysis and infrared spectroscopy of cultured and sediment derived *Lingulodinium polyedrum* (Dinoflagellata) cyst walls. *Organic Geochemistry.*

Yule, B.L., Roberts, S., Marshall, J.E.A., 2000. The thermal evolution of sporopollenin. *Organic Geochemistry*, 31, 859-870.

Zimmermann, B., 2010. Characterization of pollen by vibrational spectroscopy. *Applied Spectroscopy*, 64, 1364-1373.

Chapter 5

The Effect of meter-scale lateral oxygen gradients at the sediment-water interface on selected organic matter based alteration, productivity and temperature proxies

K. Bogus[a*], K.A.F. Zonneveld[a,b], D. Fischer[b], S. Kasten[c], G. Bohrmann[a,b] and G.J.M. Versteegh[b]

[a]*University of Bremen, Department of Geosciences, Klagenfurter Strasse, 28359 Bremen, Germany*
[b]*MARUM — Center For Marine Environmental Sciences, Loebener Strasse, 28334 Bremen, Germany*
[c]*Alfred Wegener Institute for Polar and Marine Research, Am Handelshafen 12, 27570 Bremerhaven, Germany*

** Corresponding author*
Telephone: +49 421 218 65138, Fax: +49 421 218 65159, Email: ka_bo@uni-bremen.de

Submitted to *Biogeosciences*

Abstract

A valid assessment of selective aerobic degradation on organic matter (OM) and its impact on OM-based proxies is vital to produce accurate environmental reconstructions. However, most studies investigating these effects suffer from inherent environmental heterogeneities. This includes differences in the initial OM composition, as a result of variable upper water column conditions, or from those induced by selective aerobic degradation. In this study, we used surface samples collected along two meter-scale transects and one longer transect in the northeastern Arabian Sea to constrain initial OM heterogeneity, in order to evaluate selective aerobic degradation on temperature, productivity and alteration indices at the sediment-water interface. All of the alteration indices, the higher plant alkane index, alcohol preservation index, and diol oxidation index, demonstrated that they are sensitive indicators for changes in oxygen content at the sediment-water interface. The export production indices, a cholesterol-based stanol/stenol and dinoflagellate lipid- and cyst-based ratios, showed significant (more than 20%) change over the lateral oxygen gradients. Therefore, they do not exclusively reflect surface water productivity, but can be altered after deposition with varying oxygen content at the sediment-water interface. Two of the investigated proxies, the glycerol dibiphytanyl glycerol tetraethers (GDGTs) based TEX_{86} sea surface temperature index and a productivity index based on phytol, phytane and pristane, did not show any trends related oxygen concentration at the sediment-water interface. Nevertheless, unrealistic sea surface temperatures were obtained after application of the TEX_{86}, TEX_{86}^{L}, and TEX_{86}^{H} proxies. The phytol-based ratios are likely modified by the sedimentary production of pristane. Our results demonstrate the rapid and selective impact of aerobic organic matter degradation on the lipid and palynomorph composition of surface sediments on a small spatial scale and suggests useful tracers of changing redox conditions along the sediment-water interface.

Keywords: aerobic organic matter degradation, dinoflagellate cysts, lipid biomarkers, proxy, Arabian Sea

5.1 Introduction

Organic matter (OM)-based proxies are very useful tools in paleoclimatology and environmental studies of the marine realm. Unfortunately, OM-based proxies can be diagenetically modified, which can result in overprinting of the initial signals and lead to misleading reconstructions (for a review see Zonneveld et al., 2010). For an adequate interpretation of proxy results, it is therefore essential to have detailed information about the processes responsible for overprinting and the rate at which diagenesis might alter the original signal.

Freshly deposited OM is quickly degraded at the sediment-water interface (SWI) during early diagenesis (Henrichs, 1992; Canuel and Martens, 1996; Prahl et al., 2000; Wakeham et al., 2002). One of the most significant variables influencing OM degradation is the oxygen content in bottom waters and the O_2 exposure time (e.g. Cowie et al., 1995; Hedges and Keil, 1995; Hartnett et al., 1998; Hulthe et al., 1998; Hedges et al., 1999). Furthermore, OM components such as lipid biomarkers (e.g. Hoefs et al., 2002; Sinninghe Damsté et al., 2002; Versteegh et al., 2010) and palynomorphs (e.g. Zonneveld et al., 1997; 2001; Bockelmann et al., 2007; Versteegh et al., 2010), display varying rates of degradation, as some are intrinsically more labile (e.g. Sun and Wakeham, 1994; Wakeham et al., 2002; Zonneveld et al., 2008). This is important as biomarkers and palynomorphs are widely used to reconstruct oceanographic conditions, such as productivity (e.g. Schubert et al., 1998; Schulte et al., 1999; Reichart and Brinkhuis, 2003). However, in studies of marine sediments, it is difficult to separate the effects of selective aerobic degradation from other factors, such as differences in upper water column conditions (van der Weijden et al., 1999), wind transported material (Witte and Pfannkuche, 2000), sediment accumulation rate (Hedges and Keil, 1995), as well as winnowing (Pedersen et al., 1992), lateral transport (Calvert et al., 1995; Mollenhauer et al., 2007; 2008) and advection, and water depth (Wakeham et al., 2002; Wuchter et al., 2006). These can influence the composition of OM settling on the sea floor and complicate interpretations regarding oxygen effects (Hedges and Keil, 1995).

In this study, we investigate rapid changes in biomarker- and palynomorph-based proxy ratios as a result of laterally increasing oxygen concentrations at the SWI on the Pakistan continental margin (northeastern Arabian Sea), where the primary control on OM preservation is the bottom water oxygen concentration (e.g. Paropkari et al., 1992;

1993; Cowie et al., 1999; Keil and Cowie, 1999; van der Weijden et al., 1999; Schulte et al., 2000). The higher plant alkane index (HPA; Westerhausen et al., 1993), alcohol preservation index (API; Cacho et al., 2000), and diol oxidation index (DOXI; Ferreira et al., 2001) have previously been used to indicate sediment alteration and oxygenation changes in the sedimentary record. We evaluate whether they are also sensitive indicators of redox changes at the SWI. Additionally, some molecular biomarkers commonly used to indicate changes in export production like phytol, cholesterol, and dinosterol (Volkman et al., 1998) were shown to be more rapidly degraded in an oxygenated environment (e.g. Schulte et al., 2000). In order to determine whether this degradation is selective, we incorporate them into indices along with related refractory compounds, such as pristane and phytane, cholestanol, and dinostanone and dinosterone, respectively (after Nishimura and Koyama, 1977; McCaffrey et al., 1991; Mouradian et al., 2007). Another proxy that is used to show changes in export production is the ratio between autotrophic (gonyaulacoid) and heterotrophic (peridinioid) dinoflagellate cysts (e.g. Harland, 1973; McCarthy et al., 2000; Reichart and Brinkhuis, 2003 and references therein). However, the gonyaulacoid species have been shown to be resistant to aerobic degradation while the peridinioid species are sensitive to oxygen exposure (e.g. Zonneveld et al., 1997; 2001; Combourieu-Nebout et al., 1998; Versteegh and Zonneveld, 2002). Here, we compare gonyaulacoid and peridinioid (G/P) dinoflagellate cysts to determine the extent this ratio may be affected. Finally, we investigate marine isoprenoidal archaeal glycerol dibiphytanyl glycerol tetraether (GDGT) distribution (Karner et al., 2001; Wuchter et al., 2005; Menzel et al., 2006), which is the basis for a sea surface temperature (SST) proxy based on the number of GDGT cyclopentane moieties (e.g. Schouten et al., 2002; Kim et al., 2008; Kim et al., 2010). There is conflicting evidence on the influence of selective aerobic degradation on GDGTS with some studies suggesting no selective degradation (e.g. Sinninghe Damsté et al., 2002; Schouten et al., 2004; Kim et al., 2009) while others indicate that differences in lability between the moieties are possible (e.g. Shah et al., 2008; Huguet et al., 2009). In order to provide more information, we investigate the possible effect of a lateral oxygen gradient in surface sediments on GDGT-based indices.

As the effects of selective aerobic degradation are best studied on samples with similar initial OM compositions, we utilize surface sediment samples collected along

three transects that, when used in conjunction, allow us to constrain the uncertainty associated with OM heterogeneity. The first transect encompasses the large, stable, intermediate depth (150-1300 m; e.g. Breuer et al., 2009) oxygen minimum zone (OMZ) and oxygenated deeper water. Two additional transects include methane seep sites, which are found in this region (e.g. von Rad et al., 1996; Fischer et al., submitted). One seep transect is located at the lower transition of the OMZ and thus basically records the impact of the seep environment on the OM composition. The other seep transect is located below the OMZ in well-oxygenated bottom waters with oxygen levels increasing with distance from the gas outflow. The active advection of vent fluids at a seep site reduces the oxygen penetration depth and the O_2 concentration at the SWI (Aharon and Fu, 2003). This results in a short scale lateral oxygen gradient extending from just adjacent to the active venting towards the periphery of the seep site. Essentially, the meter-scale seep transects serve to constrain environmental variability that may affect OM composition along the longer OMZ transect. Influences of OM contributed by the seep biomass and possible complications from anaerobic degradation (e.g. Saager et al., 1989; Canfield et al., 1993; Grossi et al., 2001) via bacterial sulfate reduction (e.g. Jørgensen, 1982; Lückge et al., 1999; Jørgensen and Kasten, 2006) are addressed through the comparison of the seep transects to each other and from the seep transects to the OMZ transect. This study thus provides more detail as to the rapidity of overprinting by changing oxygen content at the SWI on marine surface samples along lateral oxygen gradients.

5.2 Regional Setting

In the study area, two monsoon seasons, the boreal winter northeast monsoon (NEM) and the stronger southwest monsoon (SWM) in the summer, result from land-sea pressure gradients due to differential summer heating of the Asian continent. This produces seasonally reversing wind conditions, which induce high annual primary productivity (Wyrtki, 1973; Qasim, 1982) along the coast and in the open ocean region through upwelling (during SWM) and convective mixing (during NEM) (Bauer et al., 1991; Madhupratap et al., 1996; Prassana Kumar et al., 2001). Abundant OM in the upper water column due to the high primary production leads to a high rate of oxygen consumption as a result of OM degradation. Together with the inflow of O_2-poor intermediate waters, these cause a stable, intermediate depth OMZ that has existed for the

past 7000 years (Shapiro and Meschanov, 1991; Olson et al., 1993; von Rad et al., 1999). Current estimates place the OMZ between about 150-1000 m water depth, though there is some variability as to the depths of the upper and lower boundaries (Brand and Griffiths, 2009; Breuer et al., 2009). The OMZ was defined in this study as having oxygen concentrations below 0.5 ml l^{-1} (Fig. 5.1).

Average OM export production for the Pakistan continental margin is approximately 70 g C m^{-2} yr^{-1} with a sedimentation rate on the slope of up to 1 mm $year^{-1}$ (von Rad et al., 1995; van der Weijden et al., 1999; von Rad et al., 1999). Sedimentary OM primarily reflects marine input (e.g. Paropkari et al., 1992; Cowie et al., 1999; Lückge et al., 1999; Schulte et al., 2000), though, there is seasonal terrestrial influx of organic rich mud from the Shadi and Hingol rivers (Bohrmann et al., 2008).

The Makran accretionary prism contains numerous cold seeps, which are areas of fluid and gas emissions from the sea floor (von Rad et al., 1995; 1996). *R/V Meteor* cruise M74/2 and 3 was an interdisciplinary cruise specifically scheduled to explore the Makran continental margin for further fluid escape structures (Bohrmann et al., 2008) driven by tectonically induced overpressure (Ding et al., 2010). Evidence for twelve sites with gas bubble emissions were found (Römer et al., submitted) from which nine gas seep sites were investigated in detail by using the ROV QUEST 4000 as the major sampling instrument (Fischer et al., submitted).

Coupled to the upward gas migration at seep sites are chemosynthetic communities that rely on the supply of reduced compounds such as hydrogen sulfide and methane (Suess et al., 1985). Microbial mats composed of large sulfide-oxidizing bacteria (*Beggiatoa* and *Marithioploca* spp.) and clam fields (*Calyptogena* spp.) associated with such seep sites have been found specifically here (e.g. von Rad et al., 1995; 1996; Bohrmann et al., 2008; Fisher et al., submitted). The biogeography of the seep sites is to some degree controlled by the active fluid and gas expulsion into the water column as well as oxygen availability (Roberts and Carney, 1997; Fischer et al., submitted). Thus, these seep sites can encompass localized areas of anoxia at the SWI in otherwise oxygenated bottom waters (Aharon and Fu, 2000), such as below the OMZ (von Rad et al., 1996). The two seep fields sampled for this study are shown in Figure 5.2.

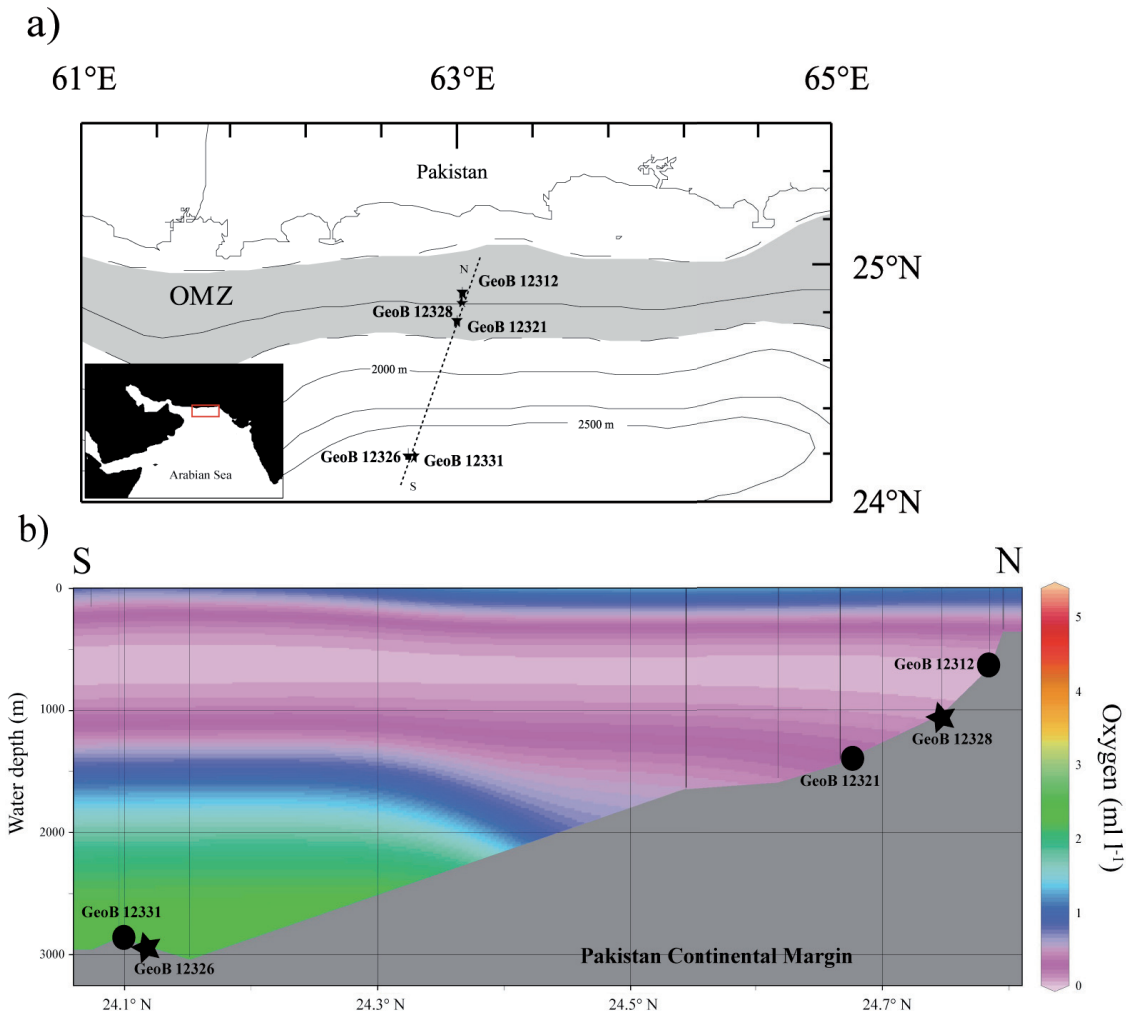

Figure 5.1: Map showing a) Sample locations b) Water column oxygen concentrations, as measured by CTD profiling, in relation to sample locations. Circles indicate multi-cores while stars denote the push core transects.

5.3 Material

Surface sediments were retrieved along three transects during *R/V Meteor* cruise M74/3 during the 2007 fall intermonsoon (Bohrmann et al., 2008). In the study area, CTD casts identified the lowest oxygen concentrations between 350–750 m water depth with 900–1200 m containing slightly higher O_2 content and well-ventilated waters found below 1600 m (Fig. 5.1; Table 5.1). Only the uppermost unconsolidated sediment layer (< 1 cm) was used.

Table 5.1: Sample location descriptions and oxygen classification scheme.

Sample	GeoB 12312	GeoB 12321	GeoB 12331	GeoB 12326-13	GeoB 12326-9	GeoB 12326-7	GeoB 12328-6	GeoB 12328-2	GeoB 12328-4
Referred in text as	OMZ-anoxic	OMZ-suboxic	OMZ-oxic	below OMZ-seep 1	below OMZ-seep 2	below OMZ-seep 3	OMZ-seep 1	OMZ-seep 2	OMZ-seep 3
Latitude (N)	24° 53'	24° 46'	24° 11'	24° 11'	24° 11'	24° 11'	24° 50'	24° 50'	24° 50'
Longitude (E)	63° 01'	62° 59'	62° 46'	62° 44'	62° 44'	62° 44'	63° 01'	63° 01'	63° 01'
Water depth (m)	655	1425	2830	2875	2875	2875	1025	1025	1025
Transect	OMZ	OMZ	OMZ	below OMZ seep	below OMZ seep	below OMZ seep	OMZ seep	OMZ seep	OMZ seep
Sample location	OMZ core	OMZ lower transition	well below OMZ	adjacent to gas orifice	50 cm from gas orifice, clam field	1 m from gas orifice, ambient sediment border	bacterial mat	15 cm from mat, clam border	75 cm from central habitat, clam field
*[O_2] ml l^{-1}	0.02	0.55	2.55	-	-	2.55	0.07	0.07	0.07
[a]Mn^{2+} at SWI	-	-	-	yes	no	-	-	-	-
Oxygen classification	anoxic	suboxic	oxic	anoxic	suboxic	oxic	anoxic	anoxic	anoxic
Based on	CTD of the station, O_2 penetration depth, Fe^{2+}			Mn^{2+} profile	Mn^{2+} profile	CTD of the station	CTD of the station		

*As measured by CTD profiling of bottom waters, [a]Based on pore water measurements of two replicate push cores (see Figure 5.4)

5.3.1 OMZ transect

Three multi-cores were retrieved along a kilometer-scale transect starting within the OMZ (GeoB 12312; 0.02 ml l^{-1} O_2; 655 mbsl) into the transition zone (GeoB 12321; 0.55 ml l^{-1} O_2; 1425 mbsl) and extending into the oxic zone below (GeoB 12331; 2.55 ml l^{-1} O_2; 2830 mbsl). This series of samples is hereafter referred to as the OMZ transect (Fig. 5.1; Table 5.1), and the samples are tentatively characterized as OMZ-anoxic (GeoB 12312), OMZ-suboxic (GeoB 12321) and OMZ-oxic (GeoB 12331). All sediment samples are composed of clay to silty clay material. They were not retrieved from areas of active seeping and thus represent background sediments of detrital OM-based ecosystems. OMZ-anoxic contained finely laminated layers and no indications of bioturbation, whereas OMZ-suboxic and OMZ-oxic appeared more homogenized, most likely due to bioturbation (Bohrmann et al., 2008). Subsamples for palynomorph analysis were sealed air tight and stored at 4°C until analysis. Subsamples for biomarker analysis were stored under argon and at -20°C until analysis.

5.3.2 Seep transects

Two seep fields (GeoB 12328 and GeoB 12326; Fig. 5.1; Table 5.1) were sampled using the remotely operated vehicle (ROV) QUEST 4000 (Bohrmann et al., 2008). This technique allowed us to know the exact push core location as well as view the surrounding environment (Fig. 5.2). The CTD bottom water oxygen measurements from the two push core stations demonstrated that site GeoB 12328 was located in the transitional OMZ zone (0.07 ml l^{-1} O_2; 1025 mbsl) and site GeoB 12326 was located in well-oxygenated bottom waters (2.55 ml l^{-1} O_2; 2875 mbsl) (Fig. 5.1; Table 5.1). Subsequently, the two seep fields are referred to as OMZ-seep (GeoB 12328) and below

OMZ-seep (GeoB 12326).

Three successive push core samples comprise the OMZ-seep transect: GeoB 12328-6 (OMZ-seep 1) was retrieved at the edge of the central bacterial mat, GeoB 12328-2 (OMZ-seep 2) where bubbles of free gas escape at the sea floor at 15 cm distance away and GeoB 12328-4 (OMZ-seep 3) at about 75 cm from the active seeping and within the clam field (Fig. 5.2a; Table 5.1). As well, three successive push core samples comprise the below OMZ-seep: GeoB 12326-13 (below OMZ-seep 1) was just adjacent to active seeping, GeoB 12326-9 (below OMZ-seep 2) was 50 cm away from the central gas orifice and within the area of small clams, and GeoB 12326-7 (below OMZ seep 3) was 1 m further away at the edge of the small clams and ambient sea floor (Fig. 5.2b; Table 5.1). When only the seep transect is stated (i.e. OMZ-seep or below OMZ-seep), this refers to all of the push cores retrieved at that respective site. All subsamples for biomarker and palynomorph analysis were stored under argon and at -20°C.

a) OMZ-seep transect (GeoB 12328)

b) below OMZ-seep transect (GeoB 12326)

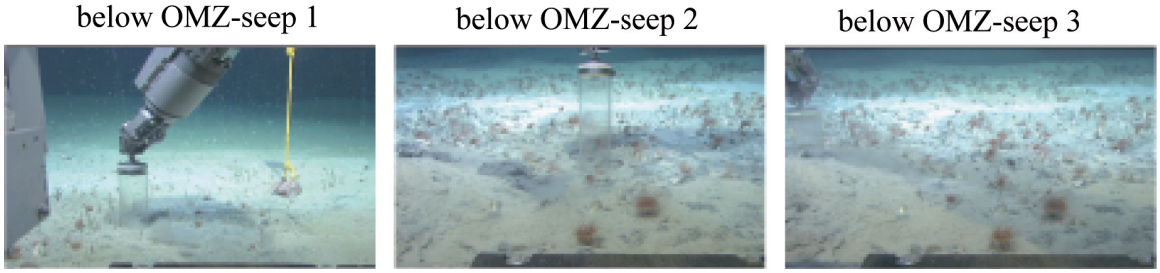

Figure 5.2: High resolution photographs taken by the ROV MARUM-QUEST 4000 of the individual push cores retrieved along the two seep transects a) OMZ-seep (GeoB 12328), and specific samples OMZ-seep 1 (GeoB 12328-6), OMZ-seep 2 (GeoB 12328-2), and OMZ-seep 3 (GeoB 12328-4), b) GeoB 12326 (below OMZ-seep), located below the OMZ.

5.4 Methods

5.4.1 Geochemical parameters

Ex situ pore water oxygen was measured on replicate whole cores to OMZ-anoxic, OMZ-suboxic, and OMZ-oxic with a FIBOX3 oxygen sensor coupled to a micromanipulator. The cores were allowed to acclimate to ambient temperature and then the O_2 probe was lowered quickly to the measurement depth and left until the O_2 reading became stable. Measurements were taken at 2.5 mm intervals and in triplicate. This method was primarily used to specify the oxygen penetration depth. The O_2 penetration depth was compared to pore water iron (Fe^{2+}) concentrations, as a way to confirm the redox boundary. For this purpose, pore water was extracted on board via rhizons (pore size 0.1 µM) according to the method of Seeberg-Elverfeldt et al. (2005). Subsamples (1 ml) were complexed with 50 µl of "Ferrospectral" and measured photometrically.

For the below OMZ-seep, manganese (Mn^{2+}) pore water concentrations were measured on two push cores replicate to below OMZ-seep 1 (central habitat, active gas ebullition) and below OMZ-seep 2 (within clam field). A pore water subsample for cation analysis was diluted 1:10 with 1M HNO_3^- and stored at 4°C. Samples were analyzed for Mn^{2+} concentrations with an ICP-OES (IRIS Intrepid, Thermo Electron). Standards were prepared from single element stock solution in 1M HNO_3^- to avoid matrix effects. Replicate measurements gave an error of ≤ 3%.

5.4.2 Lipid biomarkers

Freeze dried sediment samples (1-10 g) were ground with an agate mortar and pestle, and the total lipid extract (TLE) was extracted using an Dionex 200 ASE (Accelerated Solvent Extractor) with methanol (MeOH) and dicholoromethane (DCM) (9:1 v:v; 3 cycles of 5 min duration each) at 100 °C and 7.6 x 10^6 Pa. A small aliquot (100 µl) of the TLE was evaporated under N_2 to dryness and then redissolved in 100 µl n-hexane and propanol (99:1 v:v) for GDGT analysis following the procedure of Liu et al. (2011), modified after Hopmans et al. (2000). Briefly, a ThermoFinnigan Surveyor high performance liquid chromatography (HPLC) system was used at 30° C, a flow rate of 1 ml min^{-1}, and separation was achieved with an Econosphere N2 column (250 x 4.6 min; Alltech, Germany). The gradient used was the same as Liu et al. (2011). The HPLC was coupled to a ThermoFinnigan LCQ Deca XP Plus ion trap mass spectrometer via an

atmospheric pressure chemical ionization (APCI) interface. These settings were also the same as described in Liu et al. (2011). Relative GDGT concentrations were acquired by integrating the appropriate peak areas of their $(M + H)^+$ and $(M + H)^+ + 1$ mass chromatograms.

Another aliquot (500 µl) of the TLE was partitioned into a *n*-hexane soluble fraction and a DCM soluble fraction. The hexane soluble fraction was then derivatized with 50 µl Bis(trimethylsilyl)trifluoroacetamide (BSTFA) and pyridine (60° C, 1 hr) to produce trimethylsilylated alcohols. An internal standard mix (5 µg) containing C_{36} *n*-alkane and 1-nonadecanol was added before derivatization. Samples were then analyzed using an Agilent Technologies 7890A Gas Chromatograph (GC) equipped with a splitless injector and a HP-5MS column (i.d. 0.25 mm; film thickness 0.25 µm) operated at a flow rate of 1 ml min^{-1}. Helium was used as the carrier gas. The temperature program was as follows: 70° C (1 min), then 60-310° C at 4° C min^{-1} and 320°C (21 min). The GC was coupled to a quadripole mass spectrometer (MS) (597C VL MSD Triple Axis Detector) operated at 70 eV and a scan range of 50-800 AMU. Compounds were identified based on relative retention times and indices, and mass spectra. In general, they were quantified from comparing their peak areas in the total ion current with internal standards. The relative response factors were assumed to be 1; hence our data are only semi-quantitative. Since we were interested primarily in the relative changes of proxy ratios between samples, this analysis was sufficient. For those compounds where co-elution occurred, quantification was performed on compound specific ions after Versteegh et al. (2010).

5.4.3 Dinoflagellate cysts

Sample material (~ 0.3 g) was oven dried (60° C; 24 hrs), weighed and treated with cold 10% HCl (24 hrs) to remove carbonates and 38% HF (48 hrs after 90 min agitation) to remove silicates, then neutralized with 10% KOH. Care was taken to ensure that the solutions never became alkaline. The samples were briefly put in an ultrasonic bath (< 1 min) sieved through a 20 µm precision sieve (Stork Veco; mesh 317). Samples were centrifuged (3200 rpm; 6 min) and concentrated to 1.0 ml, after which 50 µl (100 µl for push core samples) were mounted in glycerin jelly and sealed on a glass slide with paraffin wax. Entire slides were counted blind for dinocysts with a Zeiss Axioskop light microscope. At least 200 whole specimens were counted. If necessary, additional slides were counted entirely. Taxonomy was based on Fensome and Williams (2004) and

Matsuoka et al. (2009). Dinoflagellate cyst taxa were divided into two groups, gonyaulacoid (G-cysts) and peridinioid and cysts of *Polykrikos* (P-cysts) (Table 5.2), which generally represent autotrophic and heterotrophic taxa, respectively (e.g. Mudie and Rochon, 2001). Quantification was performed via the volumetric method (e.g. Dale, 1976; Holzwarth et al., 2007).

Table 5.2: Gonyaulacoid (G) and peridinioid and cysts of *Polykrikos* (P) dinoflagellate cyst species identified in this study

P-cysts	G-cysts
Brigantedinium spp.	*Bitectatodinium spongium*
Cyst of *Diplopelta parva*	*Impagidinium aculeatum*
Cyst of *Polykrikos kofoidii*	*Impagidinium paradoxum*
Cyst of *Protoperidinium americanum*	*Impagidinium patulum*
Cyst of *Protoperidinium monospinum*	*Impagidinium sphaericum*
Cyst of *Protoperidinium stellatum*	*Impagidinium* spp.
Dubridinium spp.	*Lingulodinium machaerophorum*
Echinidinium aculeatum	*Nematosphaeropsis labyrinthus*
Echinidinium bispiniformum	*Operculodinium centrocarpum*
Echinidinium granulatum	*Operculodinium israelianum*
Echinidinium transparantum	*Operculodinium longispinigerum*
Echinidinium delicatum	*Pentapharsodinium dalei*
Echinidinium spp.	*Polysphaeridium zoharyi*
Leipokatium invisitatum	*Spiniferites membranaceous*
Lejeunacysta oliva	*Spiniferites mirabilis*
Lejeunacysta sabrina	*Spiniferites pachydermus*
Lejeunacysta spp.	*Spiniferites ramosus*
Quinquecuspis concreta	*Spiniferites* spp.
Selenopemphix nephroides	
Selenopemphix quanta	
Stelladinium robustum	
Trinovantedinium applanatum	
Votadinium calvum	
Xandarodinium xanthum	

5.4.4 Proxy ratio calculations

A proxy trend in this study is defined as a consistent increase or decrease along successive samples within a transect. Specific proxy definitions and formulae are depicted in Table 5.3. The alteration proxy HPA utilizes $\Sigma C_{24\text{-}28}$ even *n*-alcohols divided by the $\Sigma C_{27\text{-}31}$ odd *n*-alkanes (Westerhausen et al., 1993), while the API uses only *n*-hexacosanol and *n*-nonacosane (Cacho et al., 2000). The HPA and API ratios exhibit decreasing values if their respective *n*-alcohols are selectively degraded relative to the *n*-alkanes. The final alteration proxy, DOXI, involves the concentration of 1,15-long chain alkyl diols divided by the keto-ols (Ferreira et al., 2001). This proxy assumes that the

keto-ols are mainly oxidation products of the diols; thus, higher ratio values indicate higher degradation of the diols relative to the keto-ols. We initially calculated the DOXI with the dominant C_{30} isomers; the predominance of this isomer was reported previously in Arabian Sea sediments (e.g. Smallwood and Wolff, 2000; Wakeham et al., 2002). Where possible, the C_{32} isomers were also calculated.

For the three phytol-based indices, significant preferential degradation of phytol would result in overall lower ratio values as pristane and phytane are generally considered compounds produced via degradation of phytol (e.g. Didyk et al., 1978). The cholesterol-based stanol/stenol index would show an increase with more efficient cholesterol oxidation. The dinosterol-based index compares dinosterol with other dinoflagellate-derived degradation products, dinosterone, dinostanone, and dinosterane (Σdinoflagellate lipids). Thus, decreases in the proxy would indicate faster removal of dinosterol. Although the original definition of the G/P (gonyaulacoid/peridinioid) ratio is based on the number of species of each (Harland, 1973), in this study we used the quantity of G- and P-cysts in each sample because the small spatial scale of our transects made differences in species numbers highly unlikely.

The temperature indices are based on the isoprenoid GDGT distribution. The abundance of different GDGT moieties can be correlated to temperature using the GDGTs with one to three cyclopentane moieties and the crenarchaeol regioisomer, which contains four cyclopentane moieties and one cyclohexane moiety (Wuchter et al., 2004; Schouten et al., 2007). Three indices are calculated based on Kim et al. (2010): TEX_{86}, TEX_{86}^{L}, TEX_{86}^{H} (Table 5.3). From each of these indices, sea surface temperatures (SST) were calculated after Kim et al. (2010), using their linear calibration equations (5), (8), and (10) for TEX_{86}, TEX_{86}^{L}, and TEX_{86}^{H}, respectively. Changes in the distribution of the GDGTs are thus reflected in the index values and calculated SSTs. All raw data used for the calculation of these indices (lipid biomarker concentrations, GDGT peak areas, and dinoflagellate cyst counts) can be found in Appendices A3-A5.

Table 5.3: Proxy ratio descriptions and formulae as used in this study.

Proxy	Definition	Components	Source	Source references	Proxy represents	Proxy references
Alteration indices						
HPA	[ΣC_{24-28} even-OH] / {[ΣC_{24-28} even-OH] + [ΣC_{27-31} odd *n*-alkanes]}	long chain even *n*-alcohols, odd *n*-alkanes	Higher plant waxes	Eglinton and Hamilton (1967), Fukushima and Ishiwatari (1984)	Selective Preservation	Westerhausen et al. (1993), Santos et al. (1994), Yamamoto et al. (2008)
API	[C_{26}-OH] / {[C_{26}-OH] + [C_{29} *n*-alkane]}	C_{26} *n*-alcohol, C_{29} n-alkane			Bottom water oxygenation	Cacho et al. (2000), Martrat et al. (2007), Versteegh et al. (2010)
DOXI	[1,15-keto-ol] / {[1,15-diol] + [1,15-keto-ol]}	C_{30} and C_{32} 1,15 alkyl diols, keto-ols	Eustigmatophytes, unknown source for keto-ols	de Leeuw et al. (1981), Versteegh et al. (1997)	Selective Preservation	Ferreira et al. (2001), Versteegh et al. (2010)
Export production indices						
Phytol-based		Phytol, phytane, pristane	Chlorophyll-*a*	Volkman and Maxwell (1986), Didyk et al. (1978)	Selective Preservation	modified from Didyk et al. (1978), This study
index[1]	{[pristane] + [phytane]} / [phytol]					
index[2]	[phytane] / [phytol]					
index[3]	[pristane] / [phytol]					
Stanol/stenol	[cholestanol] / [cholesterol]	Cholesterol, cholestanol	Eukaryotes	Barret et al. (1995), Hudson et al. (2001)	Stenol oxidation	Nishimura and Koyama (1977), McCaffrey et al. (1991)
Dinosterol-based	{[dinosterone] + [dinostanone] + [dinosterane]} / [dinosterol]	Dinosterol, dinosterone, dinostanone, dinosterane	Dinoflagellates	Boon et al. (1979), Robinson et al. (1984), Volkman et al. (1999)	Stenol oxidation	after Mouradian et al. (2007), This study
G/P	[gonyaulacoid cysts] / {[peridinioid cysts] + [cysts of *Polykrikos*]}	Organic-walled, non-motile resting cysts		Fensome et al. (1993)	Productivity, bottom water oxygenation	McCarthy et al. (2000), Mudie and Rochon (2001)
Temperature indices						
TEX_{86}	{[GDGT-2] + [GDGT-3] + [Cren. Iso]} / {[GDGT-1] + [GDGT-2] + [GDGT-3] + [Cren. Iso]}	Glycerol dibiphanyl glycerol tetraethers	marine Crenarchaeota	Schouten et al. (2002), Karner et al. (2001)	Sea surface temperature	Schouten et al. (2002)
TEX_{86}^{L}	log {[GDGT-2] / [GDGT-1] + [GDGT-2] + [GDGT-3]}					Kim et al. (2010)
TEX_{86}^{H}	log {[GDGT-2] + [GDGT-3] + [Cren. Iso]} / {[GDGT-1] + [GDGT-2] + [GDGT-3] + [Cren. Iso]}					

* Numbers in the temperature index definitions refer to the number of cyclopentane moieties in the GDGT structure. Cren. Iso. refers to the crenarchaeol regioisomer.

5.5 Results

5.5.1 Oxygen content at the SWI

The O_2 penetration depth in the sediments increases along the OMZ transect from undetectable (OMZ-anoxic) to a maximum of about 25 mm (OMZ-oxic), and is consistent with the Fe^{2+} profiles (Fig. 5.3). At the below OMZ-seep, Mn^{2+} was present at the SWI (≈ 3 µmol l^{-1}) closest to the central habitat of active gas seepage (below OMZ-seep 1), but concentrations were lower (≈ 0.4 µmol l^{-1}) 50 cm away at the SWI in the clam field (below OMZ-seep 2) (Fig. 5.4).

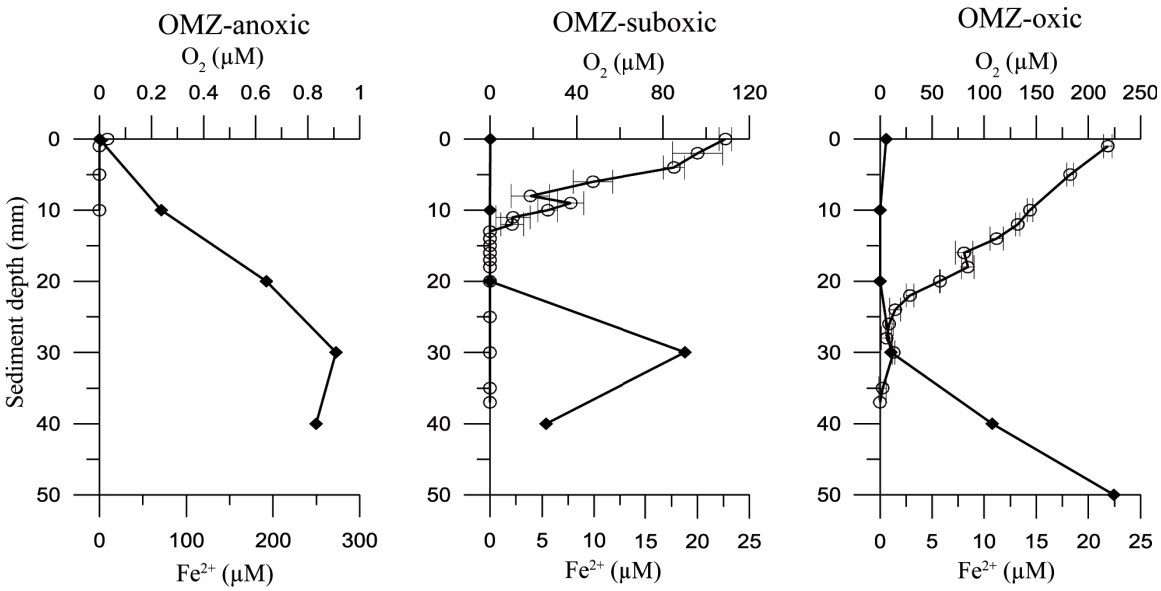

Figure 5.3: Pore water oxygen and Fe^{2+} (µM) values measured in the OMZ transect samples.

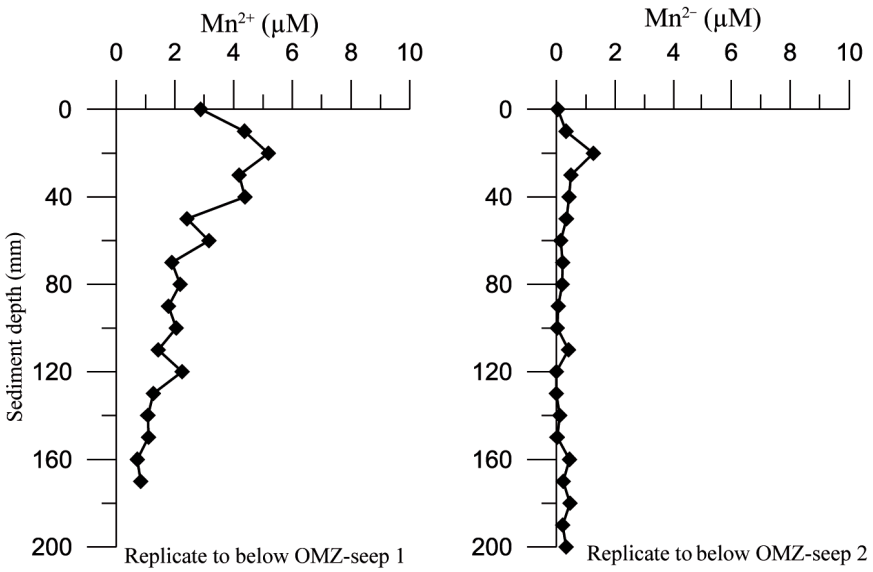

Figure 5.4: Mn^{2+} concentrations (µM) from two replicate push cores of below OMZ-seep 1 and 2.

5.5.2 Alteration indices (HPA, API, DOXI)

Along the OMZ transect, HPA (Table 5.3) values decreased from 0.58 (OMZ-anoxic) to 0.42 (OMZ-oxic). Along the below OMZ-seep, the index decreased from 0.67 (below OMZ-seep 1) to 0.55 (below OMZ-seep 3). At the OMZ-seep, the index values ranged from 0.6-0.73 with no apparent trend (Table 5.4).

Along the OMZ transect, the API (Table 5.3) values decreased from 0.47 (OMZ-anoxic) to 0.18 (OMZ-oxic). Additionally, at the below OMZ-seep, the ratio values decreased from 0.56 to 0.37 with increasing distance from the active venting. Values at the OMZ-seep were higher in general, ranged between 0.6 and 0.72, but showed no specific trend (Table 5.4).

The DOXI (Table 5.3) increased along the OMZ transect from 0.12 (OMZ-anoxic) to 0.53 (OMZ-oxic). Along the below OMZ-seep, DOXI also increased from 0.26 (below OMZ-seep 1) to 0.41 (below OMZ-seep 3). At the seep station within the OMZ, DOXI varied between 0.25-0.29. When it was possible to also calculate the ratio using the C_{32} 1, 15-diol and keto-ol, values were similar to the C_{30} ratios (Table 5.4).

5.5.3 Export production proxies (phytol, cholesterol, dinosterol indices, and dinoflagellate cysts)

Along the OMZ transect, phytol indices (Table 5.3) containing pristane, i.e. index^1 and index^3, remained around 0.25 and 0.15, respectively (Table 5.4). Phytane-containing index^2 values were between 0.08-0.16 and again showed no apparent trend. At both the OMZ-seep and below OMZ-seep, ratio values were generally higher overall, especially in the samples closest to active venting (Table 5.4). Below the OMZ-seep, all index values showed a decrease. Index^1 decreased from 0.51 (below OMZ-seep 1) to 0.25 (below OMZ-seep 3), index^2 from 0.2-0.1, and index^3 values decreased from 0.32 to 0.15. Values of index^1 at the OMZ-seep began extremely high (1.26; OMZ-seep 1) and decreased to 0.47 (OMZ-seep 3) while index^3 decreased from 0.99 to 0.32. Index^2 showed less of a decrease from 0.28 to 0.15 (Table 5.4).

The cholesterol-based stanol/stenol ratio (Table 5.3) showed an increase along the OMZ transect from about 0.23 (OMZ-anoxic) to 0.82 (OMZ-oxic). An increasing trend (0.37 to 0.75) was also apparent along the seep transect below the OMZ. A slight

decrease was exhibited along the OMZ seep with values ranging from 0.54 to 0.4 (Table 5.4).

The dinosterol-based index (Table 5.3) values increased along the OMZ transect (0.02 to 0.24) and the below OMZ-seep (0.03 to 0.20), and decreased along OMZ-seep (0.18-0.06) (Table 5.4).

The G/P ratio derived from dinoflagellate cysts (Table 5.3) increased from 0.13 (OMZ-anoxic) to 0.52 (OMZ-oxic) along the OMZ transect and from 0.15 to 0.44 along the below OMZ-seep. The ratio was consistent (0.17-0.18) at the OMZ-seep (Table 5.4).

5.5.4 Temperature proxy

The TEX_{86} index increases slightly from 0.75 (OMZ-anoxic, OMZ-suboxic) to 0.72 (OMZ-oxic) along the OMZ transect (Table 5.4). The corresponding SSTs show a decrease from 34.6-31.7° C. TEX_{86} also increases along the below OMZ-seep from 0.76 (below OMZ-seep 1) to 0.69 (below OMZ-seep 3). The calculated SSTs decreased from 35.6-29.2° C. Along the OMZ-seep, TEX_{86} ranged from 0.71-0.75, with resulting SSTs between 31.0-34.9° C. TEX_{86}^{L} showed no trends along any transect and the index values ranged from 0.33 (below OMZ-seep 2 and 3) to 0.28 (OMZ-seep 3). Subsequent SSTs vary from 24.3° C (below OMZ seep-2) to 28.3° C (OMZ-seep 3). Along the OMZ transect and below OMZ-seep, TEX_{86}^{H} values slightly increased from 0.12-0.15 and 0.12-0.16, respectively. This resulted in SSTs for the two transects as 30.1-28.6° C, and 30.6-27.4° C. The OMZ-seep showed a slight decrease (0.15-0.12) and subsequent increase (28.7-30.3° C) in TEX_{86}^{H} and SST, respectively (Table 5.4).

Table 5.4: Proxy values of the calculated indices along the three studied transects.

	OMZ transect			Below OMZ seep			OMZ seep		
	OMZ-anoxic (anoxic)	OMZ-suboxic (suboxic)	OMZ-oxic (oxic)	below OMZ-seep 1 (anoxic)	below OMZ-seep 2 (suboxic)	below OMZ-seep 3 (oxic)	OMZ-seep 1 (anoxic)	OMZ-seep 2 (anoxic)	OMZ-seep 3 (anoxic)
Alteration indices									
HPA	0.58	0.52	0.42	0.67	0.65	0.55	0.68	0.73	0.6
API	0.47	0.39	0.18	0.56	0.49	0.37	0.61	0.72	0.67
DOXI									
C_{30} isomer	0.12	0.24	0.53	0.26	0.37	0.41	0.28	0.26	0.25
C_{32} isomer	0.14	0.22	n.m.	0.27	n.m.	n.m.	0.28	0.26	n.m.
Export production indices									
Phytol-based									
index[1]	0.28	0.24	0.25	0.51	0.25	0.25	1.26	0.62	0.47
index[2]	0.16	0.08	0.15	0.2	0.1	0.11	0.28	0.19	0.15
index[3]	0.11	0.16	0.15	0.32	0.2	0.15	0.99	0.43	0.32
Stanol/stenol	0.23	0.24	0.82	0.37	0.59	0.75	0.54	0.61	0.4
Dinosterol-based	0.02	0.05	0.24	0.03	0.21	0.26	0.18	0.09	0.06
G/P	0.13	0.31	0.52	0.15	0.3	0.44	0.17	0.18	0.18
Temperature indices*									
[a]TEX_{86}	0.75 (34.6°C)	0.75 (34.7°C)	0.72 (31.7°C)	0.76 (35.6°C)	0.73 (32.7°C)	0.69 (29.2°C)	0.72 (31.7°C)	0.71 (31.0°C)	0.75 (34.9°C)
[b]TEX_{86}^{L}	-0.29 (27.5°C)	-0.32 (25.5°C)	-0.29 (27.2°C)	-0.3 (26.8°C)	-0.33 (24.3°C)	-0.33 (24.6°C)	-0.3 (26.7°C)	-0.29 (27.0°C)	-0.28 (28.3°C)
[c]TEX_{86}^{H}	-0.12 (30.1°C)	-0.12 (30.2°C)	-0.15 (28.6°C)	-0.12 (30.6°C)	-0.14 (29.2°C)	-0.16 (27.4°C)	-0.15 (28.7°C)	-0.15 (28.3°C)	-0.12 (30.3°C)

Definitions of each of the listed indices can be found in Table 5.3.

* Index alues are followed in brackets by the calculated SSTs with that value. All calculations are after Kim et al. (2010).

[a]$SST = 81.5 \times TEX_{86} - 26.6$, [b]$SST = 67.5 \times TEX_{86}^{L} + 46.9$, [c]$SST = 68.4 \times TEX_{86}^{H} + 38.6$

5.6 Discussion

5.6.1 Lateral oxygen gradients

Two of the investigated transects are characterized by differences in the oxygen content at the SWI and thus have the potential to exert a strong diagenetic overprint on our proxy ratios. The oxygen gradient through the OMZ is clear in our data (Fig. 5.3) and well known from other studies (e.g. Breuer et al., 2009). This confirms our initial classification (Table 5.1) based on CTD profiles of the study area (Fig. 5.1b) and sediment descriptions of the OMZ transect multicores (Bohrmann et al., 2008). Although there was a very small amount of oxygen measured in the bottom waters at OMZ-anoxic, we classified it as such in order to distinguish it from OMZ-suboxic, for which the bottom water oxygen concentration is one order of magnitude higher. This same logic applies to the classification of the OMZ-seep, located at the lower transition of the OMZ. The bottom water O_2 measurement of the station (0.07 ml l^{-1}; Fig. 5.1b) is very close to that of OMZ-anoxic, so all samples were classified as anoxic (Table 5.1). However, we should note that while the OMZ-seep central habitat contained a microbial mat, indicating anoxia, the presence of small vesicomyid clams further away from the gas orifice does suggest that O_2 concentrations were high enough to support them (e.g. Fischer et al., submitted). Therefore, it is likely that a lateral oxygen gradient was present at the OMZ-seep; however, the magnitude of this gradient must be smaller than along the OMZ transect or the below OMZ-seep.

The presence of a distinct spatially short-scale oxygen gradient at the below OMZ-seep was inferred from the differences in fluid/gas flow and colonization by chemosynthetic communities of the seep habitats (Bohrmann et al., 2008; Fischer et al., submitted). The pore water manganese (Mn^{2+}) profiles (Fig. 5.4) corroborate this, indicating oxygen was either absent or present in very low concentrations at below OMZ-seep 1 and higher at the SWI of below OMZ-seep 2. Mn-oxides are stable under oxic conditions and begin to dissolve as soon as the environment becomes reducing (Saager et al., 1989; Schenau et al., 2002; van der Weijden et al., 2006). So, the presence or absence of Mn^{2+} in the uppermost sediments can be used as an oxygen indicator. Subsequently, the below OMZ-seep samples are classified as follows: below OMZ-seep 1 as anoxic, below OMZ-seep 2 as suboxic, and below OMZ-seep 3 as oxic (Table 5.1). Below OMZ-seep 3 was classified as oxic since it is furthest from the central gas orifice and

more likely influenced by the bottom water oxygen content of the surrounding area.

5.6.2 Alteration proxies (HPA, API, DOXI)

5.6.2.1 HPA

In the transects incorporating lateral oxygen gradients, the HPA ratios decrease by almost 30% (OMZ transect) and 20% (below OMZ-seep) with increasing oxygen concentrations (Fig. 5.5a). In comparison, there was no change observed along the OMZ-seep (Fig. 5.5a). These trends are the result of preferential degradation of the *n*-alcohols, which are more labile than the *n*-alkanes (e.g. Yamamoto et al., 2008). Since these trends are similar along the long OMZ transect and the short below OMZ-seep, the ratio values cannot only be a result of degradation en route to the marine realm or during settling through the water column, which confirms the conclusions of Westerhausen et al. (1993). The similar HPA values along both lateral oxygen gradients indicate that the major factor affecting this ratio is the oxygen content, which indicates that this index may be a useful and sensitive to determine redox changes at the SWI.

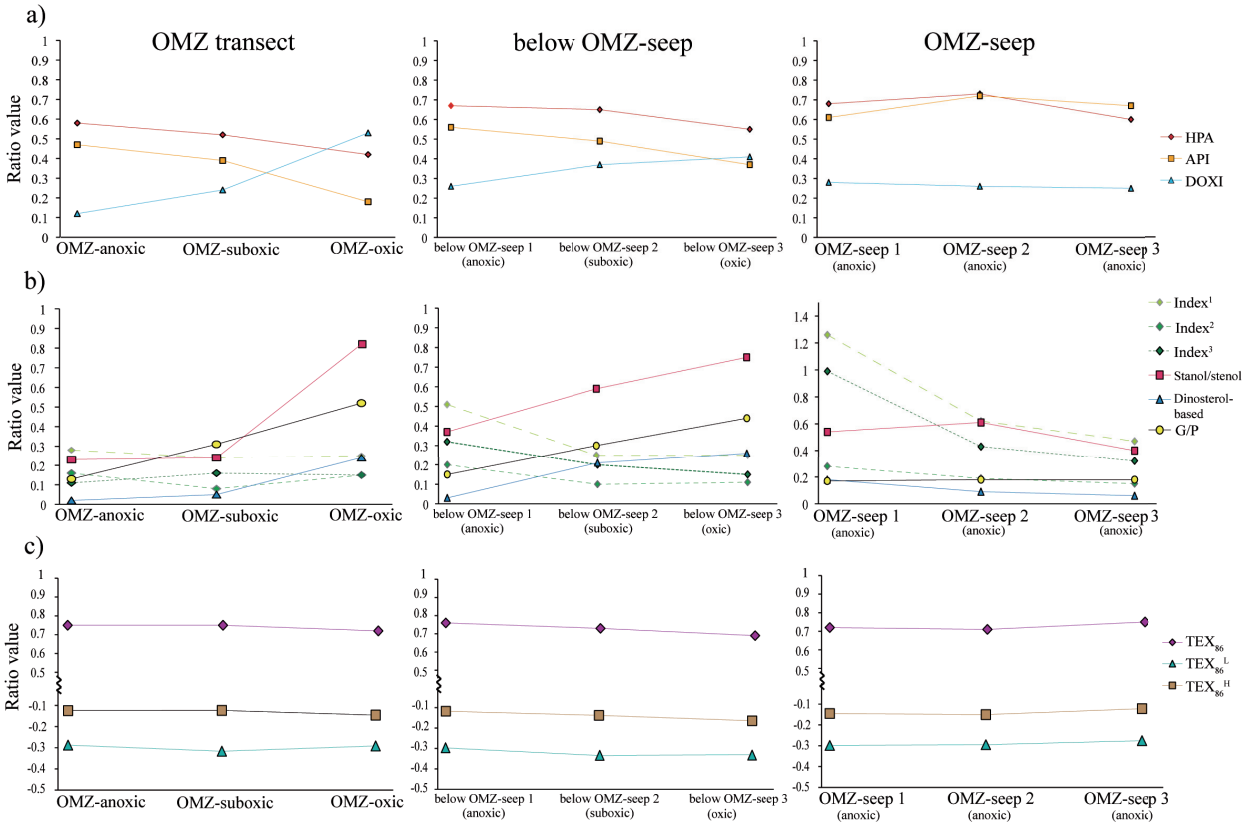

Figure 5.4: Ratios of alteration, productivity and temperature proxies.

5.6.2.2 API

The API provides very clear evidence for selective aerobic degradation at the SWI (Fig. 5.5a). The index decreased by more than 60% along the OMZ transect and more than 30% along the below-OMZ seep, whereas no trend was visible along OMZ-seep. In the studies of Cacho et al. (2000) and Martrat et al. (2007) where this ratio was used to reflect bottom water oxygenation changes in sediment cores, environmental heterogeneity, such as fluctuations in terrestrial input over time, could not be discounted as a variable possibly affecting the proxy. The short lateral oxygen transect of below OMZ-seep effectively eliminates that uncertainty. In our data, this ratio is effective as a bottom water oxygen indicator and that it is sensitive to changes in oxygen content at the SWI. Thus, we suggest that it is also a possible proxy for oxygenation changes in surface samples.

5.6.2.3 DOXI

This index reflects significant and rapid selective aerobic degradation, as a five-fold increase is present in the 1,15- C_{30} index along the OMZ transect and a doubling along the below OMZ-seep (Fig. 5.5a). Selective degradation of the diols relative to the keto-ols has previously been used to distinguish between the oxidized and unoxidized portions of the Mediterranean S1 sapropel (Ferreira et al., 2001; Versteegh et al., 2010). However, this is the first indication that this proxy is also able to reflect redox changes at the SWI in freshly deposited material. Ferreira et al. (2001) noted that the absolute concentrations of keto-ols increased as the diol concentrations decreased. They proposed that the keto-ols could be an oxidative product of the diols. In our samples, the relative concentration of the keto-ol increased as well (see Appendix A3), which is further evidence that keto-ols are oxidation products of the diols. C_{28}-C_{32} keto-ols were identified in a cultured marine eustimatophyte, *Nannochloropsis gaditana* (Méjanelle et al., 2003) and a fern species, *Osmunda regalis* (Jetter and Riederer, 1999). However, the keto-ol concentrations reported in *N. gaditana* were much smaller than what is generally measured in marine sediment (Méjanelle et al., 2003). Likewise, the terrestrial input to our samples is much less than the marine component so influence from vegetation should not be a major factor. Thus, even if there is a contributing factor of biosynthesized keto-ols, it is most likely a small amount and still would not be sufficient to explain the trend in the ratios along the seep transect below the OMZ.

5.6.3. Export production proxies (phytol, cholesterol, dinosterol indices and dinoflagellate cysts)

5.6.3.1 Phytol-based indices

The lack of any significant trends attributable to changing oxygen content from the three phytol-based indices indicates they do not reflect selective aerobic degradation. Instead, a secondary source appears to be overprinting two phytol-based indices. Index^{1} and index^{3} (Table 5.4; Fig. 5.5b) values in below OMZ-seep 1 and OMZ-seep 1 are up to an order of magnitude higher in comparison to the non-seep influenced anoxic sample, OMZ-anoxic. In contrast, index^{2} values only vary between 0.1-0.28 in all samples (Fig. 5.5b). This may suggest a sedimentary contribution of pristane. While pristane and phytane are generally considered compounds produced via degradation of phytol (e.g. Didyk et al., 1978), this assumption for pristane has been questioned in anoxic sediments (e.g. Grossi et al., 1998; Rontani and Volkman, 2003; Rontani et al., 2010). The higher index^{1} and index^{3} values in below OMZ-seep 1 and OMZ-seep 1 could indicate faster conversion of reactive phytol into a more refractory form (i.e. bound), which dominates in anoxic settings (e.g. Sun et al., 1998). If this were true, it should also be reflected in index^{2}, where in fact the values are stable. Thus, it is likely that there is a secondary source of pristane that does not involve the degradation of chlorophyll-*a* (for a review see Rontani and Bonin, 2011). Sources could include tocopherol degradation (Rontani et al., 2010) or input from archaeal lipids (Rowland, 1990). Even without the sedimentary input of pristane, the phytane-containing index^{2} does not show preferential degradation of phytol with increasing SWI oxygen concentrations. Our results agree with previous studies cautioning against the use of a proxy for redox changes based on these assumed phytol degradation products (Rontani and Volkman, 2003).

5.6.3.2 Cholesterol based stanol/stenol index

Increasing cholestanol/cholesterol index values more than double along the OMZ transect and the below OMZ-seep and suggest faster degradation of cholesterol predominantly occurs with increasing oxygen concentrations at the SWI (Fig. 5.5b). More efficient degradation of cholesterol under oxic conditions has been suggested in experiments previously (Sun and Wakeham, 1998). However, our data contrast with those from the Peru margin OMZ, where anoxic sediments generally produced the highest ratios

(McCaffrey et al., 1991). The reduction of cholesterol to cholestanol in anoxic surface sediments is generally a faster process than sterol degradation, and is the main reason for high stanol/stenol ratios in anoxic waters and sediments (Nishimura and Koyama, 1977; Wakeham, 1989). However, the presence of an increasing trend along lateral oxygen gradients suggests that the dominant process controlling this ratio is the degradation of cholesterol, so the ratio values reflect the faster degradation of cholesterol as opposed to cholestanol rather than the conversion of cholesterol to cholestanol. The higher rate of stenol degradation versus stenol hydrogenation has been suggested as one possibility for high stanol/stenol surface sediment values in an estuarine environment (Arzayus and Canuel, 2004). Therefore, in sediments with a steep lateral oxygen gradient, this ratio may be useful in determining the extent of sterol oxidation.

5.6.3.3 Dinosterol-based index

The dinosterol-based index increases by an order of magnitude along the OMZ transect and the below OMZ-seep (Fig. 5.5b), indicating faster degradation of dinosterol with increasing O_2 content at the SWI. It is unlikely that the index changes are a result of fluctuations in input from dinoflagellates, or other dinosterol-producing organisms (Volkman et al., 1993), as the trends are similar for the OMZ transect and the below OMZ-seep. Mouradian et al. (2007) indicate that inclusion of diagenetic products (Σdinflagellate lipids) of dinosterol provides evidence of preferential removal of dinosterol in oxic environments, as degradation of dinosterol would result in enrichments of its degradative products. Though dinostanone and dinosterone can be biosynthesized directly by dinoflagellates (e.g. Harvey et al., 1988; Leblond and Chapman, 2002; Chu et al., 2009), differences in input are again unlikely. Thus, we conclude that a dinosterol-based index using oxidative products of dinosterol degradation can be used to trace changes in oxygen content at the SWI.

5.6.3.4 G/P ratio

Dinoflagellate cysts are, in general, relatively resistant to degradation due to the structure of the cyst wall (e.g. Kokinos et al., 1998; Gélinas et al., 2001; de Leeuw et al., 2006; Zonneveld et al., 2008; Versteegh et al., submitted). However, it is known from laboratory (e.g. Dale, 1976; Hopkins and McCarthy, 2002) and field experiments (e.g. Kodrans-Nsiah et al., 2008) as well as natural sediments (e.g. Zonneveld et al., 1997;

2001; 2007; McCarthy et al., 2000) that P-cysts are more quickly oxidized relative to the G-cysts. In both the OMZ transect and below OMZ-seep, the G/P ratio increases by 75% and 66%, respectively (Fig. 5.5b). Thus, our data confirm the selective aerobic degradation of P-cysts and furthermore demonstrates a marked overprint along a meter-scale lateral oxygen gradient (below OMZ-seep). Previous studies have cautioned against the use of this ratio because it oversimplifies the relationship between the heterotrophic taxa that indicate productivity and P-cysts (e.g. Dale and Fjellså, 1994). Our results add another layer of caution as overprinting of the G/P ratio is likely to happen quickly with changes in oxygen content at the SWI. This overprint can be accounted for in some cases (Versteegh and Zonneveld, 2002) and, in areas of excellent preservation or when redox conditions remain stable over time, P-cysts are still valuable productivity proxies (e.g. Reichart and Brinkhuis, 2003). Therefore, the G/P ratio, based on the quantity of cysts, is also a potential proxy for tracing oxygen concentration changes at the SWI.

It is interesting to note that the dinosterol-based index and the G/P ratio demonstrated similar trends along the OMZ transect and the below OMZ-seep. There is some discrepancy between dinoflagellate cyst abundance and concentrations and dinosterol concentrations with studies either showing a weak (e.g. Marret and Scourse, 2002) or nonexistent (Pinturier-Geiss et al., 2002; Sangiorgi et al., 2005) correlation, which may be related to differences in the species that manufacture dinosterol as a membrane lipid and those that produce resting cysts (Boere et al., 2009). Our results agree with Mouradian et al. (2007) that inclusion of diagenetic transformation products of dinosterol increases the likelihood that the dinosterol-based index and dinoflagellate cyst trends will be similar. This may then reflect a correlation that is based on diagenetic factors, rather than productivity.

5.6.4 Temperature proxy

The overall small changes in the three GDGT-based indices and lack of any consistent trends (Fig. 5.5c) that could be attributed to the oxygen content at the SWI indicate that the GDGT distribution is not affected by selective aerobic degradation. Instead, it appears the GDGT signal is complicated by different factors in each transect as the TEX_{86} values and resulting SSTs are variable. SSTs calculated from these indices do not consistently reflect the annual mean SST (26.7° C) as recorded by Lornacini et al. (2010). TEX_{86} values are higher than previously reported for the Arabian Sea (e.g. Schouten et

al., 2002; 2004; Kim et al., 2008), and result in unrealistically high SSTs. The same is true for the TEX_{86}^{H}, which has shown to be suitable in subtropical waters (Kim et al., 2010). The most similar calculated SST to the reported SST of the area is derived from the TEX_{86}^{L}, which has been shown to be appropriate in (sub) polar waters (Kim et al., 2010). The difference between the three indices is the absence of the crenarcheaol regioisomer (Cren iso.) in TEX_{86}^{L}, which suggests a deviation from its observed correlation with SST at high temperatures (Kim et al., 2010) and indicates that this index may not necessarily be limited to lower temperatures (Ho et al., 2011). The crenarchaeol regioisomer has been suggested to have a different source from the other GDGTs (see the discussion in Shah et al., 2008). It was pointed out in Shah et al. (2008) that this could have implications for the TEX_{86} paleothermometer, which our data illustrate. However, the GDGT indices seem to show no clear trends that might suggest differential input of the crenarchaeol regioisomer or diagenetic alteration.

Complicating factors could include a strong seasonal signal (Wuchter et al., 2006; Leider et al., 2010), or sedimentary production in anoxic sediments (e.g. Pancost et al., 2001; Biddle et al., 2006; Lipp et al., 2008) so our data may reflect differential GDGT contributions from the water column (surface and subsurface; e.g. Huguet et al., 2007; Mollenhauer et al., 2008) as well as the seep environment. However, the lack of any consistency between OMZ-seep and below OMZ-seep would suggest that the two seep transect communities are heterogeneous. The recently proposed methane index (Zhang et al., 2011), suggests that in environments heavily impacted by methane hydrates, the contribution of GDGTs produced by methanotrophic archaea render the TEX_{86} index unreliable. However, in our data, it appears that the crenarcheaol regioisomer is the main source of variability as the TEX_{86}^{L} produces the most realistic SSTs (Table 5.4). Overall, we cannot determine which possible factors have the most influence but it seems that the three transects used in this study reflect heterogeneous input from the water column and the sediments. This suggests that, as discussed by Kim et al. (2010), there is a possibility of a significant effect from local conditions.

4.6. Conclusions

The OMZ and active methane seeps of the northeastern Arabian Sea present a natural laboratory to investigate proxy alteration as a result of changing oxygen content at the SWI. Our study investigated the effects of early selective aerobic degradation on

alteration, export production, and temperature proxies in surface samples collected along two lateral oxygen gradients. In order to constrain uncertainty regarding other environmental conditions, we utilized both the OMZ as well as methane seeps in oxic and anoxic bottom waters. The oxygen concentration at the SWI seemed to be the dominant controlling factor for most of the investigated proxy ratios, with the exception of the GDGT- and phytol-based indices, where localized environmental heterogeneity seems to be more important.

The HPA, API, and DOXI, previously used in sediment core studies as alteration proxies, appear to be quite sensitive to changing oxygen conditions at the SWI. These three proxies demonstrate sensitivity to changes in oxygen content at the SWI so that they may be used in conjunction for studies where OM composition or environmental heterogeneity is not as well constrained. The degradation of cholesterol at a well-oxygenated SWI seems to be faster than the reductive transformation of cholesterol to cholestanol so that a stanol/stenol index may be a useful proxy for changes in oxygen content. Likewise, a degradation index based on dinosterol and its transformational products might be useful to show redox changes in surface sediments. Finally, the dinoflagellate cyst based G/P index may be a useful proxy for SWI oxygenation. Our data demonstrate that even a small, localized lateral oxygen gradient at the SWI is sufficient to induce selective OM degradation. This potential to quickly and significantly affect proxy signals provides further evidence that care must be taken in order to accurately interpret the sedimentary record.

Acknowledgements

We appreciate the efforts of the captain and crew of the *R/V Meteor* cruise M74/3, as well as the ROV "MARUM-QUEST 4000" team (MARUM, Bremen) for their excellent support during the cruise. We also thank S. Forke, G. Greif, and R. Himmelsbach for laboratory assistance. X. Liu was kind enough to perform the GDGT analysis. Financial support was provided by the DFG-Research Center/Excellence Cluster MARUM "The Ocean in the Earth System", and the DFG (Deutsche Forschungsgemeinschaft) as part of the International Graduate College "Proxies in Earth History" (EUROPROX), as well as the Helmholtz group and a Heisenberg Fellowship (VE-486/2 and /3) to GJMV.

References

Aharon, P., Fu, B., 2000. Microbial sulfate reduction rates and sulfur and oxygen isotope fractionations at oil and gas seeps in deepwater Gulf of Mexico. *Geochimica et Cosmochimica Acta*, 64, 233-246.

Aharon, P., Fu, B., 2003. Sulfur and oxygen isotopes of coeval sulfate-sulfide in pore fluids of cold seep sediments with sharp redox gradients. *Chemical Geology*, 195, 201-218.

Arzayus, K.M., Canuel, E.A., 2004. Organic matter degradation in sediments of the York River estuary: Effects of biological vs. physical mixing. *Geochimica et Cosmochimica Acta*, 69, 455-463.

Barrett, S., Volkman, J.K., Dunstan, G.A., 1995. Sterols of 14 species of marine diatoms (Bacillariophyta), *Journal of Phycology*, 31, 360-369.

Bauer, S., Hitchcock, J.L., Olson, D.B., 1991. Influence of monsoonally-forced Ekman dynamics upon surface layer depth and plankton biomass distribution in the Arabian Sea. *Deep Sea Research*, 38, 531-553.

Biddle, J.F., Lipp, J.S., Lever, M.A., Lloyd, K.G., Sørensen, K.B., Anderson, R., Fredericks, H.F., Elvert, M., Kelly, T.J., Schrag, D.P., Sogin, M.L., Brenchley, J.E., Teske, A., House, C. H., Hinrichs, K.-U., 2006. Heterotrophic Archaea dominate sedimentary subsurface ecosystems off Peru. *Proceedings of the National Academy of Sciences,* 103, 3846-3851.

Bockelmann, F., Zonneveld, K.A.F., Schmidt, M., 2007. Assessing environmental control on dinoflagellate cyst distribution in surface sediments of the Benguela upwelling region (eastern South Atlantic). Limnology and Oceanography, 52, 2582-2594.

Bohrmann, G., Bahr, A., Brinkmann, F., Brüning, M., Buhmann, S., Diekamp, V., Enneking, K., Fischer, D., Gassner, A., von Halem, G., Huettich, D., Kasten, S., Klapp, S., Nasir, M., Nowald, N., Ochsenhirt, W.T., Pape, T., Ratmeyer, V., Rehage, R., Rethemeyer, J., Reuter, M., Rossel, P., Saleem, M., Schmidt, W., Seiter, C., Stephan, S., Thomanek, K., Wittenberg, N., Yoshinaga, M., Zonneveld, K., 2008. Report and preliminary results of *R/V Meteor* cruise M74/3, Fujairah – Malé, 30 October – 7 November, 2007, Cold seeps of the Makran subduction zone (Continental margin off Pakistan), *Berichte*, Fachbereich 5, Universität Bremen, edited by: Bohrmann, G. and Ohling, G., Bremen, Germany, 161 pp.

Boon, J.J., Rijpstra, W.I.C., de Lange, F., de Leeuw, J.W., 1979. Black Sea sterol – a molecular fossil for dinoflagellate blooms. *Nature*, 277, 125-126.

Brand, T.D., Griffiths, C., 2009. Seasonality in the hydrography and biogeochemistry across the Pakistan Margin of the NE Arabian Sea. *Deep Sea Research Part II*, 56, 283-295.

Breuer, E.R., Law, G.T.W., Woulds, C., Cowie, G.L., Shimmield, G.B., Peppe, O., Schwartz, M., McKinlay, S., 2009. Sedimentary oxygen consumption and microdistribution at sites across the Arabian Sea oxygen minimum zone (Pakistan margin). *Deep Sea Research Part II*, 56, 296-304.

Cacho, I., Grimalt, J.O., Sierro, F.J., Shackleton, N., Canals, M., 2000. Evidence for enhanced Mediterranean thermohaline circulation during rapid climatic coolings. *Earth and Planetary Science Letters*, 183, 417-429.

Calvert, S.E., Pedersen, T.F., Naidu, P.D., von Stackelburg, U., 1995. On the organic carbon maximum on the continental slope of the eastern Arabian Sea. *Journal of Marine Research*, 53, 279-296.

Canfield, D.E., Thamdrup, B., Hansen, J.W., 1993. The anaerobic degradation of organic matter in Danish coastal sediments: iron reduction, manganese reduction, and sulphate reduction. *Geochimica et Cosmochimica Acta*, 57, 3867-3883.

Canuel, E.A., Martens, C.S., 1996. Reactivity of recently deposited organic matter: Degradation of lipid compounds near the sediment-water interface. *Geochimica et Cosmochimica Acta*, 60, 1793-1806.

Chu, F.L.E., Lund, E.D., Littreal, P.R., Ruck, K.E., Harvey, E., 2009. Species-specific differences in long-chain n-3 essential fatty acid, sterol, and steroidal ketone production in six heterotrophic protist species. *Aquatic Biology*, 6, 159-172.

Combourieu-Nebout, N., Paterne, M., Turon, J.L., Siani, G., 1998. A high-resolution record of the last deglaciation in the central Mediterranean Sea: Palaeovegetation and palaeohydrological evolution. *Quaternary Science Reviews*, 17, 303-317.

Cowie, G.L., Hedges, J.L., Prahl, F.G., de Lange, G.J., 1995. Elemental and major biochemical changes across an oxidation front in a relict turbidite: an oxygen effect. Geochimica et Cosmochimica Acta, 59, 33-46.

Cowie, G.L., Calvert, S.E., Pedersen, T.F., Schulz, H., von Rad, U., 1999. Organic content and preservational controls in surficial shelf and slope sediments from the Arabian Sea (Pakistan Margin). *Marine Geology*, 161, 23-38.

Dale, B., 1976. Cyst formation, sedimentation, and preservation: factors affecting dinoflagellate assemblages in recent sediments from Trondheimsfjord, Norway. *Review of Palaeobotany and Palynology*, 22, 39-60.

Dale, B., Fjellså, A., 1994. Dinoflagellate cysts as paleoproductivity indicators: state of the art, potential and limits, In: Zahn, R., Pedersen, T.F., Kaminski, M.A., Labeyrie, L. (Eds.), *Carbon Cycling in the Glacial Ocean: Constraints on the Ocean's Role in Global Change*, Springer, Berlin, pp. 521-537.

de Leeuw, J.W., Rijpstra, W.I.C., Schenck, P.A., 1981. The occurence and identification of C_{30}, C_{31}, and C_{32} alkan-1,15-diols and alkan-15-one-1-ols in Unit I and Unit II Black Sea sediments. *Geochimica et Cosmochimica Acta*, 45, 2281-2285.

de Leeuw, J.W., Versteegh, G.J.M., van Bergen, P.F., 2006. Biomacromolecules of algae and plants and their fossil analogues. *Plant Ecology*, 182, 209-233.

Didyk, B.M., Simoneit, B.R.T., Brassell, S.C., Eglinton, G., 1978. Organic geochemical indicators of paleoenvironmental conditions of sedimentation. *Nature*, 272, 216-222.

Ding, F., Spiess, V., Fekete, N., Murton, B., Bruening, M., Bohrmann, G., 2010. Interaction between accretionary thrust faulting and slope sedimentation at the frontal Makran accretionary prism and its implications for hydrocarbon fluid seepage. *Journal of Geophysical Research,* 115, B08106, doi: 10.1029/2008JB006246.

Eglinton, G., Hamilton, R.J., 1967. Leaf epicuticular waxes. *Science*, 156, 1322-1335.

Fensome, R.A., Williams, G.L., 2004. *The Lentin and Williams index of fossil dinoflagellates, 2004 Edition*, American Association of Stratigraphic Palynologists, Contributions Series 42, 909 pp.

Fensome, R.A., Taylor, F.J.R., Norris, G., Sarjeant, W.A.S., Wharton, D.I., Williams, G.L., 1993. *A classification of fossil and living dinoflagellates*, Micropaleontology Press Special Paper, 7, 351 pp.

Ferreira, A.M., Miranda, A., Caetano, M., Baas, M., Vale, C., Sinninghe Damsté, J.S., 2001. Formation of mid-chain alkane keto-ols by post-depositional oxidation of mid-chain diols in Mediterranean sapropels. *Organic Geochemistry*, 32, 271-276.

Fischer, D., Sahling, H., Nöthen, K., Bohrmann, G., Zabel, M., Kasten, S. Interaction between hydrocarbon seepage, chemosynthetic communities and bottom water redox at cold seeps of the Makran accretionary prism: Insights from habitat-specific pore water sampling and modeling. Under review in *Biogeosciences*.

Fukushima, K., Ishiwatari, R., 1984. Acid and alcohol compositions of wax esters in sediments from different environments. *Chemical Geology*, 47, 41-56.

Gélinas, Y., Baldock, J.A., Hedges, J.I., 2001. Organic carbon composition of marine sediments: effect of oxygen exposure on oil generation potential. *Science*, 294, 145-148.

Grossi, V., Hirschler, D., Raphel, D., Rontani, J.F., de Leeuw, J.W., Bertrand, J.C., 1998. Biotransformation pathways of phytol in Recent anoxic sediments. *Organic Geochemistry*, 29, 845-861.

Grossi, V., Blokker, P., Sinninghe Damsté, J.S., 2001. Anaerobic biodegradation of lipids of the marine microalga *Nannochloropsis salina*. *Organic Geochemistry*, 32, 795-808.

Harland, R., 1973. Dinoflagellate cysts and acritarchs from the Bearpaw Formation (upper Campanian) of southern Alberta, Canada. *Paleontology*, 16, 665-706.

Hartnett, H.E., Keil, R.G., Hedges, J.I., Devol, A.H., 1998. Influence of oxygen exposure time on organic carbon preservation in continental margin sediments. *Nature*, 391, 572-574.

Harvey, H.R., Bradshaw, S.A., O'Hara, S.C.M., Eglinton, G., Corner, E.D.S., 1988. Lipid composition of the marine dinoflagellate *Scrippsiella trochoidea*. *Phytochemisty*, 27, 1723-1729.

Hedges, J.I., Keil, R.G., 1995. Sedimentary organic matter preservation: an assessment and speculative synthesis. Marine Chemisty, 49, 81-115.

Hedges, J.I., Hu, F.S., Devol, A.H., Hartnett, H.E., Tsamakis, E., Keil, R.G., 1999. Sedimentary organic matter preservation: a test for selective degradation under oxic conditions. *American Journal of Science*, 299, 529-555.

Henrichs, S.M., 1992. Early diagenesis of organic matter in marine sediments: progress and perplexity. *Marine Chemistry*, 39, 119-149.

Ho, S.L., Yamamoto, M., Mollenhauer, G., Minagawa, M., 2011. Core top TEX_{86} values in the south and equatorial Pacific. *Organic Geochemisty*, 42, 94-99.

Hoefs, M.J.L., Rijpstra, W.I.C., Sinninghe Damsté, J.S., 2002. The influence of oxic degradation on the sedimentary biomarker record I: Evidence from Madeira Abyssal Plain turbidites. *Geochimica et Cosmochimica Acta*, 66, 2719-2735.

Holzwarth, U., Esper, O., Zonneveld, K., 2007. Distribution of organic-walled dinoflagellate cysts in sediments of the Benguela upwelling system in relationship to environmental conditions. *Marine Micropaleontology*, 64, 91-119.

Hopkins, J.A., McCarthy, F.M.G., 2002. Post-depositional palynomorph degradation in Quaternary shelf sediments: a laboratory experiment studying the effects of progressive oxidation. *Palynology*, 26, 167-184.

Hopmans, E.C., Schouten, S., Pancost, R., van der Meer, M.T.J., Sinninghe Damsté, J.S., 2000. Analysis of intact tetraether lipids in archaeal cell material and sediments by high performance liquid chromatography/atmospheric pressure chemical ionization mass spectrometry. *Rapid Communications in Mass Spectrometry*, 14, 585-589.

Hudson, E.D., Parrish, C.C., Helleur, R.J., 2001. Biogeochemistry of sterols in plankton, settling particles and recent sediments in a cold ocean ecosystem (Trinity Bay, Newfoundland). *Marine Chemistry*, 76, 253-270.

Huguet, C., Schimmelmann, A., Thunell, R., Lourens, L.J., Sinninghe Damsté, J.S., Schouten, S., 2007. A study of the TEX_{86} paleothermometer in the water column and sediments of Santa Barbara Basin, California. *Paleoceanography*, 22, PA3203, doi: 10.10129/2006PA00131.

Huguet, C., Kim, J.H., de Lange, G.J., Sinninghe Damsté, J.S., Schouten, S., 2009. Effects of long term oxic degradation on the U^{K}_{37}, TEX_{86} and BIT organic proxies. *Organic Geochemistry*, 40, 1188-1194.

Hulthe, G., Hulth, S., Hall, P.O.J., 1998. Effect of oxygen on the degradation rate of refractory and labile organic matter in continental margin sediments. *Geochimica et Cosmochimica Acta*, 62, 1319-1328.

Jetter, R., Riederer, M., 1999. Long-chain alkanediols, ketoaldehydes, ketoalcohols and ketoalkyl esters in the cuticular waxes of *Osmunda regalis* fronds. *Phytochemistry*, 52, 907-915.

Jørgensen, B.B., 1982. Mineralisation of organic-matter in the sea-bed – the role of sulphate reduction. *Nature*, 296, 643-645.

Jørgensen, B.B., Kasten, S., 2006. Sulfur cycling and methane oxidation. In: Schulz, H.D., and Zabel, M. (Eds.), *Marine Geochemistry*, Springer, Heidelberg, pp. 263-282.

Karner, M.B., DeLong, E.F., Karl, D.M., 2001. Archaeal dominance in the mesopleagic zone of the Pacific Ocean. *Nature*, 409, 507-509.

Keil, R.G., Cowie, G.L., 1999. Organic matter preservation through the oxygen-deficient zone of the NE Arabian Sea as discerned by organic carbon: mineral surface area ratios. *Marine Geology*, 161, 13-22.

Kim, J.H., Schouten, S., Hopmans, E.C., Donner, B., Sinninghe Damsté, J.S., 2008. Global sediment core-top calibration of the TEX_{86} paleothermometer in the ocean. *Geochimica et Cosmochimica Acta*, 72, 1154-1173.

Kim, J.H., van der Meer, J., Schouten, S., Helmke, P., Willmott, V., Sangiorgi, F., Koç, N., Hopmans, E.C., Sinninghe Damsté, J.S., 2010. New indices and calibrations derived from the distribution of crenarchaeal isoprenoid tetraether lipids: Implications for past sea surface temperature reconstructions. *Geochimica et Cosmochimica Acta*, 74, 4639-4654.

Kodrans-Nsiah, M., de Lange, G.J., Zonneveld, K.A.F., 2008. A natural exposure experiment on short-term species-selective aerobic degradation of dinoflagellate cysts. *Review of Palaeobotany and Palynology*, 152, 32-39.

Kokinos, J.P., Eglinton, T.I., Goñi, M.A., Boon, J.J., Martoglio, P.A., Anderson, D.M., 1998. Characterization of a highly resistant biomacromolecular material in the cell wall of a marine dinoflagellate resting cyst. *Organic Geochemistry*, 28, 265-288.

Leblond, J.D., Chapman, P.J., 2002. A survey of the sterol composition of the marine dinoflagellates *Karenia brevis*, *Karenia mikimotoi*, and *Karlodinium micrum*: distribution of sterols within other members of the class Dinophyceae. *Journal of Phycology*, 38, 670-682.

Leider, A., Hinrichs, K.-U., Mollenhauer, G., Versteegh, G.J.M., 2010. Core-top calibration of the lipid based $U^{K'}_{37}$ and TEX_{86} temperature proxies on the southern Italian shelf (SW Adriatic Sea, Gulf of Taranto). *Earth and Planetary Science Letters*, 300, 112-124.

Lipp, J., Morono, Y., Inagaki, F., Hinrichs, K.-U., 2008. Significant contribution of Archaea to extant biomass in marine subsurface sediments. *Nature*, 454, 991-994.

Liu, X., Lipp, J.S., Hinrichs, K.-.U., 2011. Distribution of intact and core GDGTs in marine sediments. *Organic Geochemistry*, 42, 368-375.

Locarnini, R. A., Mishonov, A. V., Antonov, J. I., Boyer, T. P., Garcia, H. E., Baranova, O. K., Zweng, M. M., Johnson, D. R., 2010. *World Ocean Atlas 2009, Volume 1: Temperature,* S. Levitus (Ed.), NOAA Atlas NESDIS 68, U.S. Government Printing Office, Washington, D.C., 184 pp.

Lückge, A., Ercegovac, M., Strauss, H., Littke, R., 1999. Early diagenetic alteration of organic matter by sulfate reduction in Quaternary sediments from the northeastern Arabian Sea. *Marine Geology*, 158, 1-13.

Madhupratap, M., Prasanna Kumar, S., Bhattathiri, P.M.A., Dileep Kumar, M., Raghukumar, S., Nair, K.K.C., Ramaiah, N., 1996. Mechanism of the biological response to winter cooling in the northeastern Arabian Sea. *Nature*, 384, 549-552.

Marret, F., Scourse, J., 2002. Control of modern dinoflagellate cyst distribution in the Irish and Celtic seas by seasonal stratification dynamics. *Marine Micropaleontology*, 47, 101-116.

Martrat, B., Grimalt, J.O., Shackleton, N.J., de Abreu, L., Hutterli, M.A., Stocker, T.F., 2007. Four climate cycles of recurring deep and surface water destabilizations on the Iberian Margin. *Science*, 317, 502-507.

Matsuoka, K., Kawami, H., Nagai, S., Iwataki, M., Takayama, H., 2009. Re-examination of cyst motile relationships of *Polykrikos kofoidii* Chatton and *Polykrikos schwartzii* Bütschli (Gymnodiniales, Dinophyceae). *Review of Palaeobotany and Palynology*, 154, 79-90.

McCaffrey, M.A., Farrington, J.W., Repeta, D.J., 1991. The organic geochemistry of Peru margin surface sediments: II. Paleoenvironmental implications of hydrocarbon and alcohol profiles. *Geochimica et Cosmochimica Acta*, 55, 483-498.

McCarthy, F.M.G., Gostlin, K.E., Mudie, P.J., Scott, D.B., 2000. Synchronous palynological changes in early Pleistocene sediments off New Jersey and Iberia, and a possible paleoceanographic explanation. *Palynology*, 24, 63-77.

Méjanelle, L., Sanchez-Gargallo, A., Bentaleb, I., Grimalt, J., 2003. Long chain n-alkyl diols, hydroxy ketones and sterols in a marine eustigmatophyte, *Nannochloropsis gaditana*, and in *Brachionus plicatilis* feeding on the algae. *Organic Geochemistry*, 34, 527-538.

Menzel, D., Hopmans, E.C., Schouten, S., Sinninghe Damsté, J.S., 2006. Membrane tetraether lipids of planktonic Crenarchaeota in Pliocene sapropels of the eastern Mediterranean Sea. *Palaeogeography, Palaeoclimatology, Palaeoecology*, 239, 1-15.

Mollenhauer, G., Inthorn, M., Vogt, T., Zabel, M., Sinninghe Damsté, J.S., Eglinton, T.I., 2007. Aging of marine organic matter during cross-shelf lateral transport in the Benguela upwelling system revealed by compound-specific radiocarbon dating. *Geochemistry, Geophysics, Geosystems*, 8, Q09004, doi: 10.1029/2007GC001603.

Mollenhauer, G., Eglinton, T.I., Hopmans, E.C., and Sinninghe Damsté, J.S., 2008. A radiocarbon-based assessment of the preservation characteristics of crenarchaeol and alkenones from continental margin sediments. *Organic Geochemistry,* 39, 1039-1045.

Mouradian, M., Panetta, R.J., de Vernal, A., Gélinas, Y., 2007. Dinosterols or dinocysts to estimate dinoflagellate contributions to marine sedimentary organic matter? *Limnology and Oceanography*, 52, 2569-2581.

Mudie, P.J., Rochon, A., 2001. Distribution of dinoflagellate cysts in the Canadian Arctic marine realm. *Journal of Quaternary Science*, 16, 603-620.

Nishimura, M., Koyama, T., 1977. The occurrence of stanols in various living organisms and the behavior of sterols in contemporary sediments. *Geochimica et Cosmochimica Acta*, 41, 379-385.

Olson, D.B., Hitchcock, G.L., Fine, R.A., Warren, B.A., 1993. Maintenance of the low-oxygen layer in the central Arabian Sea. *Deep Sea Research Part II*, 40, 673-685.

Pancost, R.D., Hopmans, E.C., Sinninghe Damsté, J.S., MEDINAUT Shipboard Scientific Party, 2001. Archaeal lipids in Mediterranean cold seeps: molecular proxies for anaerobic methane oxidation. *Geochimica et Cosmochimica Acta*, 65, 1611-1627.

Paropkari, A.L., Prakash Babu, C., Mascarenhas, A., 1992. A critical evaluation of depositional parameters controlling the variability of organic carbon in Arabian Sea sediments. *Marine Geology*, 107, 213-226.

Paropkari, A.L., Prakash Babu, C., Mascarenhas, A., 1993. New evidence for enhanced preservation of organic carbon in contact with oxygen minimum zone on the western continental slope of India. *Marine Geology*, 111, 7-13.

Pedersen, T.F., Shimmield, G.B., Price, N.B., 1992. Lack of enhanced preservation of organic matter in sediments under the oxygen minimum zone on the Oman Margin. *Geochimica et Cosmochimica Acta*, 56, 545-551.

Pinturier-Geiss, L., Méjanelle, L., Dale, B., Karlsen, D.A., 2002. Lipids as indicators of eutrophication in marine coastal sediments. *Journal of Microbiological Methods*, 48, 239-257.

Prahl, F.G., Dymond, J., Sparrow, M.A., 2000. Annual biomarker record for export production in the central Arabian Sea. *Deep Sea Research Part II*, 47, 1581-1604.

Prasanna Kumar, S., Ramaiah, N., Mangesh Gauns, Sarma, V.V.S.S., Muraleedharan, P.M., Raghukumar, S., Dileep Kumar, M., Madhupratap, M., 2001. Physical forcing of biological productivity in the Northern Arabian Sea during the Northeast Monsoon. *Deep Sea Research Part II*, 48, 1115-1126.

Qasim, S.Z., 1982. Oceanography of the northern Arabian Sea. Deep Sea Research, 29, 1041-1068.

Reichart, G.J., Brinkhuis, H., 2003. Late Quaternary *Protoperidinium* cysts as indicators of paleoproductivity in the northern Arabian Sea. *Marine Micropaleontology*, 49, 303-315.

Roberts, H.H., Carney, R.S., 1997. Evidence of episodic fluid, gas, and sediment venting on the northern Gulf of Mexico continental slope. *Economical Geology*, 92, 863-879.

Robinson, N., Eglinton, G., Brassell, S.C., Cranwell, P., 1984. Dinoflagellate origin for sedimentary 4α-methylsteroids and 5α(H)-stanols. *Nature*, 308, 439-442.

Römer, M., Sahling, H., Pape, T., Bohrmann, G., Spiess, V. Gas bubble emission from submarine hydrocarbon seeps at the Makran continental margin (offshore Pakistan). Submitted.

Rontani, J.F., Volkman, J.K., 2003. Phytol degradation products as biogeochemical tracers in aquatic environments. *Organic Geochemistry*, 34, 1-35.

Rontani, J.F., Bonin, P., 2011. Production of pristane and phytane in the marine environment: role of prokaryotes. *Research in Microbiology*, doi: 10.1016/j.resmic.2011.01.012.

Rontani, J.F., Nassiry, M., Michotey, V., Guasco, S., Bonin, P., 2010. Formation of pristane from *a*-tocopherol under simulated anoxic sedimentary conditions: A combination of biotic and abiotic degradative processes. *Geochimica et Cosmochimica Acta,* 74, 252-263.

Rowland, S.J., 1990. Production of acyclic isoprenoid hydrocarbons by laboratory maturation of methanogenic bacteria. *Organic Geochemistry*, 15, 9-16.

Saager, P.M., de Baar, H.J.W., Burkill, P.H., 1989. Manganese and iron in Indian Ocean waters. *Geochimica et Cosmochimica Acta*, 53, 2259-2267.

Sangiorgi, F., Fabbri, D., Comandini, M., Gabbianelli, G., Tagliavini, E., 2005. The distribution of sterols and organic-walled dinoflagellate cysts in surface sediments of the North-western Adriatic Sea (Italy). *Estuarine, Coastal and Shelf Science*, 64, 395-406.

Schenau, S.J., Reichart, G.J., de Lange, G.J., 2002. Oxygen minimum zone controlled Mn redistribution in Arabian Sea sediments during the Late Quaternary. *Paleoceanography*, 17, 1058, doi: 10.1029/2000PA000621.

Schouten, S., Hopmans, E.C., Schefuß, E., Sinninghe Damsté, J.S., 2002. Distributional variations in marine crenarchaeotal membrane lipids: a new tool for reconstructing ancient sea water temperatures? *Earth and Planetary Science Letters*, 204, 265-274.

Schouten, S., Hopmans, E.C., Sinninghe Damsté, J.S., 2004. The effect of maturity and depositional redox conditions on archaeal tetraether lipid palaeothermometry. *Organic Geochemistry*, 35, 567-571.

Schouten, S., Forster, A., Panato, E., Sinninghe Damsté, J.S., 2007. Towards the calibration of the TEX_{86} paleothermometer in ancient greenhouse worlds. *Organic Geochemistry*, 38, 1537-1546.

Schubert, C.J., Villanueva, J., Calvert, S.E., Cowie, G.L., von Rad, U., Schulz, H., Berner, U., Erlenkeuser, H., 1998. Stable phytoplankton community structure in the Arabian Sea over the past 200,000 years. *Nature*, 394, 563-566.

Schulte, S., Rostek, F., Bard, E., Rullkötter, J., Marchal, O., 1999. Variations in oxygen-minimum and primary productivity recorded in sediments of the Arabian Sea. *Earth and Planetary Science Letters*, 173, 205-221.

Schulte, S., Mangelsdorf, K., Rullkötter, J., 2000. Organic matter preservation on the Pakistan continental margin as revealed by biomarker geochemistry. *Organic Geochemistry*, 31, 1005-1022.

Seeberg-Elverfeldt, J., Schlüter, M., Feseker, T., Kölling, M., 2005. Rhizon sampling of pore waters near the sediment-water interface of aquatic systems. *Limnology and Oceanography Methods*, 3, 361-371.

Shah, S.R., Mollenhauer, G., Ohkouchi, N., Eglinton, T.I., Pearson, A., 2008. Origins of archaeal tetraether lipids in sediments: Insights from radiocarbon analysis. *Geochimica et Cosmochimica Acta*, 72, 4577-4594.

Shapiro, G.I., Meschanov, S.L., 1991. Distribution of Red Sea Water and salt lens formation in the northwest Indian Ocean. *Deep Sea Research*, 38, 21-34.

Sinninghe Damsté, J.S., Rijpstra, W.I.C., Reichart, G.J., 2002. The influence of oxic degradation on the sedimentary biomarker record II. Evidence from Arabian Sea sediments. *Geochimica et Cosmochimica Acta*, 66, 2737-2754.

Smallwood, B.J., Wolff, G.A., 2000. Molecular characterisation of organic matter in sediments underlying the oxygen minimum zone at the Oman Margin, Arabian Sea. *Deep Sea Research Part II*, 47, 353-375.

Suess, E., Carson, B., Ritger, S.D., Moore, J.C., Jones, M.L., Kulm, L.D., Cochrane, G.R., 1985. Biological communities at vent sites along the subduction zone off Oregon. *Biological Society of Washington Bulletin*, 6, 475-484.

Sun, M.Y., Wakeham, S.G., 1994. Molecular evidence for degradation and preservation of organic matter in the anoxic Black Sea Basin. *Geochimica et Cosmochimica Acta*, 58, 3395-3406.

Sun, M.Y., Wakeham, S.G., 1998. A study of oxic/anoxic effects of degradation of sterols at the simulated sediment-water interface of coastal sediments. *Organic Geochemistry*, 28, 773-784.

Sun, M.Y., Wakeham, S.G., Aller, R.C., Lee, C., 1998. Impact of seasonal hypoxia on diagenesis of phytol and its derivatives in Long Island Sound. *Marine Chemistry*, 62, 157-173.

van der Weijden, C.H., Reichert, G.J., Visser, H.J., 1999. Enhanced preservation of organic matter in sediments deposited within the oxygen minimum zone in the northeastern Arabian Sea. *Deep Sea Research Part II*, 46, 807-830.

van der Weijden, C.H., Reichart, G.J., van Os, B.J.H., 2006. Sedimentary trace element records over the last 200 kyr from within and below the northern Arabian Sea oxygen minimum zone. *Marine Geology*, 231, 69-88.

Versteegh, G.J.M., Zonneveld, K.A.F., 2002. Use of selective degradation to separate preservation from productivity. *Geology*, 30, 615-618.

Versteegh, G.J.M., Bosch, H.J., de Leeuw, J.W., 1997. Potential palaeoenvironmental information from C_{24} to C_{36} mid-chain diols, keto-ols, and mid-chain hydroxyl fatty acids: a critical review. *Organic Geochemistry*, 27, 1-13.

Versteegh, G.J.M., Zonneveld, K.A.F., de Lange, G.J., 2010. Selective aerobic and anaerobic degradation of lipids and palynomorphs in the Eastern Mediterranean since the onset of sapropel S1 deposition. *Marine Geology*, 278, 177-192.

Versteegh, G.J.M., Blokker, P., Bogus, K., Harding, I., Lewis, J., Oltmanns, S., Rochon, A., Zonneveld, K.A.F., in press. Flash pyrolysis and infrared spectroscopy of cultured and sediment derived *Lingulodinium polyedrum* (Dinoflagellata) cyst walls. *Organic Gechemistry*.

Volkman, J.K., Maxwell, J.R., 1986. Acyclic isoprenoids as biological markers, In: Johns, R.B. (Ed.), *Biological Markers in the Sedimentary Record,* Elsevier, Amsterdam, pp. 1-46.

Volkmann, J.K., Barrett, S.M., Dunstan, G.A., Jeffrey, S.W., 1993. Geochemical significance of the occurrence of dinosterol and other 4-methyl sterols in a marine diatom. *Organic Geochemistry*, 20, 7-15.

Volkmann, J.K., Barrett, S.M., Blackburn, S.I., Mansour, M.P., Sikes, E.L., Gelin, F., 1998. Microalgal biomarkers: a review of recent research developments. *Organic Geochemistry*, 29, 1163-1179.

Volkman, J.K., Rijpstra, W.I.C., de Leeuw, J.W., Mansour, M.P., Jackson, A.E., Blackburn, S.I., 1999. Sterols of four dinoflagellates from the genus *Prorocentrum*. *Phytochemistry*, 52, 659-668.

von Rad, U., Schulz, H., Ali Khan, A., Ansari, M., Berner, U., Cepek, P., Cowie, G., Dietrich, P., Erlenkeuser, H., Geyh, M., Jennerjahn, T., Lückge, A., Marchig, V., Riech, V., Rösch, H., Schäfer, P., Schulte, S., Sirocko, F., Tahir, M., Weiss, M., 1995. Sampling the oxygen minimum zone off Pakistan: glacial-interglacial variations of anoxia and productivity (preliminary results, SONNE 90 cruise). *Marine Geology*, 125, 7-19.

von Rad, U., Rösch, H., Berner, U., Geyh, M., Marchig, V., Schulz, H., 1996. Authigenic carbonates derived from oxidized methane vented from the Makran accretionary prism off Pakistan. *Marine Geology*, 136, 55-77.

von Rad, U., Schaaf, M., Michels, K.H., Schulz, H., Berger, W.H., Sirocko, F., 1999. A 5000-yr record of climate change in varied sediments from the oxygen minimum zone off Pakistan, Northeastern Arabian Sea. *Quaternary Research*, 51, 39-53.

Wakeham, S.G., 1989. Reduction of stenols to stanols in particulate matter at oxic-anoxic boundaries in seawater. *Nature*, 342, 787-790.

Wakeham, S.G., Peterson, M.L., Hedges, J.I., Lee, C., 2002. Lipid biomarker fluxes in the Arabian Sea, with a comparison to the equatorial Pacific Ocean, *Deep Sea Research Part II*, 49, 2265-2301.

Westerhausen, L., Poynter, J., Eglinton, G., Erlenkeuser, H., Sarnthein, M., 1993. Marine and terrigenous origin of organic matter in modern sediments of the equatorial East Atlantic: the $\partial^{13}C$ and molecular record. *Deep Sea Research Part I*, 40, 1087-1121.

Witte, U., Pfannkuche, O., 2000. High rates of benthic carbon remineralisation in the abyssal Arabian Sea. *Deep Sea Research Part II*, 47, 2785-2804.

Wuchter, C., Schouten, S., Coolen, M.J.L., Sinninghe Damsté, J.S., 2004. Temperature-dependent variations in the distribution of tetraether membrane lipids of marine Crenarchaeota: implications for TEX_{86} paleothermometry. *Paleoceanography*, 19, PA4028. doi:10.1029/2004PA001041.

Wuchter, C., Schouten, S., Wakeham, S.G., Sinninghe Damsté, J.S., 2005. Temporal and spatial variation in tetraether membrane lipids of marine Crenarchaeota in particulate organic matter: implications for TEX_{86} paleothermometry. *Paleoceanography*, 20, PA3013. doi:10.1029/2004PA001110.

Wuchter, C., Schouten, S., Wakeham, S.G., Sinninghe Damsté, J.S., 2006. Archaeal tetraether membrane lipid fluxes in the northeastern Pacific and the Arabian Sea: implications for TEX_{86} paleothermometry. *Paleoceanography*, 21, PA4208. doi:10.1029/2006PA001279.

Wyrtki, K., 1973. Physical oceanography of the Indian Ocean, In: Zeitschel, B. (Ed.), *The Biology of the Indian Ocean*, Springer, Berlin, pp. 18-36.

Yamamoto, M., Okino, T., Sugisaki, S., Sakamoto, T., 2008. Late Pleistocene changes in terrestrial biomarkers in sediments from the central Arctic Ocean. *Organic Geochemistry*, 39, 754-763.

Zhang, Y.G., Zhang, C.L., Liu, X-L., Li, L., Hinrichs, K.-U., Noakes, J.E., 2011. Methane Index: A tetraether archaeal lipid biomarker indicator for detecting the instability of marine gas hydrates. *Earth and Planetary Science Letters*, 307, 525-534.

Zonneveld, K.A.F., Versteegh, G.J.M., de Lange, G.J., 1997. Preservation of organic-walled dinoflagellate cysts in different oxygen regimes: a 10,000 year natural experiment. *Marine Micropaleontology*, 29, 393-405.

Zonneveld, K.A.F., Versteegh, G.J.M., de Lange, G.J., 2001. Palaeoproductivity and post depositional aerobic organic matter decay reflected by dinoflagellate cyst assemblages of the Eastern Mediterranean S1 sapropel. *Marine Geology*, 172, 181-195.

Zonneveld, K.A.F., Bockelmann, F., Holzwarth, U., 2007. Selective preservation of organic-walled dinoflagellate cysts as a tool to quantify past net primary production and bottom water oxygen concentrations. *Marine Geology*, 237, 109-126.

Zonneveld, K.A.F., Versteegh, G.J.M., Kodrans-Nsiah, M., 2008. Preservation and organic chemistry of Late Cenozoic organic-walled dinoflagellate cysts: A review. *Marine Micropaleontology*, 68, 179-197.

Zonneveld, K.A.F., Versteegh, G.J.M., Kasten, S., Eglinton, T.I., Emeis, K.C., Huguet, C., Koch, B.P., de Lange, G.J., de Leeuw, J.W., Middelburg, J.J., Mollenhauer, G., Prahl, F.G., Rethemeyer, J., Wakeham, S.G., 2010. Selective preservation of organic matter in marine environments; processes and impact on the sedimentary record. *Biogeosciences*, 7, 483-511.

Chapter 6

Differences in composition between organic-walled resting cysts produced by autotrophic and heterotrophic dinoflagellate taxa

Kara Bogus[1*], Ian C. Harding[2], Karin A.F. Zonneveld[1,3] and Gerard J.M. Versteegh[3]

[1]*Department of Geosciences, University of Bremen, Klagenfurter Strasse, 28359 Bremen, Germany*
[2]*School of Ocean and Earth Science, National Oceanography Centre, University of Southampton, European Way, Southampton, SO14 3ZH, UK*
[3]*Marum – Center for Marine Environmental Science, Loebener Strasse, 28334 Bremen, Germany*

**Corresponding author*
Telephone: +49 421 218 65138, Email: ka_bo@uni-bremen.de

Manuscript in preparation

Abstract

Dinoflagellate cysts are widely used proxies for paleoenvironmental studies and represent an important link between biology and geology. Specifically, cysts produced by heterotrophic taxa are useful indicators of marine productivity. However, these cysts are also known to be sensitive to aerobic degradation, while the cysts produced by photosynthetic species are more resistant. This taxon specific sensitivity to degradation may result from differences in the cyst wall chemistry, namely from differences in the composition of dinosporin, the biomacromolecule that comprises them. As this variability may have the potential to explain the selective preservation of dinoflagellate cysts, we compared the cyst wall chemistry of *Brigantedinium* species, cysts of *Polykrikos kofodii* and *P. schwartzii*, which are produced by heterotrophic taxa, to *Impagidinium patulum*, *Operculodinium centrocarpum* and *Spiniferites pachydermus*, which are produced by autotrophic taxa. The cysts were isolated from surface sediments from the Bengueula upwelling area and analyzed with micro-Fourier transform infrared (FTIR) spectroscopy. The analyses show that there are intrinsic differences in the cyst wall chemistry between the two groups. The autotrophic taxa are composed of a carbohydrate-based, in some cases likely cellulosic, dinosporin while heterotrophic taxa show evidence of amide bonds in the cyst wall. We interpret these variations to reflect the ecology and feeding strategies of the two groups of dinoflagellates producing the cysts. It may thus be possible to predict the paleoecology of extinct taxa with the use of micro-FTIR. Furthermore, the observed differences in the cyst wall chemistry may also be responsible for the species-specific sensitivity to oxidation, as the presence of amide bonds may make the heterotrophic dinosporin more labile.

Keywords: dinoflagellate cyst, dinosporin, autotrophic, heterotrophic, FTIR

6.1 Introduction

Organic-walled dinoflagellate resting cysts are invaluable tools for (paleo)-environmental studies as individual cyst species can be correlated to environmental parameters and used as proxies for oceanographic conditions in the Quaternary (e.g. Marret and Zonneveld, 2003). Furthermore, dinoflagellate cysts have a long sedimentary record (MacRae et al., 1996) and are thus important tools in oceanographic reconstructions in pre-Quaternary sediments (Matthiessen et al., 2005; Sluijs et al., 2005). However, different dinoflagellate cyst taxa are known to have varying preservation efficiencies, as a result of species-specific vulnerability to oxidation. Studies showing selective cyst degradation are based on laboratory preparations (e.g. Dale, 1976; Hopkins and McCarthy, 2002), exposure experiments (e.g. Kodrans-Nsiah et al., 2008), and deposited marine sediments (e.g. Zonneveld et al., 1997; 2001; Combourieu-Nebout et al., 1998; Chapter 5). It has been suggested that the species-specific preservation potential may be related to cyst type or the cyst wall chemistry (de Leeuw et al., 2006; Zonneveld et al., 2008). The *Brigantedinium* species and cysts of the *Polykrikos* genus (together, P-cysts) are more vulnerable to aerobic degradation while gonyaulacoid (G-) cysts are more resistant (McCarthy et al., 2000; Zonneveld et al., 2001; Versteegh and Zonneveld, 2002; Chapter 5). This has implications for paleoenvironmental work as a ratio between these two cyst types (P/G ratio) is frequently used as a proxy for productivity (e.g. Harland, 1973; Mudie and Rochon, 2001; Reichart and Brinkhuis, 2003).

Dinoflagellate cysts are composed of a refractory biomacromolecule generally referred to as dinosporin (Fensome et al., 1993), the composition of which is not well understood, as only a few studies have directly investigated it (e.g. Hemsley et al., 1994; Kokinos et al., 1998; de Leeuw et al., 2006; Versteegh et al., 2007; Versteegh et al., in press). It seems plausible that differences in dinosporin composition may explain the oxidation sensitivity as well as potentially reflect the group ecology because P-cysts can be generally considered as produced by heterotrophic taxa and the G-cysts to derive from photoautotrophic species (e.g. Harland, 1973; see discussions in Reichart and Brinkhuis, 2003; Sluijs et al., 2005). Thus, the life strategies of the motile cells may influence the composition of their resting cysts, as the cyst membrane is formed from material available within the cell (e.g. Kokinos and Anderson, 1995; Rochon et al., 2009). The cyst formation process is poorly understood, although Rochon et al. (2009) provided a description for *Gonyaulax spinifera*. Briefly, the formation of the cyst membrane begins

within the cell when the flagella are expelled, the outer membrane then swells (100 μm diameter) during which the theca dislocate and the thecal plates fall off, and if the cyst has projections, they grow within the space of the membrane over a period of a few minutes to an hour. After the growth of processes, the outer membrane ruptures and the cyst is released.

In this study, we compare the dinosporin composition of Recent "resistant" G-cysts produced by phototrophic taxa and "sensitive" P-cysts produced from heterotrophic taxa using micro-Fourier transform infrared (FTIR) spectroscopy. FTIR is a rapid and non-destructive technique that allows for the identification of individual compounds in complex systems, such as large biomacromolecules, and is a commonly used technique in the analysis of palynomorphs (e.g. Pappas et al., 2003; Yule et al., 2000; Versteegh et al., 2007; in press; Zimmerman, 2010). Micro-FTIR has the same benefits but adds the additional advantage that analyses can be performed on individual specimens (e.g. Marshall et al., 2005; Steemans et al., 2010; Versteegh et al., in press).

6.2 Regional setting and material

The Benguela upwelling system (BS), located off the southwest coast of Africa (Fig. 6.1), is one of the most productive in the world (e.g. Shannon, 1985) and characterized by intense coastal upwelling (Shannon and Nelson, 1996). The Benguela area is bounded by the Walvis Ridge in the north and extends to 34° S (Nelson and Hutchings, 1983). It contains the northward flowing Benguela Current (BC), which is the eastern boundary current of the South Atlantic subtropical gyre. The BC splits at around 28° S into the Benguela Coastal Current (BCC) and the Benguela Oceanic Current (BOC; Shannon and Nelson, 1996). The BS is the only upwelling region in the world bordered by warm water currents: the Agulhas Current (AgC) in the south and the Angola Current (AC) in the north. The AgC collides with the BC around the Cape of Good Hope at the Agulhas Retroflection (Gordon, 1986), which introduces filaments of warm, saline AgC water into the BC. Southeasterly (SE) trade winds force surface water seaward along the BC, which allows the relatively nutrient rich South Atlantic Central Water (SACW) to upwell from 150-250 m depth to the surface (e.g. Jones, 1971). The strength and consistency of the SE trade winds are seasonal with a maximum in austral winter-spring (Shannon and Nelson, 1996), which leads to an upwelling maximum at the same time. Perennial

upwelling is found north of 31° S (Shannon, 1985). The upwelling area generally extends about 200 km offshore, but filaments of upwelled water can be found more than 1000km from the coast (e.g. Lutjeharms et al., 1991). The BS supports marine productivity between 125- >300 g C $m^{-2}yr^{-1}$ (Fischer et al., 2000). Additionally, inputs of aeolian dust by the SE trade winds and northeast Bergwinds (Shannon and Nelson, 1996) supply iron, a limiting factor for primary production (e.g. Martin, 1992; Jickells et al., 2005), to the region.

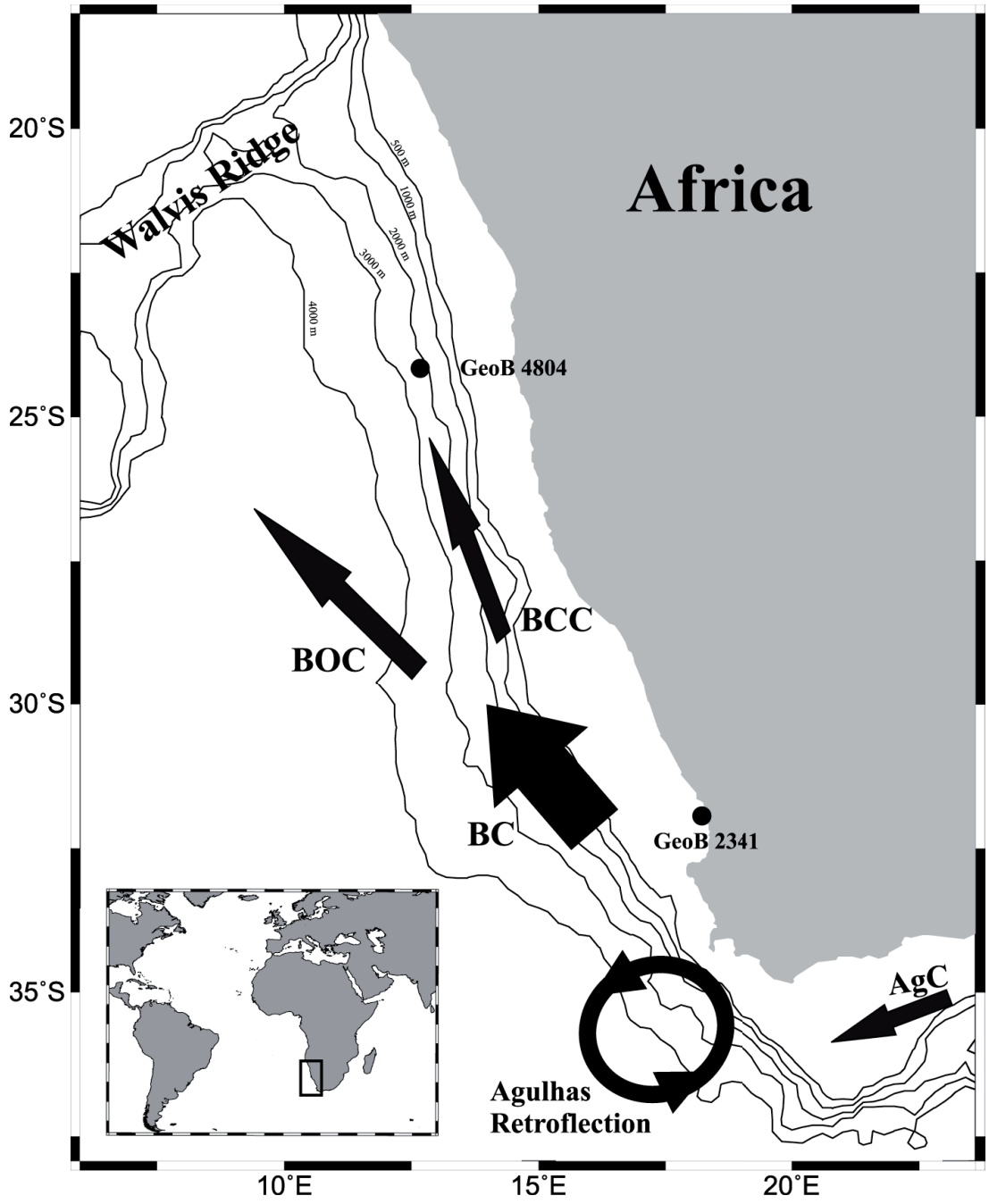

Figure 6.1: Area map of the Benguela upwelling region. Arrows depict major surface currents influencing the sampling area. BC= Benguela Current, BOC= Benguela Oceanic Current, BCC= Benguela Coastal Current, AgC= Agulhas Current.

Low concentrations of bottom water oxygen occur perennially in the BS (Kristmannsson, 1999) from two different sources (Chapman and Shannon, 1985). The upwelling SACW is oxygen-depleted and so provides a source of O_2 poor bottom water on the shelf while the degradation of organic matter consumes additional amounts of dissolved oxygen. Sedimentation rates in this region range from 2 - >16 cm yr^{-1} (Mollenhauer et al., 2004) and marine surface sediments from the area were dated at < 1000 yrs (Inthorn et al., 2006). Surface samples (0-1 cm) GeoB 2341 (31°55'48" S, 18°12'36" E; 84 m water depth) and GeoB 4804 (24°8'60" S, 12°40'12" E; 2090 m water depth) were used in this study (Fig. 6.1). Details regarding sampling conditions are described in Holzwarth et al. (2007).

6.3 Methods

6.3.1 Sample preparation

Dried samples were ultrasonicated (15 s) with a tunable ultrasonic probe in distilled water, sieved over a 50 µm mesh sieve and retained on a 20 µm precision sieve (Storck Mesh #317). The remaining material was then checked with a light microscope and, if necessary, the ultrasonication/sieving step was repeated a maximum of two additional times. These steps were performed in order to remove extraneous organic material. No chemical treatments were used. Samples were then concentrated to 4 mL each. From each sample, 50 µL was embedded in glycerine jelly between a glass slide and cover slip, and sealed with paraffin wax. Slides were coated with Zeiss 518 C immersion oil and fluorescence photographs were taken in incident light using a Zeiss Universal Microspectrophotometer 50 (UMSP 50; excitation filter 450-490 nm; long pass filter 520 nm; beam splitter 510 nm). From the aqueous sample, individual dinoflagellate cysts were then individually isolated with a Narishige IM5b microinjector attached to a Märzhauser DC3K 168 micromanipulator. Only specimens with no visibly attached particles were picked. Cysts were then dried (24 hrs) and transferred to a NaCl plate for FTIR analysis.

6.3.2 Micro-Fourier Transform Infrared Spectroscopy

Infrared spectra were recorded with a Nicolet FT-IR spectrometer coupled to a Nicplan microscope (15x objective), a Protégé™ 460 optical bench, a MCT- A detector cooled to ≤ -70°C with liquid nitrogen, Ever-Glo source, and a KBr beamsplitter. Two adjustable apertures (upper and lower) were set at a constant area of 15 x 15 µm. Interferograms were obtained in transmission mode over a spectral range of 4000-650 cm^{-1} with 256 scans at 8 cm^{-1} resolution. Multiple specimens of each species were measured. Background spectra of the NaCl plate (and air) were recorded after each specimen and all spectra show the sample beam following background subtraction. CO_2 absorptions at ~2350 cm^{-1}, an instrumental artifact, have also been removed. Assignments of the main IR group frequencies were based on Coates (2000) and Colthup et al. (1990) and published literature. Absorbance spectra were manipulated with OMNIC™ 3.1 software. The baseline correction was performed automatically. Corrected spectral areas of main deformation regions (I-IV) were integrated from the area between the band limits and the baseline. These regions correspond to the following frequencies: (I) 3010-2775 cm^{-1}, (II) 1850-1500 cm^{-1}, (III) 1500-1185 cm^{-1}, and (IV) 1185-830 cm^{-1}. The spectral areas of these regions (see Appendix A6) were used to calculate relative band intensities, and allow for the comparison of band strength between the different taxa.

6.4 Results and Discussion

The dinoflagellate cyst species analyzed were *Brigantedinium* spp., cysts of *Polykrikos kofoidii*, and cysts of *Polykrikos schwartzii*, which represent heterotrophic taxa, while *Impagidinium patulum*, *Operculodinium centrocarpum*, and *Spiniferites pachydermus* represent autotrophic taxa. These particular species were analyzed because they were shown to be among the more common species in the assemblages (Holzwarth et al., 2007). More information on the dinoflagellate cyst assemblage and distribution in these samples are detailed in Holzwarth et al. (2007). Information regarding motile affinities and ecology are depicted in Table 6.1; we chose to use the cyst names throughout this discussion, mainly due to uncertainty in motile-cyst relationships (e.g. Lewis et al., 1999; Ellegaard et al., 2003; Matsuoka et al., 2009; Rochon et al., 2009). Regardless, we were primarily interested in whether the cysts were produced by autotrophic or heterotrophic motile taxa. When comparing the two groups, the autotrophic taxa are referred to as G-cysts and the heterotrophic taxa as P-cysts.

Table 6.1: Names of the autotrophic (G) and heterotrophic (P) taxa analyzed in the study. Cyst names are after Marret and Zonneveld (2003). Motile names and cyst-motile relationships are after Wall and Dale (1968), Matsuoka et al. (2009), and Rochon et al. (2009).

Motile name	Ecology	Cyst name	Cyst type	Cyst group
Gonyaulax sp.	autotrophic	*Impagidinium patulum*	gonyaulocoid	G
Protoceratium reticulatum	autotrophic	*Operculodinium centrocarpum*	gonyaulocoid	G
Gonyaulax spinifera complex?	autotrophic	*Spiniferites pachydermus*	gonyaulocoid	G
Protoperidinium spp.	heterotrophic	*Brigantedinium* spp.	peridinioid	P
Polykrikos kofoidii	heterotrophic	cyst of *Polykrikos kofoidii*	gymnodinioid	P
Polykrikos schwartzii	heterotrophic	cyst of *Polykrikos schwartzii*	gymnodinioid	P

6.4.1 FTIR spectra of autotrophic species

The G-cysts (i.e. *S. pachydermus*, *O. centrocarpum*, *I. patulum*) show clear intra-species consistency in their spectra, though there are differences between the separate species (Fig. 6.2a). Major absorption assignments are depicted in Table 6.2. The dominant deformations are the large broad peak centered ≈ 3350 cm^{-1} (OH stretching) and the strong absorption centered at ≈ 1030 cm^{-1} (C-O stretching). This latter absorption (spectral region IV; Fig. 6.2a) is comprised of 4 separate deformations in *S. pachydermus* (Fig. 6.2a; Table 6.2). This series of absorptions is not present in *I. patulum* or *O. centrocarpum*, where the absorption (region IV) is instead smoother (Fig. 6.2a). It is possible that this may show some influence of adsorbed silica in the *O. centrocarpum* and *I. patulum* spectra as HF was not used in the preparation of the samples. Silica absorptions are generally broad and centered at ≈ 1100 cm^{-1} (Foster et al., 2002; Swann and Patwardhan, 2011). Within the broad peak, separate components at 1045-1035 cm^{-1} (strong asymmetric Si-O-Si) and 950 cm^{-1} (weak Si-OH stretching) are present (Swann and Patwardhan, 2011) and their appearance is analogous to region IV in *I. patulum*. Therefore, it is likely

Table 6.2: FTIR spectral band assignments for the main deformation peaks in the G-cysts.

Absorption (cm^{-1})	Assignment[a]	Strength[b]
980-850	γCH	w
1030	νC-O	s, br
1110	νC-O	m-sh
1160	ν^{as}C-O-C	m-w
1340-1330	δOH	m-sh
1370	δCH + δC-CH_3	m-s
1430-1400	δCH_2	m-sh
1600	νC=C + νC=O	m-sh
1650	νC=O	m-sh
2860	ν^{3}CH	m-w
2925-2920	ν^{2}CH	m
≈3400	νOH	s, br

[a]Assignments based generally on Colthup et al. (1990), Coates (2000), and specifically on Pandey (1999).
[b]Strength classifications: s=strong, br=broad, m=medium, w=weak, sh=shoulder.

that region IV in *I. patulum*, and possibly in *O. centrocarpum*, actually represents a composite signal from CO and silica bonds. The origin of the silica is likely from terrestrial material (e.g. Bremner and Willis, 1993).

The spectra of *S. pachydermus* bear the most resemblance to cellulose (Pandey 1999). The absorptions in common with cellulose are: 890 cm^{-1} (β-glycosidic linkage), 1030 cm^{-1} (C-O stretch), 1110 cm^{-1} (glucose ring stretch), 1160 cm^{-1} (C-O-C asymmetric vibration), 1330 cm^{-1} (OH in plane deformation), 1370 cm^{-1} (CH_3 bend), 1430 cm^{-1} (CH_2 bend), 1650 cm^{-1} (adsorbed OH; conjugated C=O), and the broad OH stretch ≈ 3400 cm^{-1}. From this, it appears that the dinosporin comprising *S. pachydermus* cysts is cellulosic. The spectra of *O. centrocarpum* and *I. patulum* mainly differ with respect to regions I and II, and the appearance of the deformations in region IV (Fig. 6.2a). The CH stretching (region I) consists of two clearly defined absorptions (2925 and 2860 cm^{-1}) whereas in *S. pachydermus*, there is one peak (2920 cm^{-1}) and a shoulder (2860 cm^{-1}). In spectral region II, the main absorption is at 1650 cm^{-1} for *S. pachydermus*, but this is either a shoulder (*O. centrocarpum*) or a weak peak (*I. patulum*) in the others. The stronger peak (1600 cm^{-1}) in region II of the *O. centrocarpum* and *I. patulum* spectra is a shoulder in *S. pachydermus*. This reversal represents the higher presence of C=O carbonyl stretching, and could represent carboxymethylate species (e.g. Yuen et al, 2009). This suggests that there are more ester bonds in the dinosporin of *O. centrocarpum* and *I. patulum* than *S. pachydermus*. The ester bonds could have originated from the polymerization of cell content (i.e. fatty acids) onto the dinosporin macromolecule (e.g. Versteegh et al., 2004) during settling through the water column or upon deposition at the sea floor. This explanation would support a higher aliphatic content as shown by the stronger CH stretching (region I) and bending (region III) absorptions (Fig. 6.3); however, this is unlikely as the analyzed specimens all had clearly visible archeopyles. It is more likely that these differences simply represent a different type of polysaccharide comprising the dinosporin.

In terms of relative band strength, the G-cysts seem to be characterized by generally low spectral region II/III values (≤ 0.7; Fig. 6.3). The wider separation of spectral region I/IV is explained mainly by varying degrees of aliphatic content and the possibility of non-dinosporin absorptions (i.e. silica in region IV in *I. patulum*). However, the G-cysts in general plot near to cellulose. Thus, while *S. pachydermus* is most probably cellulose like, we suggest that *I. patulum* and *O. centrocarpum* are also

carbohydrate-based. A carbohydrate backbone for the dinosporin biomacromolecule in G-cysts is in agreement with the findings of another G-cyst, *Lingulodinium machaerophorum* (Versteegh et al., in press). All of the G-cyst dinosporins may thus be composed of different β-(1→4) type polysaccharide biopolymers (Kačuráková et al., 1999; Kačuráková and Wilson, 2000).

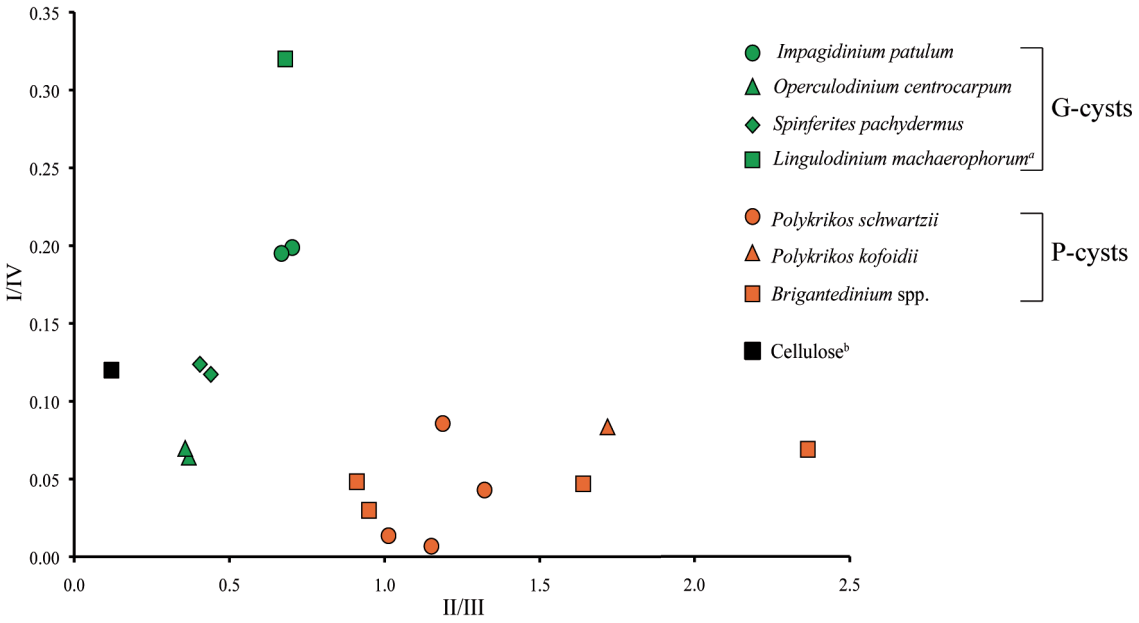

Figure 6.3: Comparison of the relative strength of major FTIR absorption regions between autotrophic (G-cysts) and heterotrophic (P-cysts) taxa. Regions I) 3010-2775 cm^{-1}, II) 1850-1500 cm^{-1}, III) 1500-1185 cm^{-1}, IV) 1185-830 cm^{-1}. [a]Values from Versteegh et al. (in press), [b]Calculated from Pandey (1999).

6.4.2 FTIR of heterotrophic species

The P-cysts, *Brigantedinium* spp., cysts of *P. kofoidii* and *P. schwartzii*, show a larger degree of intra- species variation than the G-cysts (Fig. 6.2b; Fig. 6.3). This is especially true for the *Brigantedinium* species and is probably a result of the difficulty in visually identifying species in this genus (e.g. Dale, 1992), so that the analyzed specimens may actually represent different species. Main deformation assignments are depicted in Table 6.3. The spectral region I in all of the species is weak, indicating a lack of aliphatic CH bonds. In *P. kofoidii* and two specimens of *P. schwartzii*, two deformations can be seen at 2950 and 2885 cm^{-1} (Fig. 6.2b). However, in the other two specimens of *P. schwartzii* and all *Brigantedinium* species, this deformation band is very weak and no separation is visible. Thus, the strong absorptions in region III at 1420-1390 cm^{-1} probably do not reflect only CH bending vibrations.

Table 6.3: FTIR spectral band assignments for the main deformation peaks in the P-cysts.

Absorption (cm^{-1})	Assignment[a]	Strength[b]
890-835	γ CH or amine groups	w-m
1030	ν C-O	s
1120	ν C-O	s
1260-1240	δ NH	w
1420-1390	ν C-N + δ CH + δ C-CH_3	m-s
1585-1550	ν C-N + ν C=C	m-s
2860	ν^3 CH	w
2930	ν^2 CH	w
2975-2950	ν^3 CH	sh
3100	ν NH	sh
3330	ν OH	s, br

[a]Assignments based generally on Colthup et al. (1990), Coates (2000), and specifically on Stankiewicz et al. (1998) and Cárdenas et al.(2004). [b]Strength classifications: s=strong, br=broad, m=medium, w=weak, sh=shoulder.

The strong absorptions in region II can be characteristic of amide bonds (Stankiewicz et al., 1998; Cárdenas et al., 2004). Absorptions between 1585-1560 cm^{-1} are characteristic of amide II bonds (C-N stretching and N-H bending), while the shoulder present at 1650 cm^{-1} in all of the species probably reflects amide I bonds. This deformation is the result of the influence of hydrogen bonding (C=O···H-N). These types of absorptions are typically seen in another biopolymer, chitin (e.g. Cárdenas et al., 2004). The presence of both amide bond types would increase the chemical stability of the structure (Cárdenas et al., 2004). In light of the interpretation regarding the presence of amide bonds, the absorptions in region III could primarily indicate CN stretching and NH bending (amide III; Cárdenas et al., 2004). Other evidence for nitrogen-containing functional groups is less apparent. It consists of a shoulder at 3100 cm^{-1} in two *P. schwartzii* specimens (Fig. 6.2b) that could indicate N-H stretching. Further evidence for N-H stretching could be encompassed within the broad OH stretching region as they have the same frequency range (3600-3000 cm^{-1}). Finally, absorptions between 840-875 cm^{-1} could reflect amine groups (Stankiewicz et al., 1998), as well as CH out-of-plane deformations.

The absorptions in region IV are primarily at 1120 and 1030 cm^{-1}, which correspond to sugar group vibrations and CO stretching (Stankiewicz et al., 1998). There is also a small deformation (shoulder) in most species around 900 cm^{-1} that is indicative of a β-glycosidic ring linkage. Therefore, the P-cysts may also be carbohydrate-based, albeit with nitrogen containing functional groups. The combination of the carbohydrate evidence, together with the amide bond evidence, could suggest a chitin-like β-polysaccharide compound (Stankiewicz et al., 1998; Kačuráková et al., 1999). The specific shape of spectral band IV in the *Polykrikos* cysts would further suggest 1→4

linkages (Kačuráková and Wilson, 2000). As no other FTIR spectra have been published for the P-cysts, it is impossible to compare our data with additional species.

In terms of the relative band strengths, the P-cysts all demonstrate a higher degree of intra-species variability (Fig. 6.3). As previously mentioned, the variability in *Brigantedinium* spp. could reflect the inadvertent analysis of different species; this group consists of spherical, brown cysts with no external ornamentation or defining characteristics other than the archeopyle. However, for the vast majority of specimens, the cysts were folded and an archeopyle was not clearly visible. For the greater variability seen in the *P. schwartzii* cysts, an alternative explanation related to the food source could be possible and is discussed in section 6.4.4.

All of the specimens have extremely low values for regions I/IV (< 0.1) and show a more narrow range in this ratio than the G-cysts. These low values reflect the general lack of aliphatic CH bonds in the P-cyst dinosporin. However, the absorptions of region II and III are two of the strongest absorptions in all three P-cyst species (Fig. 6.2b). It is the frequency and strength of the absorptions within these two spectral regions that most clearly distinguishes the P-cyst taxa from the G-cysts.

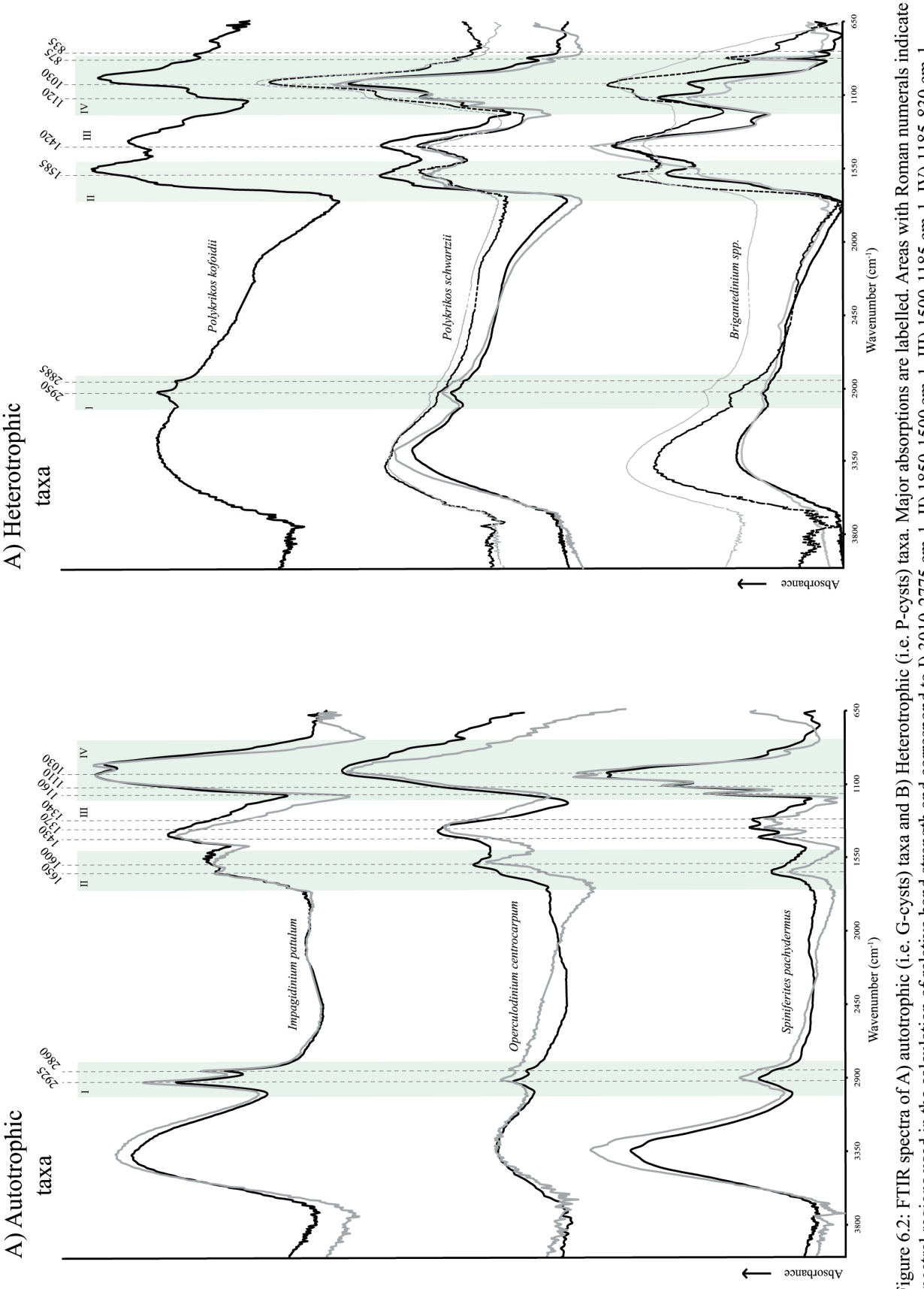

Figure 6.2: FTIR spectra of A) autotrophic (i.e. G-cysts) taxa and B) Heterotrophic (i.e. P-cysts) taxa. Major absorptions are labelled. Areas with Roman numerals indicate spectral regions used in the calculation of relative band strength and correspond to I) 3010-2775 cm-1, II) 1850-1500 cm-1, III) 1500-1185 cm-1, IV) 1185-830 cm-1.

6.4.3 Autofluorescence

Fluorescence microscopy has previously been used as a way to distinguish photosynthetic and heterotrophic dinoflagellates, as chlorophyll contains autofluorescing molecules called fluorophores (Lessard and Swift, 1986). These analyses were performed on motile cells, although more recent work demonstrates fossil and recent cysts from heterotrophic dinoflagellate do not show autofluorescence (Brenner and Biebow, 2001) and the lack of autofluorescencen has even been used to infer a heterotrophic ecology (Verleye et al., 2011). Thus, the lack of autofluorescence in the P-cysts agrees with previous studies for heterotrophic taxa (Fig. 6.4). Unfortunately, the autofluorescence of the autotrophic species was not strong enough to allow for a quantitative analysis. As a result, we are unable to determine the source of the fluorescence. It is known that cellulose exhibits autofluorescence and many other polysaccharides also contain fluorophores either within the macromolecular structure or attached to it (Castellan et al., 2007). Furthermore, increases in carbonyl and carboxylic groups have been shown to increase the intensity of fluorescence (Castellan et al., 2007), so this may contribute to the autofluorescence of the G-cysts. The lack of autofluorescence in the P-cysts is presently unexplained, but is further support for a clear difference in dinosporin between P- and G-cysts.

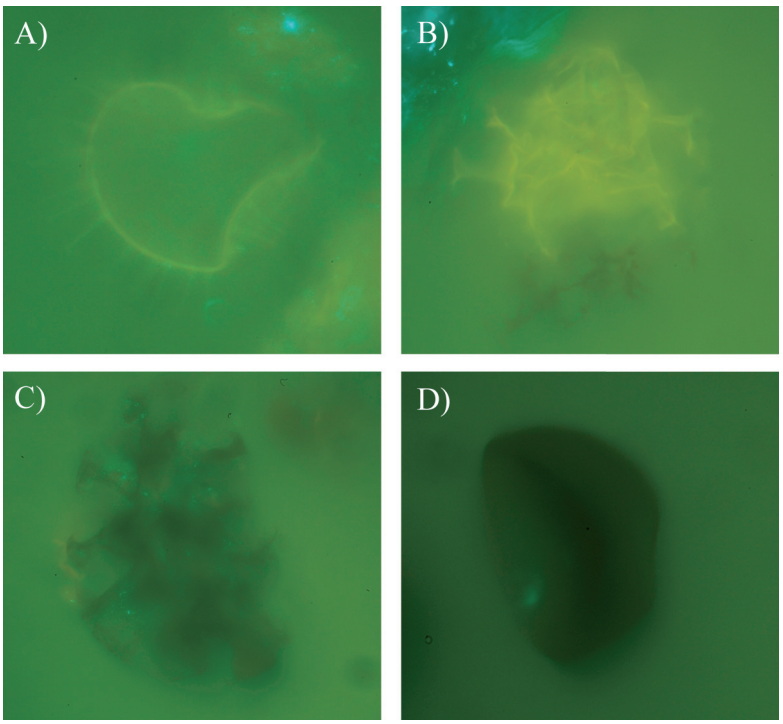

Figure 6.4: Fluorescence photographs of two G-cysts A) *O. centrocarpum*, B) *S. pachydermus* and two P-cysts C) *P. schwartzii*, D) *Brigantedinium* spp. Specimens were visually identified under a light microscope.

6.4.4 Different life strategies as a means to produce different dinosporin compositions

In general, the dinosporins of both P- and G-cysts appear to be carbohydrate-based. More specifically, they appear to be comprised of β-(1→4) linked polysaccharides. Cellulose is the most well known β-(1→4) linked glucan (Aspinall, 1983) and is the primary material comprising the theca of dinoflagellates. Additionally, other, non-cellulosic β-(1→4)-D-glucans are a common and well-documented component in plant (e.g. Kačuráková and Wilson, 2000; Burton and Fincher, 2009) and algal cell walls (e.g. Frei and Preston, 1964; Stone, 2009), including one known example in dinoflagellates (*Peridinium westii*; Nevo and Sharon, 1969). These polysaccharides, including cellulose, play a structural role in the algal cell wall (e.g. Morrill and Loeblich, 1983).

Currently, it is thought that β-(1→4)-D-glucans are biosynthesized in a two-phase process (Fincher, 2009). The first stage, as demonstrated in lower plants and fungi, involves the synthesis of small building blocks within the Golgi apparatus, which are then, in the second phase, transported to the plasma membrane where the polymer is assembled (Fincher, 2009). Thus, a cyst formation mechanism could involve altering the biosynthetic pathway for β-(1→4)-D-glucans during the induction of the quiescent stage (see Section 3.1.2) so that instead of assembling the more labile polysaccharide, the cell produces the highly resistant resting cysts. However, as this has not been examined in dinoflagellates, it is currently a hypothesis. But, alteration of a two-step biosynthetic pathway would allow for changes in the dinosporin composition, which is necessary because the G- and P-cysts clearly have different compositions, as shown by the FTIR spectra (Fig. 6.2) and the autofluorescence photographs (Fig. 6.4).

During the polymer assembly phase in the plasma membrane, other functional groups could be added to the biopolymer. This could include incorporation of amide groups in the heterotrophic taxa, which would make the dinosporin composition appear more chitin-like. The origin of the amide groups could be a result of the heterotrophy of P-cyst producing dinoflagellates. For example, some diatoms are composed of β-chitin (e.g. Kurita, 2006), and would thus represent a source of nitrogen-containing groups. During digestion, these could be released and/or stored within the dinoflagellate cell and may thus explain the incorporation of amide bonds. Heterotrophic dinoflagellates do not feed exclusively on diatoms, so different food sources could account for the greater "intra" species variability seen in their FTIR spectra (Fig. 6.3). In the autotrophic species,

formation of the resting cyst in a two phase process could result in the incorporation of photosynthetic products, namely sugars, which could account for the carbohydrate backbone proposed for the G-cyst dinosporin (Fig. 6.2a). Thus, the strongest explanation for the observed consistent differences in the dinosporin between autotrophic and heterotrophic taxa is the ecology of the two groups.

6.4.5 Implications for preservation

Carbohydrates are the most abundant form of biomass on earth (Kurita, 2006), but are generally considered labile in a native state (e.g. Imai et al., 2003). However, cellulose and chitin, known as structural polysaccharides (Allison, 1988) are more resistant because they can form complex biopolymers. Despite this ability, these two biopolymers are generally considered to preserve poorly in the sedimentary record (e.g. Lechien et al., 2006; Stankiewicz et al., 1998). If G- and P-cyst dinosporins are based on polysaccharides, then they would need to demonstrate some significant differences because both groups of cysts are non-hydrolyzable. One suggestion is that the carbohydrate backbone of G-cysts is more highly cross-linked, which increases the refractory nature of the dinosporin biomacromolecule (Versteegh et al., in press).

In terms of the species-specific sensitivity to aerobic degradation, it is possible that the incorporation of amide groups into the dinosporin biomacromolecule has made the P-cysts more susceptible to oxidation. The inclusion of nitrogen-containing functional groups would not, in and out itself, necessarily indicate a higher lability of the P-cysts. Currently, it appears that there is some relationship between the sensitivity of P-cysts to oxidation and their cyst wall chemistry; however, a mechanism for this is not clear at this time.

6.5 Conclusions

In this study, we compared the cyst wall chemistry of dinoflagellate resting cysts produced by autotrophic and heterotrophic dinoflagellate species. The dinoflagellate cysts produced by heterotrophic taxa (P-cysts) are known to be more highly sensitive to oxidation than the cysts produced by the autotrophic species (G-cysts). This has been hypothesized to be a result of variable cyst wall chemistries, arising from compositional differences in the biomacromolecule comprising the cysts – dinosporin. However, this

hypothesis had not yet been investigated. Using micro-FTIR spectroscopy and fluorescence photography, we have demonstrated that there are clear differences in the dinosporin composition between these two groups.

The G-cyst species *I. patulum* and *O. centrocarpum* seem to be composed of carbohydrate–based biopolymers and *S. pachydermus* is likely cellulosic. This carbohydrate backbone concurs with a previous study on another G-cyst species (*L. machaerophorum*; Versteegh et al., in press), and suggests this composition may be quite common in cyst-producing photoautotrophic dinoflagellates. The P-cyst species, *Brigantedinium* spp., cysts of *P. kofoidii* and *P. schwartzii*, showed a higher presence of amide bonds. This is evidence for a more chitin-like structure in the heterotrophic taxa. The autotrophic cyst species also exhibited autofluorescence, while the heterotrophic species did not.

The most likely explanation for the different dinosporin compositions between the P- and G-cyst species is their different ecologies. During the synthesis of the dinosporin macromolecule, additional structural biopolymers were included from material available within the cell. As the polysaccharides available in each cell is based on the individual contents, heterotrophic species would have more nitrogen-based polysaccharides derived from prey digestion. This further suggests that the paleoecology of extinct dinoflagellates may be inferred from the geochemistry of the cyst wall.

Acknowledgements

We appreciate the technical assistance of Mr. Ross Williams regarding the FTIR analysis. Prof. John Marshall is thanked for sharing his expertise and assisting with the fluorescence microscope. Dr. Ulrike Holzwarth is thanked for fruitful discussions. Financial support for KB was provided by the DFG (Deutsche Forschungsgemeinschaft) as part of the European Graduate College “Proxies in Earth History” (EUROPROX), and by the DFG to GJMV in the framework of a Heisenberg grant (VE-486/2 and /3).

References

Allison, P.A., 1988. Konservat-Lagerstatten: cause and classification. *Paleobiology*, 14, 331-344.

Aspinall, G.O., 1983. The polysaccharides. In: Priess, J. (Ed.), *The Biochemistry of Plants*. Academic Press, New York, NY. pp. 473-500.

Bremner, J.M., Willis, J.P., 1993. Mineralogy and geochemistry of the clay fraction of sediments from the Namibian continental margin and the adjacent hinterland. *Marine Geology*, 115, 85-116.

Brenner, W.W., Biebow, N., 2001. Missing autofluorescence of recent and fossil dinoflagellate cysts – an indication of heterotrophy? *Neues Jahrbuch fuer Geologie und Palaeontologie, Abhandlungen*, 219, 229-240.

Burton, R.A., Fincher, G.B., 2009. (1,3; 1,4)-β-D-glucans in cell walls of the Poacea, lower plants and fungi: a tale of two linkages. *Molecular Plant*, 2, 873-882.

Cárdenas, G., Cabrera, G., Taboada, E., Miranda, S.P., 2004. Chitin characterization by SEM, FTIR, XRD, and 13C cross polarization/mass angle spinning NMR. *Journal of Applied Polymer Science*, 93, 1876-1885.

Castellan, A., Ruggiero, R., Frollini, E., Ramos, L.A., Chirat, C., 2007. Studies on fluorescence of cellulosics. *Holzforschung*, 61, 504-508.

Chapman, P., Shannon, LV., 1985. The Benguela Ecosystem Part II. Chemistry and related processes. *Oceanography and Marine Biology: An Annual Review*, 23, 183-251.

Coates, J., 2000. Interpretation of Infrared Spectra, A Practical Approach. In: Meyers, R.A. (Ed.), *Encyclopedia of Analytical Chemistry*. John Wiley and Sons Ltd., pp. 10815-10837.

Colthup, N.B., Daly, L.H., Wiberly, S.E., 1990. *Introduction to Infrared and Raman Spectroscopy.* Academic Press Limited, London, 282 pp.

Combourieu-Nebout, N., Paterne, M., Turon, J.L., Siani, G., 1998. A high-resolution record of the last deglaciation in the central Mediterranean Sea: Palaeovegetation and palaeohydrological evolution. *Quaternary Science Reviews*, 17, 303-317.

Dale, B., 1976. Cyst formation, sedimentation, and preservation: factors affecting dinoflagellate assemblages in recent sediments from Trondheimsfjord, Norway. *Review of Palaeobotany and Palynology*, 22, 39-60.

Dale, B., 1992. Dinoflagellate contributions to the open ocean sediment flux. In: Honjo, S., (Ed.), *Dinoflagellate contributions to the deep sea*. Ocean Biocenosis Series 5, Woods Hole, 1-31.

de Leeuw, J.W., Versteegh, G.J.M., van Bergen, P.F., 2006. Biomacromolecules of algae and plants and their fossil analogues. *Plant Ecology*, 182, 209-233.

Ellegaard, M., Daugbjerg, N., Rochon, A., Lewis, J., Harding, I., 2003. Morphological and LSU rDNA sequence variation within the *Gonyaulax spinifera-Spiniferites* group (Dinophyceae) and proposal of *G. elongata* comb. nov. and *G. membranacea* comb. nov. *Phycologia*, 42, 151-164.

Fensome, R.A., Taylor, F.J.R., Norris, G., Sarjeant, W.A.S., Wharton, D.I., Williams, G.L., 1993. A classification of fossil and living dinoflagellates. *Micropaleontology Press Special Paper*, 7, 351 pp.

Fincher, G.B., 2009. Exploring the evolution of (1,3; 1,4)-β-D-glucans in plant cell walls: comparative genetics can help! *Current Opinion in Plant Biology*, 12, 140-147.

Fischer, G., Ratmeyer, V., Wefer, G., 2000. Organic carbon fluxes in the Atlantic and the Southern Ocean: relationship to primary production compiled from satellite radiometer data. *Deep-Sea Research Part II*, 47, 1961-1997.

Foster, G.B., Stephenson, M.H., Marshall, C., Logan, G.A., Greenwood, P.F., 2002. A revision of *Reduviasporonites* Wilson 1962: Description, illustration, comparison and biological affinities. *Palynology*, 26, 35-58.

Frei, E., Preston, R.D., 1964. Non-cellulosic structural polysaccharides in algal cell walls I. Xylan in siphoneous green algae. *Proceedings of the Royal Society of London, Series B, Biological Sciences*, 160, 293-313.

Gordon, A.L., 1986. Interocean Exchange of thermocline water. *Journal of Geophysical Research*, 91, 5037-5046.

Harland, R., 1973. Dinoflagellate cysts and acritarchs from the Bearpaw Formation (upper Campanian) of southern Alberta, Canada. *Paleontology*, 16, 665-706.

Hemsley, A.R., Barrie, P.J., Scott, A.C., Chaloner, W.G., 1994. Studies of fossil and modern spore and pollen wall biomacromolecules using ^{13}C solid state NMR. In: Eglinton, G., Kay, R.L.F. (Eds.), *Biomolecular Palaeontology*, NERC Special Publications, 94, 15-19.

Holzwarth, U., Esper, O., Zonneveld, K., 2007. Distribution of organic-walled dinoflagellate cysts in sediments of the Benguela upwelling system in relationship to environmental conditions. *Marine Micropaleontology*, 64, 91-119.

Hopkins, J.A., McCarthy, F.M.G., 2002. Post-depositional palynomorph degradation in Quaternary shelf sediments: a laboratory experiment studying the effects of progressive oxidation. *Palynology*, 26, 167-184.

Imai, T., Watanabe, T., Yui, F., Sugiyama, J., 2003. The directionality of chitin biosynthesis: a revisit. *Biochemical Journal*, 374, 755-760.

Inthorn, M., Wagner, T., Scheeder, G., Zabel, M., 2006. Lateral transport controls distribution, quality, and burial of organic matter along continental slope in high-productive areas. *Geology*, 34, 205-208.

Jickells, T.D., An, Z.S., Andersen, K.K., Baker, A.R., Bergametti, G., Brooks, N., Cao, J.J., Boyd, P.W., Duce, R.A., Hunter, K.A., Kawahata, H., Kubilay, N., la Roche, J., Liss, P.S., Mahowald, N., Prospero, J.M., Ridgwell, A.J., Tegen, I., Torres, R., 2005. Global Iron Connections Between Desert Dust, Ocean Biogeochemistry, and Climate. *Science*, 308, 67-71.

Jones, P.G.W., 1971. The southern Benguela Current region in February, 1966: Part I. Chemical observations with particular reference to upwelling. *Deep-Sea Research*, 18, 193-208.

Kristmannsson, S.S., 1999. Dissolved oxygen conditions on the shelf off Namibia in 1994. *Rit Fiskideildar*, 16, 89-95.

Kačuráková, M., Wilson, R.H., 2000. Developments in mid-infrared FT-IR spectroscopy of selected carbohydrates. *Carbohydrate Polymers*, 44, 291-303.

Kačuráková, M., Wellner, N., Ebringerová, A., Hromádková, Z., Wilson, R. H., Belton, P.S. 1999. Characterisation of xylan-type polysaccharides and associated cell wall components by FT-IR and FT-Raman spectroscopies. *Food Hydrocolloids*, 13, 35-41.

Kodrans-Nsiah, M., de Lange, G.J., Zonneveld, K.A.F., 2008. A natural exposure experiment on short-term species-selective aerobic degradation of dinoflagellate cysts. *Review of Palaeobotany and Palynology*, 152, 32-39.

Kokinos, J.P., Anderson, D.M., 1995. Morphological development of resting cysts in culture of the marine dinoflagellate *Lingulodinium polyedrum* (= *L. machaerophorum*). *Palynology*, 19, 143-165.

Kokinos, J.P., Eglinton, T.I., Goñi, M.A., Boon, J.J., Martoglio P.A., Anderson, D.M., 1998. Characterization of a highly resistant biomacromolecular material in the cell wall of a marine dinoflagellate resting cyst. *Organic Geochemistry*, 28, 265-288.

Kurita, K., 2006. Chitin and chitosan: Functional biopolymers from marine crustaceans. *Marine Biotechnology*, 8, 203–226.

Lechien, V., Rodriguez, C., Ongena, M., Hiligsmann, S., Rulmont, A., Thonart, P., 2006. Physiochemical and biochemical characterization of non-biodegradable cellulose in Miocene gymnosperm wood from the Entre-Sambre-et-Meuse, Southern Belgium. *Organic Geochemistry*, 37, 1465-1476.

Lessard, EJ; Swift, E. 1986. Dinoflagellates from the North Atlantic classified as phototrophic or heterotrophic by epifluorescence microscopy. *Journal of Plankton Research*, 8, 1209-1215.

Lewis, J., Rochon, A., Harding, I., 1999. Preliminary observations of cyst-theca relationships in Spiniferites ramosus and Spiniferites membranaceous (Dinophyceae). *Grana Supplement* 3, 1-12.

Lutjeharms, J.R.E., Shillington, F.A., Duncombe Rae, C.M., 1991. Observations of extreme upwelling filaments in the Southeast Atlantic Ocean. *Science*, 253, 774-776

MacRae, G., Fensome, R.A., Williams, G.L., 1996. Fossil dinoflagellate diversity, originations, and extinctions and their significance. *Canadian Journal of Botany*, 74, 1687-1694.

Marret, F., Zonneveld, K.A.F., 2003. Atlas of modern organic-walled dinoflagellate cyst distribution. *Review of Palaeobotany and Palynology*, 125, 1-200.

Marshall, C.P., Javaux, E.J., Knoll, A.H., Walter, M.R., 2005. Combined micro-Fourier transform infrared (FTIR) spectroscopy and micro-Raman spectroscopy of Proterozoic acritarchs: A new approach to Palaeobiology. *Precambrian Research*, 138, 208-224.

Martin, J.H., 1992. Iron as a limiting factor in oceanic productivity. In: Falkowski, P.G., Woodhead, A.D. (Eds.), *Primary Productivity and Biogeochemical Cycles in the Sea*. Plenum Press, New York, pp. 123-137.

Matsuoka, K., Kawami, H., Fujii, R., Iwataki, M., 2006. Further examination of the cyst-theca relationship of *Protoperidinium thulesense* (Peridiniales, Dinophyceae) and the phylogenetic significance of round brown cysts. *Phycologia*, 45, 632-641.

Matsuoka, K., Kawami, H., Nagai, S., Iwataki, M., Takayama, H., 2009. Re-examination of cyst-motile relationships of *Polykrikos kofoidii* Chatton and *Polykrikos schwartzii* Bütschli (Gymnodiniales, Dinophyceae), *Review of Palaeobotany and Palynology*, 154, 79-90.

Matthiessen, J., de Vernal, A., Head, M., Okolodkov, Y., Zonneveld, K.A.F., Harland, R., 2005. Modern organic-walled dinoflagellate cysts in Arctic marine environments and their (paleo-) environmental significance. *Palaeontologische Zeitschrift*, 79, 3-51.

McCarthy, F.M.G., Gostlin, K.E., Mudie, P.J., Scott, D.B., 2000. Synchronous palynological changes in early Pleistocene sediments off New Jersey and Iberia, and a possible paleoceanographic explanation, *Palynology*, 24, 63-77.

Mollenhauer, G., Schneider, R.R., Jennerjahn, T., Müller, P.J., Wefer, G., 2004. Organic carbon accumulation in the South Atlantic Ocean: its modern, mid-Holocene and last glacial distribution. *Global and Planetary Change*, 40, 249-266.

Morrill, L.C., Loeblich, A.R., 1983. Ultrastructure of the dinoflagellate amphiesma. *International Review of Cytology*, 82, 151-180.

Mudie, P.J., Rochon, A., 2001. Distribution of dinoflagellate cysts in the Canadian Arctic marine region. *Journal of Quaternary Science*, 16, 603-620.

Nelson, G., Hutchings, L., 1983. The Benguela upwelling area. *Progress in Oceanography*, 12, 333-356.

Nevo, Z., Sharon, N., 1969. The cell wall of *Peridinium westii*, a non cellulosic glucan. *Biochimica et Biophysica Acta*, 173, 161-175.

Pandey, K.K., 1999. A study of chemical structure of soft and hardwood and wood polymers by FTIR spectroscopy. *Journal of Applied Polymer Science*, 71, 1969-1975.

Pappas, C.S., Tarantillis, P.A. Harizanis, P.C., Polissiou, M.G., 2003. New method for pollen identification by FT-IR spectroscopy. *Applied Spectroscopy*, 57, 23-27.

Reichart, G.J., Brinkhuis, H., 2003. Late Quaternary *Protoperidinium* cysts as indicators of paleoproductivity in the northern Arabian Sea. *Marine Micropaleontology*, 49, 303-315.

Rochon, A., Lewis, J., Ellegaard, M., Harding, I.C., 2009. The Gonyaulax spinifera (Dinophyceae) "complex": Perpetuating the paradox? *Review of Palaeobotany and Palynology*, 155, 52-60.

Shannon, L.V., 1985. The Benguela ecosystem Part I: Evolution of the Benguela, physical features and processes. *Oceanography and Marine Biology: An Annual Review*, 23, 105-182.

Shannon, L.V., Nelson, G., 1996. The Benguela: large scale features and system variability. In: Wefer, G., Berger, W.H., Seidler, G., Webb, D.J, (Eds.), *The South Atlantic: Present and Past Circulation*. Springer Verlag, Berlin, pp. 163-210.

Sluijs, A., Pross, J., Brinkhuis, H., 2005. From greenhouse to icehouse; organic-walled dinoflagellate cysts as paleoenvironmental indicators in the Paleogene. *Earth-Science Reviews*, 68, 281-315.

Stankiewicz, B.A., Mastalerz, M., Hof, C.H.J., Bierstedt, A., Flannery, M.B., Briggs, D.E.G., Evershed, R.P., 1998. Biodegradation of the chitin-protein complex in crustacean cuticle. *Organic Geochemistry*, 28, 67-76.

Steemans, P., Lepot, K., Marshall, C.P., Le Hérissé, A., Javaux, E.J., 2010. FTIR characterisation of the chemical composition of Silurian miospores (cryptospores and trilete spores) from Gotland, Sweden. *Review of Palaeobotany and Palynology*, 162, 577-590.

Stone, B.A., 2009. Chemistry of β-glucans. In: Bacic, A., Fincher, G.B., Stone, B.A. (Eds.), 2009. *Chemistry, biochemistry, and biology of (1-3)-β-glucans and related polysaccharides*. Academic Press, Elsevier Inc., London. pp. 5-46.

Swann, G.E.A., Patwardhan, S.V., 2011. Application of Fourier Transform Infrared Spectroscopy (FTIR) for assessing biogenic silica sample purity in geochemical analyses and palaeoenvironmental research. *Climate of the Past*, 7, 65-74.

Verleye, T.J., Pospelova, V., Mertens, K.N., Louwye, S., 2011. The geographical distribution and (palaeo) ecology of *Selenopemphix undulata* sp. nov., a late Quaternary dinoflagellate cyst from the Pacific Ocean. *Marine Micropaleontology*, 78, 65-83.

Versteegh, G.J.M., Zonneveld, K.A.F., 2002. Use of selective degradation to separate preservation from productivity, *Geology*, 30, 615-618.

Versteegh, G.J.M., Blokker, P., Wood, G., Collinson, M.E., Sinninghe Damsté, J.S., de Leeuw, J.W., 2004. An example of oxidative polymerization of unsaturated fatty acids as a preservation pathway for dinoflagellate organic matter. *Organic Geochemistry*, 35, 1129-1139.

Versteegh, G.J.M., Blokker, P., Marshall, C.P., Pross, J., 2007. Macromolecular composition of the dinoflagellate cyst Thalassiphora pelagica (Oligocene, SW Germany). *Organic Geochemistry*, 38, 1643-1656.

Versteegh, G.J.M., Blokker, P., Bogus, K., Harding, I.C., Lewis, J., Oltmanns, S., Rochon, A., Zonneveld, K.A.F., in press. Flash pyrolysis and infrared spectroscopy of cultured and sediment derived *Lingulodinium polyedrum* (Dinoflagellata) cyst walls. *Organic Geochemistry*.

Wall, D., Dale, B., 1968. Modern dinoflagellate cysts and evolution of the Peridiniales. *Micropaleontology*, 14, 265–304.

Yuen, S.N., Choi, S.-M., Phillips, D.E., Ma, C.-Y., 2009. Raman and FTIR spectroscopic study of carboxymethylated non-starch polysaccharides. *Food Chemistry*, 114, 1091-1098.

Yule, B.L., Roberts, S., Marshall, J.E.A., 2000. The thermal evolution of sporopollenin. *Organic Geochemistry*, 31, 859-870.

Zimmermann, B., 2010. Characterization of pollen by vibrational spectroscopy. *Applied Spectroscopy*, 64, 1364-1373.

Zonneveld, K.A.F., Versteegh, G.J.M., de Lange, G.J., 1997. Preservation of organic-walled dinoflagellate cysts in different oxygen regimes: a 10,000 year natural experiment. *Marine Micropaleontology*, 29, 393-405.

Zonneveld, K.A.F., Versteegh, G.J.M., de Lange, G.J., 2001. Palaeoproductivity and post-depositional aerobic organic matter decay reflected by dinoflagellate cyst assemblages of the Eastern Mediterranean S1 sapropel. *Marine Geology*, 172, 181-195.

Zonneveld, K.A.F., Versteegh, G.J.M., Kodrans-Nsiah, M., 2008. Preservation and organic chemistry of Late Cenozoic organic-walled dinoflagellate cysts: A review, *Marine Micropaleontology*, 68, 179-197.

Chapter 7

The composition and diversity of dinosporin in species of the *Apectodinium* complex (Dinoflagellata)

Kara Bogus[1,2*], Ian C. Harding[3], Adrian King[3], Adam J. Charles[3], Karin A.F. Zonneveld[1,2] and Gerard J.M. Versteegh[2]

[1]*Department of Geosciences, University of Bremen, Klagenfurter Strasse, D-28334 Bremen, Germany*
[2]*Marum – Center for Marine Environmental Sciences, Loebener Strasse, D-28359 Bremen, Germany*
[3]*School of Ocean and Earth Science, National Oceanography Centre Southampton, University of Southampton, European Way, Southampton, SO14 3ZH, UK*

**Corresponding author:*
Telephone: +49 421 218 65138, Email: ka_bo@uni-bremen.de

Submitted to *Review of Palaeobotany and Palynology*

Abstract

Organic-walled dinoflagellate cysts, produced as a result of sexual reproduction, are important tools for studies of recent and past environments. Additionally, the organic-walled cysts can be used as proxies for understanding the composition and chemical tranformations of marine kerogen, the largest global organic carbon pool. However, any usage of dinoflagellate cysts in this manner is predicated on an understanding of the composition and transformations of this potential proxy. Dinoflagellate cyst walls are composed of "dinosporin", a refractory biomacromolecule that probably represents a suite of chemically distinct biopolymers. In order to investigate both the nature of dinosporin and the extent to which the composition of this biomacromolecule may differ between dinoflagellate cyst taxa, we analyzed cyst species from the genus *Apectodinium*. The species defined within this genus are visually similar with several seeming to represent end-members along a continuum of morphological variation. Micro-Fourier transform infrared (FTIR) analysis was performed on three of these morphospecies (identified visually as *A. paniculatum, A. parvum* and *A. augustum*) from two regionally distinct samples. The analyses showed consistent patterns with clear differences between the species. The dinosporin of *A. paniculatum* closely resembles cellulose and is rich in ether bonds (C-O), while the dinosporin of *A. augustum* contains more carboxyl (COOH) groups. The dinosporin of *A. parvum* appears intermediate in many respects, despite representing an end-member in terms of morphology. These differences are consistent regardless of the regional setting or post-depositional conditions, and strongly suggest that the original cyst wall composition of the species differed when the cysts were formed. These data are the first to clearly show differences in cyst wall composition between species of the same genus and indicate that the chemical diversity of dinosporins is greater than previously thought.

Keywords: dinosporin, dinoflagellate, *Apectodinium,* cyst wall, biomacromolecule, FTIR

7.1 Introduction

Palynomorphs, organic-walled microfossils, are taxonomically well-defined kerogen particles that can be reliably linked to their biological source long after incorporation into the sedimentary record (for reviews see de Leeuw et al., 2006; Zonneveld et al., 2010). Therefore, understanding the formation, composition, and chemical transformations of palynomorphs can provide more information as to the composition and fate of kerogen in general, which is of crucial importance to understand because marine kerogen represents the largest global organic carbon pool, and therefore plays a central role in the global carbon cycle (e.g. Durand, 1980; Tegelaar et al., 1989; de Leeuw and Largeau, 1993; Vandenbroucke and Largeau, 2007). The organic-walled resting cysts of dinoflagellates are one group of palynomorphs that can enhance our knowledge of kerogen as dinoflagellates constitute a major portion of global marine plankton (Marret and Zonneveld, 2003) and dinoflagellate cysts have a long sedimentary record (MacRae et al., 1996). However, their applicability as a proxy for chemical transformations of kerogen is first dependent on an understanding of the composition and compositional diversity of dinoflagellate cysts.

Dinoflagellate cyst walls are said to be composed of "dinosporin" (Fensome et al., 1993), a poorly characterized compound that differs from other resistant biopolymers like algaenan and sporopollenin (de Leeuw et al., 2006), although it has previously been referred to as sporopollenin-like (Fensome et al., 1993). However, the structure of dinosporin has only been investigated in a few Recent (Hemsley et al., 1994; Kokinos et al., 1998; Versteegh et al., in press) and fossil species of dinoflagellates (de Leeuw et al., 2006; Versteegh et al., 2007) with contradictory results. Some studies suggest that the dinosporin macromolecule probably contains both aromatic and aliphatic components, and that the composition may vary between taxa (de Leeuw et al., 2006) whereas more recently, a predominantly carbohydrate-based biopolymer has been suggested (Versteegh et al., in press). However, the structural diversity of dinosporin has never been systematically studied and so its variability is almost completely unknown.

There are some factors that may increase the variability of the dinosporin macromolecule, including genetics (i.e. cysts produced from different living species), adaptations to different environmental settings and post-depositional alteration. These factors have never been examined in dinoflagellate cysts, but have been shown to induce

variability in sporopollenin (e.g. Hemsley et al., 1993; Domínguez et al., 1999; Yule et al., 2000; Zimmermann et al., 2010 and references therein). Due to the long geological record of dinoflagellate cysts, it is plausible that evolution has had ample time to come up with a genotypic blueprint for the cyst morphology and wall chemistry that suits each species. This is supported by the many taxa that demonstrate a morphologically stable cyst shape despite the sometimes wide range of environmental conditions that these organisms may experience. However, some taxa change their cyst morphology in response to environmental gradients, such as salinity and temperature. For example, this has been observed directly in the extant dinoflagellate species *Lingulodinium polyedrum* (e.g. Lewis and Hallett, 1997; Hallett, 1999; Mertens et al., 2009), *Pyrophacus steinii* (Zonneveld and Susek, 2007), *Protoceratium reticulatum* (e.g. Ellegaard, 2000) and the genus *Gonyaulax* (e.g. Lewis et al., 2001; Ellegaard et al., 2002; Rochon et al., 2009) and also inferred for extinct taxa such as *Thalassiphora pelagica* (Pross, 2001), *Homotryblium* (e.g. Dybkjaer, 2004), and *Apectodinium* (Sluijs et al., 2005). Post-depositional alteration can overprint the original biomacromolecule as it is mineralized into a geomacromolecule; for dinosporin, there is evidence of natural sulfurization in suboxic to anoxic marine sediments (e.g. Versteegh et al., 2007). Furthermore, dinosporin has the potential to be oxidatively polymerized, in a manner similar to algaenan (Versteegh et al., 2004), though this has not been specifically demonstrated in dinoflagellate cysts as yet. Both sulfurization and oxidative polymerization may contribute to the high preservation potential of dinosporin, but have the disadvantage of complicating the interpretation of the original biopolymer composition.

Thus, although dinosporin is different from other resistant biomacromolecules it is (1) still poorly characterized (2) its structural diversity is hardly known, and (3) the factors influencing this diversity have not been explored. This study attempts to address all of these aspects through geochemical analyses of different morphospecies of the genus *Apectodinium* (Paleocene age) from two different geographical regions, which experienced different post-depositional conditions. Many species of *Apectodinium* appear to have been adapted to warm surface water masses (e.g. Bujak and Brinkhuis, 1998; Crouch et al., 2003; Sluijs et al., 2006; 2011) and this genus demonstrates a global abundance peak coincident with the Paleocene-Eocene Thermal Maxium (PETM; e.g. Crouch et al., 2001; Sluijs et al., 2007). The PETM occurred at about 56 Ma (Westerhold

et al., 2008; 2009; Charles et al., 2011) and was a short period (~157-217 kya; Röhl et al., 2007; Abdul Aziz et al., 2008; Murphy et al., 2010) of extreme global warmth (e.g. Kennett and Stott, 1991; Zachos et al., 2001; 2003; 2006; Sluijs et al., 2006; Weijers et al., 2007).

Specifically, we have investigated whether differences in cyst morphology, as demonstrated by the different morphospecies of the genus *Apectodinium*, are reflected in the overall chemical composition shown by micro-Fourier transform infrared (FTIR) spectroscopy. FTIR has been used in kerogen characterization studies (e.g. Landais et al., 1993), as well as being a common spectroscopic technique in the study of ancient microfossils (e.g. Arouri et al., 1999; 2000; Marshall et al., 2005; Javaux and Marshall, 2006; Dutta et al., 2007; Jacob et al., 2007; Moczydłowska and Willman, 2009; Steemans et al., 2010). The main advantage of micro-FTIR in the analysis of complex organic molecules is that it allows for the characterization of the chemical bonds present and provides information on the abundance of functional groups in individual specimens. Our results indicate that the initial chemical composition of dinoflagellate cysts can vary greatly and represent the first data that demonstrate differences in cyst wall composition between species from the same genus. These data may further suggest a relationship between environment and cyst morphology, and we discuss to what extent this may relate to chemistry.

7.2 Materials and Methods

7.2.1 Sample locations and Apectodinium species

Samples were taken from sediments deposited during the PETM in two regions (Fig. 7.1): the Longyearbyen section of the Spitsbergen Central Basin (Harding et al., 2011) and exploration well 22/10a-4 from the Everest Field in the Central Graben of the North Sea (Knox and Holloway, 1992; Thomas, 1996). During the PETM, the Spitsbergen Central Basin experienced low bottom water oxygen concentrations as indicated by laminated sediments, although the presence of organic linings of benthic foraminifera suggests that periods of oxygenation (possibly seasonal) may have occurred (Harding et al., 2011). In the North Sea, the entire basin was extremely restricted during the PETM and fine, uninterrupted laminations indicate persistent bottom water anoxia (King, 2001).

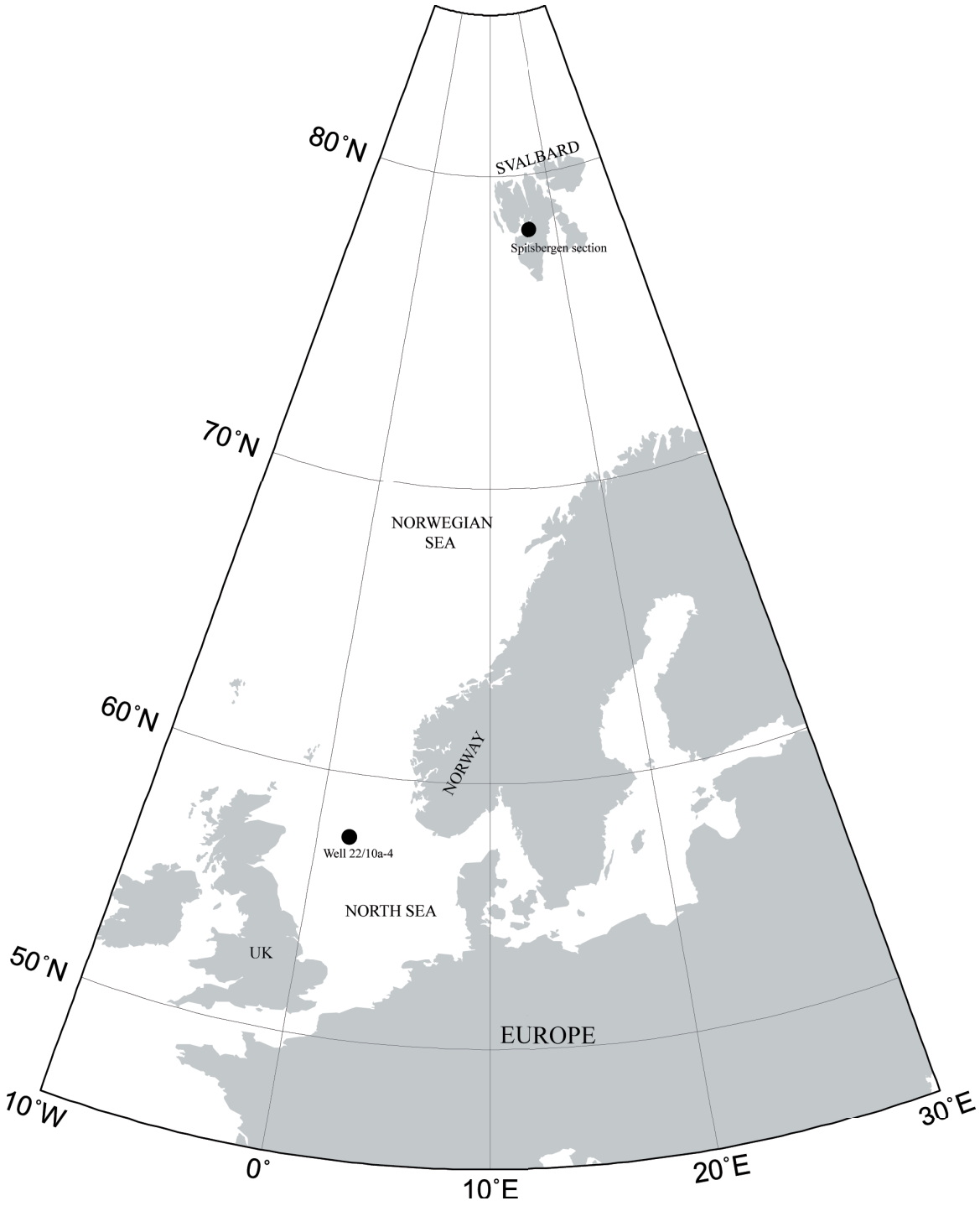

Figure 7.1: Locations of the PETM successions sampled in this study.

The different species of the genus *Apectodinium* are largely distinguished by apical, antapical and lateral horn development (Table 7.1). Four species from the *Apectodinium* complex were used in this study (Fig. 7.2): *A. augustum*, *A. hyperacanthum*, and *A. parvum* were used in the morphometric analysis, and *A. augustum*, *A. paniculatum*, and *A. parvum* were used for micro-FTIR analysis. *A. hyperacanthum* was used in the morphometric analysis as *A. paniculatum* was initially not described from the North Sea samples we used (King, 2001). These species are similar in having intermediate lateral horn development. While *A. parvum* is distinctive because it possesses less than the full complement of horns seen in other members of the genus, it can be difficult to speciate *A. hyperacanthum* and *A. paniculatum* under the light microscope. Therefore, *A. parvum* and *A. augustum* represent morphological end-members and *A. hyperacanthum* and *A. paniculatum* are intermediate species.

Table 7.1: Morphological characteristics of the four *Apectodinium* species used in this study.

Species	Characteristics*
A. augustum	A large, pentagonal cyst with variable apical horn development, well-developed asymmetrical antapical horns and long lateral horns (max. ¾ of cyst diameter), the axes of which are characteristically shifted towards the apex.
A. paniculatum	A pentagonal cyst with well developed antapical and lateral horns. The apical horn is either absent or consists of a short blunt projection surmounted by a tuft of processes. The lateral horns are long and bifurcate distally, whilst the antapical horns are symmetrical, and bear long ramified processes.
A. hyperacanthum	A rounded-pentagonal cyst with well developed apical, antapical and lateral horns, the lateral horns being the most conspicuous.
A. parvum	A pentagonal cyst bearing only an apical and two antapical horns, although some swelling of the periphragm in the lateral positions may occur.

*summarized from (Harland, 1979) and (Costa and Downie, 1976)

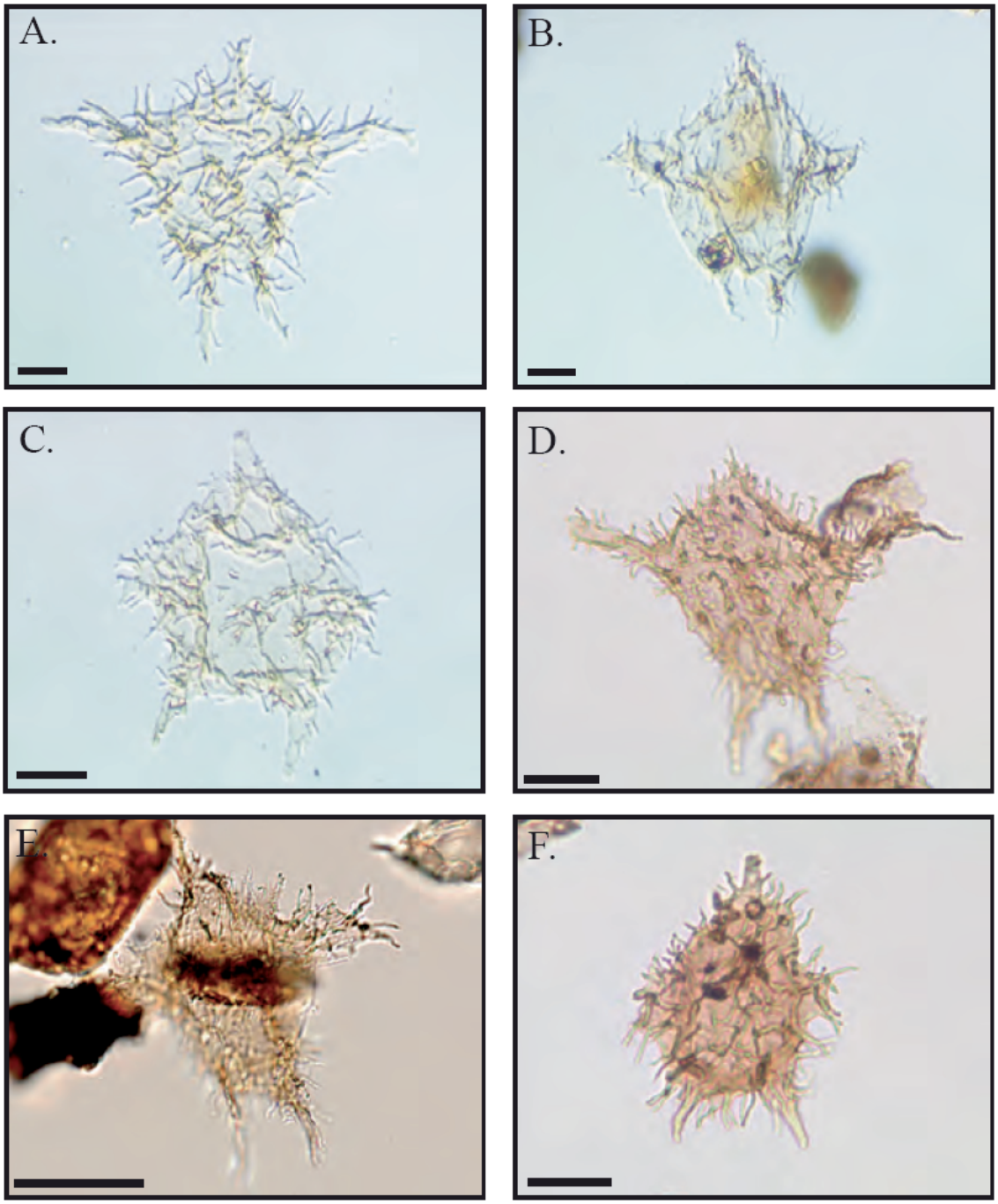

Figure 7.2: Photographs of the Apectodinium species investigated in this study: A) *A. augustum*, B) *A. hyperacanthum*, C) *A. parvum*, are from the North Sea (Well 22/10a-4). D) *A. augustum*, E) *A. paniculatum*, F) *A. parvum* from the Spitsbergen succession. Scale bars indicate 25 µm.

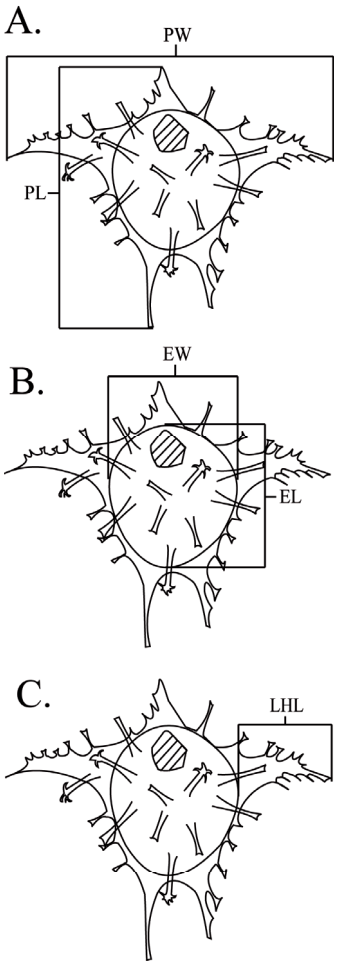

Figure 7.3: Diagrammatic illustration of the different measurements taken for the morphological analysis. A) Pericyst measurements: PW = pericyst width, PL = pericyst, B) Endocyst measurements: EW = endocyst width, EL = endocyst length, C) Horn measurement: LHL = lateral horn length

7.2.2 Morphological analysis

Samples used in the morphometric analysis were from North Sea well 22/10a-4 (sample depths between 2565-2614 m) and processed as described in Harding et al. (2011). The following morphological features were measured under a light microscope: average lateral horn length (LHL), endocyst width (EW) and length (EL), and pericyst width (PW) and length (PL). Lateral horn length was measured for both the right and left horns and then averaged. EW and EL measurements were made at the widest and longest points of the endocyst, respectively. PW was the measured distance between the tips of the lateral horns; PL refers to the measured distance from the tip of the apical horn to the longest antapical horn (Fig. 7.3).

7.3 Micro-FTIR spectroscopic methods

Micro-FTIR spectroscopy was performed on individual cysts isolated from one sample residue (after a modified acid maceration treatment) from each location. The Spitsbergen sample is from a height of 6.18 m above the base of the Gilsonryggen Member, which was deposited during the carbon isotope excursion (CIE; see Harding et al., 2011). The sample from the North Sea Central Graben (2613 m) is from a mudstone intercalation in the Forties Sandstone Member of the Sele Formation. Approximately 1.5 g of each sample was treated with 60% HF, neutralized with water and decanted. HCl was not used as a pre-treatment as previous studies indicated that very little carbonate was present. No oxidizing agents were used. Material was ultrasonicated (≤ 1 min) with a tunable ultrasonic probe to remove amorphous organic matter and then sieved over a 20 μm precision sieve (Storck Mesh #317). Individual dinoflagellate cysts were isolated following the method of Versteegh et al. (2007) with a Narishige IM5b microinjector attached to a Märzhauser

DC3K 168 micromanipulator. Care was taken to pick specimens with no attached particles and no visible pyrite crystals. After picking, cysts were dried and transferred to a NaCl plate for FTIR analysis.

Each cyst species had multiple separate specimens analyzed. Infrared spectra were recorded with a Nicolet FT-IR spectrometer with a Nicplan microscope (15x objective), a Protégé™ 460 optical bench, a MCT- A detector cooled to ≤ -70°C with liquid nitrogen, Ever-Glo source, and a KBr beamsplitter. Two adjustable apertures (upper and lower) were set at a constant area of 15 x 15 µm. Interferograms were obtained in transmission mode with 256 scans at 8 cm^{-1} resolution over a spectral range of 4000-650 cm^{-1}. Background spectra of the NaCl plate (and air) were recorded after each specimen and all reported spectra depict the sample beam following background subtraction. CO_2 absorptions at 2400 cm^{-1}, a result of the system not being purged, have also been removed. All spectra were manipulated with OMNIC™ 3.1 software in absorbance mode. Assignments of the main IR characteristic group frequencies were primarily based on Coates (2000) and Colthup et al. (1990). Relative strengths of the main frequency bands within a species spectrum were calculated by integrating the area between the band limits using the program ImageJ64 in order to allow comparisons to published spectra. This analysis provides a means for the comparison of the size (and concentration) of frequency bands (and therefore functional groups) between different species and biopolymers.

7.3 Results and discussion

7.3.1 Morphology and cyst wall composition of the Apectodinium species

Forty-eight *A. augustum*, 25 *A. hyperacanthum*, and 22 *A. parvum* specimens were analyzed morphometrically. In all cases, the cysts were visually well preserved, but the morphometric data demonstrate the quantitative difficulties in separating the various species of the *Apectodinium* genus. This is especially apparent in the consistent overlap between the end-member species *A. parvum* and *A. augustum* and the morphologically intermediate species, *A. hyperacanthum* (Fig. 7.4). In the distribution of average lateral horn length, *A. augustum* and *A. parvum* demonstrate a unimodal distribution with peaks at 32.5 µm and 5 µm, respectively. *A. hyperacanthum* exhibits an intermediate, bimodal distribution with peaks at 17.5 µm and 30 µm (Fig. 7.4a). *A. hyperacanthum* also shows

intermediate values in width and length ranges (Table 7.2). The best separation was achieved with a ratio representing endocyst (EW:EL) plotted against pericyst (PW:PL) measurements where there is still little discrete grouping amongst the species (Fig. 7.4b), although it seems that *A. parvum* and *A. augustum* do represent end-members along a continuum. These results imply that morphology alone may not be the most reliable indicator of speciation, despite the fact it is still the primary method used to recognize fossil dinoflagellate cyst species (Fensome et al., 1999; Sluijs et al., 2005). In fact, the unusual bimodal distribution of the *A. hyperacanthum* LHL could be an artifact of uncertainty in visual species determination.

Table 7.2: Morphological size ranges for endocyst and pericyst features.

Morphological characteristic* (µm)	*A. augustum*	*A. hyperacanthum*	*A. parvum*
EW	55-95	50-87.5	37.5-70
EL	50-100	50-100	45-72.5
PW	100-187.5	80-137.5	50-102.5
PL	82.5-147.5	72.5-150	57.5-135

*EW= endocyst width, EL= endocyst length, PW= pericyst width, PL= pericyst length

The taxonomic separation of these species of *Apectodinium* is, however, supported by the systematic differences in their FTIR spectra (Fig. 7.5); all specimens of individual species produced similar spectra, and thus, representative spectra are shown. The species can be clearly distinguished on the basis on the relative strengths of the absorption bands in the FTIR spectra (Fig. 7.5; Table 7.3). The 3000-2800 cm^{-1} region is dominated by methyl (CH_3) and methylene (CH_2) symmetric and asymmetric stretching vibrations (frequency band I). *A. augustum* and *A. parvum* exhibit two peaks located between 2925-2850 cm^{-1}, which correspond mainly to methylene (CH_2) asymmetric and symmetric stretching, respectively. This suggests a strong dominance of CH_2 over CH_3 groups. The absorption (2920 cm^{-1}) in this region in *A. paniculatum* appears weaker relative to the other frequency bands (Table 7.3), in contrast to *A. parvum* and especially *A. augustum*, and also lacks the two clearly separate peaks present in the other two species. In all species, there are corresponding CH_3 and CH_2 bending deformations between 1470-1430 cm^{-1} and 1380-1360 cm^{-1}, respectively (frequency band III; Fig. 7.5). In *A. parvum*, frequency band III is stronger in the North Sea specimens, which is reflected in the I/III ratio value difference (Table 7.3). This stronger absorption in the North Sea *A. parvum* is

not supported by frequency band I, so an additional absorption, such as $(CH_3)_n$, may play a role.

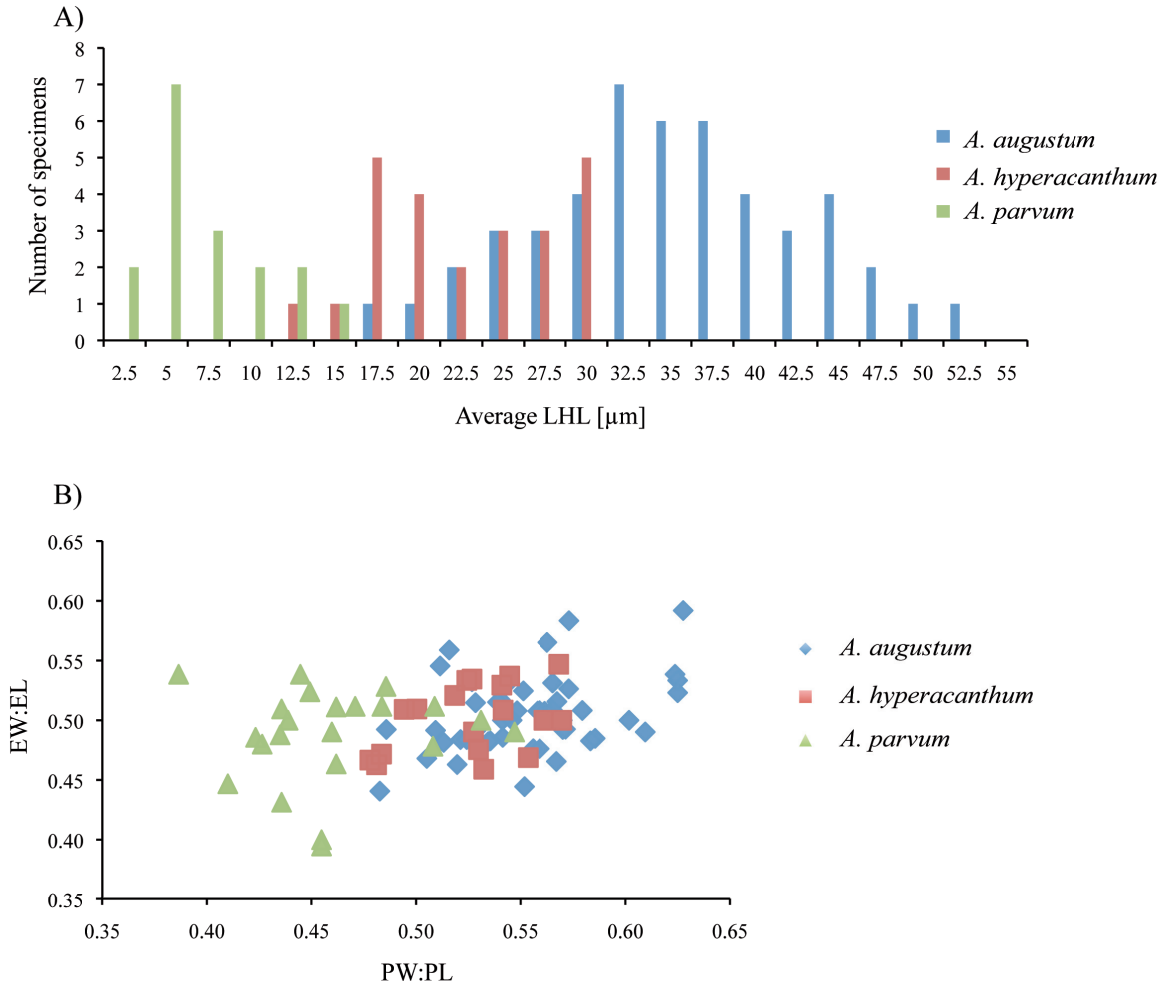

Figure 7.4: Morphological characteristics of *A. augustum*, *A. hyperacanthum*, and *A. parvum* from the North Sea. A) Average lateral horn length distribution of *A. augustum* (blue bars), *A. hyperacanthum* (red bars), and *A. parvum* (green bars), B) comparison of endocyst (endocyst width:length, EW:EL) with pericyst (pericyst width:length, PW:PL) measurements of *A. augustum* (blue diamonds), *A. hyperacanthum* (red squares), and *A. parvum* (green triangles).

The lowest frequency band (IV; Fig. 7.5) consists of peaks characteristic of ether bonds. The presence of three shoulders within this strong deformation, at 1160 cm^{-1} (C-O-C asymmetric vibration), 1110 cm^{-1} and 1050 cm^{-1} (C-O stretching), is unique to *A. paniculatum*. There are also small deformations present between 903-910 cm^{-1}, characteristic of CH out-of-plane bending. *A. augustum* demonstrates two weak absorptions at 1130-1120 cm^{-1} and 1050 cm^{-1}, while *A. parvum* exhibits a broad absorption centered at 1130 cm^{-1} (Spitsbergen) and 1050 cm^{-1} (North Sea); both species also exhibit a small CH out-of-plane deformation at 890-870 cm^{-1} (Fig. 7.5). Frequency

band IV completely dominates the ratio values in *A. paniculatum* (Table 7.3) as the strongest series of absorptions. By comparison, it is the weakest set of absorptions in *A. augustum*. *A. parvum* is intermediate in terms of frequency band strength (Table 7.3). Overall, the *A. paniculatum* spectra show very strong similarities to cellulose (Fig. 7.6) so that the absorptions at 1110 cm^{-1} and about 900 cm^{-1} could represent the glucose ring stretching (Pandey, 1999). The spectra of *A. parvum* and *A. augustum* do not resemble cellulose. Most importantly, they lack the strong series of absorptions in frequency range IV. They also have a higher proportion of CH_3 and CH_2 absorptions (Table 7.3). Overall it seems that the dinosporin comprising *A. paniculatum* is cellulose-like, while *A. parvum* and *A. augustum* dinosporins have a more aliphatic component.

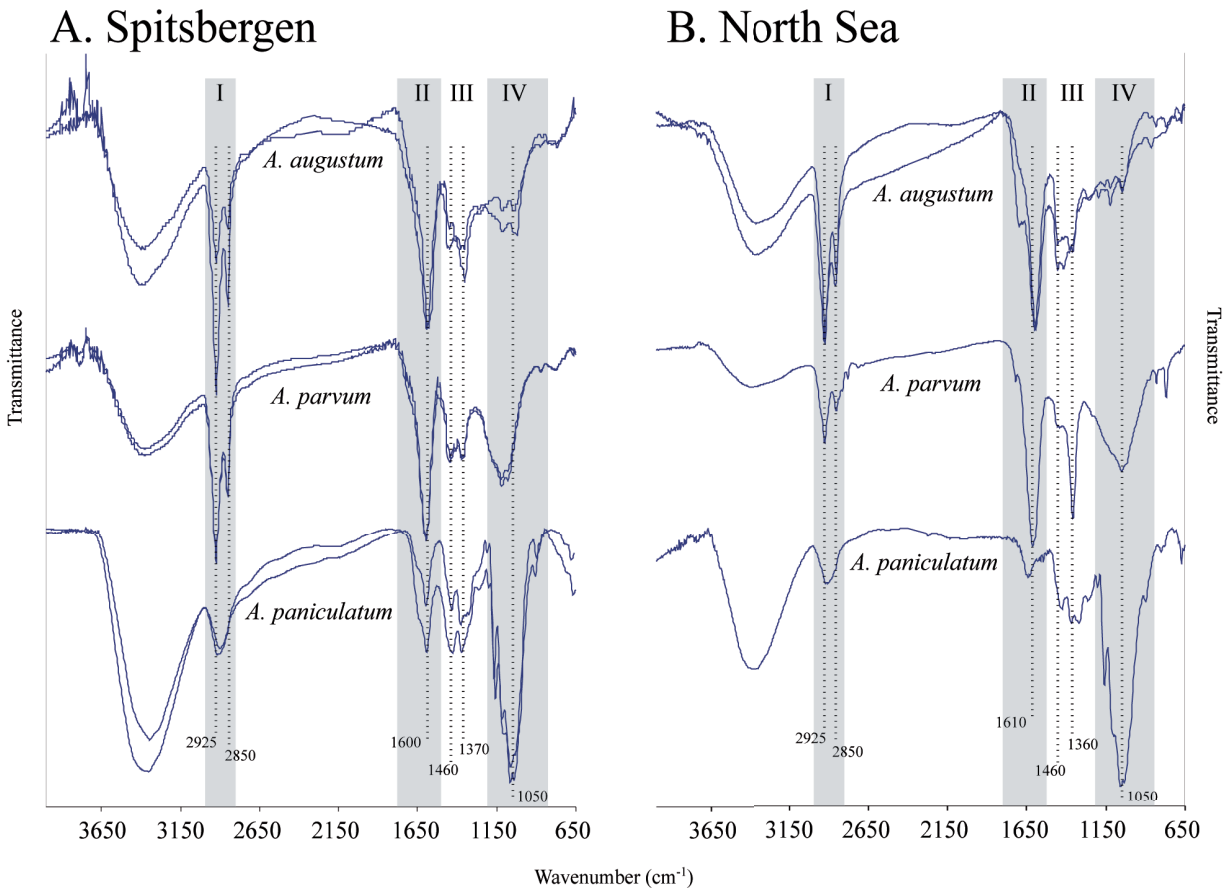

Figure 7.5: FTIR spectra of *A. augustum*, *A. parvum*, and *A. paniculatum* from A) Spitsbergen and B) central North Sea. Roman numerals (I-IV) indicate frequency bands used in the calculation of relative band intensities (Table 7.3). Ranges of these bands are: (I) 3010-2775 cm-1, (II) 1850-1500 cm-1, (III) 1500-1185 cm-1, (IV) 1185-860 cm-1.

Despite the differences, there are some commonalities between the species' FTIR spectra. First of all, it appears that the dinosporins are probably non-aromatic, although the deformation centered at 1600 cm^{-1} is somewhat ambiguous (frequency band II; Fig. 7.5), as it can result from aromatic C=C-C stretching. However, in a primarily aromatic compound, there should be additional C-H stretching frequencies between 3100-3000 cm^{-1} and aromatic skeletal vibrations at around 1500 cm^{-1}, as well as stronger C-H out of plane bending frequencies between 900-670 cm^{-1}.

Another explanation for this series of absorptions in frequency band II is an alkenyl C=C stretch influenced by a carbonyl (C=O) group because most specimens actually demonstrate a main peak at 1600 cm^{-1} and a shoulder at 1650-1730 cm^{-1}. The only digression from this pattern is in the North Sea *A. paniculatum* spectrum, where the band is weaker and centered at 1640 cm^{-1}. This explanation is supported by the strong, broad hydroxy (O-H) absorption and could be suggestive of a keto-enol (OCC asymmetric stretching). Thus, for this series of absorptions, enolization of sugars could play a role, and is a process that happens with exposure to higher temperatures (Yaylayan and Ismail, 1995). However, absorptions as a result of enolization are more common around 1630 cm^{-1}, and so may not be the most plausible explanation. Moreover, it is unlikely that thermal alteration would vary between the species as they are all derived from one sample at each site.

A final possibility is that this absorption represents carboxymethyl derivatives (e.g. Šandula et al., 1999; Yuen et al., 2009), which may increase the stability of the dinosporin biopolymer (e.g. Yang et al., 1996). The stronger absorption of band II in *A. augustum* and *A. parvum* thus indicates a higher amount of ester bonds than in *A. paniculatum*. Therefore, *A. augustum* contains a stronger aliphatic and carboxyl contribution, while *A. parvum* appears to have an intermediate structure (Fig. 7.5), despite being the most distinct in terms of morphology of these three species (Fig. 7.4). Finally, the FTIR results demonstrate that while there may be slight morphological variation between species in this genus, the cysts clearly differ chemically.

Table 7.3: Relative band strengths of frequency ranges in FTIR spectra.

	Ratio of frequency bands*						
Spectrum origin	I/II	I/III	I/IV	II/III	II/IV	III/IV	I/II+III
Cellulose[a]	2.20	0.25	0.12	0.12	0.06	0.46	0.23
Dinosporins							
A. paniculatum (North Sea)	1.52	0.41	0.10	0.27	0.07	0.26	0.32
(Spitsbergen)	0.52	0.40	0.12	0.77	0.23	0.30	0.23
A. parvum (North Sea)	0.50	0.98	0.57	1.95	1.13	0.58	0.33
(Spitsbergen)	0.91	1.72	0.82	1.90	0.91	0.48	0.59
A. augustum (North Sea)	1.11	1.84	4.01	1.65	3.60	2.18	0.69
(Spitsbergen)	1.06	2.60	1.79	2.46	1.69	0.69	1.00
T. pelagica[b]	0.95	2.23	7.30	2.36	7.71	3.27	0.67
L. machaerophorum[c]	0.94	0.64	0.32	0.68	0.33	0.49	0.38
Algaenan							
Chlorella emersonii[d]	1.18	1.08	1.18	0.91	1.01	1.10	0.56
Sporopollenin							
Typha angustifolia L.[e]	0.75	0.82	0.73	1.1	0.97	0.88	0.39

*Bands: (I) 3010-2775 cm-1, (II) 1850-1500 cm-1, (III) 1500-1185 cm-1, (IV) 1185-860 cm-1. FTIR from a) Pandey (1999), b) Versteegh et al. (2007), c) Versteegh et al. (in press), d) Allard and Templier (2000) e) Bubert et al. (2002).

7.3.2 Influence of diagenesis

The combination of samples and sites enables us to considerably narrow down the origin of the link between the cyst morphology and chemistry. As both the North Sea and Spitsbergen samples provide extremely similar FTIR spectra with regards to the different morphospecies (Fig. 7.5), only factors that are common to both sites would be able to explain the observed differences in cyst chemistry. Furthermore, within each sample the morphospecies have a characteristic chemical "fingerprint", as demonstrated by the relative band strengths (Table 7.3), and implies that any influence affecting all of the morphospecies is unlikely to be responsible for the chemical differences in the cysts. In other words, the consistency in the FTIR spectra between species indicates that modification of identical dinosporin macromolecules into spectrally different geomacromolecules is probably not the major source of variability.

However, as this material was deposited during the late Paleocene, we may expect some modification of the original dinosporin biomacromolecule through processes such as coalification (e.g. Yule et al., 2000; Versteegh and Blokker, 2004), oxidative polymerization (e.g. Versteegh et al., 2004; Gupta et al., 2006), or, in light of the anoxic

depositional environment, sulfurization (e.g. Sinninghe Damsté et al., 1989; Kok et al., 2000; Versteegh et al., 2007). It is known that natural sulfurization can aid in the preservation of carbohydrates, though this would then lead to an overprinting of the original biomacromolecular structure (e.g. Kok et al., 2000; van Dongen et al., 2003). In one species of dinoflagellate cyst, *Thalassiphora pelagica*, sulfurization was shown to result in such an overprinting (Versteegh et al., 2007). Since sulfur species are not well-resolved in FTIR spectra, we cannot determine the extent to which sulfurization may have affected the *Apectodinium* dinosporins in the present study.

However, the remarkable resemblance of *A. paniculatum* to cellulose is evidence that minimal alteration of the biomacromolecule has taken place in these two locations, despite the Spitsbergen material having a vitrinite reflectance (R_o) of around 0.7% (Ćmiel and Fabiańska, 2004). The only digression is the shift of frequency band II between the two sites. An absorption at 1640 cm^{-1} (North Sea) is more consistent with cellulose (Fig. 7.6). In the Spitsbergen *A. paniculatum* spectra, this absorption is shifted to 1600 cm^{-1} and is relatively stronger in comparison with the other frequency bands (Table 3). This could be due to the material being more thermally mature (Soares et al., 2001), or might reflect the intermittent presence of oxygen in the bottom waters of this area during deposition (Harding et al., 2011).

Despite this, the signal from *A. paniculatum* in both locations is an example of extremely good carbohydrate preservation. Cellulose, and carbohydrates in general, have been described as labile and easily degraded by bacteria (e.g. Arnosti et al., 1994; Arnosti, 1995). Few studies have found evidence for cellulose preservation in the Cenozoic (e.g. Lechien et al., 2006). The higher preservation potential of dinosporin has been attributed to a higher degree of cross-linking between carbohydrate monomers (Versteegh et al., in press). Thus, if diagenetic processes like sulfurization and thermal maturation are not the major source of variability in the cyst wall chemistry between the species, it appears that the species-specific differences in the FTIR spectra reflect intrinsic differences in the cyst wall chemistry.

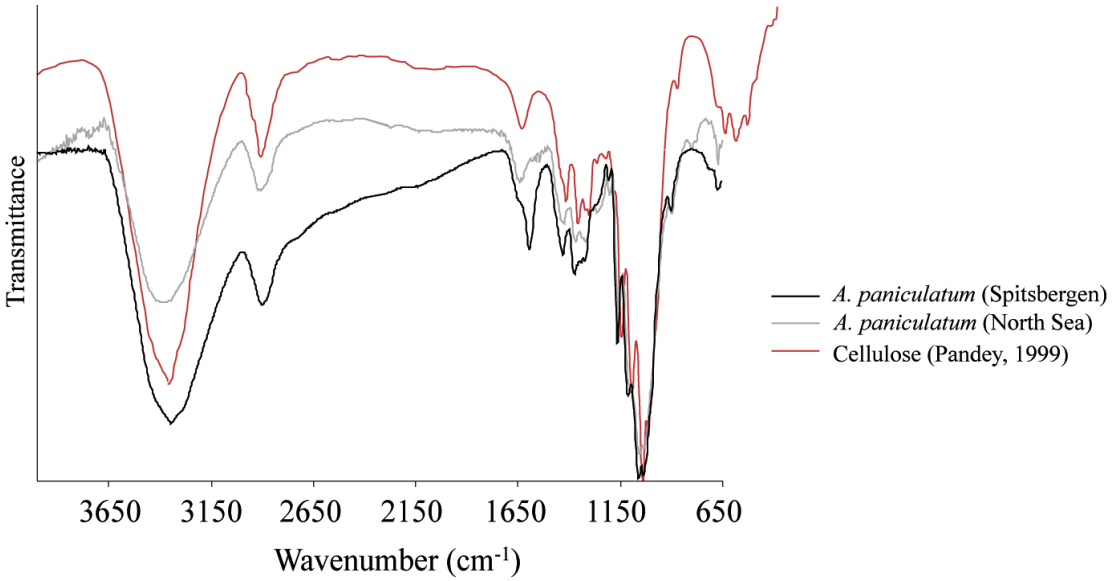

Figure 7.6: Comparison of the FTIR spectra of A. paniculatum from the two study locations, the North Sea (gray line) and Spitsbergen (black line), to cellulose (red line; modified after Pandey, 1999).

7.3.3 Origin of the intrinsic differences in Apectodinium *dinosporin*

If the cause of the differences in cyst chemistry is an intrinsic property then there are several possible biological mechanisms that can contribute to taxon specific dinosporin compositions. First, the differences in dinosporin could be explained if there were several motile species, each with an unique cyst wall chemistry, which produced the different cyst morphospecies of the *Apectodinium* complex. The current understanding is that morphological overlap between cysts of different species is primarily absent, in that one genotype produces one phenotype (e.g. Ellegaard et al., 2003). However, there are exceptions, as recently shown for the *Gonyaulax spinifera* complex (Rochon et al., 2009), so the extent to which a single motile species may produce multiple morphologically distinct cyst types is still unclear. Unfortunately, this hypothesis is impossible to examine in the extinct *Apectodinum* species.

It is also possible that the *Apectodinium* morphotypes were produced by a single motile species but that the cyst morphology and chemistry reflect a response to fluctuating environmental conditions, such as salinity and temperature, during the PETM. Changes in surface water salinity and temperature have been suggested during the PETM (Sluijs et al., 2006; Sluijs and Brinkhuis, 2009; Harding et al., 2011). In extant species, salinity, for example, has been linked with changes in cyst morphology, which typically leads to distinct end-members with a wide range of intermediate morphologies (e.g. Wall

and Dale, 1973; Mudie, 1992; Nehring, 1994; Dale, 1996; Matthiessen and Brenner, 1996; Mertens et al., 2009) and is analogous to what we observe in the species of *Apectodinium*. However, this connection is not unequivocal, as a wide range of morphologies has been found in single culture experiments (e.g. Kokinos and Anderson, 1995; Lewis et al., 1999).

Furthermore, it is known that microalgae alter their lipid content as a result of changing environmental conditions (e.g. Abid et al., 2008; Fuentes-Grünewald et al., 2009; 2011). This has been shown specifically for dinoflagellates in response to changes in salinity and temperature (e.g. Garcia-Martin and Casais-Laiño, 1991). Unfortunately, it is not known whether these differences in the cell would be reflected in changes in dinosporin composition. For the extinct *Apectodinium* species, we can therefore speculate that cyst production/formation or the actual composition of the cell changed in a fundamental way as a response to environmental stress such as fluctuating salinity or temperature.

These two properties could covary and produce the observed differences in the FTIR spectra in a couple of ways. The first is a direct link between between the environment and the dinosporin composition through changes in the cell content of the dinoflagellate. The result may be a "unimodal" relationship between morphology and cyst wall chemistry where the morphologically intermediate species, *A. paniculatum*, represents the optimum dinosporin composition of a cellulosic backbone from a non-stressed dinoflagellate. In that case, both *A. parvum* and *A. augustum* would represent cysts formed in periods of environmental stress. This leads to a higher biosynthesis of fatty acids and could explain the more prominent absorption at 1600 cm^{-1}. Thus, these cyst species would deviate from the "optimum" both morphologically (Fig. 7.4) and chemically (Fig. 7.5). However, this also implies that the formation pathways of the cysts changed in a fundamental way. Therefore, another explanation is that environmental conditions led to the biosynthesis of higher amount of lipids (e.g. Garcia-Martin and Casais-Laiño, 1991) and influenced the morphology, but did not change the cyst wall chemistry during formation. During early diagenesis (syn-depositional), remnants of cell material were polymerized (Versteegh et al., 2004) or attached to the dinosporin macromolecule (e.g. Gupta et al., 2006), and resulted in a higher contribution of aliphatic components. This combination could account for both the higher aliphatic absorptions

(region I) and explain the lower absorptions in region IV in *A. parvum* and *A. augustum* (Fig. 7.5; Versteegh et al., 2007). Presently, such explanations for the observed dinosporin diversity are merely speculation, but in either case, can provide links between the environment, cyst morphology and cyst wall chemistry.

7.3.4 Comparison to algaenan, sporopollenin and other dinosporins

The structure of dinosporin suggested by the *Apectodinium* species indicates that it may be more effectively thought of as a suite of chemically different biopolymers. Our results also complement previous assertions that dinosporin differs from other resistant biomacromolecules. While algaenan is a component in the motile cell wall of one dinoflagellate species (*G. catenatum*; Gelin et al., 1999), it is unlikely that dinosporin is derived from an algaenan-like biopolymer. Algaenans contain abundant long chain aliphatic and carboxyl groups. The primary differences in our spectra when compared to algaenan (Allard and Templier, 2000) are the lack of strong carbonyl absorptions, the presence of strong absorptions at 1600 cm^{-1} in *A. augustum* and *A. parvum*, and the strong presence of ether bonds in *A. paniculatum* (Fig. 7.7). The comparison between the *Apectodinium* frequency band ratios also shows differences from algaenan (Table 7.3). Additionally, in contrast to fossil algaenan (e.g. Derenne et al., 1997), there is no evidence of a characteristic absorption for longer chain aliphatics (720 cm^{-1}) in the *Apectodinium* dinosporins. While it has been shown that algaenan may lose its oxygen-containing functional groups after thermal degradation, the strong aliphatic signal remains unchanged (e.g. Salmon et al., 2009). The lack of any absorption characteristic of long chain aliphatics indicates that the dinosporins of *Apectodinium* species comprise shorter chain lengths.

None of the *Apectodinium* species appear to demonstrate a composition similar to sporopollenin, which is a predominantly oxygenated aromatic compound, formed from a para-coumaric acid and ferrulic acid backbone (de Leeuw et al., 2006 and references therein). The main difference between their FTIR spectra is that dinosporin lacks the characteristic absorptions at 1510 cm^{-1} and ~840 cm^{-1}, representative of C-H ring vibrations, present in sporopollenin (e.g. Bubert et al., 2002). As additional evidence, the published FTIR spectra of fossil sporopollenin differ from all the *Apectodinium* species analyzed here, especially *A. paniculatum* (e.g. Steemans et al., 2010; Yule et al., 2000; see Fig. 7.7). This is most likely a result of dinosporin and sporopollenin having different

pathways of formation (de Leeuw et al., 2006), and provides more evidence for the assertion that dinosporin differs significantly from sporopollenin (e.g. Versteegh et al., in press).

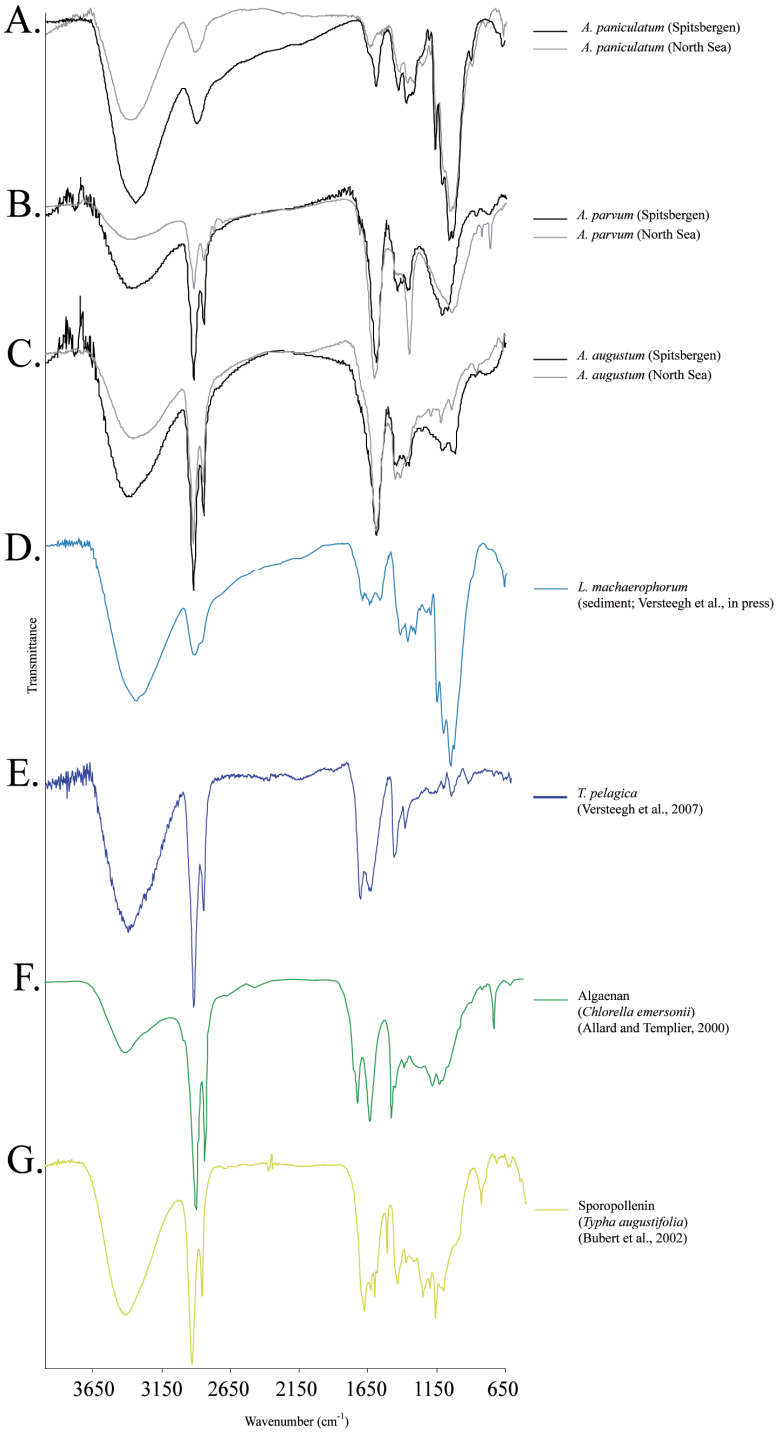

Figure 7.7: FTIR spectra comparison between *Apectodinium* species (A-C) from Spitsbergen (black lines) and the North Sea (gray lines), other fossil dinoflagellate cysts D) *L. machaerophorum* (modified from Versteegh et al., in press, E) *T. pelagica* (modified after Versteegh et al., 2007), and other resistant biomacromolecules F) algaenan (*C. emersonii*; after Allard and Templier, 2000) and G) sporopollenin (*T. angustifolia* L.; modified from Bubert et al., 2002).

There is a paucity of FTIR data for other dinoflagellate cyst species to compare with our analyses of species of *Apectodinium*. Of the *Apectodinium* species, *A. paniculatum* bears the most resemblance to the spectra derived from the cyst species *L. machaerophorum* (Fig. 7.7; Table 7.3; Versteegh et al., in press). The similarities between these two species, despite the millions of years difference in age, are further support for the contention that the *Apectodinium* spectra closely resemble the original dinosporin biomacromolecule. All appear to be carbohydrate-based. This is of interest because the dinoflagellates that produced the *Apectodinium* morphotypes have been presumed to be possibly related to extant heterotrophic dinoflagellates such as *Protoperidinium* (e.g. Sluijs and Brinkhuis, 2009), whereas *L. polyedrum*, the dinoflagellate producing *L. machaerophorum* cysts, is autotrophic (e.g. Lewis and Hallett, 1997). The similarity between *A. paniculatum* and *L. machaerophorum* could suggest that dinosporin structure may be independent of whether the dinoflagellate cyst is classified as heterotrophic or autotrophic. Another option is that the dinoflagellate that produced the *A. paniculatum* cysts was autotrophic. However, this suggestion would require further study, as no published spectra of heterotrophic species (i.e. *Protoperidinium* species) are currently available[1].

There are only two other fossil (Oligocene) dinoflagellate cyst species for which reliable details of the cyst wall chemistry have been published: *Chiropteridium* (de Leeuw et al., 2006) and *Thalassiphora pelagica* (Versteegh et al., 2007). Other fossil dinoflagellate cyst species have been investigated (see Table 3 in de Leeuw et al., 2006), but the impurity of the samples complicates the overall interpretations. The *Chiropteridium* cysts were analyzed by flash pyrolysis gas chromatography-mass spectrometry (py-GC-MS) with tetramethylammonium hydroxide (TMAH) and the results show a dominance of aliphatic moieties (de Leeuw et al., 2006), which, in light of the results presented here, would suggest a diagenetic overprint due to a post-mortem migration and subsequent condensation of aliphatic moieties on to the macromolecule. However, FTIR spectroscopy was not performed and so a direct comparison with the dinosporin of the *Apectodinium* species is not possible. An FTIR spectrum is available for *T. pelagica*, which is different to the *Apectodinium* species (Fig. 7.7). It mainly differs from *A. paniculatum* and *A. parvum* because there is no evidence for ether bonds

[1] However, in light of the results of Chapter 6, we may say with more confidence that *A. paniculatum* resembles the spectra of autotrophic species.

in *T.pelagica* and seems most similar to *A. augustum* in that respect. As discussed previously, *T. pelagica* cysts have been subject to sulfurization processes (Versteegh et al., 2007), which could explain the dissimilarity between the spectra. Regrettably, this overprinting thus prevents any further discussion about dinosporin compositional diversity, except that the *Apectodinium* dinosporins do not resemble other fossil dinoflagellate cyst species analyzed to date.

7.4 Conclusions

As an identifiable component of kerogen, dinoflagellate cysts provide us with a proxy to trace the nature of kerogen transformations, but only once the composition and nature of the transformations of the refractory biomacromolecule of which they are comprised - dinosporin - is understood. In this study, we have therefore investigated the compositional variability in dinosporin between species of the dinoflagellate cyst genus *Apectodinium*. In particular, we have examined whether the morphological parameters used to define the fossil morphospecies can be related to differences in the chemical composition of the dinoflagellate cyst wall by undertaking both a quantitative assessment of morphological features and a geochemical analysis using micro-FTIR spectroscopy. While morphometric variations alone do not provide a clear separation of species of the *Apectodinium* complex, end-member morphospecies can be differentiated. The three species of *Apectodinium* we analyzed geochemically produce completely different FTIR spectra. The morphologically identified end-member species present more similar FTIR spectra to each other than to the intermediate species. *A. paniculatum*, as the morphologically intermediate species, closely resembles the spectrum of cellulose. This indicates that the dinosporin of this species is cellulosic in nature and therefore provides an example of an exceptionally well-preserved biopolymer. *A. augustum* and *A. parvum* show a higher degree of ester bonds, shown by the higher absorption of carboxymethyl derivatives.

The characteristic differences in the cyst wall structure between these closely related species indicates that the term “dinosporin“ does indeed encompass a group of chemically distinct biopolymers. Importantly, we have also been able to show that the structure of dinosporin in *Apectodinium* species differs from both algaenan and sporopollenin, and is probably carbohydrate-based. The structural diversity observed in

the dinosporins could be both taxon-specific as well as a result of environmental factors. The differences in dinosporin were shown to be regionally independent and most likely point to different initial compositions. We speculate that environmental stress, such as salinity variations, may be responsible for producing the different morphotypes within the *Apectodinium* complex and that this stress further resulted in different dinosporin compositions, through either alteration of the cell content chemistry and cyst formation processes or by a combination of altered cell content chemistry and early diagenetic processes. These results are the first to demonstrate clear differences in dinosporin structure between species of the same genus.

Acknowledgements

S. Akbari is thanked for laboratory assistance. We appreciate the technical assistance of R. Williams regarding the FTIR analysis. Financial support for KB and KAFZ was provided by the DFG (Deutsche Forschungsgemeinschaft) as part of the European Graduate College "Proxies in Earth History" (EUROPROX), and by the DFG to GJMV in the framework of a Heisenberg grant (VE-486/2 and /3). Financial support for AK was kindly provided by a NERC PhD studentship and for AJC by a NERC CASE PhD studentship (NE/F006721/1), in conjunction with Shell UK.

References

Abdul Aziz, H., Hilgen, F.J., Van Luijk, G.M., Sluijs, A., Kraus, M.J., Pares, J.M., Gingerich, P.D. 2008. Astronomical climate control on the paleosol stacking patterns in the upper Paleocene-lower Eocene Willwood Formation, Bighorn Basin, Wyoming. *Geology*, 36, 531-534.

Abid, O., Sellami-Kammoun, A., Ayadi, H., Drira, Z., Bouain, A., Aleya, L., 2008. Biochemical adaptation of phytoplankton to salinity and nutrient gradients in a coastal solar saltern, Tunisia. *Estuarine, Coastal and Shelf Science*, 80, 391-400.

Allard, B., Templier, J., 2000. Comparison of neutral lipid profile of various trilaminar outer cell wall (TLS)-containing microalgae with emphasis on algaenan occurrence. *Phytochemistry*, 54, 369-380.

Arnosti, C., 1995. Measurement of depth- and site-related differences in polysaccharide hydrolysis rates in marine sediments. *Geochimica et Cosmochimica Acta*, 59, 4247-4257.

Arnosti, C., Repeta, D.J., Blough, N.V., 1994. Rapid bacterial degradation of polysaccarides in anoxic marine systems. *Geochimica et Cosmochimica Acta*, 58, 2639-2652.

Arouri, K.F., Greenwood, P.F., Walter, M.R., 1999. A possible chlorophycean affinity of some Neoproterozoic acritarchs. *Organic Geochemistry*, 30, 1323-1337.

Arouri, K.F., Greenwood, P.F., Walter, M.R., 2000. Biological affinities of Neoproterozoic acritarchs from Australia: microscopic and chemical charaterisation. *Organic Geochemistry*, 31, 75-89.

Bubert, H., Lambert, J., Steuernagel, S., Ahlers, F., Wiermann, R., 2002. Continuous decomposition of sporopollenin from pollen of *Typha angustifolia* L. by acidic methanolysis. *Zeitschrift für Naturforschung*, 57, 1035-1041.

Bujak, J., Brinkhuis, H., 1998. Global warming and dinoflagellate cyst changes across the Paleocene/Eocene epoch boundary. In: Aubry, M.-P., Lucas, S., Berggren, W. (Eds.), *Late Paleocene–Early Eocene Biotic and Climatic Events in the Marine and Terrestrial Records*. Columbia University Press, New York, pp. 277–295.

Charles, A.J., Condon, D.J., Harding, I.C., Pälike, H., Marshall, J.E.A., Cui, Y., Kump, L., Croudace, I.W., 2011. Constraints on the numerical age of the Paleocene-Eocenc boundary. *Geochemistry, Geophysics, Geosystems*, 12, QOAA17. doi: 10.1029/2010GC003426.

Coates, J., 2000. Interpretation of Infrared Spectra: A Practical Approach. In: Meyers, R.A. (Ed.), *Encyclopedia of Analytical Chemistry*. John Wiley and Sons Inc., pp. 10815-10837.

Colthup, N.B., Daly, L.H., Wiberly, S.E., 1990. *Introduction to Infrared and Raman Spectroscopy.* Academic Press Limited, London, 282 pp.

Costa, L.I., Downie, C., 1976. The distribution of the dinoflagellate *Wetzeliella* in the Palaeogene of North-Western Europe. *Palaeontology*, 19, 591-614.

Crouch, E.M., Heilmann-Clausen, C., Brinkhuis, H., Morgans, H.E.G., Rogers, K.M., Egger, H., Schmitz, B., 2001. Global dinoflagellate event associated with the late Paleocene thermal maximum. *Geology*, 29, 315-318.

Crouch, E.M., Dickens, G.R., Brinkhuis, H., Aubry, M.P., Hollis, C.J., Rogers, K.M., Visscher, H., 2003. The *Apectodinium* acme and terrestrial discharge during the Paleocene-Eocene thermal maximum: new palynological, geochemical, and calcareous nannoplankton observations at Tawanui, New Zealand. *Palaeogeography, Palaeoclimatology, Palaeoecology*, 194, 387-403.

Ćmiel, S.R., Fabiańska, M.J., 2004. Geochemical and petrographic properties of some Spitsbergen coals and dispersed organic matter. *International Journal of Coal Geology*, 57, 77-97.

Dale, B., 1996. Dinoflagellate cyst ecology: modelling and geological applications. In: Jansonius, J., McGregor, D.C. (Eds.), *Palynology: Principles and Applications.* American Association of Stratigraphic Palynologists Foundation, Salt Lake City, Utah, pp. 1249-1275.

de Leeuw, J.W., Largeau, C., 1993. A review of macromolecular organic compounds that comprise living organisms and their role in kerogen, coal and petroleum formation. In: Engel, M.H., Macko, S.A. (Eds.), *Organic Geochemistry: principles and applications.* Plenum Publishing Corp., New York, pp. 23-72.

de Leeuw, J.W., Versteegh, G.J.M., van Bergen, P.F., 2006. Biomacromolecules of algae and plants and their fossil analogues. *Plant Ecology*, 182, 209-233.

Derenne, S., Largeau, C., Hetényi, M., Brukner-Wein, A., Connan, J., Lugardon, B., 1997. Chemical structure of the organic matter in a Pliocene maar-type shale: Implicated *Botryococcus* race strains and formation pathways. *Geochimica et Cosmochimica Acta*, 61, 1879-1889.

Domínguez, E., Mercado, J.A., Quesada, M.A., Heredia, A., 1999. Pollen sporopollenin: degradation and structural elucidation. *Sexual Plant Reproduction*, 12, 171-178.

Durand, B., 1980. Sedimentary organic matter and kerogen: Definition and quantitative importance of kerogen. In: Durand, B. (Ed.), *Kerogen, Insoluble Organic Matter from Sedimentary Rocks.* Editions Technip, Paris, pp 13-34.

Dutta, S., Brocke, R., Hartkopf-Fröder, C, Littke, R., Wilkes, H., Mann, U., 2007. Highly aromatic character of biogeomacromolecules in Chitinozoa: A spectroscopic and pyrolytic study. *Organic Geochemistry*, 38, 1625-1642.

Dybkjaer, K., 2004. Morphological and abundance variations in *Homotryblium*-cyst assemblages related to depositional environments; uppermost Oligocene - Lower Miocene, Jylland, Denmark. *Palaeogeography, Palaeoclimatology, Palaeoecology*, 206, 41-58.

Ellegaard, M., 2000. Variations in dinoflagellate cyst morphology under conditions of changing salinity during the last 2000 years in the Limfjord, Denmark. *Review of Palaeobotany and Palynology*, 109, 65-81.

Ellegaard, M., Lewis, J., Harding, I., 2002. Cyst-theca relationship, life cycle, and effects of temperature and salinity on the cyst morphology of *Gonyaulax baltica* sp. nov. (Dinophyceae) from the Baltic Sea area. *Journal of Phycology*, 38, 775-789.

Ellegaard, M., Daugbjerg, N., Rochon, A., Lewis, J., Harding, I., 2003. Morphologic and genetic (LSU rDNA) variation within *Spiniferites/Gonyaulax* (Dinophyceae), including the cyst-theca relationship of *Spiniferites elongatus* and phylogenetic analysis of the position of *Spiniferites* and *Bitectatodinium* within the Gonyaulacales. *Phycologia*, 42, 151-164.

Fensome, R.A., Taylor, F.J.R., Norris, G., Sarjeant, W.A.S., Wharton, D.I., Williams, G.L., 1993. A classification of fossil and living dinoflagellates. *Micropaleontology Press Special Paper*, 7, 351 pp.

Fensome, R.A., Saldarriaga, J.F., Taylor, F.J.R., 1999. Dinoflagellate phylogeny revisited: reconciling morphological and molecular based phylogenies. *Grana*, 38, 66-80.

Fuentes-Grünewald, C., Garcés, E., Rossi, S., Camp, J., 2009. Use of the dinoflagellate *Karlodinium veneficum* as a sustainable source of biodiesel production. *Journal of Industrial Microbiology and Biotechnology*, 36, 1215-1224.

Fuentes-Grünewald, C., Garcés, E., Alacid, E., Sampedro, N., Rossi, S., Camp, J., 2011. Improvement of lipid production in the marine strains *Alexandrium minutum* and *Heterosigma akashiwo* by utilizing abiotic parameters. *Journal of Industrial Microbiology and Biotechnology*, doi: 10.1007/s10295-011-1016-6.

Garcia-Martin, M.S., Casais-Laiño, C., 1991. Effects of temperature and salinity on the dinoflagellate *Alexandrium lusitanicum*. I. cell volume, cell concentrations in the culture and cellular composition. *Environmental Technology*, 12, 997-1005.

Gelin, F., Volkman, J.K., Largeau, C., Derenne, S., Sinninghe Damsté, J.S., de Leeuw, J.K., 1999. Distribution of aliphatic, nonhydrolyzable biopolymers in marine microalgae. *Organic Geochemistry,* 30, 147-159.

Gupta, N.S., Collinson, M.E., Briggs, D.E.G., Evershed, R.P., Pancost, R., 2006. Reinvestigation of the occurrence of cutan in plants: implications for the leaf fossil record. *Paleobiology*, 32, 432-449.

Hallett, R.I., 1999. Consequences of environmental change on the growth and morphology of *Lingulodinium polyedrum* (Dinophyceae) in culture. University of Westminster, London, pp. 1-109.

Harding, I.C., Charles, A.J., Marshall, J.E.A., Pälike, H., Roberts, A.P., Wilson, P.A., Jarvis, E., Thorne, R., Morris, E., Moremon, R., Pearce, R.B., Akbari, S., 2011. Sea-level and salinity fluctuations during the Paleocene-Eocene thermal maximum in Arctic Spitsbergen. *Earth and Planetary Science Letters*, 303, 97-107.

Harland, R., 1979. The *Wetzeliella* (*Apectodinium*) *homomorpha* plexus from the Palaeogene/earliest Eocene of North-west Europe. *Proceedings of the IV International Palynological Conference*, Lucknow, India, pp. 59-70.

Hemsley, A.R., Chaloner, W.G., Groombridge, C.J., Scott, A.C., 1992. Carbon-13 solid state nuclear magnetic resonance of sporopollenin from modern and fossil plants. *Annals of Botany*, 69, 545-549.

Hemsley, A.R., Barrie, P.J., Chaloner, W.G., Scott, A.C., 1993. The composition of sporopollenin and its use in living and fossil plant systematics. *Grana,* Supplement 1, 2-11.

Hemsley, A.R., Barrie, P.J., Scott, A.C., Chaloner, W.G., 1994. Studies of fossil and modern spore and pollen wall biomacromolecules using ^{13}C solid state NMR. In: Eglinton, G., Kay, R.L.F. (Eds.), *Biomolecular Palaeontology,* NERC Special Publications, 94, 15-19.

Jacob, J., Paris, F., Monod, O., Miller, M.A., Tang, P., George, S.C., Bény, J.M., 2007. New insights into the chemical composition of chitinozoans. *Organic Geochemistry*, 38, 1782-1788.

Javaux, E.J., Marshall, C.P., 2006. A new approach in deciphering early protist paleobiology and evolution: combined microscopy and microchemistry of single Proterozoic acritarchs. *Review of Palaeobotany and Palynology*, 139, 1-15.

Kennett, J.P., Stott, L., 1991. Abrupt deep-sea warming, palaeoceanographic changes and benthic extinctions at the end of the Palaeocene. *Nature*, 353, 225-229.

King, A., 2001. Terminal Palaeocene events in the North Sea and Faeroe-Shetland Basins. Unpublished PhD thesis. University of Southampton, UK.

Knox, R.W.O'B., Holloway, S., 1992. Paleogene of the Central and Northern North Sea. In: Knox, R.W.O'B., Cordey, W.G. (Eds.), *Lithostratigraphic Nomenclature of the UK North Sea*. British Geological Survey, Nottingham, 133 pp.

Kok, M.D., Schouten, S., Sinninghe Damsté, J.S., 2000. Formation of insoluble, nonhydrolyzable, sulfur-rich macromolecules via incorporation of inorganic sulfur species into algal carbohydrates. *Geochimica et Cosmochimica Acta*, 64, 2689-2699.

Kokinos, J.P., Anderson, D.M., 1995. Morphological development of resting cysts in cultures of the marine dinoflagellate *Lingulodinium polyedrum* (*=L. machaerophorum*). *Palynology*, 19, 143-166.

Kokinos, J.P., Eglinton, T.I., Goñi, M.A., Boon, J.J., Martoglio P.A., Anderson, D.M., 1998. Characterization of a highly resistant biomacromolecular material in the cell wall of a marine dinoflagellate resting cyst. *Organic Geochemistry*, 28, 265-288.

Landais, P., Rochdi, A., Largeau, C., Derenne, S., 1993. Chemical characterization of torbanites by transmission micro-FTIR spectroscopy: origin and extent of compositional heterogeneities. *Geochimica et Cosmochimica Acta*, 57, 2529-2539.

Lechien, V., Rodriguez, C., Ongena, M., Hiligsmann, S., Rulmont, A., Thonart, P., 2006. Physiochemical and biochemical characterization of non-biodegradable cellulose in Miocene gymnosperm wood from the Entre-Sambre-et-Meuse, Southern Belgium. *Organic Geochemistry*, 37, 1465-1476.

Lewis, J., Hallett, R., 1997. *Lingulodinium polyedrum* (*Gonyaulax polyedra*), a blooming dinoflagellate. *Oceanography and Marine Biology Annual Review*, 35, 97-161.

Lewis, J., Rochon, A., Harding, I.C., 1999. Preliminary observations of cyst-theca relationships in *Spiniferites ramosus* and *Spiniferites membranaceus* (Dinophyceae). *Grana*, 38, 113-124.

Lewis, J., Rochon, A., Ellegaard, M., Mudie, P.J., Harding, I., 2001. The cyst-theca relationship of *Bitectatodinium tepikiense* (Dinophyceae). *European Journal of Phycology*, 36, 137-146.

MacRae, G., Fensome, R.A., Williams, G.L., 1996. Fossil dinoflagellate diversity, originations, and extinctions and their significance. *Canadian Journal of Botany*, 74, 1687-1694.

Marret, F., Zonneveld, K.A.F., 2003. Atlas of modern organic-walled dinoflagellate cyst distribution. *Review of Palaeobotany and Palynology*, 125, 1-200.

Marshall, C.P., Javaux, E.J., Knoll, A.H., Walter, M.R., 2005. Combined micro-Fourier transform infrared (FTIR) spectroscopy and micro-Raman spectroscopy of Proterozoic acritarchs: A new approach to Palaeobiology. *Precambrian Research*, 138, 208-224.

Matthiessen, J., Brenner, W., 1996. Chlorococcalalgen und dinoflagellaten-zysten in rezenten sedimenten des greifswalder boddens (südliche Ostsee). *Senckenbergiana Maritima*, 27, 33-48.

Mertens, K.N., Ribeiro, S., Bouimetarhan, I., Caner, H., Combourieu Nebout, N., Dale, B., de Vernal, A., Ellegaard, M., Filipova, M., Godhe, A., Goubert, E., Grøsfjeld, K., Holzwarth, U., Kotthoff, U., Leroy, S.A.G., Londeix, L., Marret, F., Matsuoka, K., Mudie, P.J., Naudts, L., Peña-Manjarrez, J.L., Persson, A., Popescu, S.M., Pospelova, V., Sangiorgi, F., van der Meer, M.T.J., Vink A., Zonneveld, K.A.F., Vercauteren, D., Vlassenbroeck, J., Louwye, S., 2009. Process length variation in cysts of a dinoflagellate, *Lingulodinium machaerophorum*, in surface sediments: Investigating its potential as salinity proxy. *Marine Micropaleontology*, 70, 54-69.

Moczydłowska, M., Willman, S., 2009. Ultrastructure of cell walls in ancient microfossils as a proxy to their biological affinities. *Precambrian Research*, 173, 27-38.

Mudie, P., 1992. Circum-arctic Quaternary and Neogene marine palynofloras: paleoecology and statistical analysis. In: Head, M.J., Wrenn, J.H. (Eds.), *Neogene and Quaternary dinoflagellate cysts and acritarchs*. American Association of Stratigraphic Palynologists Foundation, College Station, Texas, pp. 347-390.

Murphy, B.H., Farley, K.A., Zachos, J.C., 2010. An extraterrestrial ^{3}He-based timescale fort he Paleocene-Eocene thermal maximum (PETM) from Walvis Ridge, IODP Site 1266. *Geochimica et Cosmochimica Acta*, 74, 5098-5108.

Nehring, S., 1994. Spatial distribution of dinoflagellate resting cysts in Recent sediments of Kiel Bight, Germany (Baltic Sea). *Ophelia*, 39, 137-158.

Pandey, K.K., 1999. A study of chemical structure of soft and hardwood and wood polymers by FTIR spectroscopy. *Journal of Applied Polymer Science*, 71, 1969-1975.

Pross, J., 2001. Paleo-oxygenation in Tertiary epeiric seas: evidence from dinoflagellate cysts. *Palaeogeography, Palaeoclimatology, Palaeoecology*, 166, 369-381.

Rochon, A., Lewis, J., Ellegaard, M., Harding, I.C., 2009. The *Gonyaulax spinifera* (Dinophyceae) "complex": Perpetuating the paradox? *Review of Palaeobotany and Palynology*, 155, 52-60.

Röhl, U., Westerhold, T., Bralower, T.J., Zachos, J.C., 2007. On the duration of the Paleocene Eocene thermal maximum (PETM). *Geochemistry, Geophysics, Geosystems*, 8, Q12002. doi:10.1029/2007GC001784.

Salmon, E., Behar, F., Lorant, F., Hatcher, P.G., Metzger, P., Marquaire, P.M., 2009. Thermal decomposition processes in algaenan of *Botryococcus braunii* race L. Part 1: Experimental data and structural evolution. *Organic Geochemistry*, 40, 400-415.

Šandula, J., Kogan, G., Kačuráková, M., Machová, E., 1999. Microbial (1→3)-β-D-glucans, their preparation, physico-chemical characterization and immunomodulatory activity. *Carbohydrate Polymers*, 38, 247-253.

Sinninghe Damsté, J.S., Rijpstra, W.I.C., Kock-Van Dalen, A.C., de Leeuw, J.W., Schenck, P.A., 1989. Quenching of labile functionalized lipids by inorganic sulfur species: evidence for the formation of sedimentary organic compounds at the early stages of diagenesis. *Geochimica et Cosmochimica Acta*, 53, 1343-1355.

Sluijs, A., Brinkhuis, H., 2009. A dynamic climate and ecosystem state during the Paleocene Eocene Thermal Maximum: inferences from dinoflagellate cyst assemblages on the New Jersey shelf. *Biogeosciences*, 6, 1755-1781.

Sluijs, A., Pross, J., Brinkhuis, H., 2005. From greenhouse to icehouse; organic-walled dinoflagellate cysts as paleoenvironmental indicators in the Paleogene. *Earth-Science Reviews*, 68, 281-315.

Sluijs, A., Schouten, S., Pagani, M., Woltering, M., Brinkhuis, H., Sinninghe Damsté, J.S., Dickens, G.R., Huber, M., Reichart, G.J., Stein, R., Matthiessen, J., Lourens, L.J., Pedentchouk, N., Backman, J., Moran, K., Expedition 302 Scientists, 2006. Subtropical Arctic Ocean temperatures during the Palaeocene/Eocene thermal maximum. *Nature*, 441, 610-613.

Sluijs, A., Brinkhuis, H., Schouten, S., Bohaty, S.M., John, C.M., Zachos, J.C., Reichart, G.J., Sinninghe Damsté, J.S., Crouch, E.M., Dickens, G.R., 2007. Environmental precursors to rapid light carbon injection at the Paleocene/Eocene boundary. *Nature*, 450, 1218-1221.

Sluijs, A., Bijl, P.K., Schouten, S., Röhl, U., Reichart, G.-J., Brinkhuis, H., 2011. Southern ocean warming, sea level and hydrological change during the Paleocene-Eocene thermal maximum. *Climate of the Past,* 7, 47-61.

Soares, S., Ricardo, S.M.P.S., Jones, S., Heatley, F., 2001. High temperature thermal degradation of cellulose in air studied using FTIR and ^{1}H and ^{13}C solid-state NMR. *European Polymer Journal*, 37, 737-745.

Steemans, P., Lepot, K., Marshall, C.P., Le Hérissé, A., Javaux, E.J., 2010. FTIR characterisation of the chemical composition of Silurian miospores (cryptospores and trilete spores) from Gotland, Sweden. *Review of Palaeobotany and Palynology*, 162, 577-590.

Tegelaar, E.W., de Leeuw, J.W., Derenne, S., Largeau, C., 1989. A reappraisal of kerogen formation. *Geochimica et Cosmochimica Acta*, 53, 3103-3016.

Thomas, J.E., 1996. The occurrence of the dinoflagellate cyst *Apectodinium* (Costa and Downie, 1976) Lentin and Williams 1977 in the Moray and Montrose Groups (Danian to Thanetian) of the UK central North Sea. *Geological Society of London*, Special Publications, 101, 115-120.

Vandenbroucke, M., Largeau, C., 2007. Kerogen origin, evolution and structure. *Organic Geochemistry*, 38, 719-833.

van Dongen, B.E., Schouten, S., Baas, M., Geenevasen, J.A.J., Sinninghe Damsté, J.S., 2003. An experimental study of the low-temperature sulfurization of carbohydrates. *Organic Geochemistry*, 34, 1129-1144.

Versteegh, G.J.M., Blokker, P., 2004. Resistant macromolecules of extant and fossil microalgae. *Phycological Research*, 52, 325-339.

Versteegh, G.J.M., Blokker, P., Wood, G., Collinson, M.E., Sinninghe Damsté, J.S., de Leeuw, J.W., 2004. An example of oxidative polymerization of unsaturated fatty acids as a preservation pathway for dinoflagellate organic matter. *Organic Geochemistry*, 35, 1129-1139.

Versteegh, G.J.M., Blokker, P., Marshall, C.P., Pross, J., 2007. Macromolecular composition of the dinoflagellate cyst *Thalassiphora pelagica* (Oligocene, SW Germany). *Organic Geochemistry*, 38, 1643-1656.

Versteegh, G.J.M., Blokker, P., Bogus, K., Harding, I.C., Lewis, J., Oltmanns, S., Rochon, A., Zonneveld, K.A.F., in press. Flash pyrolysis and infrared spectroscopy of cultured and sediment derived *Lingulodinium polyedrum* (Dinoflagellata) cyst walls. *Organic Geochemistry.*

Wall, D., Dale, B., 1973. Paleosalinity relationships of dinoflagellates in the late Quaternary of the Black Sea – a summary. *Geosciences, Environment, and Man,* VII, 95-102.

Weijers, J.W.H., Schouten, S., Sluijs, A., Brinkhuis, H., Sinninghe Damsté, J.S., 2007. Warm arctic continents during the Palaeocene-Eocene thermal maximum. *Earth and Planetary Science Letters*, 261, 230-238.

Westerhold, T., Röhl, U., Raffi, I., Fornaciari, E., Monechi, S., Reale, V., Bowles, J., Evans, H.F., 2008. Astronomical calibration of the Paleocene time. *Palaeogeography, Palaeoclimatology, Palaeoecology,* 257, 377-403.

Westerhold, T., Röhl, U., McCarren, H.K., Zachos, J.C., 2009. Latest on the absolute age of the Paleocene-Eocene Thermal Maximum (PETM): New insights from exact stratigraphic position of key ash layers +19 and -17. *Earth and Planetary Science Letters*, 287, 412-419.

Yang, C.Q., Xu, Y., Wang, D., 1996. FT-IR spectroscopy study of the polycarboxylic acids used for paper wet strength improvement. *Industrial and Engineering Chemistry Research*, 35, 4037-4042.

Yaylayan, V.A., Ismail, A.A., 1995. Investigation of the enolization and carbonyl group migration in reducing sugars by FTIR spectroscopy. *Carbohydrate Research*, 276, 253-265.

Yuen, S-N., Choi, S-M., Phillips, D.L., Ma, C-Y., 2009. Raman and FTIR spectroscopic study of carboxymethylated non-starch polysaccharides. *Food Chemistry*, 114, 1091-1098.

Yule, B.L., Roberts, S., Marshall, J.E.A., 2000. The thermal evolution of sporopollenin. *Organic Geochemistry*, 31, 859-870.

Zachos, J.C., Pagani, M., Sloan, L., Thomas, E., Billups, K., 2001. Trends, rhythms, and aberrations in global climate 65 Ma to present. *Science*, 292, 686-693.

Zachos, J.C., Wara, M.W., Bohaty, S., 2003. A transient rise in tropical sea surface temperature during the Paleocene-Eocene Thermal Maximum. *Science*, 302, 1551-1554.

Zachos, J.C., Schouten, S., Bohaty, S., Quattlebaum, T., Sluijs, A., Brinkhuis, H., Gibbs, S.J., Bralower, T.J., 2006. Extreme warming of mid-latitude coastal ocean during the Paleocene-Eocene Thermal Maximum: Inferences from TEX_{86} and isotope data. *Geology*, 34, 737-740.

Zimmermann, B., 2010. Characterization of pollen by vibrational spectroscopy. *Applied Spectroscopy*, 64, 1364-1373.

Zonneveld, K.A.F., Susek, E., 2007. Effects of temperature, light and salinity on cyst production and morphology of *Tuberculodinium vancampoae* (the resting cyst of *Pyrophacus steinii*). *Review of Palaeobotany and Palynology*, 145, 77-88.

Zonneveld, K.A.F., Versteegh, G.J.M., Kasten, S., Eglinton, T.I., Emeis, K.C., Huguet, C., Koch, B.P., de Lange, G.J., de Leeuw, J.W., Middelburg, J.J., Mollenhauer, G., Prahl, F.G., Rethemeyer, J., Wakeham, S.G., 2010. Selective preservation of organic matter in marine environments; processes and impact on the sedimentary record. *Biogeosciences*, 7, 483-511.

Chapter 8

Diagenetic changes in dinosporin composition in Cretaceous age gonyaulacoid dinoflagellate cysts

Kara Bogus[1*], Ian C. Harding[2], Karin A.F. Zonneveld[1,3] and Gerard J.M. Versteegh[3]

[1]*Department of Geosciences, University of Bremen, Klagenfurter Strasse, 28359 Bremen, Germany*
[2]*School of Ocean and Earth Science, National Oceanography Centre, University of Southampton, European Way, Southampton, SO14 3ZH, UK*
[3]*Marum – Center for Marine Environmental Science, University of Bremen, 28334 Bremen, Germany*

**Corresponding author*
Telephone: +49 421 218 65138; Email: ka_bo@uni-bremen.de

Manuscript in preparation

Abstract

Organic-walled dinoflagellate cysts are discrete particles within the kerogen fraction, the largest reservoir of organic carbon in the global sedimentary carbon pool. The structure of kerogen is notoriously difficult to analyze as it is heterogeneous and insoluble in most organic solvents. Since dinoflagellate cysts can be reliably linked to a biological source, it may be possible to utilize these palynomorphs to gain information about kerogen composition and the processes involved in its formation. Dinoflagellate cyst walls are composed of dinosporin, which are non-hydrolyzable biopolymers. The composition of modern gonyaulacoid cysts seems to be carbohydrate-based, so it can be inferred that fossil gonyaulacoid cysts would have also been initially composed of a carbohydrate backbone. However, during diagenesis, the dinosporin biomacromolecule may have undergone chemical transformations that converted it into a geomacromolecule. These chemical alterations may be possible to identify by comparing the modern gonyaulacoid dinosporin composition with older material. In order to investigate this, multiple dinoflagellate cyst species from the Late Hauterivian-Early Barremian (Early Cretaceous) were analyzed with micro-Fourier transform infrared (FTIR) spectroscopy. The results suggest that the general composition of these gonyaulacoid dinoflagellate cysts was originally similar to their modern counterparts, as shown by one excellently preserved specimen of *P. brevicornutum*. The remainder of the dinoflagellate cyst species exhibited similar FTIR spectra. These characteristics include a reduction in the amount of oxygen containing functional groups, and a higher presence of aromatics. These specific alterations indicate considerable diagenetic alteration of the original cyst wall. The analysis of these resistant microfossils has thus provided valuable information on the chemical transformations of some aspects of organic matter as well as preservation processes of biomolecules.

Keywords: biomacromolecule, geomacromolecule, diagenesis, selective preservation, dinoflagellate cyst, dinosporin, Cretaceous

8.1 Introduction

Kerogen is a complex and heterogeneous compound that is notoriously difficult to analyze (e.g. Vandenbroucke and Largeau, 2007 and references therein) but extremely important to understand, as it represents the largest reserve of organic carbon in the global carbon system (Durand, 1980). As discrete and biologically identifiable particles within the kerogen fraction, palynomorphs, or more specifically the resistant biomacromolecules that comprise them, present a unique opportunity to trace diagenetic transformations of organic matter (OM) (de Leeuw et al., 1991; de Leeuw et al., 2006). As kerogen is essentially altered OM, this thus provides information regarding the composition of kerogen. Therefore, elucidating the nature and transformations of resistant biomacromolecules present in palynomorphs can be important for understanding kerogen composition and formation.

These biomacromolecules are generally well preserved in the sedimentary record due to their resistance against chemical and biological attack. However, the mechanisms that provide them with this resistance are not well understood. There are a few pathways that are proposed to contribute to the high preservation potential of these biomacromolecules (e.g. de Leeuw and Largeau, 1993; van Bergen et al., 2004; Versteegh and Blokker, 2004; de Leeuw et al., 2006). They include selective preservation (e.g. Tegelaar et al., 1989; 1991; Derenne et al., 1992; Flaviano et al., 1994; Largeau and Derenne, 1993; Baas et al., 1995), condensation and polymerization (e.g. Stankiewicz et al., 2000; Riboulleau et al., 2001; Versteegh et al., 2004; Gupta et al., 2006; 2007a) and natural sulfurization (e.g. Sinninghe Damsté and de Leeuw, 1990; Kok et al., 2000; Versteegh et al., 2007).

One of the most understudied biomacromolecule in this respect comprises the resting cysts of dinoflagellates. These are an abundant group of microfossils described morphologically since the Triassic that are composed of the non-hydrolyzable biopolymer termed “dinosporin” (Fensome et al., 1993). This refractory compound seems to be unique to dinoflagellates, as it differs from biomacromolecules found in other algae (algaenan) and pollen and spores (sporopollenin) (de Leeuw et al., 2006; Versteegh et al., 2007; Versteegh et al., in press; Chapter 7). The composition of dinosporin has only recently begun to be intensively investigated (e.g. Kokinos et al., 1998; de Leeuw et al., 2006; Versteegh et al., in press; Chapters 6; 7) despite the wide usage of dinoflagellate cysts in paleoenvironmental studies, biostratigraphy, and fossil fuel exploration. With the

exception of Versteegh et al. (2007), no other published study has specifically investigated diagenetic changes in the dinosporin macromolecule, while numerous studies have shown distinct changes attributed to diagenesis in other resistant biomacromolecules (e.g. Hemsley et al., 1994; Baas et al., 1995; Collinson et al., 1998; 2000; Mösle et al., 1997; 1998; 2002; Stankiewicz et al., 1998; Briggs, 1999; Cody and Sághi-Szabó, 1999; Blokker et al., 2000; 2001; Yule et al., 2000; Almendros et al., 2005; Bernard et al., 2007; Gupta et al., 2007a, b; 2009; Cody et al., 2011).

Therefore, in order to provide more information on diagenetic alteration of the dinosporin biomacromolecule and the possible mechanisms that lead to its high preservation potential, we investigated the composition of gonyaulacoid cysts from Otto Gott claypit (Early Cretaceous) in northwestern Germany (e.g. Mutterlose and Harding, 1987). The geochemical analyses were performed using micro-Fourier transform infrared spectroscopy (FTIR). This technique provides qualitative as well as quantitative information on individual specimens and is a common technique used in the investigations of more ancient material (e.g. Marshall et al., 2005; Javaux and Marshall, 2006; Steemans et al., 2010).

8.2 Material

The Otto Gott claypit succession in northwest Germany (Fig. 8.1a) spans the Late Hauterivian - Late Aptian of the Lower Cretaceous (e.g. Below, 1982; Mutterlose, 1983, 1984; Mutterlose and Harding, 1987; Harding, 1990). Two samples, 100/1/79 and 61/1/83 from Late Hauterivian- and Early Barremian-age beds, respectively, were used in the analysis (Fig. 8.1b). Details on the dinoflagellate species present in both 61/1/79 and 100/1/83 can be found in Harding (1990). The Late Hauterivian beds are characterized by evidence of frequent bioturbation and alternate between light and darker grey clay layers (Harding, 1990). The Early Barremian section contains an identifying horizon known as the Hauptblätterton (Mutterlose, 1983), which consists of very fine laminations of coccolith microlenses (pale layers) and black clay (dark layers), and is enriched in dinoflagellate cysts. Overall, the horizon is organic carbon rich and has high carbonate and pyrite contents (Harding, 1990). Due to its fine laminae, the lack of evidence for benthic fauna, and excellent faunal preseration, the sediment-water interface during this

time was likely anoxic (Mutterlose and Harding, 1987). Sample 100/1/79 is specifically from this horizon (C_{org} = 3.87%; Mutterlose and Harding, 1987).

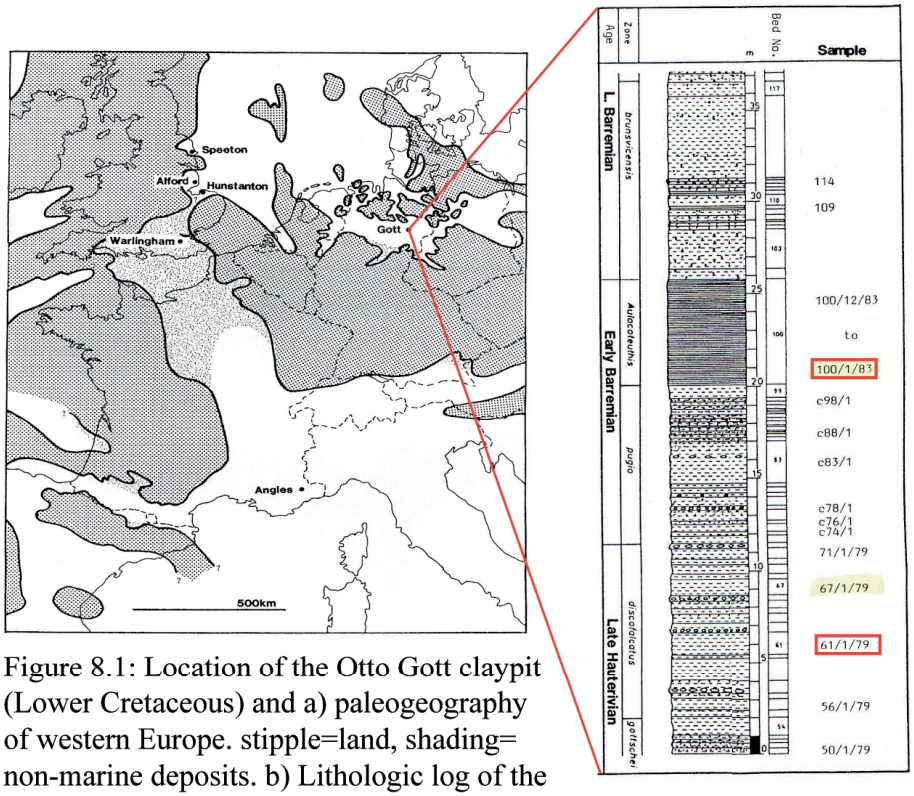

Figure 8.1: Location of the Otto Gott claypit (Lower Cretaceous) and a) paleogeography of western Europe. stipple=land, shading= non-marine deposits. b) Lithologic log of the Gott succession; zones refer to belemnite zonation. Modified from Harding (1990).

8.3 Methods

Approximately 1.5 g of lithified material was treated with HF, neutralized with water and then sieved over a 20 µm precision sieve (Storck Mesh #317). Samples were briefly ultrasonicated (< 20 s) with a tunable ultrasonic probe to remove amorphous organic matter (AOM), and re-sieved. Individual dinoflagellate cysts were identified with a light microscope and then isolated with a Narishige IM5b microinjector attached to a Märzhauser DC3K 168 micromanipulator. Cysts were dried for 24 hrs and then transferred to a NaCl plate for infrared analysis with a Nicolet FT-IR spectrometer coupled to a Nicplan microscope (15x objective). The spectrometer consisted of a Protégé™ 460 optical bench, a MCT- A detector cooled to ≤ -70°C with liquid nitrogen, Ever-Glo source, and a KBr beamsplitter. Two adjustable apertures (upper and lower) were set at a constant area of 15 x 15 µm. Interferograms were obtained in transmission mode with 256 scans at 8 cm^{-1} resolution over a spectral range of 4000-650 cm^{-1}.

Background spectra of the NaCl plate (and air) were recorded after each specimen and all reported spectra depict the sample beam following background subtraction. Each cyst species had several separate specimens analyzed. CO_2 absorptions at 2350 cm^{-1}, a result of the system not being purged, have also been removed. All spectra were manipulated with OMNIC™ 3.1 software in absorbance mode. Assignments of the main IR characteristic group frequencies were primarily based on Colthup et al. (1990) and Coates (2000).

8.4 Results

The cyst species analyzed from sample 61/1/79 were: *Cassiculosphaeridia magna*, *Hystrichosphaeridium* spp., *Pseudoceratium brevicornutum,* and *Pseudoceratium pelliferum.* From the Hauptblätterton sample (100/1/83), the analyzed cyst species included: *Oligosphaeridium complex* and *Pseudoceratium anaphrissum*. Cyst names are after Harding (1990) with the exception of *Pseudoceratium brevicornutum* (Herngreen et al., 2000). All specimens of the same species were similar so representative spectra are shown in Figure 8.2 with absorption assignments listed in Table 8.1.

Table 8.1: FTIR frequency assignments of the analyzed dinocyst species

Absorption (cm^{-1})	Assignment[b]	Strength
900-760	γCH aromatic deformations	m
1060	νC-O	w-s
1370	$\delta CH + \delta C\text{-}CH_3$	m-s
1430-1400	δCH_2	sh
1600	ν C=C aromatic ring	s
1700	ν C=O	w-sh
2860	$\nu^{s}CH_2$	m-w
2930	$\nu^{as}CH_2$	m
≈3400	ν OH	s, br

[b]Based on Colthup et al. (1990) and Coates (2000).

The majority of the species showed similar spectra. The major absorptions present in those species included: a broad band centered at 3400 cm^{-1} (OH stretching), two absorptions at 2930 and 2860 cm^{-1} (CH stretching), a shoulder at 1700 cm^{-1} (C=O stretching), a strong absorption at 1600 cm^{-1} (C=C stretching), a strong absorption between 1360-1400 cm^{-1} (CH bending), a variable strength absorption at about 1060 cm^{-1} (C-O stretching), and deformations at 830 and 760 cm^{-1} (CH out of plane). The only clearly different spectrum originated from *P. brevicornutum*. That species showed a

shifted absorption from the other species at 1640 cm^{-1} and a shoulder at 1730 cm^{-1}. Furthermore, the C-O stretching is stronger and more developed with a shoulder at 1110 cm^{-1} and a second peak at 1160 cm^{-1}.

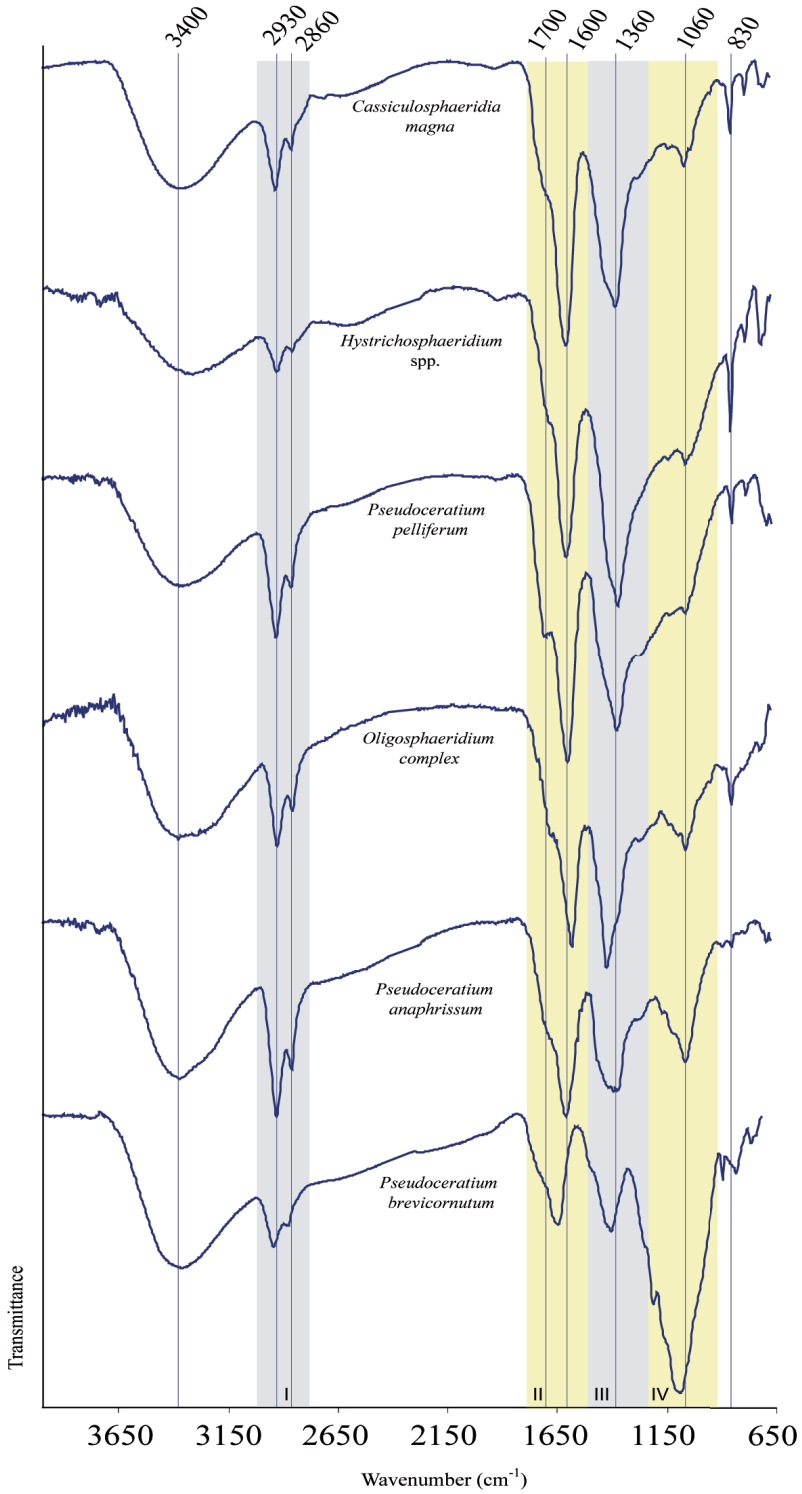

Figure 8.2: FTIR spectra of the Cretaceous dinocyst species analyzed in this study. Shaded areas indicate spectral bands discussed in the text: I) 3010-2775 cm^{-1}, II) 1850-1500 cm^{-1}, III) 1500-1185 cm^{-1}, IV) 1185-760 cm^{-1}.

The relative strengths of the main frequency bands within a species spectrum were calculated by integrating the area between the band limits. This analysis provided a means for the comparison of the size (and concentration) of frequency regions (and therefore functional groups) between the different species. The spectral regions were as follows: (I) 3010-2775 cm^{-1}, (II) 1850-1500 cm^{-1}, (III) 1500-1185 cm^{-1}, (IV) 1185-760 cm^{-1}. Spectral band areas and calculated ratios are depicted in Appendix A9. The comparison of the relative band strength shows no clear pattern between the different species or samples (Fig. 8.3). The only outlier is *P. brevicornutum*, which shows much lower values for I/IV that reflect the stronger CO absorption (Fig. 8.2).

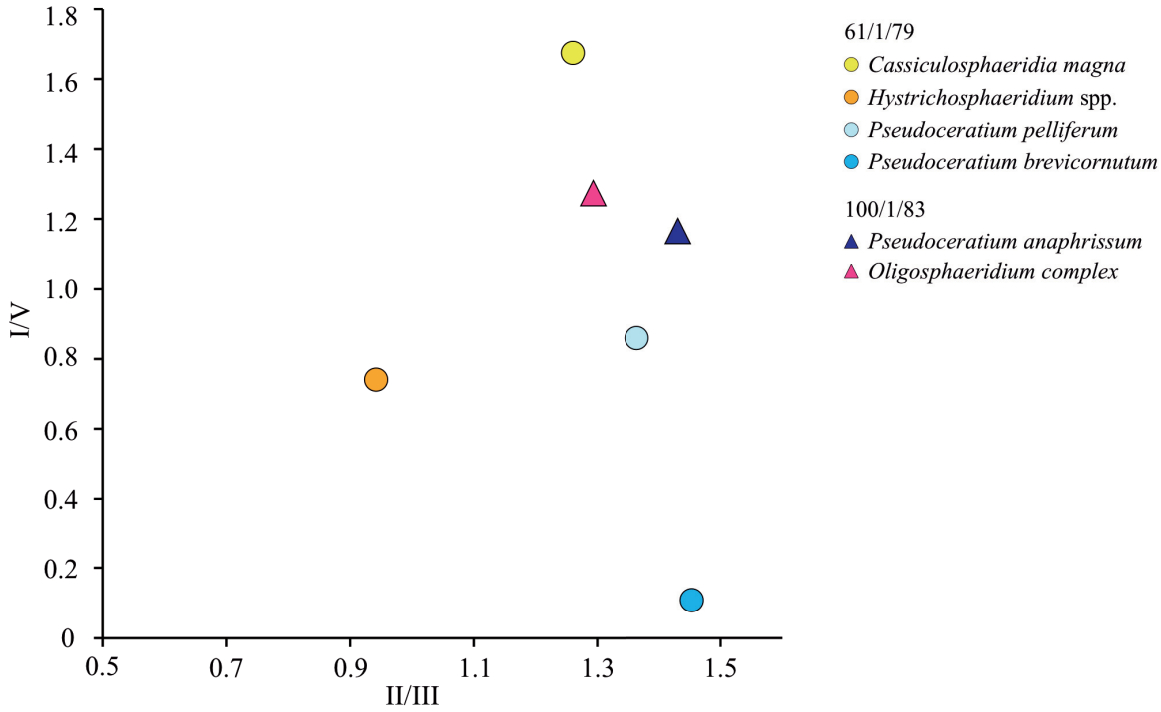

Figure 8.3: Relative band strength comparison between dinoflagellate cysts from the Otto Gott claypit (Lower Cretaceous). I) 3010-2775 cm^{-1}, II) 1850-1500 cm^{-1}, III) 1500-1185 cm^{-1}, IV) 1185-830 cm^{-1}.

8.5 Discussion

8.5.1 FTIR spectral similarities

Despite the fact that the analyzed dinoflagellate cysts are all different species, most of them show fairly similar FTIR spectra. The main similarities consist of the broad OH absorptions, the dominant peak at 1600 cm^{-1}, and the single absorption that corresponds to CH bending at about 1360 cm^{-1}. The peak at 1600 cm^{-1} was previously linked to

carboxymethylate species in other analyzed dinosporins (e.g. Chapters 6 and 7); however, the lack of evidence for C-O bonds in spectral region IV and the distinct shoulder at 1700 cm^{-1} (carbonyl stretching) makes it more likely that the 1600 cm^{-1} absorption is unrelated to carboxyl groups. Instead, it is probably indicative of C=C stretching of aromatic structures (e.g. Steemans et al., 2010). This is supported by the presence of stronger C-H out-of-plane aromatic deformations at about 760 and 830 cm^{-1} (Steemans et al., 2010). The evidence for ether bonds (C-O) is the most variable spectral band (IV) in the species. The strength of the absorptions varies from broad and strong (*P. brevicornutum*) to medium (*Oligosphaeridium complex*, *P. anaphrissum*) to weak (*C. magna*, *Hystrichosphaeridium* spp., *P. pelliferum*).

There are multiple reasons why the majority of the species demonstrate similar FTIR spectra. The first is that the FTIR spectra represent the composition of the original biopolymer, so these species simply have similar dinosporin compositions. This explanation would suggest that dinosporin composition is not species specific, which contrasts with previous research that suggests it is (de Leeuw et al., 2006; Chapter 7). Another, more likely explanation, is that the dinosporins have been diagenetically altered. The reasoning and supporting evidence for all of the dinoflagellate cyst species, except *P. brevicornutum*, representing geomacromolecules are discussed in more detail in the following sections.

8.5.2 The spectrum of P. brevicornutum

The only cyst species that shows a distinct dinosporin composition is *P. brevicornutum* (Fig. 8.2; 8.3). The reason that this species would exhibit such a drastically different dinosporin composition is unclear. This species is thought to be indicative of the Ryazanian and Valanginian (Davey, 2001; Riding et al., 2003), the stage before the Hauterivian, and is quite rare in this sample. However, there was no indication for reworking of material in any of the beds in this succession (Harding, 1990).

The FTIR spectrum for *P. brevicornutum* is very similar to the spectra exhibited by *Lingulodinium machaerophorum* (Versteegh et al., in press), *Spiniferites pachydermus* (Chapter 6), and *Apectodinium paniculatum* (Chapter 7), and all resemble cellulose (Pandey, 1999; see Fig. 8.4). A carbohydrate-based composition has been demonstrated for all of the gonyaulacoid dinoflagellate cyst species (i.e. G-cysts) analyzed thus far in

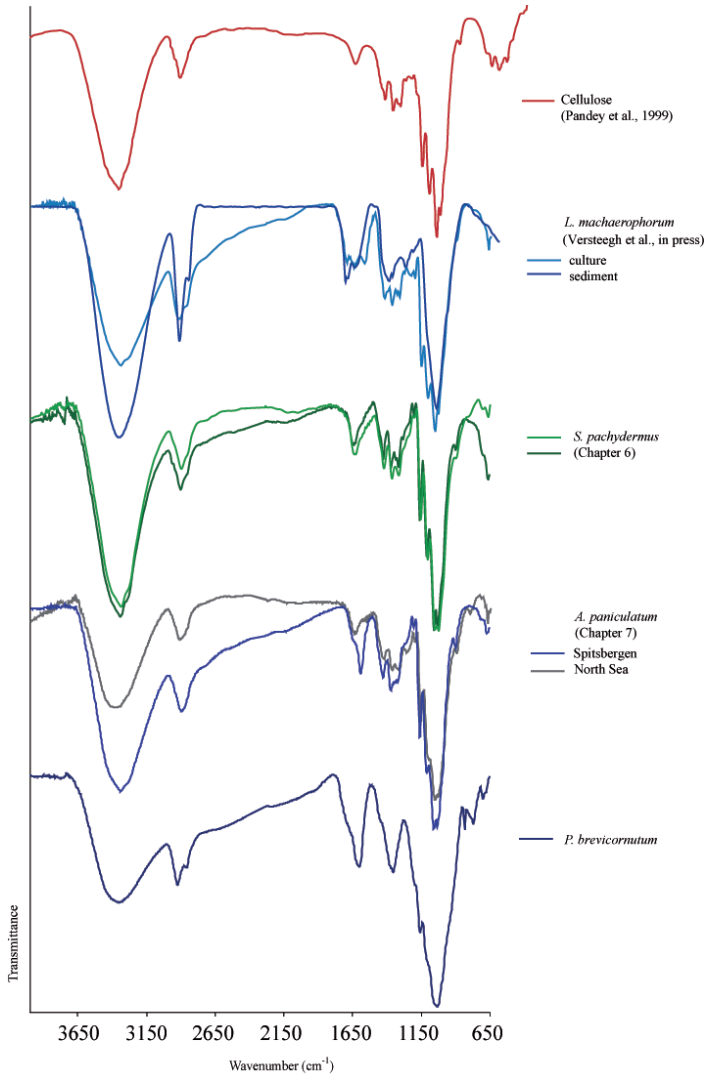

Figure 8.4: Comparsion of the transmittance spectra of extant and extinct gonyaulacoid dinocysts to cellulose (Pandey, 1999).

this work, with some of the cyst species even exhibiting a cellulosic composition (Versteegh et al., in press; Chapter 6; 7). It is therefore likely that the gonyaulacoid dinosporin biomacromolecule is composed of a β-(1→4)-linked polysaccharide, either cellulose or another compound such as xylan (Kačuráková et al., 1999; Kačuráková and Wilson, 2001; Chapter 6).

Therefore, if we assume that the composition of most G-cyst dinosporin is initially carbohydrate-based, does not contain high amounts of aliphatic or aromatic groups and possesses strong C-O absorptions (spectral area IV), then deviations from this composition may be attributed to taphonomic processes.

8.5.3 Evidence of diagenetic overprints

Though the plots of relative band strength show no discrete grouping between the two samples analyzed, the FTIR spectra do show slight, but consistent differences between the samples. These include a stronger aromatic signal in the species of 61/1/79 and a greater amount of C-O bonds in the 100/1/83 species. The Hauptblätterton horizon (100/1/83) was deposited under anoxic conditions, while the Late Hauterivian sample (61/1/79) was deposited during oxygenated bottom water conditions (Harding, 1990). Thus, the

differences between these two samples could reflect a greater degree of early diagenetic alteration of sample 61/1/79 as a result of a longer oxygen exposure time. This would then produce a dinosporin composition that demonstrates a higher degradative influence. Yule et al. (2000) observed an increase in the aromatic content of sporopollenin and a decrease in oxygen-related functional groups with increasing degradation, which is analogous to what is observed in the dinosporin of these cysts.

Another possible result of diagenesis is natural sulfurization. The incorporation of sulfur species into carbohydrates have been shown to increase the preservation potential of biomolecules, including carbohydrates (e.g. Kok et al., 2000; van Dongen et al., 2003). This was shown to occur in anoxic settings (e.g. Kok et al., 2000; Versteegh et al., 2007) and so would really be expected to only affect the dinoflagellate cysts isolated from the Hauptblätterton sample. However, sulfur species are not well resolved in FTIR spectra so it is difficult to determine in the present study the extent to which sulfurization may have altered the dinosporin in the species *Oligosphaeridium complex* and *P. anaphrissum*. However, in comparison to dinoflagellate cyst species (*Thalassiphora pelagica*) that has shown effects of natural sulfurization, the Hauptblätterton dinoflagellate cyst species show some similar trends. These include the loss of oxygen groups, especially C-O bonds and an increase in CH aliphatic stretching (Versteegh et al., 2007). Therefore, we cannot rule out sulfurization as a diagenetic influence.

Overall, this study provides an example for dinoflagellate cysts that morphological preservation does not necessarily indicate good chemical preservation, which concurs with data from plants (Mösle et al., 1998; Collinson et al., 2000; Gupta et al., 2009) and pollen (Yule et al., 2000).

8.6 Conclusions

In this study, we investigated the composition of dinosporin, the resistant biomacromolecule comprising the organic-walled resting cysts of dinoflagellates, in gonyaulacoid cysts isolated from an Early Cretaceous deposit (Otto Gott claypit, Germany). We were primarily interested in whether we could ascribe any portions of the FTIR spectra to diagenetic changes in the dinosporin structure. We based our interpretations of diagenetic changes in the dinosporin structure on previous work that suggests that gonyaulacoid cysts are comprised of a highly cross-linked carbohydrate-

based backbone (Versteegh et al., in press; Chapter 6, 7). One cyst species, *P. brevicornutum*, shows a dinosporin composition that is likely cellulosic and is very similar to modern species of gonyaulacoid dinoflagellate cysts. This is the only species that shows a cellulosic composition, although the reasons for this are unclear.

The other dinoflagellate cyst species, *P. anaphrissum*, *P. pelliferum*, *Oligosphaeridium complex*, *Hystrichosphaeridium* spp., and *C. magna*, show consistent trends in their dinosporin composition. These include a reduction in the relative strength (and thus concentration) of oxygen-containing functional groups and an increase in the aromaticity of the dinosporin macromolecule. This could simply indicate that these species all have similar dinosporin compositions and would be supported by the evidence that multiple species demonstrate a cellulosic composition. However, this is probably not the case. For one, although different G-cyst species have demonstrated a cellulosic dinosporin, this does not seem to be the case in the majority of species. Within one surface sample, Chapter 6 showed inter-species variations in dinosporin content. Furthermore, Chapter 7 showed that dinosporin composition varies within species of the same genus. Thus, it is unlikely that the different species in this study would show the same dinosporin compositions. Additionally, the dinosporin structure of the majority of these analyzed dinoflagellate cysts demonstrate FTIR absorptions that are characteristic of macromolecules that have undergone diagenetic alteration. Therefore, we conclude that the species analyzed here show a geomacromolecular structure of dinosporin; however, the pathway of these alterations still needs to be examined.

Acknowledgements

Shir Akbari (National Oceanography Centre, Southampton, UK) is thanked for assistance with the palynological preparation. Ross Williams (National Oceanography Centre, Southampton, UK) is thanked for technical assistance regarding the FTIR analysis. Financial support was provided by the DFG (Deutsche Forschungsgemeinschaft) as part of the European Graduate College “Proxies in Earth History” (EUROPROX).

References

Almendros, G., Zancada, M.C., González-Vila, F.J., Lesiak, M.A., Álvarez-Ramis, C., 2005. Molecular features of fossil organic matter in remains of the Lower Cretaceous fern *Weichselia reticulata* from Przenosza basement (Poland). *Organic Geochemistry*, 36, 1108-1115.

Baas, M., Brigg, D.E.G., van Heemst, J.D.H., Kear, A.J., de Leeuw, J.W., 1995. Selective preservation of chitin during the decay of shrimp. *Gechimica et Cosmochimica Acta*, 59, 945-951.

Below, R., 1982. Zur Kenntnis der Dinoflagellaten-Zysten- Populationen im Ober Apt der Tongrube "Otto Gott" in Sarstedt/Norddeutschland. *Neues Jahrbuch für Geologie und Paläontologie Abhandlungen*, 164, 339-363.

Blokker, P., Schouten, S., de Leeuw J.W., Sinninghe Damsté, J.S., 2000. A comparative study of fossil and extant algaenans using ruthenium tetroxide degradation. *Geochimica et Cosmochimica Acta*, 64, 2055-2065.

Blokker, P., van Bergen, P., Pancost, R., Collinson, M.E., de Leeuw, J.W., Sinninghe Damsté, J.S., 2001. The chemical structure of *Gloeocapsomorpha prisca* microfossils: implications for their origin. *Geochimica et Cosmochimica Acta*, 65, 885-900.

Briggs, D.E.G., 1999. Molecular taphonomy of animal and plant cuticles: Selective preservation and diagenesis. *Royal Society of London Philosophical Transactions*, 354, 7-17.

Coates, J., 2000. Interpretation of Infrared Spectra, A Practical Approach. In: Meyers, R.A. (Ed.), *Encyclopedia of Analytical Chemistry*. John Wiley and Sons Ltd., pp. 10815-10837.

Cody, G.D., Sághi-Szabó, G., 1999. Calculation of the ^{13}C NMR chemical shift of ether linkages in lignin derived geopolymers: constraints on the preservation of lignin primary structure with diagenesis. *Geochimica et Cosmochimica Acta*, 63, 193-205.

Cody, G.D., Gupta, N.S., Briggs, D.E.G., Kilcoyne, A.L.D., Summons, R.E., Kenig, F., Plotnick, R.E., Scott, A.C., 2011. Molecular signature of chitin-protein complex in Paleozoic arthropods. *Geology*, 39: 255-258.

Collinson, M.E., Mösle, B.M., Finch, P., Scott, A.C., Wilson, R., 1998. The preservation of plant cuticle in the fossil record: A chemical and microscopical investigation. *Ancient Biomolecules*, 2, 251-265.

Collinson, M.E., Finch, P.F., Mösle, B., Wilson, R., Scott, A.C., 2000. Preservations of plant cuticles. *Acta Palaeobot. Supplement*, 2, 629-632.

Colthup, N.B., Daly, L.H., Wiberly, S.E., 1990. *Introduction to Infrared and Ramna Spectroscopy*. Academic Press Limited, London, 282 pp.

Davey, R.J., 2001. A summary of the palynology of the lower Hauterivian (Lower Cretaceous) from Speeton, east England. *Neues Jahrbuch für Geologie und Paläontologie, Abhandlungen,* 219, 83-93.

de Leeuw, J.W., Largeau, C., 1993. A review of macromolecular organic compounds that comprise living organisms and their role in kerogen, coal and petroleum formation. In: Engel, M.H., Macko, S.A., (Eds.), *Organic Geochemistry: principles and applications.* Plenum Publishing Corp., New York. pp. 23-72.

de Leeuw, J.W., van Bergen, P.F., van Aarssen, B.G.K., Gatellier, J.-P.L.A., Sinninghe Damsté, J.S., Collinson, M.E., 1991. Resistant biomacromolecules as major contributors to kerogen, *Philosophical Transactions of the Royal Society London B*, 333, 329-337.

de Leeuw, J.W., Versteegh, G.J.M., van Bergen, P.F., 2006. Biomacromolecules of algae and plants and their fossil analogues. *Plant Ecology*, 182, 209-233.

Derenne, S., Le Berre, F., Largeau, C., Hatcher, P., Connan, J., Raynaud, J.F., 1992. Formation of ultralaminae in marine kerogens via selective preservation of thin resistant outer walls of microalgae. *Organic Geochemistry*, 19, 345-350

Durand, B., 1980. Sedimentary organic matter and kerogen: Definition and quantitative importance of kerogen. In: Durand, B. (Ed.), *Kerogen, Insoluble Organic Matter from Sedimentary Rocks.* Editions Technip, Paris. pp 13-34.

Fensome, R.A., Taylor, F.J.R., Norris, G., Sarjeant, W.A.S., Wharton, D.I., Williams, G.L., 1993. A classification of fossil and living dinoflagellates. *Micropaleontology Press Special Paper*, 7, 351 pp.

Flaviano, C., Le Berre, F., Derenne, S., Largeau, C., Connan, J., 1994. First indications of the formation of kerogen amorphous fractions by selective preservation. Role of non-hydrolysable macromolecular constituents of Eubacterial cell walls. *Organic Geochemistry*, 22, 759-771.

Gupta, N.S., Collinson, M.E., Briggs, D.E.G., Evershed, R.P., Pancost, R., 2006. Reinvestigation of the occurrence of cutan in plants: implications for the leaf fossil record. *Paleobiology*, 32, 432-449.

Gupta, N.S., Briggs, D.E.G., Collinson, M.E., Evershed, R.P., Michels, F., Jack, K.S., Pancost, R.D., 2007a. Evidence for the in situ polymerisation of labile aliphatic organic compounds during the preservation of fossil leaves: implications for organic matter preservation. *Organic Geochemistry*, 38, 499-522.

Gupta, N.S., Michels, R., Briggs, D.E.G., Collinson, M.E., Evershed, R.P., Pancost, R.D., 2007b. Experimental evidence for fomation of geomacromolecules from plant leaf lipids. *Organic Geochemistry*, 38, 28-36.

Gupta, N.S., Yang, H., Leng, Q., Briggs, D.E.G., Cody, G.D., Summons, R.E., 2009. Diagenesis of plant biopolymers: Decay and macromolecular preservation of *Metasequoia*. *Organic Geochemistry*, 40, 802-809.

Harding, I.C., 1990. A dinocyst calibration of the European Boreal Barremian. *Palaeontographica Abteilung B*, 218, 1-76.

Hemsley, A.R., Barrie, P.J., Scott, A.C., Chaloner, W.G., 1994. Studies of fossil and modern spore and pollen wall biomacromolecules using ^{13}C solid state NMR. In: Eglinton, G., Kay, R.L.F. (Eds.), *Biomolecular Palaeontology*, NERC Special Publications, 94, 15-19.

Herngreen, G.F.W., Kerstholt, S.J., Munsterman, D.K., 2000. Callovian-Ryazanian (Upper Jurassic) palynostratigraphy of the Central North Sea Graben and Vlieland Basin, The Netherlands. *Mededelingen Nederlands Instituut voor Toegepaste Geowetenshappen TNO*, 63, 99 pp.

Javaux, E.J., Marshall, C.P., 2006. A new approach in deciphering early protist paleobiology and evolution: combined microscopy and microchemistry of single Proterozoic acritarchs. *Review of Palaeobotany and Palynology*, 139, 1-15.

Kačuráková, M., Wilson, R.H., 2001. Developments in mid-infrared FT-IR spectroscopy of selected carbohydrates. *Carbohydrate Polymers*, 44, 291-303.

Kačuráková, M., Wellner, N., Ebringerová, A., Hromádková, Z., Wilson, R.H., Belton, P.S., 1999. Characterisation of xylan-type polysaccharides and associated cell wall components by FT-IR and FT-Raman spectroscopies. *Food Hydrocolloids*, 13, 35-41.

Kok, M.D., Schouten, S., Sinninghe Damsté, J.S., 2000. Formation of insoluble, nonhydrolyzable, sulfur-rich macromolecules via incorporation of inorganic sulfur species into algal carbohydrates. *Geochimica et Cosmochimica Acta*, 64, 2689-2699.

Kokinos, J.P., Eglinton, T.I., Goñi, M.A., Boon, J.J., Martoglio P.A., Anderson, D.M., 1998. Characterization of a highly resistant biomacromolecular material in the cell wall of a marine dinoflagellate resting cyst. *Organic Geochemistry*, 28, 265-288.

Largeau, C., Derenne, S., 1993. Relative efficiency of the selective preservation and degradation recondensation pathways in kerogen formation. Source and environmental influence on their contributions to type I and II kerogens. *Organic Geochemistry*, 20, 611-615.

Marshall, C.P., Javaux, E.J., Knoll, A.H., Walter, M.R., 2005. Combined micro-Fourier transform infrared (FTIR) spectroscopy and micro-Raman spectroscopy of Proterozoic acritarchs: a new approach to palaeobiology. *Precambrian Research*, 138, 208-224.

Mösle, B., Finch, P., Collinson, M.E., Scott, A.C., 1997. Comparison of modern and fossil plant cuticles by selective chemical extraction monitored by flash pyrolysis-gas chromatography-mass spectrometry and electron microscopy. *Journal of Analytical and Applied Pyrolysis*, 40-41, 585-597.

Mösle, B., Collinson, M.E., Finch, P., Stankiewicz, B.A., Scott A.C., Wilson, R., 1998. Factors influencing the preservation of plant cuticles: a comparison of morphology and chemical composition of modern and fossil examples. *Organic Geochemistry*, 29, 1369-1380.

Mösle, B., Collinson, M.E., Scott, A.C., Finch, P., 2002. Chemosystematic and microstructural investigations on Carboniferous seed plant cuticles from four North American localities. *Review of Palaeobotany and Palynology*, 120, 41-52.

Mutterlose, J., 1983. Phylogenie und Biostratigraphie der Unterfamilie Oxyteuthinae (Belemnitida) aus dem Barrême (Unter-Kreide) NW-Europas. *Palaeontographica Abteilung A*, 180, 1-90.

Mutterlose, J., Harding, I., 1987. Phytoplankton from the anoxic sediments of the Barremian (Lower Cretaceous) of North-West-Germany. *Abhandlungen der Geologischen Bundesanstalt-A*, 39, 177-215.

Pandey, K.K., 1999. A study of chemical structure of soft and hardwood and wood polymers by FTIR spectroscopy. *Journal of Applied Polymer Science*, 71, 1969-1975.

Riboulleau, A., Derenne, S., Largeau, C., Baudin, F., 2001. Origin of contrasting features and preservation pathways in kerogens from the Kashpir oil shales (Upper Jurassic, Russian Platform). *Organic Geochemistry*, 32, 647-665.

Riding, J.B., Rose, J., Booth, S.J., 2003. Allochthonous and indigenous palynomorphs from the Devensian of the Warham Borehole, Stiffkey, north Norfolk, England; evidence for sediment provenance. *Proceedings of the Yorkshire Geological Society*, 54, 223-235.

Sinninghe Damsté, J.S., de Leeuw, J.W., 1990. Organically-bound sulphur in the geosphere: state of the art and future research. *Organic Geochemistry*, 16, 1077-1101.

Stankiewicz, B.A., Mastalerz, M., Hof, C.H.J., Bierstedt, A., Flannery, M.B., Briggs, D.E.G., Evershed, R.P., 1998. Biodegradation of the chitin-protein complex in crustacean cuticle. *Organic Geochemistry*, 28, 67-76.

Stankiewicz, B.A., Briggs, D.E.G., Michels, R., Collinson, M.E., Flannery, M.B., Evershed, R.P., 2000. Alternative origin of aliphatic polymer in kerogen. *Geology*, 28, 559-562.

Steemans, P., Lepot, K., Marshall, C.P., Le Hérissé, A., Javaux, E.J., 2010. FTIR characterisation of the chemical composition of Silurian miospores (cryptospores and trilete spores) from Gotland, Sweden. *Review of Palaeobotany and Palynology*, 162, 577-590.

Tegelaar, E.W., de Leeuw, J.W., Derenne, S., Largeau, C., 1989. A reappraisal of kerogen formation. *Geochimica et Cosmochimica Acta*, 53, 3103-3106.

Tegelaar, E.W., Kerp, H., Visscher, H., Schenk, P.A., de Leeuw, J.W., 1991. Bias of the paleobotanical record as a consequence of variations in the chemical composition of higher vascular plant cuticles. *Paleobiology*, 17, 133-144.

Vandenbroucke, M., Largeau, C, 2007. Kerogen origin, evolution and structure. *Organic Geochemistry*, 38, 719-833.

van Bergen, P.F., Blokker, P., Collinson, M.E., Sinninghe Damsté, J.S., de Leeuw, J.W., 2004. Structural biomacromolecules in plants: what can be learnt from the fossil record? In: Hemsley, A.R., Poole, I., (Eds.), *Evolution of Plant Physiology*. Elsevier, Amsterdam, pp. 133-154.

van Dongen, B.E., Schouten, S., Baas, M., Geenevasen, J.A.J., Sinninghe Damsté, J.S., 2003. An experimental study of the low-temperature sulfurization of carbohydrates. *Organic Geochemistry*, 34, 1129-1144.

Versteegh, G.J.M., Blokker, P., 2004. Resistant macromolecules of extant and fossil microalgae. *Phycological Research*, 52, 325-339.

Versteegh, G.J.M., Blokker, P., Wood, G., Collinson, M.E., Sinninghe Damsté, J.S., de Leeuw, J.W., 2004. An example of oxidative polymerization of unsaturated fatty acids as a preservation pathway for dinoflagellate organic matter. *Organic Geochemistry*, 35, 1129-1139.

Versteegh, G.J.M., Blokker, P., Marshall, C.P., Pross, J., 2007. Macromolecular composition of the dinoflagellate cyst *Thalassiphora pelagica* (Oligocene, SW Germany). *Organic Geochemistry*, 38, 1643-1656.

Versteegh, G.J.M., Blokker, P., Bogus, K., Harding, I.C., Lewis, J., Oltmanns, S., Rochon, A., Zonneveld, K.A.F., in press. Flash pyrolysis and infrared spectroscopy of cultured and sediment derived *Lingulodinium polyedrum* (Dinoflagellata) cyst walls. *Organic Geochemistry.*

Yule, B.L., Roberts, S., Marshall, J.E.A., 2000. The thermal evolution of sporopollenin. *Organic Geochemistry*, 31, 859-870.

Chapter 9

Conclusions and Outlook

The studies presented and discussed in this thesis represent the first data systematically evaluating the chemistry of dinocyst walls. Very little was previously known about the composition of dinosporin, which is the refractory biopolymer that comprises dinocysts. Overall, the cyst species analyzed in this work exhibited cyst wall chemistries that were dissimilar to other resistant biomacromolecules (Chapter 7), which clearly suggests that dinosporin is a unique biopolymer. Furthermore, the results indicate that the composition of the dinosporin macromolecule is dependent on numerous factors, including the ecology of the dinoflagellate producing the cyst (Chapter 6), environmental conditions at the time of cyst formation (Chapter 7), and taphonomic processes (Chapter 8).

All of these sources of variability influence the cyst wall chemistry so that is quite likely taxon specific. It is this species-specific dinosporin composition that may explain the selective preservation of dinocyst species. This differential preservation potential has implications for paleoenvironmental investigations, as was shown in Chapter 5. The rapid effect of selective aerobic degradation on dinocyst signals, and other OM-based proxies, can lead to misinterpretations of the sedimentary proxy record if these changing redox conditions are not considered during interpretation of proxy signals. Furthermore, the selective preservation of dinocysts can bias the sedimentary record towards those cysts that are either composed of a more resistant dinosporin or have undergone chemical transformations that converted the biomacromolecule into a more refractory form. The nature of these chemical transformations is an important component towards understanding the composition and formation of marine kerogen, the largest global sedimentary organic carbon pool. The taphonomic changes that could be seen in the cyst wall chemistry of the Lower Cretaceous dinocysts (Chapter 8) may be another piece of the puzzle in this regard.

Of the two manuscripts that are currently in preparation (Chapters 6, 8), there are some specific suggestions that could strengthen the micro-FTIR based interpretations. For Chapter 6, a Fourier self-deconvolution would allow for greater specificity in pinpointing the different bond types present in the autotrophic and, especially, the

heterotrophic taxa. For Chapter 8, micro-Raman spectroscopy may be a feasible and relatively quick analysis that can be performed. Micro-Raman spectroscopy would allow for the determination of the degree of aromaticity as well as the thermal maturity of the dinosporin macromolecule. Micro-FTIR and micro-Raman have been shown to be powerful characterization tools when used in conjunction for the analysis of acritarchs (e.g. Marshall et al., 2005; Javaux and Marshall, 2006) as well as general kerogen typing (e.g. Landais et al., 1993).

The results of this thesis also illustrate important questions that remain regarding the nature of dinosporin, so further studies are therefore recommended. The ecology of dinoflagellates was shown to affect the dinosporin composition, specifically in that the composition of peridinioid (representing heterotrophic taxa) and gonyaulacoid (representing photoautotrophic taxa) cysts differs (Chapter 6). This likely reflects the group ecology and so may be used to predict the paleoecology of extinct taxa. However, many dinoflagellate taxa are actually mixotrophs, in that their life strategy combines both photoautotrophy and heterotrophy (Stoecker et al., 1999), so it would be interesting to investigate to what extent mixotrophy may affect cyst wall chemistry. Second, it appears that environmental variability, such as fluctuating salinity and/or temperature, may play a pivotal role in the composition of dinosporin (Chapter 7). While this was speculated to result from an intrinsic feature of cyst formation processes as a response to environmental stress, it is impossible to test with the investigated genus, *Apectodinium*, as it is an extinct taxon. Therefore, these findings should to be evaluated in extant species. The previous points that arose based on the studies in Chapters 6 and 7 lead to three specific questions that have potential as avenues of investigation:

(1) What is the effect on dinosporin composition with varying salinity, temperature and pH in cultured dinoflagellates?

(2) What is the effect of mixotrophy on the dinosporin composition in cultured dinoflagellates? Do they show an intermediate dinosporin composition between autotrophic or heterotrophic, or does it reflect the primary strategy at the time that cyst formation is induced?

(3) Can we observe different dinosporin compositions as a result of seasonal factors through measurements of cysts

collected from sediment traps? As in, is there a changing environmental signal that may alter the cyst chemistry throughout the year?

Finally, diagenetic processes were shown to alter the dinosporin macromolecular composition (Chapter 8), which effectively converted the dinosporin biomacromolecule into a geomacromolecule. If it would be possible to trace these diagenetic changes in one (or more) dinocyst species over time, through both degradation experiments as well as investigations of dinocysts within the same lithologic succession, this may provide us with a powerful tool to elucidate changes in kerogen composition. Thus, the final questions:

(4) Can we induce diagenetic composition changes of dinosporin in degradation experiments from cultured material?

(5) Can we observe progressive diagenesis of the dinosporin biomacromolecule by tracing a single species through time?

Much still remains unknown with regards to dinosporin, so additional research into the nature of dinosporin has potential implications for many fields, including paleoclimatology, paleoceanography, palynology, biostratigraphy, and the petroleum industry. This thesis merely represents a first step in using a specific proxy, dinocysts, in an investigation that links biology, palynology and geochemistry in an attempt to provide more information regarding fundamental questions of the global carbon cycle and climatic changes through Earth's history.

References

Javaux, E.J., Marshall, C.P., 2006. A new approach in deciphering early protist paleobiology and evolution: combined microscopy and microchemistry of single Proterozoic acritarchs. *Review of Palaeobotany and Palynology*, 139, 1-15.

Landais, P., Rochdi, A., Largeau, C., Derenne, S., 1993. Chemical characterization of torbanites by transmission micro-FTIR spectroscopy: origin and extent of compositional heterogeneities. *Geochimica et Cosmochimica Acta*, 57, 2529-2539.

Marshall, C.P., Javaux, E.J., Knoll, A.H., Walter, M.R., 2005. Combined micro-Fourier transform infrared (FTIR) spectroscopy and micro-Raman spectroscopy of Proterozoic acritarchs: a new approach to palaeobiology. *Precambrian Research*, 138, 208-224.

Stoecker, D.K., 1999. Mixotrophy among Dinoflagellates. *Journal of Eukaryotic Microbiology*, 46, 397-401.

Appendix A1

Infrared spectroscopy, flash pyrolysis, thermally assisted hydrolysis and methylation (THM) in the presence of tetramethylammonium hydroxide (TMAH) of cultured and sediment-derived *Lingulodinium polyedrum* (Dinoflagellata) cyst walls

Gerard J.M. Versteegh[a,b*], Peter Blokker[c], Kara Bogus[b] Ian Harding[d] Jane Lewis[e], Sven Oltmanns[f] André Rochon[e,1], Karin Zonneveld [a,b]

[a] *Organic Geochemistry Group, MARUM Center for Marine Environmental Sciences University of Bremen, D-28359 Bremen, Germany*
[b] *Fachbereich 5 Geowissenschaften, Universität Bremen, PO Box 330440 D-28334 Bremen, Germany*
[c] *Water R&D Europe, Nalco Europe B.V., Ir. G. Tjalmaweg 1, 2342 BV Oegstgeest, The Netherlands*
[d] *School of Ocean and Earth Science, National Oceanography Centre Southampton, University of Southampton, European Way, Southampton, SO14 3ZH, UK*
[e] *School of Biosciences, University of Westminster, 115 New Cavendish Street, London W1W 6UW, United Kingdom*
[f] *Bruker Optik GmbH, Fahrenheitstraße 4, D-28359, Bremen Germany*

[*] *Corresponding author: Tel.: +49 421 218 65709.*
E-mail address: versteegh@uni-bremen.de (G.J.M. Versteegh).

[1] *Present address: Institut des sciences de la mer de Rimouski, Université du Québec à Rimouski, 310 allée des Ursulines, G5L 3A1 Rimouski, Québec, Canada*

Accepted in *Organic Geochemistry*

The macromolecular composition of dinoflagellate cyst walls is poorly understood and is usually referred to as 'sporopollenin-like'. Our micro-Fourier transform infra red (micro-FTIR) analyses on chemically untreated sediment-derived and enzymatically and chemically purified culture-derived L. polyedrum cyst walls suggest an aliphatic polymer rich in C-O bonds and relatively poor in CH_2 and CH_3 groups and which is much closer to cellulose than to sporopollenin or algaenan. This is in agreement with flash pyrolysis gas-chromatography mass-spectrometry (py-GC/MS), with and without tetramethylammonium hydroxide (TMAH) on purified culture derived cyst walls, which indicates an oxygen-rich polymer without normal or isoprenoid carbon chains. Our results support a strongly cross-linked carbohydrate-based polymer and as such confirm earlier hypotheses that the cysts are unlike algaenan or sporopollenin and contrast with the suggestion that the cyst walls are highly aromatic and contain tocopherol as a major monomeric building block.

Keywords: dinosporin, dinoflagellate, algal culture, pyrolysis, macromolecule, FTIR, cyst wall, sediment

Appendix A2

Diagenetic barium cycling in Black Sea sediments – A case study for anoxic marine environments

Susann Henkel[1*], José M. Mogollón[1], Kerstin Nöthen[1], Christine Franke[2], Kara Bogus[3], Eric Robin[4], André Bahr[5], Martin Blumenberg[6], Thomas Pape[7], Richard Seifert[8], Christian März[9], Gert J. de Lange[10], and Sabine Kasten[1]

[1]*Alfred Wegener Institute for Polar and Marine Research, Am Handelshafen 12, 27570 Bremerhaven, Germany.*
[2]*Centre des Géosciences, Mines ParisTech, 35, rue Saint Honoré, 77305 Fontainebleau Cedex, France.*
[3]*Department of Geosciences, University of Bremen, Klagenfurter Str., 28359 Bremen, Germany.*
[4]*Laboratoire des Sciences du Climat et de l'Environnement, (CEA/CNRS/UVSQ), Avenue de la Terrasse, Bâtiment 12, 91198 Gif-sur-Yvette Cedex, France.*
[5]*Institute of Geoscience, Goethe-University Frankfurt, Altenhöferallee 1, 60438 Frankfurt am Main, Germany.*
[6]*Geoscience Center, Geobiology Group, Georg-August-University Göttingen, Goldschmidtstr. 3, 37077 Göttingen, Germany.*
[7]*MARUM – Center for Marine Environmental Sciences and Department of Geosciences, University of Bremen, Klagenfurter Str., P.O. Box 330440, D-28334 Bremen, Germany.*
[8]*Institute of Biogeochemistry and Marine Chemistry, University of Hamburg, Bundesstr. 55, 20146 Hamburg, Germany.*
[9]*School of Civil Engineering and Geosciences (CEG), Newcastle University, Newcastle upon Tyne, NE1 7RU, United Kingdom.*
[10]*Department of Earth Sciences - Geochemistry, Utrecht University, P.O. Box 80.021, 3508 TA Utrecht, The Netherlands.*
**corresponding author, current address: Institute of Geology and Mineralogy, Zülpicher Str. 49a, 50674 Cologne, Germany; susann.henkel@uni-koeln.de*

Under revision for publication in *Geochimica et Cosmochimica Acta*

High-resolution sedimentary records of major and minor elements (Al, Ba, Ca, Sr, Ti), total organic carbon (TOC), and pore water profiles (SO_4^{2-}, CH_4, Ca^{2+}, Ba^{2+}, Mg^{2+}, alkalinity) were obtained for two gravity cores (755 and 214) from the northwestern Black Sea (501 and 1686 m water depth). The records were examined to gain insight into the cycling of Ba in anoxic marine sediments characterized by a shallow sulfate-methane transition (SMT). The Ba records are strongly overprinted by diagenetic barite ($BaSO_4$) precipitation and remobilization; authigenic Ba enrichments were found at both sites at and slightly above the current SMT. Transport reaction modeling was applied to simulate the downward migration of the SMT in response to the increase in bottom water SO_4^{2-} concentrations after the Holocene seawater intrusion into the Black Sea. Based on this, sediment intervals affected by diagenetic Ba redistribution were identified. At site 214, a sapropel unit is located below the SMT favoring microbial methanogenesis. An increase in the formation rate of microbial methane, as evidenced by $\delta^{13}C_{CH4}$, initiated an upward migration of the SMT in the recent past. We emphasize that apart from being controlled by the presence/absence of sulfate, diagenetic $BaSO_4$ dissolution and precipitation are indirectly controlled by anoxia enhancing TOC preservation and stimulating higher rates of (microbial) methanogenesis. Elevated methane formation rates shift the SMT closer to the sediment surface and provoke diagenetic barite redistribution at shallow depth. The excess Ba (Ba_{xs}; non-detrital fraction) records differ significantly from those known for the Mediterranean Sea. In the latter, barite-Ba appears to be a good tracer for initial productivity and TOC fluxes. In the Black Sea, in contrast, the intense overprint of Ba and Ba_{xs} hardly allows drawing conclusions with respect to primary productivity. These findings have implications for other modern and ancient anoxic basins, e.g., sections covering the Oceanic Anoxic Events for which the Ba-proxy is frequently used. Our study also demonstrates the limitations concerning the use of Ba_{xs} as a tracer for SMT migrations: due to high sedimentation rates at the investigated sites, diagenetic barite fronts are buried below the shallow SMT within a relatively short period. If at all, "relict" barite fronts would therefore be preserved only for a few thousands of years.

Appendix A3

Appendix A3: Lipid biomarker concentrations as measured by GC-MS used in the calculation of proxy ratios in Chapter 5.

Compound*	GeoB 12312 Anoxic	GeoB 12321 Suboxic	GeoB 12331 Oxic	GeoB 12326-13 Anoxic	GeoB 12326-9 Suboxic	GeoB 12326-7 Oxic	GeoB 12328-6 Anoxic	GeoB 12328-2 Anoxic	GeoB 12328-4 Anoxic
Even long chain n alcohols (ΣC_{24-28})	173.1	303.9	72.2	243.6	246.7	233.6	241.4	159.3	384
Odd long chain n alkanes (ΣC_{27-31})	123.5	286.2	101.1	122.2	134	192.3	112.5	57.9	284.4
C_{30} 1,15-diol	125.5	123.4	46	206.9	145.9	44.9	301.7	223.2	201.8
C_{32} 1,15-diol	180	268.3	n.d.	198.7	n.d.	n.d.	24.3	136.8	n.d
C_{30} 1,15-keto-ol	21.3	39.8	52	73.2	87.4	30.7	117.7	78.8	68.8
C_{32} 1,15-keto-ol	29.8	76.2	19.5	73.9	n.d.	20.9	n.d.	49.3	n.d.
Phytol	1321.7	1392.3	477.4	1782.5	1947.4	355.9	2059.3	2419.6	1354
Phytane	216	112.8	34.6	346.3	123.6	38.2	569.8	460.8	199.9
Pristane	150.2	217.6	134.4	570	363.2	52.3	2037.3	1050.9	432.8
Total sterols (ΣC_{27-30})	9900.3	7031	1882.4	4117.34	6243.97	7796.6	9512.9	5742.13	13563.9
Cholesterol	1945.9	1286.9	287.1	1282.4	1240.6	877.2	783.8	1073.2	1179.4
Cholestanol	449.6	304.5	236.1	476.5	602	661.9	426.3	655.6	466.2
Dinosterol	1995.5	905	317	789.7	513.9	342	1105.7	1067.5	980.5
Dinostanol	131.7	n.d.	n.d.	n.d.	n.d.	n.d.	n.d.	n.d.	n.d.
Dinostanone	16.4	25.3	24.6	27.2	59.1	22.7	191.1	86.7	56.3
Dinosterone	19.2	16.6	28.1	n.d.	47.1	65.7	n.d.	n.d.	n.d.
Dinosterane	n.d.	3.9	23	n.d.	n.d.	1.5	5.2	4.3	7.4

* All reported values are in ng g sediment^{-1}, normalized abundance to a standard (see text) and have not been corrected for compound specific response factors.

Appendix A4

Appendix A4: GDGT peak areas and distribution (%) used in the calculation of TEX_{86} indices in Chapter 5.

	OMZ transect			Below OMZ seep			OMZ seep		
	OMZ-anoxic (anoxic)	OMZ-suboxic (suboxic)	OMZ-oxic (oxic)	below OMZ-seep 1 (anoxic)	below OMZ-seep 2 (suboxic)	below OMZ-seep 3 (oxic)	OMZ-seep 1 (anoxic)	OMZ-seep 2 (anoxic)	OMZ-seep 3 (anoxic)
GDGT peak areas									
GDGT-0	3537659115	646466944	287373213	96387435	96387435	300390774	641392516	650377801	444243057
GDGT-1	1403675844	219408981	157159514	37611649	37611649	125094161	367976047	358778708	237579676
GDGT-2	2052767023	321549319	230836278	52242107	52242107	137712830	492488974	485423709	379931095
GDGT-3	523460998	125463678	63630757	13768514	13768514	31808931	119225241	113036605	99260914
Crenarchaeol	11342322473	2132374476	1019610762	294990212	294990212	842971451	2377313797	2359268582	2285539610
Crenarchaeol iso.	1656878913	220565762	99945007	54905802	54905802	102573230	313690101	267210214	252901252
GDGT relative abundance									
GDGT-0	17.24	17.63	15.46	17.53	16.42	19.50	14.87	15.36	12.01
GDGT-1	6.84	5.99	8.46	6.84	6.41	8.12	8.53	8.47	6.42
GDGT-2	10.01	8.77	12.42	9.50	7.94	8.94	11.42	11.46	10.27
GDGT-3	2.55	3.42	3.42	2.50	2.81	2.06	2.76	2.67	2.68
Crenarchaeol	55.28	58.17	54.86	53.64	60.03	54.72	55.13	55.72	61.78
Crenarchaeol iso.	8.08	6.02	5.38	9.98	6.40	6.66	7.27	6.31	6.84

APPENDIX A5

Appendix A5: Dinocyst counts from Arabian Sea surface sediments as described in Chapter 5.

Sample	**GeoB 12312**		**GeoB 12321**		**GeoB 12331**		**GeoB 12326-13**		**GeoB 12326-9**		**GeoB 12326-7**		**GeoB 12328-6**		**GeoB 12328-2**		**GeoB 12328-4**	
Oxygen classification	**Anoxic**		**Suboxic**		**Oxic**		**Anoxic**		**Suboxic**		**Oxic**		**Anoxic**		**Anoxic**		**Anoxic**	
Dinoflagellate cysts	# cysts	cysts/g*	# cysts	cysts/g*	# cysts	cysts/g*	# cysts	cysts/g*	# cysts	cysts/g*	# cysts	cysts/g*	# cysts	cysts/g*	# cysts	cysts/g*	# cysts	cysts/g*
Bitectatodinium spongium	10	161.97	12	194.05	7	76.03	8	82.20	9	55.43	11	73.25	4	80.00	10	163.45	6	68.49
Brigantedinium spp.	144	2332.36	115	1859.64	170	1846.42	145	1489.93	142	874.60	103	685.84	84	1680.00	103	1683.56	77	879.00
cyst of *Protoperidinium monospinum*	10	161.97	7	113.20	8	86.89	9	92.48	4	24.64	17	113.20	3	60.00	5	81.73	6	68.49
Diplopelta minor	0	0.00	0	0.00	0	0.00	0	0.00	0	0.00	0	0.00	1	20.00	1	16.35	0	0.00
Diplopelta parva	0	0.00	2	32.34	0	0.00	0	0.00	3	18.48	0	0.00	0	0.00	2	32.69	1	11.42
Dubridinium spp.	3	48.59	9	145.54	0	0.00	7	71.93	10	61.59	2	13.32	1	20.00	1	16.35	0	0.00
Echinidinium aculeatum	12	194.36	6	97.02	7	76.03	3	30.83	1	6.16	6	39.95	4	80.00	2	32.69	10	114.16
Echinidinium bispiniformum	0	0.00	0	0.00	0	0.00	0	0.00	0	0.00	1	6.66	0	0.00	0	0.00	0	0.00
Echinidinium delicatum	1	16.20	1	16.17	0	0.00	0	0.00	0	0.00	0	0.00	0	0.00	0	0.00	1	11.42
Echinidinium granulatum	6	97.18	36	582.15	28	304.12	10	102.75	12	73.91	19	126.51	12	240.00	23	375.94	12	136.99
Echinidinium transparantum	11	178.17	7	113.20	16	173.78	4	41.10	4	24.64	10	66.59	4	80.00	7	114.42	6	68.49
Echinidinium zonneveldii	2	32.39	1	16.17	1	10.86	0	0.00	0	0.00	0	0.00	0	0.00	0	0.00	0	0.00
Echinidinium spp.	17	275.35	23	371.93	26	282.39	16	164.41	10	61.59	22	146.49	13	260.00	26	424.98	19	216.89
Impagidinium aculeatum	0	0.00	1	16.17	1	10.86	1	10.28	0	0.00	0	0.00	0	0.00	0	0.00	0	0.00
Impagidinium paradoxum	0	0.00	0	0.00	1	10.86	0	0.00	0	0.00	0	0.00	0	0.00	0	0.00	0	0.00
Impagidinium patulum	0	0.00	0	0.00	3	32.58	0	0.00	0	0.00	2	13.32	1	20.00	0	0.00	0	0.00
Leipokatium invisitatum	1	16.20	0	0.00	0	0.00	0	0.00	0	0.00	0	0.00	0	0.00	0	0.00	0	0.00
Lingulodinium machaerophorum	1	16.20	0	0.00	0	0.00	0	0.00	0	0.00	1	6.66	0	0.00	0	0.00	0	0.00
*Lejeunecysta oliva (*cyst of *P. leonis?)*	0	0.00	0	0.00	0	0.00	0	0.00	0	0.00	0	0.00	1	20.00	0	0.00	0	0.00
*Lejeunecysta sabrina (*cyst of *P. leonis?)*	2	32.39	1	16.17	1	10.86	2	20.55	0	0.00	0	0.00	0	0.00	2	32.69	0	0.00
Lejeunecysta spp.	0	0.00	4	64.68	1	10.86	0	0.00	0	0.00	0	0.00	0	0.00	0	0.00	1	11.42
Nematosphaeropsis labyrinthus	4	64.79	3	48.51	73	792.87	4	41.10	15	92.39	20	133.17	2	40.00	4	65.38	2	22.83
Operculodinium centrocarpum sensu Wall and Dale (1966)	0	0.00	1	16.17	2	21.72	0	0.00	0	0.00	0	0.00	0	0.00	2	32.69	2	22.83
Operculodinium centrocarpum s.s.	0	0.00	1	16.17	0	0.00	0	0.00	0	0.00	0	0.00	0	0.00	0	0.00	0	0.00
Operculodinium israelianium	6	97.18	3	48.51	21	228.09	2	20.55	3	18.48	17	113.20	5	100.00	5	81.73	6	68.49
Operculodinium longispinigerum	2	32.39	2	32.34	6	65.17	2	20.55	3	18.48	5	33.29	2	40.00	2	32.69	3	34.25
Operculodinium spp.	1	16.20	3	48.51	2	21.72	0	0.00	4	24.64	2	13.32	1	20.00	3	49.04	4	45.66
Pentapharsodinium daleii	1	16.20	0	0.00	1	10.86	0	0.00	0	0.00	0	0.00	0	0.00	0	0.00	0	0.00
Polykrikos kofoidii	0	0.00	2	32.34	3	32.58	0	0.00	3	18.48	4	26.63	1	20.00	2	32.69	2	22.83
Polysphaeridium zoharyi	1	16.20	9	145.54	9	97.75	1	10.28	0	0.00	8	53.27	0	0.00	0	0.00	0	0.00
cyst of *Protoperidinium americanum*	0	0.00	3	48.51	0	0.00	0	0.00	0	0.00	0	0.00	0	0.00	0	0.00	0	0.00
*Trinovantedinium applanatum (*cyst of *P. pentagonum)*	4	64.79	5	80.85	9	97.75	5	51.38	4	24.64	5	33.29	3	60.00	6	98.07	4	45.66
cyst of *P. conicoides*	0	0.00	0	0.00	0	0.00	0	0.00	0	0.00	0	0.00	0	0.00	0	0.00	0	0.00
*Stelladinium robustum (*cyst of *P. robustum)*	2	32.39	3	48.51	3	32.58	3	30.83	3	18.48	2	13.32	3	60.00	1	16.35	1	11.42
*Stelladinium stellatum/reidii (*cyst o*f P. compressum/reidii)*	1	16.20	3	48.51	2	21.72	4	41.10	4	24.64	6	39.95	1	20.00	7	114.42	2	22.83
cyst of *Peridinoid* spp.	4	64.79	12	194.05	8	86.89	6	61.65	2	12.32	13	86.56	7	140.00	13	212.49	7	79.91
Pyxidinopsis reticulata	0	0.00	0	0.00	3	32.58	0	0.00	0	0.00	0	0.00	0	0.00	0	0.00	0	0.00
*Quinquecuspis concreta (*cyst of *P. leonis?)*	0	0.00	0	0.00	0	0.00	0	0.00	0	0.00	0	0.00	0	0.00	1	16.35	1	11.42
*Selenopemphix nephroides (*cyst o*t P. subinerme)*	1	16.20	5	80.85	4	43.45	0	0.00	3	18.48	5	33.29	2	40.00	5	81.73	2	22.83
*Selenopemphix quanta (*cyst of *P. conicum)*	5	80.98	3	48.51	3	32.58	0	0.00	1	6.16	3	19.98	3	60.00	3	49.04	2	22.83
Spiniferites membranaceus	0	0.00	0	0.00	0	0.00	0	0.00	0	0.00	0	0.00	0	0.00	1	16.35	0	0.00
Spiniferites mirabilis	0	0.00	0	0.00	0	0.00	0	0.00	1	6.16	0	0.00	0	0.00	0	0.00	0	0.00
Spiniferites pachydermus	2	32.39	41	663.00	20	217.23	10	102.75	21	129.34	22	146.49	4	80.00	5	81.73	2	22.83
Spiniferites ramosus	0	0.00	1	16.17	0	0.00	0	0.00	0	0.00	0	0.00	0	0.00	0	0.00	0	0.00
Spiniferites spp.	1	16.20	1	16.17	4	43.45	4	41.10	6	36.95	10	66.59	5	100.00	5	81.73	3	34.25
*Votadinium calvum (*cyst of *P. oblongum)*	3	48.59	2	32.34	6	65.17	1	10.28	4	24.64	3	19.98	0	0.00	1	16.35	0	0.00
*Xandarodinium xanthum (*cyst o*f P. divaricatum)*	0	0.00	0	0.00	0	0.00	1	10.28	0	0.00	0	0.00	1	20.00	0	0.00	0	0.00
Total dinoflagellate cysts	258		328		449		248		272		319		168		248		182	
Volume (ml) on slides	0.1		0.1		0.15		0.2		0.4		0.3		0.2		0.2		0.4	
Dry weight sediment (g)	0.3087		0.3092		0.3069		0.4866		0.4059		0.5006		0.25		0.3059		0.219	
Total concentration (cysts/g)	4178.814		5304.010		4876.724		2548.294		1675.289		2124.118		3360.000		4053.612		2077.626	

* indicates cysts per gram dry sediment

APPENDIX A6

Appendix A6: Spectral areas (I-IV) and subsequent calculated band strength ratios of autotrophic and heterotrophic taxa from the Benguela upwelling region (GeoB 2341 and 4804). Spectral areas were calculated from the integration of peak areas using OMNIC 3.1 software.

Species	**Spectral areas***				**Ratios**						
	I (3010-2775)	**II** (1850-1500)	**III** (1500-1185)	**IV** (1185-830)	**I/II**	**I/III**	**I/IV**	**II/III**	**II/IV**	**III/IV**	**I/II+III**
S. pachydermus	0.5336	0.5363	1.3244	4.3112	0.995	0.403	0.124	0.405	0.124	0.307	0.287
	0.7137	0.8197	1.8624	6.0853	0.871	0.383	0.117	0.440	0.135	0.306	0.266
O. centrocarpum	0.761	2.634	7.136	11.87	0.289	0.107	0.064	0.369	0.222	0.601	0.078
	0.994	2.238	6.26	14.274	0.444	0.159	0.070	0.358	0.157	0.439	0.117
I. patulum	0.8171	0.883	1.2574	4.1103	0.925	0.650	0.199	0.702	0.215	0.306	0.382
	0.9478	0.9982	1.4951	4.8602	0.950	0.634	0.195	0.668	0.205	0.308	0.380
P. schwartzii	0.083	0.8199	0.8098	6.1075	0.101	0.102	0.014	1.012	0.134	0.133	0.051
	0.0158	0.5088	0.4422	2.3087	0.031	0.036	0.007	1.151	0.220	0.192	0.017
	1.0608	4.7595	4.0093	12.3803	0.223	0.265	0.086	1.187	0.384	0.324	0.121
	0.2056	1.3171	0.6	1.4134	0.156	0.343	0.145	2.195	0.932	0.425	0.107
P. kofoidii	1527	36220	27402	35547	0.042	0.056	0.043	1.322	1.019	0.771	0.024
Brigantedinium spp.	0.1839	4.4114	2.6906	3.9176	0.042	0.068	0.047	1.640	1.126	0.687	0.026
	0.2108	5.3988	5.9299	4.3662	0.039	0.036	0.048	0.910	1.236	1.358	0.019
	0.0979	1.6745	0.708	1.4203	0.058	0.138	0.069	2.365	1.179	0.498	0.041
	0.2164	2.5868	0.7075	3.1915	0.084	0.306	0.068	3.656	0.811	0.222	0.066

* Spectral area ranges for regions I-IV are in wavenumbers (cm^{-1})

Appendix A7

Appendix A7: *Apectodinium* species measurements from Chapter 7. All values are in microns. Data were collected by King (2001) and modified for this study.

Species	Species No.*	Pericyst Width	Pericyst Length	Endocyst Width	Endocyst Length	Right Lateral Horn Length	Left Lateral Horn Length	Average Lateral Horn Length
A.au	1	125	112.5	82.5	72.5	25	17.5	21.25
A.au	1	125	117.5	95	75	27.5	30	28.75
A.au	1	117.5	102.5	67.5	72.5	25	27.5	26.25
A.au	1	122.5	105	85	80	17.5	17.5	17.5
A.au	1	100	95	65	70	30	22.5	26.25
A.au	1	132.5	112.5	80	80	32.5	17.5	25
A.au	1	142.5	112.5	77.5	75	32.5	32.5	32.5
A.au	1	102.5	110	65	82.5	25	30	27.5
A.au	1	145	115	82.5	80	45	25	35
A.au	1	187.5	112.5	85	77.5	35	40	37.5
A.au	1	127.5	107.5	67.5	60	25	32.5	28.75
A.au	1	170	112.5	70	70	42.5	57.5	50
A.au	1	162.5	115	80	85	45	45	45
A.au	1	162.5	125	85	75	35	37.5	36.25
A.au	1	157.5	130	80	77.5	47.5	35	41.25
A.au	1	157.5	95	70	60	40	22.5	31.25
A.au	1	150	120	75	82.5	50	37.5	43.75
A.au	1	160	102.5	62.5	65	52.5	50	51.25
A.au	1	147.5	120	80	100	35	35	35
A.au	1	137.5	125	75	80	30	32.5	31.25
A.au	1	140	100	70	75	35	35	35
A.au	1	152.5	132.5	70	75	37.5	55	46.25
A.au	1	165	147.5	87.5	82.5	45	45	45
A.au	1	125	115	75	80	20	30	25
A.au	1	115	110	90	75	25	12.5	18.75
A.au	1	137.5	102.5	75	67.5	35	27.5	31.25
A.au	1	150	112.5	82.5	85	35	37.5	36.25
A.au	1	140	125	72.5	75	40	30	35
A.au	1	152.5	130	75	70	45	45	45
A.au	1	132.5	130	55	62.5	45	35	40
A.au	1	120	100	55	55	32.5	42.5	37.5
A.au	1	127.5	95	70	50	22.5	37.5	30
A.au	1	132.5	100	67.5	67.5	30	35	32.5
A.au	1	152.5	115	80	82.5	45	32.5	38.75
A.au	1	162.5	132.5	80	72.5	42.5	42.5	42.5
A.au	1	137.5	105	67.5	77.5	32.5	37.5	35
A.au	1	155	112.5	77.5	75	30	30	30
A.au	1	135	125	62.5	72.5	35	37.5	36.25
A.au	1	142.5	112.5	75	82.5	37.5	25	31.25
A.au	1	165	140	85	90	32.5	47.5	40
A.au	1	162.5	125	75	72.5	35	57.5	46.25
A.au	1	125	132.5	80	82.5	15	27.5	21.25
A.au	1	142.5	137.5	72.5	75	42.5	42.5	42.5
A.au	1	137.5	82.5	60	52.5	40	37.5	38.75
A.au	1	147.5	87.5	72.5	50	32.5	35	33.75
A.au	1	112.5	87.5	65	50	20	27.5	23.75
A.au	1	147.5	112.5	82.5	77.5	30	32.5	31.25
A.au	1	160	125	85	82.5	42.5	32.5	37.5

Species	Species No.	Pericyst Width	Pericyst Length	Endocyst Width	Endocyst Length	Right Lateral Horn Length	Left Lateral Horn Length	Average Lateral Horn Length
A.hy	2	125	95	87.5	72.5	30	15	22.5
A.hy	2	112.5	100	72.5	80	40	15	27.5
A.hy	2	125	110	70	82.5	30	27.5	28.75
A.hy	2	80	87.5	52.5	60	10	15	12.5
A.hy	2	95	95	67.5	65	10	20	15
A.hy	2	97.5	87.5	62.5	65	20	20	20
A.hy	2	107.5	90	72.5	62.5	17.5	17.5	17.5
A.hy	2	102.5	105	70	67.5	12.5	20	16.25
A.hy	2	137.5	125	80	70	30	30	30
A.hy	2	115	97.5	75	72.5	20	37.5	28.75
A.hy	2	112.5	85	65	65	25	30	27.5
A.hy	2	130	105	75	85	12.5	35	23.75
A.hy	2	125	135	77.5	90	30	25	27.5
A.hy	2	107.5	100	62.5	57.5	25	25	25
A.hy	2	107.5	115	62.5	70	17.5	27.5	22.5
A.hy	2	125	113	77.5	67.5	17.5	25	21.25
A.hy	2	92.5	72.5	50	50	17.5	15	16.25
A.hy	2	100	85	67.5	60	17.5	20	18.75
A.hy	2	137.5	150	77.5	100	25	35	30
A.hy	2	137.5	123	85	72.5	22.5	25	23.75
A.hy	2	137.5	113	80	75	27.5	30	28.75
A.hy	2	107.5	90	75	70	17.5	15	16.25
A.hy	2	115	92.5	77.5	75	17.5	20	18.75
A.hy	2	97.5	87.5	62.5	65	20	20	20
A.hy	2	102.5	105	70	67.5	12.5	20	16.25
A.pv	3	62.5	90	52.5	65	5	2.5	3.75
A.pv	3	67.5	87.5	55	72.5	10	7.5	8.75
A.pv	3	82.5	87.5	70	62.5	7.5	5	6.25
A.pv	3	75	87.5	57.5	55	5	7.5	6.25
A.pv	3	65	87.5	60	65		5	5
A.pv	3	55	75	42.5	45	7.5	5	6.25
A.pv	3	72.5	77.5	55	52.5		2.5	2.5
A.pv	3	80	100	70	60	7.5	5	6.25
A.pv	3	85	100	62.5	65	12.5	10	11.25
A.pv	3	85	135	70	60			
A.pv	3	62.5	75	37.5	57.5	7.5		7.5
A.pv	3	60	67.5	55	52.5	5	5	5
A.pv	3	62.5	80	57.5	57.5		5	5
A.pv	3	65	57.5	57.5	57.5		7.5	7.5
A.pv	3	82.5	80	55	60	12.5	12.5	12.5
A.pv	3	75	87.5	47.5	55	12.5	12.5	12.5
A.pv	3	50	65	50	52.5			
A.pv	3	67.5	87.5	67.5	65			
A.pv	3	75	90	40	60		15	15
A.pv	3	102.5	85	62.5	65			
A.pv	3	75	72.5	55	52.5	10	10	10
A.pv	3	55	67.5	55	50			

*Species numbers: 1) *A. augustum*, 2) *A. hyperacanthum*, 3) *A. parvum*

Appendix A8

Appendix A8: Spectral areas (I-IV) and subsequent calculated band strength ratios of *Apectodinium* species from the North Sea (NS) and Spitsbergen (S) as described in Chapter 7. Spectral areas are arbitrary units from the integration of peak areas using ImageJ64 software.

Species		*A. augustum* (NS)	*A. augustum* (S)	*A. paniculatum* (NS)	*A. paniculatum* (S)	*A. parvum* (NS)	*A. parvum* (S)
Spectral areas*	**I** (3010-2775)	16036	8205	4406	3997	8095	15167
	II (1850-1500)	14413	16007	2893	7680	16196	16734
	III (1500-1185)	8721	8419	10815	9913	8293	8815
	IV (1185-860)	4003	5059	42198	32821	14318	18486
Ratios	**I/II**	1.113	0.513	1.523	0.520	0.500	0.906
	I/III	2.179	0.975	0.407	0.403	0.976	1.721
	I/IV	1.839	1.622	0.104	0.122	0.565	0.820
	II/III	3.601	1.901	0.267	0.775	1.953	1.898
	II/IV	4.006	3.164	0.069	0.234	1.131	0.905
	III/IV	1.653	1.664	0.256	0.302	0.579	0.477
	I/II+III	0.693	1.188	0.321	0.227	0.331	0.594

* Spectral areas are in wavenumbers (cm^{-1})

APPENDIX A9

Appendix A9: Spectral areas (I-IV) and subsequent calculated band strength ratios of dinocysts from the Otto Gott claypit (Lower Cretaceous) as described in Chapter 8. Spectral areas are arbitrary units from the integration of peak areas using ImageJ64 software.

Species		*C. magna*	*Hystrichosphaeridium* spp.	*P. pelliferum*	*P. brevicornutum*	*Oligosphaeridium complex*	*P. anaphrissum*
Spectral areas*	**I** (3010-2775)	7374	3870	10415	5340	7840	12042
	II (1850-1500)	24679	22493	27656	12171	24035	19287
	III (1500-1185)	19582	23880	20278	8380	18583	13480
	IV (1185-760)	4403	5224	12114	48875	6155	10335
Ratios	**I/II**	0.299	0.172	0.377	0.439	0.326	0.624
	I/III	0.377	0.162	0.514	0.637	0.422	0.893
	I/IV	1.675	0.741	0.860	0.109	1.274	1.165
	II/III	1.260	0.942	1.364	1.452	1.293	1.431
	II/IV	5.605	4.306	2.283	0.249	3.905	1.866
	III/IV	4.447	4.571	1.674	0.171	3.019	1.304
	I/II+III	0.167	0.083	0.217	0.260	0.184	0.368

* Spectral areas are in wavenumbers (cm^{-1})

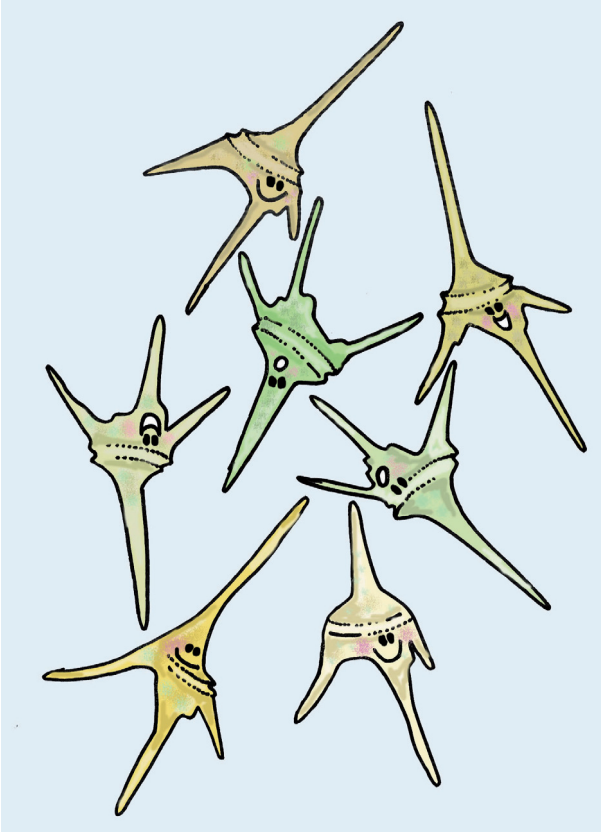

The creatures that inhabit this earth - be they human beings or animals - are here to contribute, each in its own particular way, to the beauty and prosperity of the world.

-H.H. Dalai Lama